INVESTIGATING THE IMPACT OF ELECTRONIC CIGARETTES ON NEUTROPHIL FUNCTION

by

ALICE EMILY JASPER

A thesis submitted to the University of Birmingham for the degree of DOCTOR OF PHILOSOPHY.

Supervisors:

Dr Aaron Scott, Professor Elizabeth Sapey & Professor David Thickett.

Institute of Inflammation and Ageing

College of Medical and Dental Sciences

University of Birmingham

February 2022

UNIVERSITY OF
BIRMINGHAM

University of Birmingham Research Archive

e-theses repository

This unpublished thesis/dissertation is copyright of the author and/or third parties. The intellectual property rights of the author or third parties in respect of this work are as defined by The Copyright Designs and Patents Act 1988 or as modified by any successor legislation.

Any use made of information contained in this thesis/dissertation must be in accordance with that legislation and must be properly acknowledged. Further distribution or reproduction in any format is prohibited without the permission of the copyright holder.

Abstract

Electronic (e-) cigarettes were developed in the early 2000s as safer alternatives to tobacco smoking. Their popularity continues to rise amongst current smokers, ex-smokers and never smokers despite uncertainties in their long-term safety. Studies have begun to uncover early indicators of potential harm including changes in function, transcription, and communication of important cells of the respiratory immune system.

This thesis aimed to investigate the impact of e-cigarette vapour on neutrophil functions and uncover potential drivers of dysfunction. A novel and adaptable model of direct e-cigarette vapour exposure was developed, validated, and applied to the treatment of human peripheral blood neutrophils. Neutrophils were isolated from the whole blood of otherwise healthy non-smokers/non-vapers and exposed to e-cigarette vapour. Two generations of e-cigarette device, along with two e-liquids of different nicotine strengths were tested, to understand the contribution of device power and nicotine content to the neutrophil functions examined.

Key neutrophil effector functions including chemotaxis, transmigration, phagocytosis, and oxidative burst were blunted by e-cigarette vapour exposure. In all cases, higher-powered e-cigarette devices had a more inhibitory effect on neutrophil functions. Nicotine-free e-cigarette vapour prevented key neutrophil effect functions including phagocytosis and transmigration, indicating this effect cannot only be attributed to nicotine. To understand the mechanistic drivers of these changes, neutrophil transcriptome, metabolism (glycolytic function), and calcium signalling were explored. In addition, neutrophils were pre-treated with a nicotinic receptor inhibitor,

phosphoinositide 3-kinase (Pi3K) inhibitors and the antioxidant and anti-aldehyde agent N-acetyl cysteine (NAC), and the ability to restore e-cigarette-induced dysfunction was assessed. Pre-treatment of neutrophils with NAC appeared to provide the greatest protection against e-cigarette vapour-induced dysfunctional phagocytosis and transmigration, providing rationale for this effect to be further elucidated.

Overall, this thesis demonstrated e-cigarette vapour-induced neutrophil dysfunction, which could have persistent consequences for lung health, and raises concerns over the long-term safety of e-cigarette use.

For my Mum and Dad.

Acknowledgements

I could write another thesis thanking every person who has helped me get here, but I will try to keep this brief.

Firstly, to my supervisors. I have to say an enormous thank you to Aaron, who has dedicated himself to guiding me through this project. It has been a pleasure to have been your first PhD student and I can't thank you enough for your time, support, and commitment. Sorry for using up much more than your allotted 20 minutes per week! To Liz, thank you for your guidance throughout my journey in Team Neutrophil, and for being a fantastic role model for women in science. To David, thank you for your advice and feedback throughout the duration of this project, and for always having an idea for the next experiment! To all three of you, thank you for trusting me with this project. Without your expertise and guidance, I would not be where I am now, and I feel so lucky to have had such a great experience completing this PhD.

To my colleagues and friends, past and present, in Team Neutrophil and Team Respiratory. The best advice I ever got was that you can fall in love with a PhD topic, but it is much harder to fall in love with a lab group, so pick them wisely; and that I have done. There are far too many of you to name individually who have helped me in all manner of ways through every step of this PhD, you know who you are! Thank you for being like family when we couldn't see our own during the pandemic. Thank you for being honest about lab mishaps, writers block, and receiving unwanted criticism. I am so grateful for your genuine interest in my project, your advice, and your concern over

whether I had stopped for lunch! I'll miss the lab meetings, pub trips and coffee breaks and wish every single one of you all the best in the future.

To my Mum and Dad, who have dedicated their lives to raising my brother and I. You two are my inspirations, and truly the best parents anyone could ever wish for. I hope I have done you proud, this thesis is dedicated to you both. I am extremely grateful to my other half, Freddie, who has been my rock throughout this journey. Thank you for your unwavering support, and for believing in me even when I didn't believe in myself. Somehow, you always knew exactly what I needed to hear and helped me find joy even in the tough times. I'm not sure I could have done this without you. To my wonderful friends and incredible family who have been there for me through this rollercoaster of a journey; thank you for your endless support, understanding and encouragement. Without you, life outside of this PhD would have been very boring and I am so lucky to have you all.

Finally, to the University of Birmingham who have funded me to complete this PhD. Birmingham has been home to me for the past 6.5 years and I will never forget the time I have had here. For providing a place for me to be nurtured and become a woman I am proud of, thank you.

COVID-19 Declaration

My project was significantly impacted by the COVID-19 pandemic which struck part-way through my second year. The laboratory was shut down from 20th March-22nd June 2020 just as I completed validation of my experimental methodology and was beginning a significant data collection phase.

During this time, I focussed on writing a literature review which has been published in a peer-reviewed journal (Jasper et al AJP-Lung 2021 PMID: 34009037). I also contributed to a peer-reviewed guideline manuscript for safe return to clinical research (Walker et al JMIR Res Protoc PMID: 33146625). On reopening, significant restrictions applied which hampered the use of blood and blood products in the laboratory due to significant delays in risk assessment approval. As SARS-CoV-2 virus is a hazard group 3 agent, work with fresh blood samples was not possible under law until these assessments were in place. As my project depended entirely on the isolation of neutrophils with no appropriate cell line to use as an alternative, I was unable to progress with data collection. Instead, I focussed on non-cellular assays using stored samples.

On 20th August 2020, the risk assessments were approved, however, adopting a bubble-based system on return limited us to 50% time in the lab and 50% work from home. This system of 50/50 working continued until June 2021, by which point I had taken the decision to stop lab work and begin writing my thesis as my PhD was due to finish at the end of September of that same year. Safety restrictions limiting use of

fresh blood products remained in place. This reduced capacity significantly hampered the development of my final thesis chapter examining the mechanisms of effect.

The University recognised the significant impact COVID-19 had on my project and kindly granted me a 4-month funded extension which allowed me to return to the lab to complete some of the essential mechanistic experiments. During this time, I tried to maximise output capacity and introduced elements such as transcriptomics to again capitalise on stored samples. The body of work required to compete these studies was very large so despite this extension some of the results presented in this thesis have low numbers of biological replicates.

Despite this caveat, I believe the work presented in this thesis represents a significant contribution to the field, advancing our knowledge of the effects of e-cigarettes on cells intricately linked to smoking related and chronic lung disease, which may have serious implications for e-cigarette user’s lung health.

Table of contents

Chapter 1 - INTRODUCTION 1

1.1 E-cigarettes 2

1.1.1 A brief history of smoking 2

1.2 Device design and evolution 4

1.2.1 E-liquids and vapour constituents 8

1.2.2 E-cigarette use and topography 9

1.2.3 EVALI 12

1.3 Neutrophils 16

1.3.1 Neutrophil production and release into circulation 17

1.3.2 Neutrophil activation 19

1.3.3 Neutrophil migration and chemotaxis 21

1.3.4 Phagocytosis 22

1.3.5 Neutrophil granules 24

1.3.6 Neutrophil extracellular traps (NETs) 26

1.3.7 Neutrophil metabolism ..... **Error! Bookmark not defined.**

1.3.8 Neutrophil clearance 28

1.3.9 Neutrophils in health and disease ..... **Error! Bookmark not defined.**

1.3.9.1 Health ..... **Error! Bookmark not defined.**

1.3.9.2 Neutrophils in COPD 29

1.3.9.3 Neutrophils in cigarette smoking 30

1.4 Limitations in current e-cigarette model systems 36

1.5 The effect of e-cigarettes on cells of the respiratory system 39

1.5.1 Epithelial cells 39

1.5.2 Alveolar macrophages 40

1.5.3 Current understanding of the effect of e-cigarettes and neutrophils 44

1.5.4 Parallels between e-cigarette and cigarette studies 48

1.6 Gap in knowledge and the importance of this work 49

1.7 Hypothesis and aims 50

Chapter 2 - MATERIALS AND METHODS 51

2.1 Ethical approval 52

2.2 Subject recruitment 52

2.3 Blood sample collection 52

2.4 Neutrophil isolation 52
2.4.1 Percoll™ density gradient separation 52
2.4.2 Assessing neutrophil purity by cytospin 55
2.5 E-cigarette devices 57
2.6 E-cigarette vapour exposure system 58
2.7 Neutrophil viability 61
2.8 Neutrophil migration assays 63
2.8.1 Insall chamber – chemotaxis 63
2.8.2 Transwell migration 66
2.9 Neutrophil phagocytosis of *E. coli* and *S. aureus* 66
2.10 Neutrophil NETosis assays 68
2.10.1 Immunofluorescence staining for NETs 68
2.10.2 Quantification of NET release 69
2.11 Neutrophil degranulation - protein release 69
2.12 Neutrophil metabolic assay 72
2.13 Calcium signalling assay 77
2.14 Graph and figure generation 77
2.15 Statistical analysis 78
2.15.1 Power calculations 78
Chapter 3 - ASSAY OPTIMISATION AND VALIDATION 80
3.1 Chapter 3 introduction 81
3.2 Aims of chapter 3 82
3.3 Materials and Methods linked to chapter 3 82
3.3.1 Nicotine deposition - Gas chromatography with flame ionization detector 82
3.3.2 Calcein AM staining for transwell migration 82
3.3.3 Measuring pHrodo™ bioparticle fluorescence 83
3.3.4 Validation of cytochalasin D concentration for inhibition of phagocytosis. 83
3.3.5 Assessing the effect of CellTak on neutrophil viability 84
3.4 Chapter 3 results 85
3.4.1 Donor demographics 85
3.4.2 E-cigarette vapour model validation 87

3.4.2.1 GC-FID results 87
3.4.2.2 Neutrophil viability after e-cigarette exposure 89
3.4.3 CXCL8 as a chemoattractant for neutrophil chemotaxis in the Insall chamber model 92
3.4.4 Transwell migration validation work 94
3.4.4.1 Measuring migration by fluorescence 94
3.4.4.2 Measuring migration by FACS 96
3.4.4.3 CXCL8 as a chemoattractant for neutrophil transmigration in the transwell model 98
3.4.5 pHrodo™ bioparticle assay validation 99
3.4.5.1 Inter -batch variation and pHrodo™ bioparticle colour consideration 99
3.4.5.2 Fluorescence intensity 101
3.4.5.3 pHrodo™ assay gating strategy 103
3.4.5.4 Timecourse 105
3.4.5.5 Cytochalasin D concentration 107
3.4.6 Seahorse validation 110
3.4.6.1 Cell-Tak and neutrophil viability 110
3.4.6.2 Cell seeding density 112
3.4.6.3 PMA concentration validation 115
3.4.7 SYTOX® green / anti-histone H3 NET co-staining 117
3.4.8 Calcium assay validation 118
3.4.9 RNA extraction validation 120

3.5 Chapter 3 discussion 122

3.5.1 E-cigarette vapour chamber model 122
3.5.2 Neutrophil migration assays 124
3.5.3 Neutrophil phagocytosis model 125
3.5.4 Neutrophil bioenergetics – seahorse assay 127
3.5.5 Staining for NETs using SYTOX® green 128
3.5.6 Neutrophil intracellular calcium signalling assay 129
3.5.7 Limitations 129
3.5.8 Conclusion 130

Chapter 4 - IMPACT OF E-CIGARETTE VAPOUR EXPOSURE ON NEUTROPHIL FUNCTIONS 131

4.1 Chapter 4 introduction 132

4.2 Aims of chapter 4 133

4.3 Materials and methods linked to chapter 4 134

4.3.1 Transwell staining and visualisation 134
4.3.2 Nicotine treatment 134

4.4 Chapter 4 results 135
4.4.1 Neutrophil migratory parameters 135
4.4.1.1 E-cigarette vapour exposure and neutrophil chemotaxis to CXCL8 135
4.4.1.2 E-cigarette vapour exposure and neutrophil transmigration to CXCL8 137
4.4.2 E-cigarette vapour exposure and neutrophil phagocytosis of *E. coli* and *S. aureus* 139
4.4.2.1 *E. coli* 139
4.4.2.2 *S. aureus* 140
4.4.2.3 Nicotine-dependent effects on neutrophil phagocytosis of *E. coli* and *S. aureus*. 140
4.4.2.4 Device power-dependent effects on neutrophil phagocytosis of *E. coli* and *S. aureus* 141
4.4.3 Neutrophil protein secretion in response to e-cigarette vapour exposure 143
4.4.4 Neutrophil bioenergetics 147
4.4.4.1 E-cigarette vapour exposure and basal neutrophil metabolism 147
4.4.4.2 E-cigarette vapour exposure and neutrophil oxidative burst response 149
4.4.5 E-cigarette vapour exposure and NET generation 152
4.4.5.1 Spontaneous NET generation 152
4.4.5.2 PMA-stimulated NET generation 153
4.4.6 Direct treatment of neutrophils with nicotine 157
4.4.6.1 Nicotine treatment and neutrophil viability 157
4.4.6.2 Nicotine treatment and neutrophil transwell migration 159
4.4.6.3 Nicotine treatment and NET generation 160
4.4.6.4 Nicotine treatment and neutrophil phagocytosis of *E. coli* and *S. aureus* bioparticles 162

4.5 Chapter 4 discussion 165
4.5.1 Neutrophil migratory parameters 165
4.5.2 Neutrophil phagocytosis 166
4.5.3 Neutrophil degranulation 168
4.5.4 Neutrophil oxidative burst 171
4.5.5 Neutrophil NET generation 172
4.5.6 Impact of device generation on neutrophil functions 174
4.5.7 Nicotine-dependent neutrophil dysfunction 174
4.5.8 Nicotine-independent neutrophil dysfunction 176
4.5.9 Limitations 178
4.5.10 Conclusion 181

Chapter 5 - MECHANISTIC WORK 182

5.1 Chapter 5 introduction 183
5.1.1 Neutrophil transcriptome 183

5.1.2 Neutrophil metabolism 184
5.1.3 Nicotine receptors 185
5.1.3.1 Nicotine receptor signalling 185
5.1.3.2 Calcium signalling 186
5.1.4 Restoration of function – Pi3K signalling 187
5.1.5 Restoration of function – antioxidants 188
5.2 Aims of Chapter 5 190
5.3 Materials and methods linked to chapter 5 191
5.3.1 RNAseq 191
5.3.1.1 Sample collection, storage, and extraction 191
5.3.1.2 RNA extraction 191
5.3.1.3 DNase I treatment and DNase inactivation 192
5.3.1.4 RNA purity check 192
5.3.1.5 RNA sequencing 193
5.3.1.6 RNA sequencing data analysis 193
5.3.2 6NBDG glucose uptake assay 196
5.3.3 Inhibitor treatment 196
5.3.4 Antioxidant treatment 197
5.4 Chapter 5 results 198
5.4.1 E-cigarette vapour and the neutrophil transcriptome 198
5.4.2 E-cigarette vapour and neutrophil glycolysis 204
5.4.2.1 Glycolytic parameters 204
5.4.2.2 Glucose uptake 208
5.4.3 Pre-treatment of neutrophils exposed to e-cigarette vapour with α4β2 and α7 nAChR inhibitor 210
5.4.3.1 Phagocytosis 210
5.4.3.2 Transwell migration 213
5.4.4 E-cigarette vapour and calcium signalling 215
5.4.5 Pre-treatment of neutrophils exposed to e-cigarette vapour with Pi3K inhibitors 217
5.4.5.1 Phagocytosis 217
5.4.5.2 Transwell migration 220
5.4.6 Pre-treatment of neutrophils exposed to e-cigarette vapour with NAC 223
5.4.6.1 Phagocytosis 223
5.4.6.2 Transwell migration 225
5.5 Chapter 5 discussion 227
5.5.1 Neutrophil transcriptome 227
5.5.2 Neutrophil glycolytic metabolism 228

5.5.3 Nicotine receptors 230
5.5.3.1 Calcium signalling 231
5.5.4 Restoration of function – Pi3K signalling 233
5.5.5 Restoration of function – antioxidants 234
5.5.6 Limitations 235
5.5.7 Conclusion 237

Chapter 6 - GENERAL DISCUSSION 239

6.1 Overall findings 240
6.1.1 Neutrophil migration 241
6.1.2 Neutrophil phagocytosis 242
6.1.3 Neutrophil degranulation 244
6.1.4 Neutrophil oxidative burst 246
6.1.5 NET formation 247
6.1.6 Driving mechanisms 248

6.2 *In vivo* evidence of e-cigarette-induced harm 253

6.3 What does this study contribute to the field? 255

6.4 Clinical implications 255

6.5 Study strengths 259

6.6 Study limitations 260

6.7 Future direction 262

6.8 Conclusions 264

Chapter 7 - REFERENCES 266

List of Figures

Figure 1.1*:* A diagram of the structure of an e-cigarette device. 6
Figure 1.2: The evolution of e-cigarette devices. 7
Figure 1.3*:* Neutrophil granule subsets and their matrix and membrane proteins. 25
Figure 1.4: Neutrophil extracellular traps and their components. 27
Figure 1.5: Modulation of chronic airway inflammation driven by cigarette smoke exposure 35
Figure 1.6*:* A schematic diagram of the main e-cigarette exposure models used in *in vitro* models. 38
Figure 1.7: A summary of the effects of e-cigarette vapour exposure on lung homeostasis driven by alterations in important lung cells. 47
Figure 2.1: A schematic diagram of the percoll gradient neutrophil isolation method. 54
Figure 2.2: Cytospin slide photograph after Quick-Diff staining to allow identification of blood cell subtypes. 56
Figure 2.3: The e-cigarette vapour exposure system developed to expose cells directly to e-cigarette vapour. 59
Figure 2.4*:* An example of flow cytometry analysis plots used to assess cell viability. 62
Figure 2.5: A schematic diagram of the Insall chamber used to assess neutrophil chemotaxis. 64
Figure 2.6: A schematic diagram of the injection ports of the Agilent Seahorse XF96 sensor cartridge. 75
Figure 2.7: Schematic diagrams of ECAR and OCR traces generated during the glyco stress test and oxidative burst test. 76
Figure 2.8*:* An overview of the approach to statistical analysis used in this thesis 79
Figure 3.1: Heat maps showing the distribution of nicotine across the e-cigarette vaping chamber used in this study. 88
Figure 3.2: The gating strategy used to assess neutrophil viability. 90
Figure 3.3: The effect of e-cigarette vapour exposure on neutrophil viability at baseline. 91

Figure 3.4: Neutrophil chemotaxis is upregulated in response to 100 nM CXCL8 using the Insall chamber. 93
Figure 3.5: Fluorescence intensity of neutrophils stained with calcein AM before and after e-cigarette vapour exposure....95
Figure 3.6: Comparing plate reader to flow cytometer methods of measuring neutrophil transmigration....97
Figure 3.7: Neutrophil transmigration is upregulated in response to 100 nM CXCL8 using the transwell migration model. 98
Figure 3.8: Inter-batch variation in pHrodo™ red E. coli bioparticles....100
Figure 3.9: pHrodo™ bioparticle fluorescence over time....102
Figure 3.10: Representative flow cytometry plots to describe the gating strategy for phagocytosis assays. 104
Figure 3.11: Neutrophil phagocytosis of *E. coli* and *S. aureus* bioparticles over time. 106
Figure 3.12: Validation of cytochalasin D concentration for inhibition of phagocytosis. 109
Figure 3.13: Viability staining for neutrophils adhered to a well via Cell-Tak and BSA. 111
Figure 3.14: Representative photographs of the cell seeding densities of neutrophils used in the Seahorse assay. 113
Figure 3.15*:* Neutrophil oxidative burst test cell seeding densities. 114
Figure 3.16: Neutrophil glyco stress test parameters and cell seeding densities. ...114
Figure 3.17: PMA induced-oxidative burst dose responses. 116
Figure 3.18: Neutrophil extracellular traps co-stained with SYTOX® green and Anti-Histone H3 antibody. 117
Figure 3.19: Neutrophil treatment with thapsigargin increases cytoplasmic calcium. 119
Figure 3.20: Extracted RNA yield (concentration) and quality (RNA integrity number). 121
Figure 4.1: The effect of e-cigarette vapour exposure on neutrophil chemotaxis to CXCL8....136

Figure 4.2: The effect of e-cigarette vapour exposure on neutrophil transwell migration. 138
Figure 4.3: The effect of e-cigarette vapour exposure on neutrophil phagocytosis of *E. coli* and *S. aureus* pHrodo™ bioparticles. 142
Figure 4.4: Neutrophil phagocytosis of E. coli and S. aureus pHrodo™ bioparticles over time 143
Figure 4.5: Neutrophil secretion of MMP-2, MMP-8, MMP-9 and MPO in response to e-cigarette vapour exposure. 146
Figure 4.6: Baseline metabolism of neutrophils treated with e-cigarette vapour. 148
Figure 4.7: The effect of e-cigarette vapour exposure on neutrophil oxidative burst response to 160 nM PMA. 151
Figure 4.8: The effect of e-cigarette vapour exposure on neutrophil NETosis. 155
Figure 4.9: Infographic summary of the effects of e-cigarette vapour on key neutrophil effector functions studied in chapter 4. 156
Figure 4.10: The effect of nicotine treatment on neutrophil viability. 158
Figure 4.11: The effect of nicotine treatment on neutrophil transwell migration. 159
Figure 4.12*:* The effect of nicotine treatment on neutrophil NET generation. 161
Figure 4.13: The effect of direct nicotine treatment on neutrophil phagocytosis. 164
Figure 5.1*:* A summary of the RNA analysis workflow described in section 5.3.1.6.195
Figure 5.2: Volcano plots generated from DESeq2 analysis of gene counts comparing UTC to paired treated samples. 200
Figure 5.3: Volcano plots generated from DESeq2 analysis of gene counts comparing all UTC samples to all treated samples, regardless of which e-cigarette vapour condition was used. 201
Figure 5.4 KEGG pathway analysis of all DEGs caused by e-cigarette treatments. 203
Figure 5.5: The effect of e-cigarette vapour exposure on neutrophil glycolysis. 207
Figure 5.6: The effect of e-cigarette vapour exposure on neutrophil uptake of fluorescent 6NBDG analogue of glucose. 209
Figure 5.7: The effect of nicotine receptor inhibition prior to 4th generation e-cigarette exposure on neutrophil phagocytosis of *E. coli* and *S. aureus* bioparticles. 212
Figure 5.8: The effect of nicotine receptor inhibition prior to 4th generation e-cigarette exposure on neutrophil transmigration to 100 nM CXCL8. 214

Figure 5.9: The effect of e-cigarette and nicotine treatment on neutrophil intracellular calcium signalling 216
Figure 5.10: The effect of Pi3Kδ and γ inhibition prior to 4th generation e-cigarette exposure on neutrophil phagocytosis of *E. coli* and *S. aureus* bioparticles. 219
Figure 5.11: The effect of Pi3Kδ and γ inhibition prior to 4th generation e-cigarette exposure on neutrophil transmigration to 100 nM CXCL8. 222
Figure 5.12: The effect of antioxidant treatment prior to 4th generation e-cigarette exposure on neutrophil phagocytosis of *E. coli* and *S. aureus* bioparticles. 224
Figure 5.13: The effect of N-acetyl-cystine pre-treatment on neutrophil transwell migration prior to e-cigarette vapour exposure. 226

List of Tables

Table 1.1: Details of the current understanding of the effects of cigarette smoke and e-cigarette vapour on alveolar macrophages and epithelial cells. 43
Table 2.1: Group definitions for each e-cigarette vapour exposure method. ...60
Table 2.2 Definitions of parameters used to assess neutrophil migration as defined by Greenwood et al in 2014 (Greenwood, 2014).....65
Table 2.3: ELISA kits used to measure protein release by e-cigarette treated neutrophils.....71
Table 2.4: Inhibitors and stimulants used in the Agilent Seahorse XF96 neutrophil metabolism protocol. 75
Table 3.1*:* The demographics of study participants who donated blood for the purposes of this project. 86
Table 5.1: The top 20 differentially expressed genes associated with each e-cigarette vapour treatment, and the corresponding statistical significance. 202
Table 6.1: Details of current understandings of neutrophil functions in a range of diseases as well as the effect of smoking and e-cigarettes on the same functions. 258

List of Abbreviations

2-DG	2-Deoxy- d-glucose
2GECV	Second generation electronic cigarette vapour (containing nicotine)
2GNF	Second generation nicotine free (electronic cigarette vapour)
4GECV	Fourth generation electronic cigarette vapour (containing nicotine)
4GNF	Fourth generation nicotine free (electronic cigarette vapour)
6NBDG	6-(*N*-(7-Nitrobenz-2-oxa-1,3-diazol-4-yl)amino)-6-Deoxyglucose
AA	Antimycin-A
AAT	Alpha-1 anti-trypsin
AATD	Alpha-1 anti-trypsin deficiency
ACE2	Angiotensin-converting enzyme 2
Akt	Protein kinase B
ANOVA	Analysis of variance
ATP	Adenosine triphosphate
BALF	Bronchoalveolar lavage fluid
BSA	Bovine serum albumin
C/EBPa	CCAAT-enhancer-binding proteins
CBD	Cannabidiol
CD	Cluster of differentiation
CDC	Centres for Disease Control and Prevention
CFTR	Cystic fibrosis transmembrane conductance regulator
CGD	Chronic granulomatous disease
Cit H3	Citrullinated histone H3
COPD	Chronic obstructive pulmonary disease
COVID-19	Coronavirus disease 2019
CR	Complement receptor
CRAC	Calcium release-activated channels
CReSS	Clinical research support system
CT	Computed tomography
CXCL	CXC-chemokine ligand
CXCR	CXC-chemokine receptor
CytD	Cytochalasin D
DEGs	Differentially expressed genes
DNA	Deoxyribonucleic acid
E-cigarette	Electronic cigarette
E-liquid	Electronic cigarette liquid
E. coli	*Escherichia coli*
ECAR	Extracellular acidification rate
ELISA	Enzyme-linked immunosorbent assay

ENDS	Electronic nicotine delivery system
ERK	Extracellular-signal regulated kinase
EVALI	E-cigarette or vaping use-associated lung injury
F. nucleatum	*Fusobacterium nucleatum*
FACS	Fluorescence-activated cell sorting
FcRs	Fc receptors
FCS	Fetal calf serum
FEF	Forced expiratory flow
FEV	Forced expiratory volume in 1 second
fMLP	*N*-Formylmethionyl-leucyl-phenylalanine
fMLPR	fMLP receptor
FVC	Forced vital capacity
GC-FID	Gas chromatography with flame ionisation detection
GCSF	Granulocyte colony stimulating factor
Gfi-1	Growth factor independent transcription repressor
GPCR	G-protein coupled receptors
GTP	Guanosine-5'-triphosphate
HBSS	Hanks' balanced salt solution
HEPES	4-(2-hydroxyethyl)-1-piperazineethanesulfonic acid
HNEC	Human nasal epithelial cells
HSC	Haematopoietic stem cells
ICAM	Intracellular adhesion molecule
Ig	Immunoglobulin
IL	Interleukin
IPF	Idiopathic pulmonary fibrosis
IQR	Interquartile range
IRF3	Interferon regulator factor 3
JAM	Junctional adhesion molecule
LAIV	Live-attenuated influenza virus
LFA1	Lymphocyte function-associated antigen 1
LPS	Lipopolysaccharide
LTA	Lipoteichoic acid
LTB_4	Leukotriene B_4
Mac-1	Macrophage-1 antigen
MAPK	Mitogen-activated protein kinase
MCP	Monocyte chemoattractant protein
MFI	Median fluorescence intensity
MFI	Median fluorescence intensity
MHRA	Medicines and Healthcare products Regulatory Agency
MIP	Macrophage inflammatory protein
MMP	Matrix metalloproteinases

MPO	Myeloperoxidase
mRNA	Messenger Ribonucleic acid
mRNA	Messenger ribonucleic acid
MRSA	Methicillin-resistant Staphylococcus aureus
NAC	N-acetyl cysteine
NADPH	Nicotinamide adenine dinucleotide phosphate
NE	Neutrophil elastase
NET	Neutrophil extracellular trap
NF-kB	Nuclear factor kappa-light-chain-enhancer of activated B cells
NHBE	Normal human bronchial epithelial
NRT	Nicotine replacement therapy
NTHI	Non-typeable Haemophilus influenzae
OCR	Oxygen consumption rate
OD	Optical density
PAMP	Pathogen associated molecular pattern
PATH	Population Assessment of Tobacco Health
PBMC	Peripheral blood mononuclear cell
PBS	Phosphate buffered saline
PCR	Polymerase chain reaction
PECAM1	Platelet endothelial cell adhesion molecule -1
PER	Proton efflux rate
PG	Propylene glycol
PI	Propidium iodide
Pi3K	Phosphoinositide 3-kinase
PKC	Protein kinase C
PMA	Phorbol 12-myristate 13-acetate
PR3	Proteinase 3
PRRs	Pattern recognition receptors
PSGL	P-selectin glycoprotein ligand
RCS	Reactive carbonyl species
RFU	Relative fluorescence units
Rho	Ras homology
RIN	RNA integrity number
RNA	Ribonucleic acid
ROCK	Rho-association protein kinase
ROS	Reactive oxygen species
Rot	Rotenone
RT	Room temperature
RT-PCR	Real time polymerase chain reaction
S. aureus	*Staphylococcus aureus*
S. pneumoniae	*Streptococcus pneumoniae*

SARS-CoV-2	Severe acute respiratory syndrome coronavirus 2
SD	Standard deviation
SEM	Standard error of the mean
SERCA	Sarco/endoplasmic reticulum Ca^{2+} ATPase
SLPI	Secretory leucocyte proteinase inhibitor
SOCE	store operated calcium entry
STAT1	Signal transducer and activator of transcription 1
THC	Tetrahydrocannabinol
TICAM2	TIR domain-containing adapter molecule 2
TLR	Toll-like receptor
TNF	Tumour necrosis factor
UTC	Untreated control
V-type H^+ ATPase	Vacuolar ATPase
VEA	Vitamin E acetate
VG	Vegetable glycerin
WHIM	Warts, hypogammaglobulinemia, infections, myelokathexis
α2M	α2-macroglobulin

Chapter 1 -

INTRODUCTION

Foreword: Chapter 1 draws heavily on first author work previously published in peer-reviewed journals (Jasper et al., 2021, Jasper et al., 2019) but has been adapted for the purpose of this thesis.

1.1 E-cigarettes

1.1.1 A brief history of smoking

Records of tobacco smoking exist from as early as the first century BC in indigenous America. Native Americans developed tobacco smoking for use in religious rituals and medical treatment (Mishra and Mishra, 2013). After the invention of the first automated cigarette manufacturing machines in the 1880s, the Duke brothers began mass producing cigarettes in their factory. The popularity of cigarettes soared, and the global company British American Tobacco was born. The ability to mass produce cigarettes increased their accessibility, and they grew in glamour and popularity throughout the 1950s (National Center for Chronic Disease Prevention and Health Promotion (US), 2014, Peto et al., 2000).

Beginning as early as the 1920s, possible ill-effects of smoking on human health were noted, but in 1950, the British Medical Journal published a preliminary report suggesting a possible link between smoking and lung cancer (Doll and Hill, 1950). In 1964, the US Surgeon General published a damming report attributing cigarette smoking to lung cancer and the rising death rate (U.S. Department of Health, 1964). It is now understood that smoking is a major risk factor for cancer, heart disease, stroke, lung diseases, diabetes and chronic obstructive pulmonary disease (COPD) (National Center for Chronic Disease Prevention and Health Promotion (US) (NCCDPHP),

2014). The hallmarks of COPD mirror those of smoking-related lung diseases: inflammation of the small airways (bronchiolitis) and breakdown of lung parenchyma (emphysema), resulting in abnormalities in airflow through the respiratory system.

Smoking drives these physiological changes because tobacco smoke contains over 5,000 chemicals including nicotine, carbon monoxide and carcinogens including polycyclic aromatic hydrocarbons, formaldehyde and arsenic (Centers for Disease Control and Prevention, 2010). These toxins, along with thousands of reactive oxygen species (ROS), directly damage the epithelial cells lining the upper airways by peroxidation of cell membrane lipids, activating oxidative stress pathways, and inducing DNA damage (Lee et al., 2012, Valavanidis et al., 2009). This promotes inflammation and drives chronic immune cell recruitment. In addition, tar - a sticky dark brown viscous fluid containing many carcinogens - collects in the lungs of smokers and increases the risk of developing lung cancer and lung diseases including COPD. As a result, tobacco smoke activates a cycle of chronic lung inflammation. Tobacco smoking represents a slow burning model of disease development, commonly taking decades to develop detectable disease after initiation of smoking, often when it is irreversible (Lokke et al., 2006). Tobacco smoking remains the leading preventable cause of death worldwide, killing over 8 million people each year and costing the global economy US $1.4 trillion per year (WHO, 2021).

Electronic (e-) cigarettes, also known as electronic nicotine delivery systems (ENDS) are devices which deliver nicotine without combustion, which were developed in 2003 as a safer alternative to tobacco cigarettes. By removing the factors which create

harmful tar and carbon monoxide, it was thought that nicotine could be delivered in a vapourised form without the long-term health consequences associated with cigarette smoking.

1.2 Device design and evolution

E-cigarette devices have five main components: battery, activator switch, atomiser, tank, and mouthpiece. E-liquids are used to refill the tank, and saturate the wick of the atomiser coil, usually made of cotton or silica. E-cigarettes are activated by the user engaging the activator switch and inhaling via the mouthpiece which together generates an electrical current (see Figure 1.1). The electrical current heats the atomiser and the e-liquid is vaporised, which is inhaled by the user via the mouthpiece.

The first devices to be invented - first generation or cig-a-like devices - were disposable, non-refillable and looked like tobacco cigarettes. Later came the more advanced pen-like second generation devices, with refillable tanks and rechargeable batteries. Second generation devices rapidly overtook first generation due to the cost-effectiveness of a refillable and rechargeable device. However, development of larger volume tanks and higher-power batteries formed the basis of third generation devices. Most recently, the fourth generation of e-cigarettes allows user modification of temperature, power output and airflow settings. Additionally, these devices have larger tanks, longer battery life and more customisable features than ever. The devices mentioned thus far vapourise e-liquids containing freebase nicotine. However, in 2015, closed pod e-cigarettes which vapourised protonated nicotine in the form of nicotine salts were invented under the brand name Juul. These devices resemble USB devices,

use disposable nicotine salt pods and operate on lower power than traditional e-cigarette devices. Nicotine salts produce a quicker nicotine “hit” when inhaled, due to increased speed of diffusion across the alveolar epithelium and reduce throat-bur associated with freebase nicotine (Duell et al., 2018, Davis et al., 2022). The evolution of e-cigarette devices can be seen in Figure 1.2.

The e-cigarette market is ever-growing in diversity from devices to e-liquids. However, this poses its own challenges in assessing effects of vaping on health as the combination of device, settings and e-liquid differ from user to user. In the UK in 2020, 75% of vapers used tank models, while only 15% used cartridge models, such as Juul devices (McNeill et al., 2021). However, among 11-18 year olds, cartridge devices were the most popular, with 21.8% of vapers using a Juul device (McNeill et al., 2021).

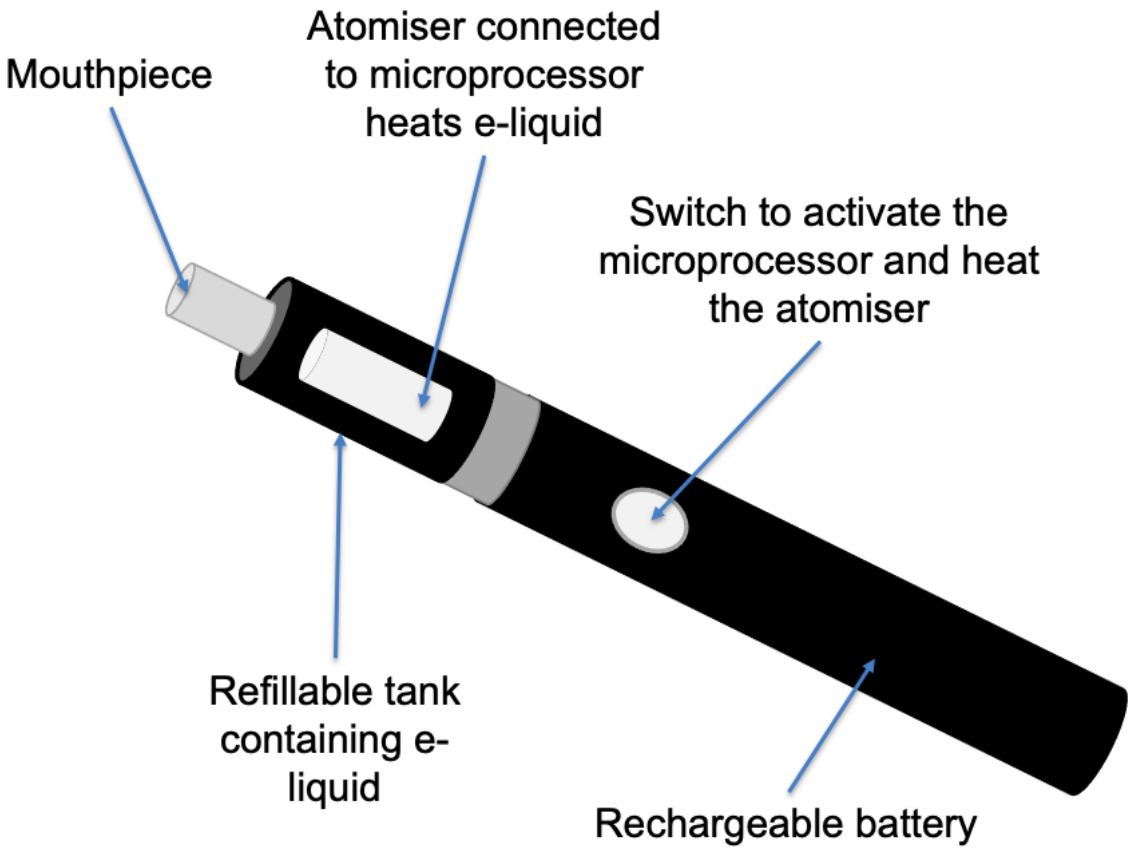


Figure 1.1*: A diagram of the structure of an e-cigarette device.*
Electronic cigarettes contain the main elements: mouthpiece, tank, atomiser, switch and battery. To activate the device, engagement of the switch and/or suction via the mouthpiece is required, depending on the device design. This activates the heating element made up of the atomiser and cotton or silica wick. The atomiser is a coil wire made of metal such as Nichrome, Kanthal, Nickel, Titanium or stainless steel; wrapped around a wick which is usually made of cotton or silica. Upon activation, the heating element warms up the wick saturated with e-liquid, generating a puff of vapourised e-liquid which is inhaled by the user. The elements of an e-cigarette device can come in multiple shapes, sizes and powers and can be largely customised by the user.

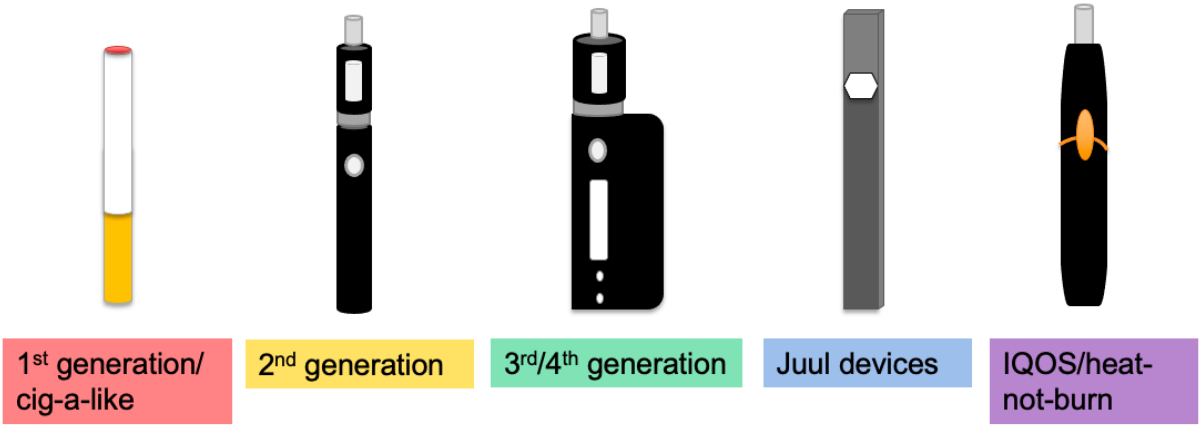


Figure 1.2: The evolution of e-cigarette devices.
1st generation, or cig-a-like devices were designed to closely mimic tobacco cigarettes. They were disposable, small and the end glowed, similar to cigarettes. 2nd generation devices had a tank system and remained small, pen-like devices but had refillable tanks and rechargeable batteries so were much more cost-effective for the users. These evolved to the 3rd generation devices which had larger tanks and battery outputs but users were limited in the number of settings they could customise. 4th generation devices looked very much like 3rd generation devices but users could modify additional settings such as airflow, battery output and temperature. Then, pod devices developed by the brand Juul were invented which were USB rechargeable, light weight and heat nicotine salts. Alongside this evolution was the development of IQOS, or "heat not burn" devices which warm a tobacco tab, without combustion.

1.2.1 E-liquids and vapour constituents

E-liquids usually contain nicotine, a variety of flavouring compounds with over 7,700 currently described (Zhu et al., 2014), and vehicles; propylene glycol (PG) and vegetable glycerine (VG). PG and VG provide the benefit that they vapourise easily, will carry nicotine and are both “generally recognised as safe” by the FDA as food additives. However, the heating process necessary to convert the e-liquid into an inhalable vapour results in thermal degradation and oxidation of e-liquid components, changing the chemical composition and behaviour of the e-liquid elements (Jaegers et al., 2021). In the presence of oxygen and heat, PG and VG decompose to form highly reactive carbonyl species (RCS) including the aldehydes: formaldehyde (group 1 human carcinogen), acetaldehyde (group 2B human possible carcinogen), acrolein (nasal cavity irritant and causes lung lining damage) and acetone (mucus membrane irritant and causes olfactory neuroepithelial damage) (Kosmider et al., 2014, Jensen et al., 2015, Ogunwale et al., 2017, Goniewicz et al., 2014). Studies have shown that increasing battery output (from 3.2 V to 4.8 V) can lead to increased acetaldehyde levels by 4 times, acetone levels by 10 times and formaldehyde levels by 200 times from PG/VG based e-liquids (Kosmider et al., 2014, Salamanca et al., 2018), with formaldehyde levels reaching the levels reported in tobacco smoke (Counts et al., 2005).

Many of the flavouring agents used in e-liquids are food additives generally considered safe for oral consumption, but the effect on human health of their inhalation after vapourisation remains uncertain. Popular flavours include tobacco, cinnamon and cherry, all of which have been suggested to be particularly toxic (Bahl et al., 2012,

Behar et al., 2014, Kosmider et al., 2016). For example, Diacetyl is a flavouring agent commonly added to sweet-flavoured e-liquids, and was detected in 118 of 159 e-liquid samples (Farsalinos et al., 2015). Diacetyl is approved for use in food but is associated with bronchiolitis obliterans, also known as “popcorn lung” when inhaled (Kreiss et al., 2002). Due to a lack of manufacturing regulation, e-liquid nicotine levels have been reported to not match those labelled, with one study finding 9 of 20 tested e-liquids containing actual nicotine concentrations differing by more than 20% of that labelled (Goniewicz et al., 2013). Further, impurities and contamination, such as endotoxin has been detected in some e-liquids (Lee et al., 2019). Flavouring agents such as vanillin (vanilla flavour), ethyl maltol (caramel flavour) and diketones (butter flavour) have been shown to induce ROS production and proinflammatory cytokine release from alveolar macrophage and bronchial epithelial cell lines (THP-1 and BEAS-2B) (Morris et al., 2021). In addition, neutrophil phagocytosis and oxidative burst are impaired by cinnamaldehyde (cinnamon flavour), benzaldehyde (almond/cherry flavour) and ethyl vanillin (vanilla flavour) (Hickman et al., 2019).

1.2.2 E-cigarette use and topography

In 2019, sale of ENDS products generated US$ 15 billion, supported by over 2.7 million e-cigarette users in the UK (WHO, 2021, McNeill, 2021) and an estimated 68 million e-cigarette users worldwide (Jerzyński et al., 2021). Use of e-cigarettes has been supported by the Royal College of Physicians (UK) and Public Health England have reported e-cigarettes as 95% less harmful than tobacco smoking, resulting in a huge increase in popularity. This estimation was based on scoring criteria assessing harm to individuals, the environment and the community including: morbidity, mortality,

crime, environmental damage, economic cost and dependence (Nutt et al., 2014). A range of nicotine products were scored including tobacco products, ENDS products, nicotine replacement therapy (NRT)s and snus, and ENDS were allocated a score of 5 compared to the cigarette's score of 100, hence the 95% safer statistic (Nutt et al., 2014). This assessment took place in 2014, and has not been reviewed since even with further evidence emerging on use, device development and potential harm.

Despite origins as a smoking cessation tool, only 29.7% of e-cigarette users have cigarette quitting intentions (McNeill et al., 2021). In 2021, approximately 30% of e-cigarette users in the UK continued to use tobacco cigarettes (Action on Smoking and Health (ASH), 2021). This represents the first group of e-cigarette users: dual users who both vape and smoke.

A landmark study investigating the efficacy of e-cigarettes as a quit smoking tool found only 18% of those using e-cigarettes had stopped smoking compared to 9.9% in the NRT arm (Hajek et al., 2019). Despite appearing to increase quitting rates by nearly double, 80% of those who switch from cigarettes to e-cigarettes continued to use the device 1 year after switching (Hajek et al., 2019). This represents the second group of e-cigarette users: ex-smokers who are now using e-cigarettes long-term. Therefore, it is important that e-cigarettes are not considered only as short-term therapy.

The gateway hypothesis states that uptake of one habit which is considered harmless (or less harmful) may lead to the subsequent taking up of another habit which is considered harmful (or more harmful). The gateway hypothesis is a theory which has

been tested extensively and there are still gaps which need addressing to prove or disprove the hypothesis (Miller and Hurd, 2017). However, production of sweet and fruity e-liquid flavours and exposure to advertising has increased the uptake of e-cigarette use by non-smoker adolescents who are consequently 3.5 times more likely to initiate cigarette smoking, supporting the gateway hypothesis (Soneji et al., 2017). This represents the third group of e-cigarette users: never-smokers who initiate vaping behaviours, the popularity of which is increasing (Miech et al., 2019, Dutra and Glantz, 2014).

Early puffing topography studies relied on a variety of methods including usage diaries, analysing YouTube videos of e-cigarette users, and asking users to demonstrate their vaping habits in a laboratory. The invention of clinical research support system (CReSS) devices allowed the revolution of e-cigarette topography studies whereby the user could take the device away and use it in their normal environment; but all the topography data would be recorded and stored by the device until it was returned to the research team, allowing accurate recordings of real-world use. It was found that actual mean puff number per day (225 ± 59 puffs/day) was almost double that of the self-reported values in previous studies (Robinson et al., 2015). Average puff duration, measured by a combination of analysis methods has been reported between 2.3 and 5 seconds (Evans and Hoffman, 2014, Norton et al., 2014, Hua et al., 2013, Behar et al., 2015, Lee et al., 2018). Puff duration has been found to be longer for e-cigarette devices than tobacco cigarettes (4.3 seconds (e-cigarette) vs 2.4 seconds (tobacco cigarettes) (Hua et al., 2013) and longer by established cigarette users (2.3-4.3 seconds) compared to non-established users (1.5-2.1 seconds) (Lee et al., 2018);

representing a compensatory behaviour for lower nicotine delivery by e-cigarette devices. This was reinforced by a recent study examining vaping behaviours by e-cigarette users given e-liquids containing 6 mg/mL and 18 mg/mL nicotine where puff duration was longer and average puff number higher when lower nicotine e-liquids were used (Kosmider et al., 2020). The compensatory behaviour was also shown to be associated with greater toxicant exposure (Kośmider et al., 2018). Topography parameters, such as puff duration and average number of puffs helps to inform *in vitro* studies to ensure they represent real life use.

1.2.3 EVALI

The emergence of e-cigarette or vaping associated lung injury (EVALI) in the US - acute severe respiratory distress with an absence of infection in otherwise healthy adults - has highlighted the potential dangers of e-cigarette use. Clinical presentation of EVALI includes dyspnoea, fever, and tachycardia with bilateral ground glass opacities on computed tomography (CT). Of 81 EVALI patients, 89% reported having used tetrahydrocannabinol (THC) and 9% used cannabidiol (CBD) e-liquids in the previous 90 days before symptom onset (Layden et al., 2019). Vitamin E acetate has been strongly linked with EVALI cases, particularly those where THC use has been reported (Blount et al., 2019). Vitamin E acetate is a supplement used to thicken some e-liquids and is considered safe for ingestion and skin application (Reboul, 2017). However, upon inhalation vitamin E acetate is delivered directly to the surfactant lining of the epithelium, interfering with the chemical properties and contributing to respiratory dysfunction in EVALI (Blount et al., 2019, Massey et al., 1982, Zuo et al., 2008). The discovery of the dangers of vitamin E acetate raises further concern about e-liquid

ingredients and the potential toxicity caused by vapourisation. Since August 2019, over 2800 cases of EVALI have been confirmed by the Centres for Disease Control and Prevention (CDC) with 68 confirmed deaths in the US and at least 2 in the UK (CDC, 2020, MHRA, 2020). EVALI patients have been shown to exhibit airway neutrophilia (on average 61% of all cells collected from bronchoalveolar lavage fluid (BALF) were neutrophils), and 63% of patients exhibited a predominance of neutrophils in BALF, a marker of lung inflammation (Blagev et al., 2019). The contribution of neutrophils to this fast-onset acute pneumonitis disease has not yet been fully established, however, their function and dysfunction could play a major role in patient outcomes as the largely predominant cell in the airways. The emergence of EVALI highlights the potentially devastating impact of e-cigarette use on respiratory health and advances the urgency at which we need to develop a full understanding of these effects.

It has been established that smoking related lung disease results in chronic airway inflammation, tissue destruction and small airways dysfunction before development of emphysema, which will be expanded on in section 1.4.9.2. In addition, COPD is a progressive chronic lung disease associated with small airways damage, neutrophilic inflammation, increased protease burden and considerable morbidity and mortality, but often takes decades to develop. Neutrophils are thought to be key drivers of this pathophysiology, and this will be discussed in section 1.4.9.1. Evidence to date suggests e-cigarettes may also induce a similar lung neutrophilia, therefore it is vital we ascertain the impact of e-cigarette vapour on these cells to determine if this is a signal of harm similar to that seen in smoking-related disease.

1.3 The role of inflammatory cells in the lung

Inhalation of pollutants, toxicants, and microbes requires a defence system equipped for protecting the respiratory system from frequent illness (Nicod, 2005). In health, the respiratory system is kept in a homeostatic state by a combination of defence mechanisms which quickly survey and clear particulates. Firstly, ciliated epithelial cells, goblet cells and submucosal glands make up the Mucociliary escalator which traps particulates in the sticky mucus and prevents them from entering the lower respiratory tract (Kuek and Lee, 2020). Secondly, alveolar macrophages residing in the airways and alveolar spaces of the lungs, survey inhaled particulates and clear foreign substances, initiating an immune response when necessary (Belchamber et al., 2020). When appropriate, alveolar macrophages release inflammatory cytokines which change the receptor expression on the vascular endothelial cell wall to rapidly recruit an army of neutrophils, T-lymphocytes and monocytes from the circulation. Neutrophils possess an arsenal of proteinases such as NE, proteinase 3 (PR3) and MMPs which are released from azurophilic granules during migration. Substrates for these proteinases include elastin (Janoff and Scherer, 1968), collagen (Kafienah et al., 1998) and fibronectin (Grinnell and Zhu, 1994) which are major components of the extracellular matrix, leading to its digestion. To limit tissue destruction, antiproteinases including alpha-1 anti-trypsin (AAT), secretory leucocyte proteinase inhibitor (SLPI) and α2-macroglobulin (α2M) inhibit the activity of proteinases. In health, there is an obligate area of tissue damage caused by neutrophil migration through tissues due to a time delay in the concentration balances between NE and its inhibitors, in a phenomenon known as “quantum proteolysis”.

Once the cause of insult or injury has been cleared, the inflammatory site must be resolved to prevent chronic inflammation. Alveolar macrophages are the main initiators of inflammatory resolution, by phagocytosing apoptotic neutrophils and leukocytes in a process called efferocytosis. Efferocytosis prevents the dying cells from releasing pro-inflammatory and toxic compounds and triggers the release of anti-inflammatory and reparative factors (Allard et al., 2018). Inflammatory resolution happens in two phases: first an anti-inflammatory phase with the release of anti-inflammatory cytokines such as IL-4 and IL-10 and downregulation of nuclear factor (NF)-κB, and then a pro-resolution phase characterised by release of specialised pro-resolving mediators by alveolar macrophages including lipoxins, resolvins, protectins and maresins (Bannenberg and Serhan, 2010) which promote tissue resolution and limit further leukocyte recruitment (Levy and Serhan, 2014).

Changes in this fine balance of neutrophil function have been implicated in a range of diseases including sepsis, bronchiectasis, asthma, alpha-1 antitrypsin deficiency, cystic fibrosis and pneumonia (Sapey et al., 2019, Patel et al., 2018, Crisford et al., 2021, Bedi et al., 2018, Houston et al., 2013). Airway inflammation precedes the development of chronic lung diseases. Airway neutrophilia is a common feature of many chronic inflammatory lung diseases and is associated with disease progression, generally regardless of the initiating cause (Jasper et al., 2019). Often neutrophil dysfunction drives disease pathophysiology and severity of symptoms is directly associated with extent of neutrophil disruption (Thompson et al., 1989, Sapey et al.,

2011). However, the role of neutrophils in causality vs correlation in disease is poorly understood.

1.4 Neutrophils

Neutrophils are innate immune cells from the myeloid lineage, constituting 70% of circulating leukocytes, and are rapidly recruited to sites of infection or injury (Dancey et al., 1976). Mature neutrophils are characterised by their distinctive segmented, lobular nucleus and a granular cytoplasm. Neutrophils have an arsenal of killing mechanisms which can be deployed in response to infection including phagocytosis, degranulation and neutrophil extracellular traps (NET)osis (Kolaczkowska and Kubes, 2013). Neutrophils play an important role in tissue homeostasis including inflammation initiation and resolution.

1.4.1 Neutrophil metabolism

Cells rely on adenosine triphosphate (ATP) generated from 1) oxidative phosphorylation which takes place in the mitochondrial membrane, or 2) glycolysis which takes place in the cell cytoplasm to perform their functions including proliferation, transcription/translation and movement (Fernandez-de-Cossio-Diaz and Vazquez, 2018). The majority of ATP in a cell is produced via mitochondrial oxidative phosphorylation (Alberts, 2002). The role of mitochondria in neutrophils has been debated since the 1950s and extensively reviewed (Kumar and Dikshit, 2019, Injarabian et al., 2019) however remains a topic of question. It is thought that neutrophil chemotaxis, apoptosis and differentiation rely on mitochondria as energy producers and Ca^{2+} regulators (Maianski et al., 2004, Bao et al., 2015).

Neutrophils largely rely upon glycolysis as their source of ATP, with glycolytic inhibitors abolishing ATP levels and consequent effector functions (Sbarra and Karnovsky, 1959, Borregaard and Herlin, 1982). Neutrophil functions including NET formation and phagocytosis are dependent on glycolysis (Fossati et al., 2003, Rodriguez-Espinosa et al., 2015). As highly glycolytic cells, neutrophils are significant sources of lactate (produced by conversion from pyruvate in the production of ATP via aerobic and anaerobic glycolysis) (Grudzinska et al., 2020). Neutrophils can adapt their ATP production in a largely oxygen-independent manner, which is beneficial in inflammatory states where oxygen supply is limited (Fossati et al., 2003, Silver, 1977, Edwards et al., 1984).

1.4.2 Neutrophil production and release into circulation

Neutrophils develop in the bone marrow from haematopoietic stem cells (HSCs) which differentiate into committed myeloid progenitor cells, upon induction by transcription factors such as PU.1 (Nerlov and Graf, 1998, Iwasaki et al., 2005). Other growth factors, including CCAAT-enhancer-binding proteins (C/EBPα) and Growth factor independent transcription repressor (Gfi-1) direct further differentiation from progenitor cells to terminally differentiated neutrophils (Hock et al., 2003, Karsunky et al., 2002). Once fully differentiated, neutrophils are characterised by a multi-lobed nucleus and granular cytoplasm, due to the presence of Azurophillic (primary), Specific (secondary) and Gelatinase (tertiary) granules, as well as secretory vesicles (Kolaczkowska and Kubes, 2013). Neutrophils are produced continuously, with basal production approximately 1-2 x 10^{11} neutrophils/day in a normal adult; though this can increase to

10^{12} neutrophils/day during infection (Mayadas et al., 2014, Summers et al., 2010, Butcher et al., 2000).

Neutrophil homing is a tightly controlled process to ensure there are enough neutrophils in circulation, but also a bone marrow residing population which can quickly be mobilised when infection is detected. Neutrophils express CXC-chemokine receptor (CXCR)2 on their membrane, which is induced by CXC-chemokine ligand (CXCL)1 and CXCL2 on bone marrow stromal cells and causes release of neutrophils into the blood stream (Eash et al., 2010, Christopher et al., 2009). Antagonistically, neutrophil CXCR4 is engaged by bone marrow stromal cell CXCL12 which causes retention in the bone marrow niche (Eash et al., 2010, Hernandez et al., 2003). Developing neutrophils express CXCR4, retaining them in the bone marrow. With maturity, CXCR4 expression reduces, and engagement of CXCR2 with its ligands causes release into the circulation (Suratt et al., 2004). As the neutrophil ages, expression of CXCR4 increases once more, homing it back to the bone marrow (Martin et al., 2003). Mutations in CXCR4 are the leading cause of warts, hypogammaglobulinemia, infections, myelokathexis (WHIM) syndrome, with which patients exhibit a neutropenia despite normal to increased neutrophil numbers in the bone marrow (Gorlin et al., 2000).

Macrophages and dendritic cells produce interleukin (IL)-23 which stimulates T helper cells to produce IL-17 (Ley et al., 2006). IL-17 is a pro-inflammatory cytokine which induces further release of Granulocyte colony stimulating factor (G-CSF) which promotes mobilisation of neutrophils into circulation (Schwarzenberger et al., 2000).

G-CSF upregulates expression of CXCL1 and CXCL12 on the bone marrow endothelial cells, tilting the CXCR4/CXCR2 balance in favour of CXCR2 which encourages neutrophil release from the bone marrow (Eash et al., 2010). Conversely, when neutrophils die by apoptosis, they are phagocytosed by macrophages and dendritic cells which lowers the levels of IL-23, consequently suppressing IL-17 production and G-CSF signalling, reducing the number of neutrophils released into circulation. Neutrophils released from the bone marrow into circulation are dormant cells, resting with a round morphology and must undergo a series of activation steps before they are able to employ their full armoury of killing mechanisms (Borregaard, 2010).

1.4.3 Neutrophil activation

Neutrophils exist in 3 main states: quiescent, primed or activated, and can transition between the three states in response to controlled signals (Sapey and Stockley, 2014). In circulation, neutrophils exist in a quiescent state, with low transcriptional activity, non-adherence, and low response to activator signals to protect against unwarranted inflammatory responses and tissue damage (Miralda et al., 2017, Sheppard et al., 2005). Neutrophils adopt a primed state upon interaction with pro-inflammatory cytokines, bacterial products such as lipopolysaccharide (LPS) or activated endothelial cells, amongst others (El-Benna et al., 2008, Miralda et al., 2017). Priming results in a “ready to go” state, enhancing superoxide production by a secondary stimulus, making responses faster (El-Benna et al., 2008, McPhail et al., 1984). Previous work has highlighted the ease in which primed neutrophils degranulate, and subsequently easily get caught in the lung (Summers et al., 2014, Condliffe et al., 1998). Upon secondary

stimulation after priming, neutrophils are able to respond quickly and aggressively through degranulation, respiratory burst and increased lifespan (Vogt et al., 2018).

Vascular endothelial cells have the capability to prime neutrophils by changing the array of receptors expressed on the luminal surface to signpost a site of infection or inflammation. Bacterial-derived LPS and *N*-formylmethionyl-leucyl-phenylalanine (fMLP), or host derived tumour necrosis factor alpha (TNFα), IL-1β and IL17 accumulate in inflamed tissues (Amulic et al., 2012). Responding to these signals, the vascular endothelium upregulates adhesion molecules P- and E-selectin, intracellular adhesion molecule (ICAM) and other integrins on the apical surface (Borregaard, 2010, Phillipson and Kubes, 2011). Neutrophils express receptors for these adhesion molecules including P-selectin glycoprotein ligand (PSGL-1) and L-selectin, and the neutrophil-endothelial interaction induces tethering of the neutrophils to the vessel wall, associated with activation of intracellular kinases including p38 mitogen-activated protein kinase (MAPK) (Kansas, 1996, Yago et al., 2010, Ley et al., 2007). Secretory vesicles fuse with the surface membrane, upregulating Macrophage-1 antigen (Mac1) (integrin $\alpha_M\beta_2$), complement receptor (CR)1 and pattern recognition receptors (PRRs) (including Toll-like receptor (TLR)4 (LPS) and fMLP receptor (fMLPR)) on the neutrophil surface (Faurschou and Borregaard, 2003, Sengelov et al., 1995, Borregaard et al., 1993). Due to shear stress associated with laminar blood flow, selectin-mediated bonds detach and reattach sequentially, inducing neutrophil “rolling” along the luminal surface of the endothelium (Yago et al., 2010, Pospieszalska and Ley, 2009). β2-integrins including Mac-1 facilitate intraluminal crawling of neutrophils and lymphocyte function-associated antigen 1 (LFA1) binding to adhesion molecules

on the endothelial cell surface induces firm adhesion, which is characterised by the cessation of rolling (Phillipson et al., 2006, Ley et al., 2007, Mocsai et al., 2015).

1.4.4 Neutrophil migration and chemotaxis

Upon the initiation of firm adhesion caused by LFA-1 engagement, Ras homology (Rho)G and Rho A signalling molecules become activated and intracellular Ca^{2+} levels increase by Ca^{2+} store release and extracellular Ca^{2+} influx (Ley et al., 2007). As a result, small guanosine-5'-triphosphate (GTP)ases become activated which induces actin polymerisation to form a leading edge lamellipodium, with concentrated chemokine receptors on the surface (Phillipson et al., 2006). The neutrophil begins to spread along the intraluminal surface of the endothelium and the lamellipodium extends (Goldfinger et al., 2003). At the trailing edge, myosin contraction controlled by cell division control protein (CDC)42, RhoA, Rho-association protein kinase (ROCK) results in the propulsion of neutrophils along the endothelial surface, in a crawling motion, until a preferred site of transmigration is reached (Van Keymeulen et al., 2006). At the transmigration site, there is loosening of cell-cell adhesion junctions between endothelial cells which is exploited by neutrophils who, with assistance from ICAM-2 and junctional adhesion molecule- A (JAM-A), can pass between endothelial cells via the paracellular route of migration (Woodfin et al., 2009). Alternatively, and less regularly, neutrophils can pass the endothelial layer transcellularly (Ley et al., 2007).

After crossing the endothelial cell layer, neutrophils must migrate through the endothelial basement membrane, composed of a protein network of collagen IV and laminins (Hallmann et al., 2005). Engagement of the platelet endothelial cell adhesion

molecule -1 (PECAM-1) leads to upregulation of integrin α6β1 on the surface of the neutrophil to aid migration through the basement membrane (Woodfin et al., 2009). In addition, gelatinase and azurophilic granules can be mobilised and fuse with the neutrophil surface membrane, allowing digestion of the basement membrane matrix by serine proteases such as neutrophil elastase (NE) and metalloproteases such as matrix metalloprotease 9 (MMP-9) to aid transmigration (Borregaard, 2010).

Now in the tissue, neutrophils continue to follow a chemotactic gradient of bacterial derived (e.g. LPS, fMLP) or host derived (e.g. CXCL8, TNF-α, IL-1β and IL-17) signalling molecules which have accumulated in affected tissues (Wang, 2009). At the leading edge, actin polymerisation, and at the trailing edge, myosin contraction, synergistically propel the neutrophil towards the source of chemoattractant at the site of infection or inflammation (Wang, 2009, Ley et al., 2007).

1.4.5 Phagocytosis

Phagocytosis is the receptor-mediated ingestion of pathogens into a vesicle, termed the phagosome. Phagocytosis is initiated by the engagement of PRRs such as TLRs or opsonic receptors such as Fc receptors (FcRs) and CRs (Kobayashi et al., 2018). PRRs recognise pathogen associated molecular patterns (PAMPs) such as LPS and peptidoglycan while opsonic receptors recognise host-derived molecules which have bound targets, such as immunoglobulin (Ig)G or IgA antibodies and complement components (Uribe-Querol and Rosales, 2020).

Neutrophils which have migrated into tissues are more phagocytically active than peripheral blood neutrophils (Sørensen et al., 2001). Upon engagement of PRRs with their ligands, actin polymerisation in the target area of the neutrophil results in formation of pseudopods around the particle, until it is fully engulfed into the neutrophil phagosome (Uribe-Querol and Rosales, 2020). Phagocytosis triggers the mobilisation of pre-formed neutrophil specific and azurophilic granules which fuse with the phagosome, releasing antimicrobial factors such as Myeloperoxidase (MPO) and lactoferrin into the phagosomal lumen, now termed the phagolysosome (Kobayashi et al., 2018, Hager et al., 2010). In addition, Nicotinamide adenine dinucleotide phosphate (NADPH) oxidase assembles itself on the phagolysosomal membrane which is responsible for the generation of ROS including superoxide (O_2^-) (Babior, 2004). Superoxide dismutates to hydrogen peroxide (H_2O_2) which can react with Cl^- ions to form hypochlorous acid which is highly microbicidal (Uribe-Querol and Rosales, 2020, Babior, 2004). This results in a drop in pH (to pH ~ 6.0) inside the phagolysosome and ultimately leads to the breakdown of the phagocytosed microbe. Evidence suggests a rapid (2-3 minutes) initial alkalisation of the phagolysosome, as a result of H^+ consumption as superoxide dismutates (Segal et al., 1981, Levine et al., 2015). This would support evidence of optimal Cathepsin G and NE activity at pH 7-9 and pH 8-10 respectively, aiding microbial breakdown (Levine et al., 2015). It is thought that the initial respiratory burst later (10-15 minutes) subsides, meaning vacuolar ATPase (V-type H^+ ATPase) activity predominates, pumping H^+ into the phagolysosome and causing a drop in pH to around 6.0 (Segal et al., 1981, Jankowski et al., 2002). This then corresponds to the optimal pH of MPO, which is 6.0. However,

evidence has challenged this biphasic change in pH within the phagosome (Jankowski et al., 2002).

1.4.6 Neutrophil granules

Neutrophil cytoplasm contains azurophilic (primary), specific (secondary) and gelatinase (tertiary) granules, as well as secretory vesicles. Some of the contents of azurophilic granules include lysozyme, NE and MPO, specific granules include collagenase, lysozyme and lactoferrin, gelatinase granules contain gelatinase and lysozyme and secretory vesicles contain CR1 and FCγRIII, which is expanded on in Figure 1.3. When activated, neutrophils mobilise specific and azurophilic granules in a process known as degranulation (Hager et al., 2010). These granules can fuse with either the phagosomal membrane, releasing antimicrobial factors into the phagosome, or fuse with the neutrophil surface membrane, releasing proteins into the extracellular space. Neutrophil granules require different levels of activation to be mobilised: secretory vesicles are released during minimal stimulation to facilitate migration and adhesion and azurophilic granules require the most stimulation as they contain the most cytotoxic contents (Jasper et al., 2019). Degranulation must be tightly regulated by receptor-mediated signalling, as excessive release of granule contents into the extracellular matrix has the potential to induce serious tissue damage and extreme inflammation, such as that seen in severe asphyxial episodes of asthma and septic shock (Lacy, 2006).

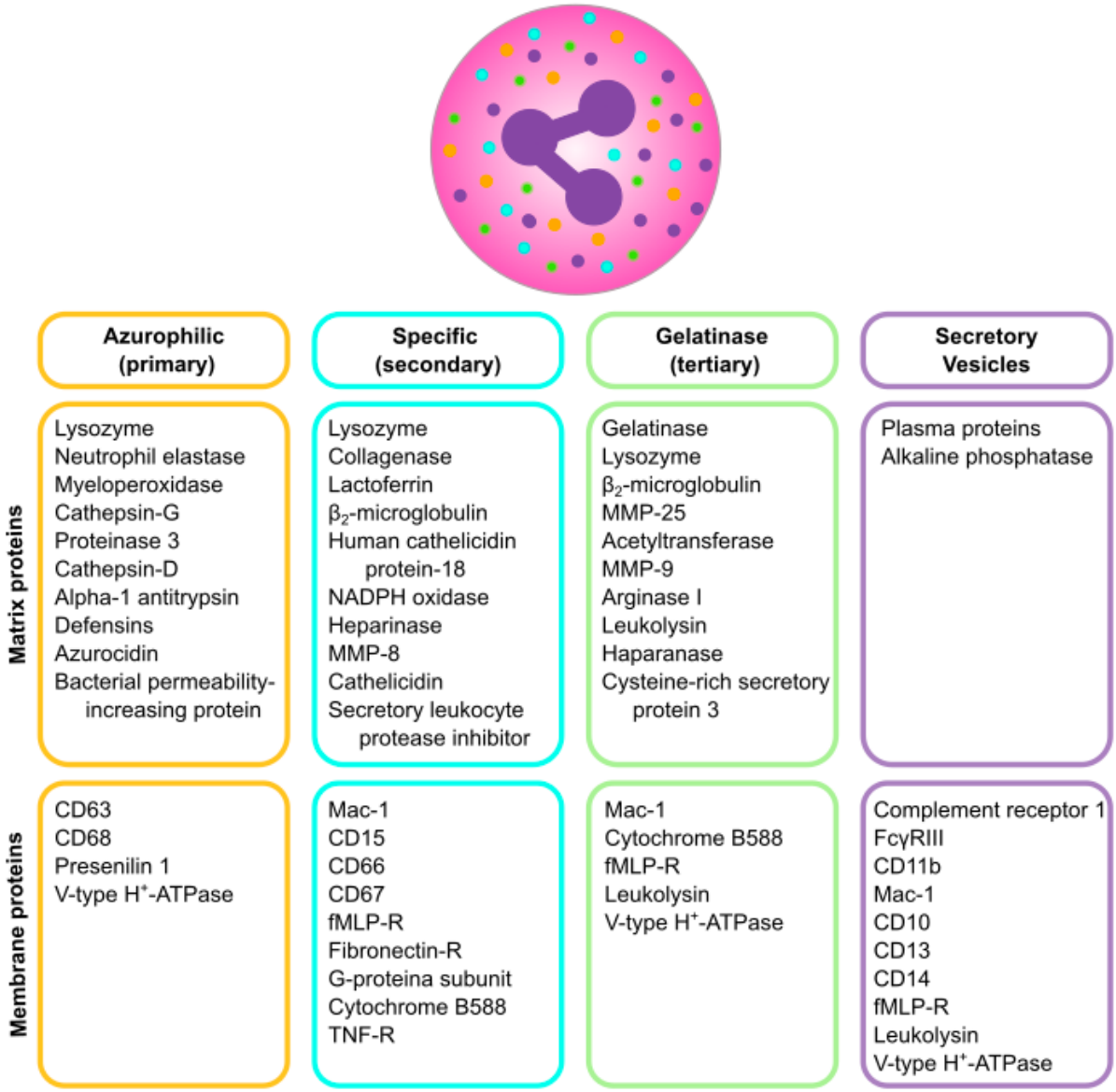


Figure 1.3*:* Neutrophil granule subsets and their matrix and membrane proteins. Neutrophil cytoplasmic granule subsets: azurophilic, specific, gelatinase and secretory vesicles contain proteins encased inside a vesicle lumen as well as surface membrane proteins, as indicated. Upon stimulation, neutrophils can mobilise these granules to fuse with either the phagosomal membrane or the neutrophil surface membrane, releasing the granule contents into the phagosome or extracellular space. Different forms of stimulation enable different granules to be mobilised to assist neutrophils in their required functions. Figure adapted from (Jasper et al., 2019, Völs et al., 2017)

1.4.7 Neutrophil extracellular traps (NETs)

In the event of an overwhelming infection, neutrophils have been described to extrude their cellular deoxyribonucleic acid (DNA) in the form of a web-like structure. This structure consists of a DNA and histone protein backbone decorated with cytotoxic and antimicrobial proteins and enzymes, including NE, lactoferrin and gelatinase, in structures called NETs (see Figure 1.4) (Brinkmann et al., 2004). The generation of NETs, in a process known as NETosis, represents an alternative cell death pathway independent of apoptosis and necrosis. NETs immobilise bacteria and prevent the further spread of infection (Brinkmann et al., 2004). NET stimuli include fungi, large pathogens, immune complexes, ionomycin and nicotine (Branzk et al., 2014, Papayannopoulos, 2018). Most commonly, ROS generated by NADPH oxidase or mitochondria stimulates NE to translocate from azurophilic granules to the nucleus where it causes chromatin decondensation (Papayannopoulos et al., 2010). However, it should be noted that the disruption of any of these contributors does not prevent NET generation, but only delays it (Metzler et al., 2011, Papayannopoulos, 2018). Following decondensation of chromatin, ROS promote the breakdown of the nuclear membrane which releases chromatin into the cytoplasm before it begins to leave the neutrophil via membrane pores, ending with cellular lysis (Delgado-Rizo et al., 2017). NETs protect the host against infection but also extruding DNA leaves the host vulnerable to auto-antibodies. Excessive NET generation has been linked to tissue damage and autoimmune diseases including systemic lupus erythematosus and rheumatoid arthritis (Papayannopoulos, 2018).

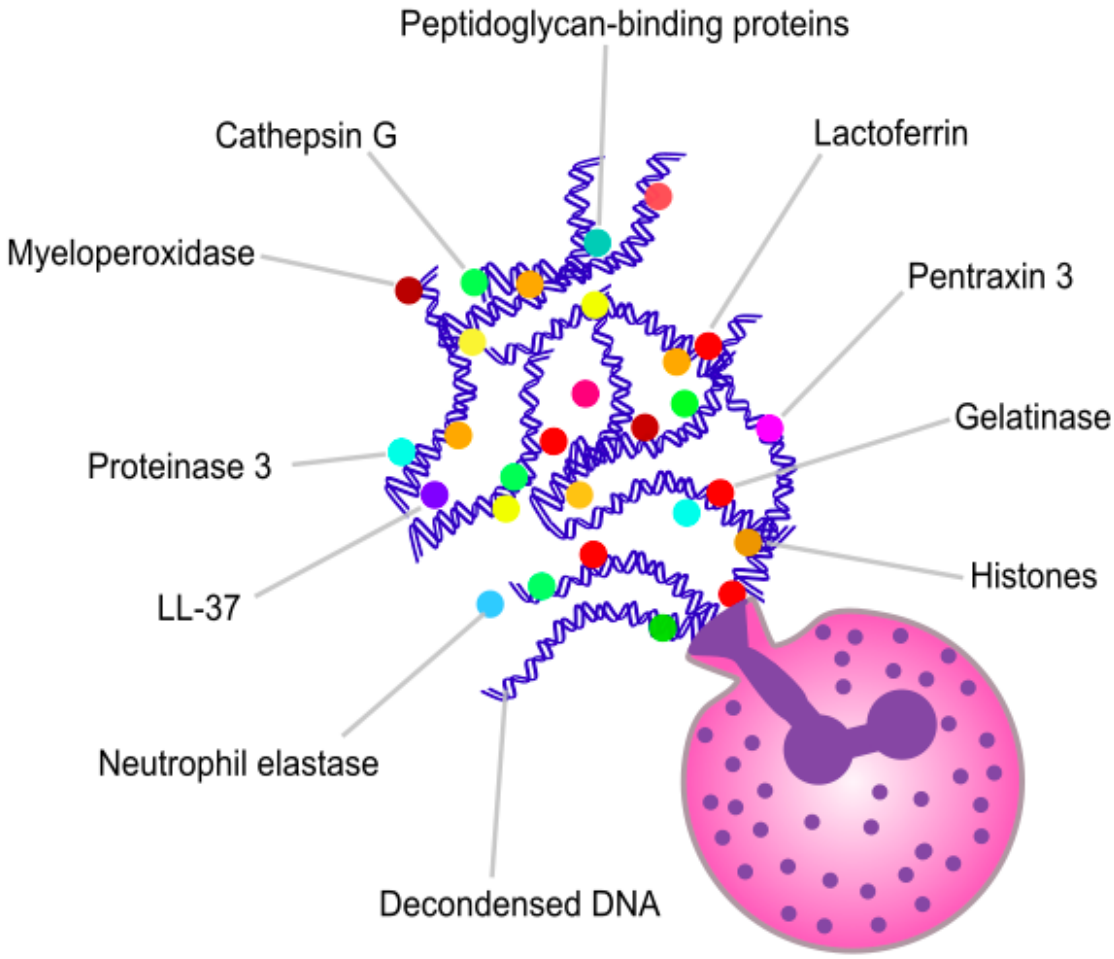


Figure 1.4: Neutrophil extracellular traps and their components.
In the event of an overwhelming infection, neutrophils can extrude their DNA in the form of a neutrophil extracellular trap (NET) in a suicidal process known as NETosis. NETs consist of decondensed DNA decorated with histone proteins, and a range of antimicrobial peptides (Delgado-Rizo et al., 2017), such as those labelled. NETs trap and immobilise and kill bacteria, preventing further spread of infection. Neutrophils which have undergone NETosis are consequently cleared by macrophages and dendritic cells via efferocytosis.

1.4.8 Recruitment of other inflammatory cells

Neutrophils are capable of actively recruiting other inflammatory cells to sites of infection and inflammation and are known to be involved in the cross-talk between the innate and adaptive immune systems. Neutrophils have been shown to upregulate transcription of several genes relating to the recruitment of macrophages, T cells, and further neutrophils as well as those involved in modulating immune responses (including CXCL8, Monocyte chemoattractant protein (MCP)-1, CXCL2, Macrophage inflammatory protein (MIP)-1α, CXCL2, IL-1β and TNF-α) (Theilgaard-Mönch et al., 2004, Scapini et al., 2000, Scapini et al., 2005). This challenges the longstanding paradigm that neutrophils are transcriptionally inactive cells incapable of *de novo* synthesis of proteins after terminal differentiation.

1.4.9 Neutrophil clearance

Neutrophils are short-lived cells which will die by apoptosis approximately 8-20 hours after leaving the bone marrow, but this may be extended up to several days when neutrophils enter tissues (Edwards, 1994). Neutrophil lifespan can be extended by adhesion, transmigration, hypoxia and cytokines to ensure they fulfil their requirements, or shortened by phagocytosis or NETosis where necessary (Lee et al., 1993). In the blood stream, at the end of their lifespan, neutrophils will undergo apoptosis and are cleared by the spleen, liver and bone marrow (Sadik et al., 2011). If they have been recruited into a tissue due to injury or infection, neutrophils will perform their roles and undergo apoptosis or NETosis and be cleared by tissue-resident macrophages and dendritic cells (Borregaard, 2010). The clearance of dead and dying

neutrophils by tissue-resident immune cells is an essential step in the resolution of inflammation and the return to tissue homeostasis.

1.4.9.1 Neutrophils in COPD

In COPD, airway neutrophil numbers are directly correlated with severity of airflow obstruction, decline in forced expiratory volume in 1 second (FEV_1), reduction in gas transfer, and development of emphysema (Thompson et al., 1989, Pilette et al., 2007, Donaldson et al., 2005, Parr et al., 2006, Sapey et al., 2011). Despite airway neutrophilia, COPD patients also experience airway colonisation and recurrent infections (Fagon et al., 1990, Donaldson and Wedzicha, 2006). This raises the possibility that the function of neutrophils is impaired, leading to reduced anti-microbial function and at the same time contributing to lung damage.

Evidence around NETs in COPD has been largely conflicting. Increased levels of NET components have been detected in sputum from COPD patients compared to controls, and the amount of NETs correlated with decline in FEV_1 (Grabcanovic-Musija et al., 2015). However, *in vitro*, neutrophils from COPD patients exhibit a diminished ability to undergo NETosis compared to controls (Pullan et al., 2015). Despite the direction of change remaining to be elucidated, alterations in NET generation represent issues for tissue homeostasis, and can have implications for auto-immunity, antimicrobial defences and inflammatory status. Reduced phagocytosis of non-typeable *Haemophilus influenzae* (NTHI), *Streptococcus pneumoniae* (*S. pneumoniae*), fungi and apoptotic neutrophils by macrophages in COPD has been well documented (Wrench et al., 2018, Taylor et al., 2010, Belchamber et al., 2019). However, there has

not been a strong focus on the phagocytic ability of neutrophils in COPD to date. Published data exhibits conflicting results with some demonstrating no difference (Müns et al., 1995, Tortorella et al., 1992) while some suggest a reduction in neutrophil phagocytosis in COPD compared to controls (Fietta et al., 1988). The phagocytic ability during stable and acute exacerbations of COPD is an area which needs further investigation. Previous work has found peripheral blood neutrophils from COPD patients migrate with increased speed but reduced directional accuracy compared to age-matched healthy controls, resulting in greater obligate tissue damage (Sapey et al., 2011). The proteinase-antiproteinase imbalance theory states that the mismatch between the amount of enzymes breaking down lung tissue parenchyma (proteinases e.g. MMPs, NE, PR3) and the enzymes opposing this proteolytic activity (antiproteinases e.g. TIMPs, AAT, SLPI) drives the pathophysiology of COPD and emphysema. The extent of the imbalance of proteinases and antiproteinases dictates the degree of tissue destruction. This theory is supported by findings of increased NE and PR3 activity footprints in plasma from patients with COPD and increased fibronectin degradation by COPD neutrophils (Carter et al., 2011, Crisford et al., 2018, Burnett et al., 1987).

1.4.9.2 Neutrophils in cigarette smoking

Smoking related lung disease exhibits hallmark features of chronic airway inflammation (predominantly neutrophilic), increased proteinase burden and small airways dysfunction.

Cigarette smoke induces airway inflammation driven by oxidative stress, resulting in the recruitment of inflammatory cells, including neutrophils, to the airways, as shown in Figure 1.5 (Lugg et al., 2022). Neutrophils, capable of extensive tissue damage and perpetuation of inflammation, have been linked to cigarette-associated lung ill-health and extensively researched. There is evidence of a direct detriment of cigarette smoke on neutrophil functions and indirectly via aberrant immune activation and regulation. It is yet to be fully understood whether neutrophils represent a key link between cigarette smoking and COPD, but they have been described to drive persistent inflammation and tissue damage and there are many parallels in the aberrant function of neutrophils in both contexts.

Neutrophils are recruited to the airways due to increased secretion of chemokines from bronchial epithelial cells and alveolar macrophages caused by cigarette smoking (Mio et al., 1997). Cell recovery from BALF samples of smokers showed an increase in neutrophil numbers by more than double, from 1.63 to 3.96 $x10^6$/L (Karimi et al., 2012) which is supported by murine models (Vlahos et al., 2006). Excessive recruitment of neutrophils to the airways leads to increased obligate tissue damage, increasing inflammation in the lung tissue and the risk of developing emphysema, a feature of COPD.

Cigarette smoke extract has been shown to delay apoptosis in neutrophils *in vitro* via suppression of protein kinase B (Akt) deactivation and can lead to neutrophil persistence and delayed resolution of inflammation (Xu et al., 2013, Guzik et al., 2011). In addition, pro-inflammatory cytokines released from activated alveolar macrophages

and epithelial cells promote neutrophil survival (Lee et al., 2012). This effect is exacerbated by cigarette smoke-induced downregulation of CD36, a scavenger receptor for the efferocytosis of apoptotic neutrophils expressed on the surface of alveolar macrophages, reducing clearance of apoptotic neutrophils (Dewhurst et al., 2017). Persistent inflammation and delayed resolution leads to increased tissue damage and remodelling and results in aberrant immune responses, which can promote auto-attack and increase the risk of developing chronic lung disease.

Mimicking that of COPD, analysis of NET generation in response to cigarette smoke has conflicting results, driven by differing methodologies. In one study, *ex vivo* treatment of neutrophils with cigarette smoke extract impaired phorbol 12-myristate 13-acetate (PMA)-stimulated NET release (White et al., 2018). Conversely, treatment of human neutrophils with nicotine induced NET formation in a dose-dependent manner (Hosseinzadeh et al., 2016). In the nicotine study, NETs were induced at all nicotine concentrations as low as 10µM, while cigarette smoke extract measured to contain 25 µM nicotine significantly suppressed NETosis, highlighting the importance of studying the role of smoke/vapour constituents other than nicotine in effect on neutrophils. Neutrophils isolated from the blood of smokers exhibited increased spontaneous NET generation and increased sensitivity to the NET stimulator PMA (Lee et al., 2017). This highlights the potential for systemic effects of smoking on neutrophil functions. NETosis requires further understanding in the context of smoking. NET generation is a finely balanced process which requires stringent regulation, only occurring as a last resort to contain an overwhelming infection. Increased sensitivity to undergo NETosis leaves the host vulnerable to persistent infection and auto-

antibodies, while resistance to NETs can promote microbial infections to grow and spread to an uncontrollable level.

Nicotine is a chemoattractant for neutrophils (Totti et al., 1984) which, combined with pro-inflammatory cytokines heightens neutrophil recruitment into the airspaces. Accurate and directed chemotaxis responses are required for rapid recruitment and minimal obligate tissue damage. However, speed, velocity, and directionality of neutrophil chemotaxis to CXCL8 and fMLP is impaired by cigarette smoke extract, the same combination of defects which was reported in COPD neutrophils (Sapey et al., 2011, White et al., 2018). It is thought that ROS are required for the destruction of pseudopods produced in the opposing direction to the chemoattractant source. ROS has previously been shown to be reduced by cigarette smoke extract treatment (Matthews et al., 2011), which may contribute to dysregulated chemotaxis. Aberrant neutrophil chemotaxis coupled with amplified recruitment to the lungs results in increased tissue destruction.

Phagocytosis of *E. coli* has been shown to be reduced by 33.4% compared to untreated controls (UTC) by treatment with cigarette smoke extract (Stringer et al., 2007) as well as a reduced ability to generate an oxidative burst response when stimulated with *F. nucleatum,* opsonised *S. aureus,* and *E. coli*-derived LPS (Matthews et al., 2011, Matthews et al., 2012). This reduction in antimicrobial activity by cigarette smoke-treated neutrophils exaggerates the already suppressed innate antimicrobial responses, leading to increased recurrent infections, exaggerating the chronic lung inflammation observed in smokers.

Neutrophils are known drivers of harm and have been implicated in smoking-related disease development. Neutrophil dysfunction after cigarette smoke exposure has been recapitulated *in vitro*, providing rationale for examining neutrophil functions after e-cigarette vapour exposure; examining early indicators of change and helping to predict the long-term consequences of potential changes.

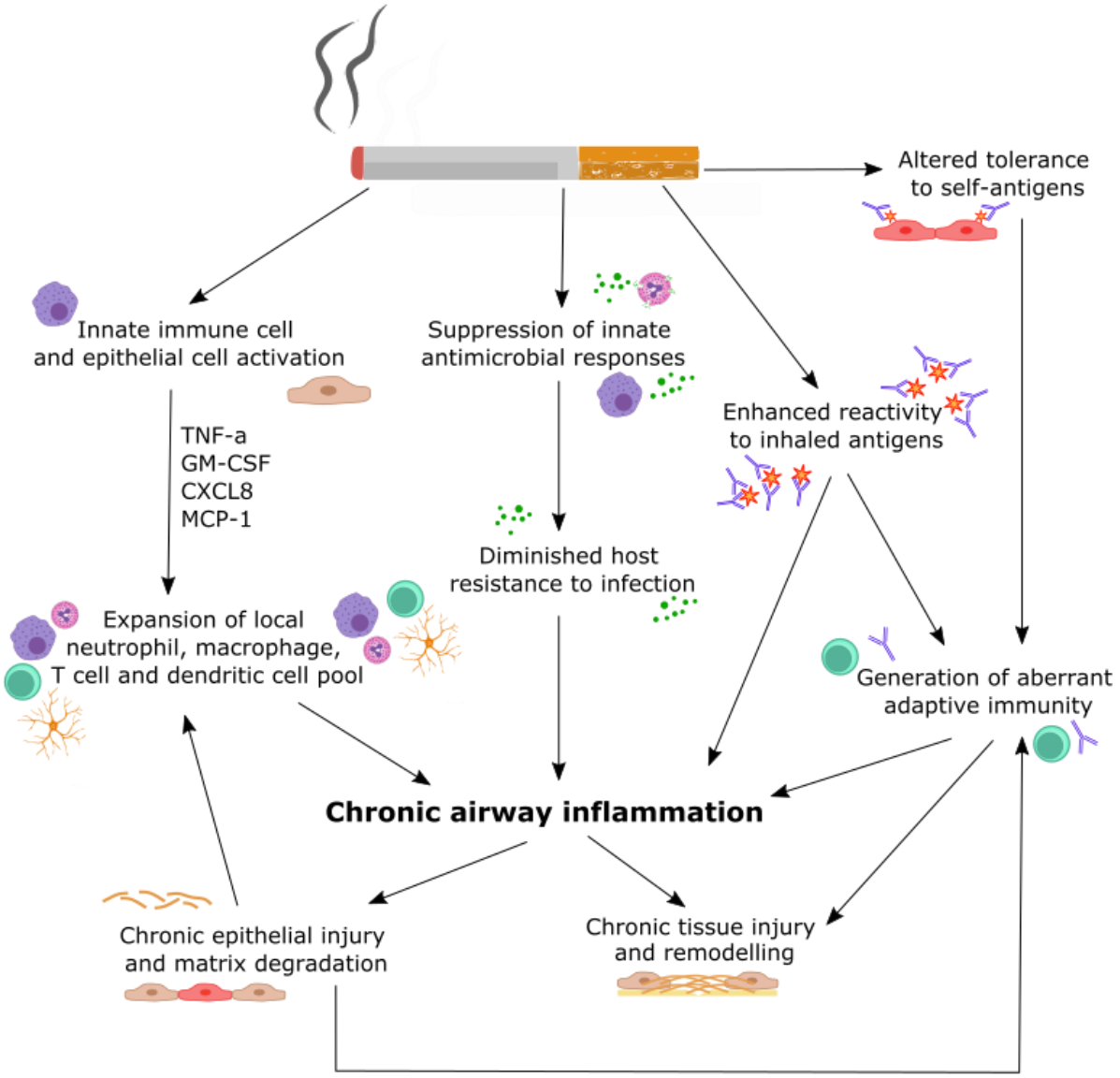


Figure 1.5: Modulation of chronic airway inflammation driven by cigarette smoke exposure.
Activation of innate immune cells and epithelial cells leads to recruitment of other immune cells including T lymphocytes, neutrophils, monocytes, and dendritic cells to the airspaces. Cells produce pro-inflammatory factors due to cigarette smoke exposure, promoting activation, recruitment, and survival of inflammatory cells, causing persistent inflammation. By simultaneously promoting an aberrant adaptive immune response, this leads to chronic airway inflammation. Lung tissue becomes injured and undergoes extensive remodelling. Repeated exposure perpetuates this cycle of injury and inflammation. Adapted from (Lee et al., 2012).

1.5 Limitations in current e-cigarette model systems

To determine the potential long-term impact of e-cigarettes, models to mimic e-cigarette exposure conditions have been developed by researchers; yet lack of standardisation in experimental methods has resulted in differing experimental methods. E-cigarette vapour extract systems rely on vapour constituents quickly dissolving into media with high degrees of dilution and loss of some insoluble elements. E-cigarette vapour extract allows direct comparison with studies using cigarette smoke extract, the standard model for cigarette studies.

E-cigarette vapour condensate is generated by vapourising e-liquids then condensing the vapour, followed by diluting with media and treating the cells. This represents the physiological behaviour of e-cigarette vapour - vapourising in the device and condensing in the airway - more accurately than e-cigarette vapour extract treatment. However, the extent to which the vapour phase is captured in these models remains in question. Both e-cigarette vapour extract and e-cigarette vapour condensate exposure models account for chemical changes induced by vapourisation, preferable compared to unvapourised e-liquid treatment.

The models mentioned thus far (detailed in Figure 1.6) do not utilise whole vapour exposure, however in the air-liquid interface model cells are cultured on membranes and e-cigarette vapour is drawn over the apical surface of the cells. Various measurements have been used to quantify and compare the level of exposure including particulate deposition by optical density and nicotine quantification by mass spectrometry. In addition to variations in exposure model is the further complication of

variations in devices, device settings, duration of exposure and e-liquid compositions. Recently, automated vaping machines have revolutionised *in vitro* studies, capable of producing a puff of e-cigarette vapour automatically with controlled time intervals, air flow intensity and cell exposures. These provide the benefit of improving consistency of exposures, but are expensive investments where in-house alternatives can be developed.

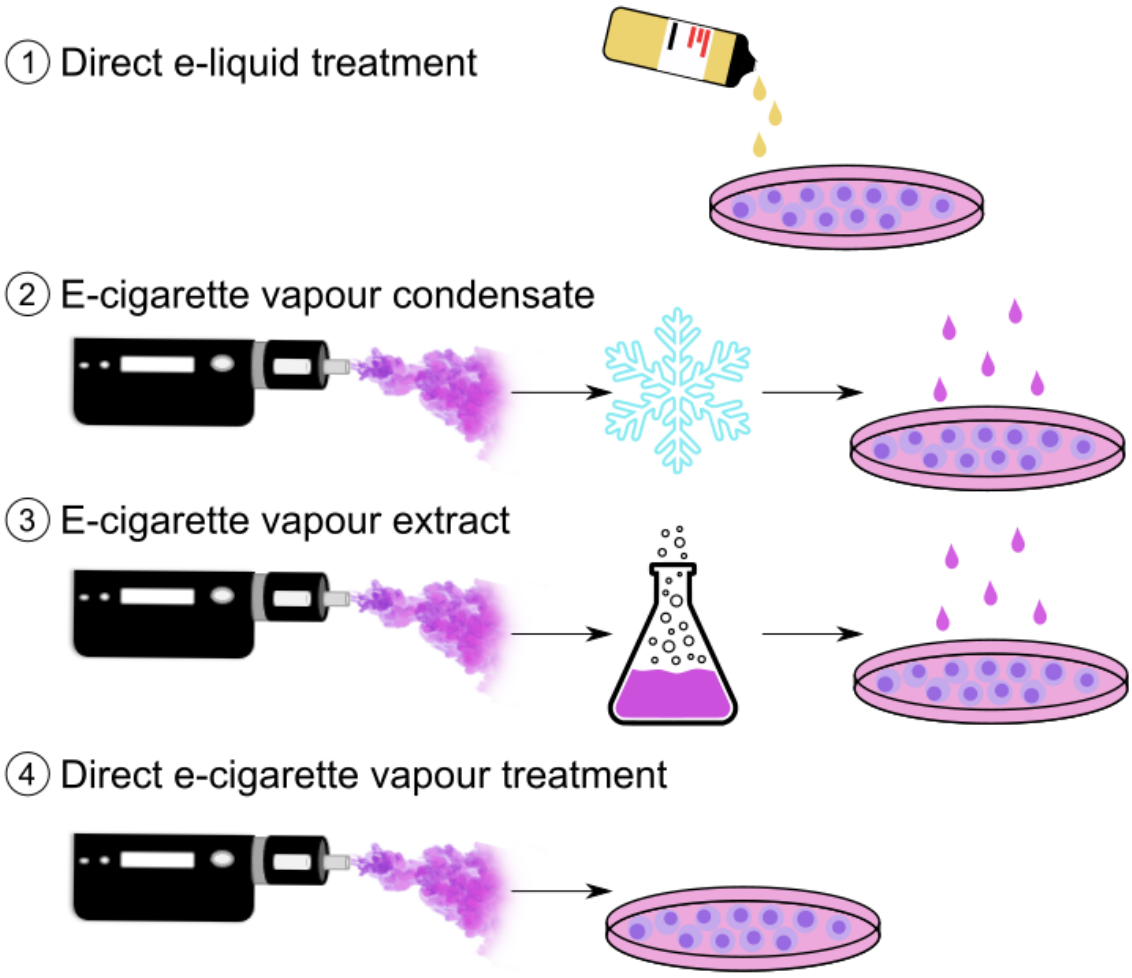


Figure 1.6*: A schematic diagram of the main e-cigarette exposure models used in *in vitro* models.*
1) Direct e-liquid treatment technique involves treating cells directly with e-liquid before examining the effects. No vapourisation is involved, meaning the effects of thermal decomposition of e-liquids is not assessed and this is not the most physiologically relevant model as cells are unlikely to be exposed to e-liquid in its raw form *in vivo*. 2) E-cigarette vapour condensate is produced by quickly cooling the e-cigarette vapour to condense the vapour constituents before treating cells with the condensate either raw or diluted. This model incorporates the chemical changes associated with vapourisation of e-liquids and mimics e-cigarette vapour condensing in the airway *in vivo*. 3) E-cigarette vapour extract models are most commonly used as they can directly compare to the cigarette smoke extract models employed in cigarette studies. The generation of e-cigarette vapour extract involves bubbling e-cigarette vapour through a media, before treating cells with that media. This method does, however, rely on the vapour constituents dissolving into media and significantly dilutes the products. 4) Direct e-cigarette vapour treatment involves generating puffs of e-cigarette vapour directly onto cells, using a chamber. This mimics exposure of cells in the lower respiratory tract to e-cigarette vapour particulates.

1.6 The effect of e-cigarettes on cells of the respiratory system

Due to their relatively recent invention, it is not possible to recruit a cohort of decade or life-long e-cigarette users to examine physiological effects of long-term use. Instead, short-term cohort studies, murine, and *in vitro* work modelling exposure in the short-medium term, enable early indicators of biological change to be understood (Davis et al., 2022). Published literature has uncovered changes in function, transcription, and communication of cells of the respiratory immune system (including epithelial cells and alveolar macrophages), providing rationale to investigate this further to understand the interaction between e-cigarette vapour and the first responders to respiratory harm, neutrophils. The functional implications of e-cigarette vapour compared to cigarette smoke have been outlined in Table 1.1, and a summary of the effects of e-cigarettes on lung health can be seen in Figure 1.7.

1.6.1 Epithelial cells

Type I and type II alveolar epithelial cells are directly exposed to e-cigarette vapour upon inhalation. As a dynamic cell type, with large influences on tissue homeostasis, it is important to understand its response to e-cigarette vapour exposure. Visual inspection of the airways of e-cigarette users has revealed erythematous mucosa and cases of life-threatening bronchial injury have been reported (Ghosh et al., 2018, Carter et al., 2017).

High concentrations of e-cigarette vapour extract trigger epithelial cell toxicities comparable to cigarette smoke extract exposure but how these doses compare to user exposure is unclear as no data regarding e-cigarette vapour extract characteristics

were provided by this study (Sohal et al., 2019). Other findings have indicated no induction of apoptosis or necrosis by unflavoured e-cigarette exposure (Ween et al., 2020, Garcia-Arcos et al., 2016, Lin et al., 2019). Dysfunctional cilia beat frequency and motility have been reported in human nasal epithelial cells (HNEC) and normal human bronchial epithelial (NHBE) cells exposed to e-cigarettes in a manner similar to that seen with cigarette smoke extract (Garcia-Arcos et al., 2016, Carson et al., 2017). Although the authors described a return to baseline function over time, they did not rule out the potential of lasting damage with chronic exposure (Carson et al., 2017). This could have significant implications for the clearance of mucus and a resulting impact on recurrent lung infections and sustained inflammation.

Consistently, epithelial cells exposed to e-cigarette vapour (via a variety of exposure models) exhibit an increase in CXCL8 secretion (Sohal et al., 2019, Garcia-Arcos et al., 2016, Reidel et al., 2018). In addition, increases in IL-6, MCP-1, TNF-a, MIP-1B and IL-10 have been reported (Garcia-Arcos et al., 2016, Herr et al., 2020, Ween et al., 2020, Wu et al., 2014). Extracellular matrix proteins, collagen 1 and fibronectin, are secreted in a concentration-dependent manner by Beas-2B and airway smooth muscle cells exposed to e-cigarette vapour extract, leading to formation of mesh-like fibres observed in e-cigarette vapour exposed HNECs and contributing to tissue remodelling (Sohal et al., 2019, Carson et al., 2017).

1.6.2 Alveolar macrophages

Alveolar macrophages are essential in maintaining tissue homeostasis and controlling inflammatory responses. Bronchoscopy cohort studies have enabled the collection of

alveolar macrophages from e-cigarette users, smokers and healthy individuals in order to investigate e-cigarette-induced changes *ex vivo*. In alveolar macrophages collected from BALF from healthy non-smokers, e-cigarette vapour exposure altered expression of over 60 genes including those associated with inflammation after only 20 puffs (Staudt et al., 2018). In addition, lipid-laden macrophages have been identified in over half of e-cigarette users in a bronchoscopy study, and were associated with elevated immunosuppressive cytokines IL-4 and IL-10 and reduced surfactant protein A (Shields et al., 2020, Ghosh et al., 2021a). Despite the value of bronchoscopy studies, there is a lack of longitudinal studies in the literature which would provide further data on long term use of e-cigarettes.

In vitro, treatment of alveolar macrophages with e-cigarette vapour condensate showed a nicotine-independent reduction in viability (Scott et al., 2018) whereas e-cigarette vapour extract treatment on macrophage-like THP-1 cells did not affect viability (Gómez et al., 2020). However, stark differences in the preparation of e-cigarette vapour condensate and extract along with behaviours of *ex vivo* cells that cannot be replicated in cell lines would explain these differences in findings. Our group have previously shown that nicotine-containing e-cigarette vapour condensate increased secretion of pro-inflammatory cytokines: IL-6, TNF-a, CXCL8, MCP-1 and MMP-9 compared to controls in alveolar macrophages (Scott et al., 2018). Increased CXCL8 and MMP-9 secretion was replicated in e-cigarette vapour extract models using THP-1 cell lines in the presence of nicotine (Ghosh et al., 2019, Gómez et al., 2020). Conversely, effects on antimicrobial activity appear to be independent of nicotine content. Alveolar macrophages exposed to e-cigarettes exhibit reduced antimicrobial

activity to gram-positive and gram-negative bacteria regardless of nicotine content and this is exacerbated by the reported increased virulence and growth rates of infecting pathogens caused by e-cigarette exposure (Hwang et al., 2016, Scott et al., 2018, Clapp et al., 2017, Gómez et al., 2020). Furthermore, alveolar macrophages exposed to nicotine-containing e-cigarette vapour extract exhibit significant reduction in efferocytosis of apoptotic epithelial cells (Ween et al., 2020). Inability to clear cellular debris and dying cells may lead to persistent inflammation of the airway.

Evidence detailed in sections 1.6.1 and 1.6.2 highlight the pro-inflammatory effects that have been uncovered of e-cigarette vapour on epithelial cells and alveolar macrophages. These changes suggest the respiratory inflammation cascade is activated upon inhalation of e-cigarette vapour. Inflammatory responses in the lung lead to recruitment of neutrophils to the airspaces, and therefore, given the impact neutrophils can have on lung disease pathophysiology, understanding the impact of e-cigarette vapour on this important cell type is essential.

	Epithelial cells				Alveolar macrophages			
Cellular function	Cigarette smoke		E-cigarette vapour		Cigarette smoke		E-cigarette vapour	
Viability	↓	(Kode et al., 2006) (Hoshino et al., 2001) (Jiao et al., 2006)	↔	(Ween et al., 2020) (Garcia-Arcos et al., 2016) (Lin et al., 2017)	↔	(Pauly et al., 2005)	↓	(Scott et al., 2018)
Reactive oxygen species	↑	(Khan et al., 2008) (Lerner et al., 2015)	↑	(Zhao et al., 2018) (Lerner et al., 2015)	↑	(Ko et al., 2015) (Larson-Casey et al., 2018)	↑	(Scott et al., 2018)
Pro-inflammatory cytokine release (e.g. IL-1β, IL-6, TNF-a, CXCL8)	↑	(Yang et al., 2006) (Kode et al., 2006)	↑	(Sohal et al., 2019) (Herr et al., 2020) (Xu et al., 2013)	↑	(Hodge et al., 2011) (Ween et al., 2017)	↑	(Scott et al., 2018) (Gomez et al., 2020)
Phagocytosis/antimicrobial activity	N/a		N/a		↓	(Hodge et al., 2007)	↓	(Hwang et al., 2016) (Clapp et al., 2017) (Scott et al., 2018) (Gomez et al., 2020)
Efferocytosis	N/a		N/a		↓	(Hodge et al., 2011)	↓	(Ween et al., 2020)
Ciliary function	↓	(Wyatt et al., 2000) (Gindele et al., 2020)	↓	(Garcia-Arcos et al., 2016) (Carson et al., 2017)	N/a		N/a	

Table 1.1: Details of the current understanding of the effects of cigarette smoke and e-cigarette vapour on alveolar macrophages and epithelial cells.
The effect of cigarette smoke on epithelial cells and alveolar macrophages is well established while the effect of e-cigarette vapour is more exploratory. There are common patterns between cigarette smoke and e-cigarette vapour, indicating the potential for similar effects on respiratory health. ↑ = there is a reported increase in that function compared to controls, ↔ = there is reportedly no change in the function compared to controls, or it is unknown, ↓ = there is a reduction in that function compared to controls.

1.6.3 Current understanding of the effect of e-cigarettes and neutrophils

Cytopathological findings from the recently reported EVALI cases revealed neutrophil infiltration into the airways (58% of BAL cells were neutrophils) (Layden et al., 2019). However, analysis of BALF from e-cigarette users and smokers did not reveal an upregulation in neutrophil numbers compared to controls in BALF or induced sputum (Ghosh et al., 2019, Reidel et al., 2018). The participants were asked to abstain from vaping the morning of the bronchoscopy, therefore, neutrophils could have been rapidly recruited to the lung and undergone apoptosis and cleared before the samples were collected. Despite no changes in neutrophil numbers, both studies reported significant changes to neutrophil-related products. E-cigarette users had significantly elevated granule enzymes and activity including NE, MMP-2 and MMP-9 in BALF (Ghosh et al., 2019). Neutrophil granule and NET-related proteins including MPO, azurocidin, protein-arginine deiminase 4 and MMP-9 were all elevated in induced sputum from e-cigarette users, again, despite no increase in neutrophil numbers (Reidel et al., 2018). Importantly, secretion of destructive proteinases such as NE and MMPs were elevated with a lack of corresponding increase in anti-proteinases (Higham et al., 2016, Reidel et al., 2018, Ghosh et al., 2019), indicating a potential proteinase-antiproteinase imbalance and a shift towards increased bystander tissue damage upon neutrophil recruitment to the airways. There is potential these findings were due to previous smoking history, and the development of early-stage COPD, however, in most cases there were no differences in protease concentration between smokers and vapers, and in the Reidel study, NE concentration was significantly higher in e-cigarette users than smokers.

The underlying causes of these potential changes in neutrophil behaviour remain poorly understood. Much of the literature has performed functional experiments on neutrophils exposed to e-cigarettes but have not fully elucidated a mechanism of harm. E-cigarette vapour extract generated from e-liquids containing 24 mg nicotine was not reported to be cytotoxic to neutrophils however, markers of neutrophil activation were elevated after exposure, including morphological shape change and activation marker expression (CD11b and CD66b) (Higham et al., 2016). However, it should be noted that the exposure time in those experiments was 6 hours, at which point activation and neutrophil shape change would be expected. After just a 20 minute exposure to nicotine-containing e-cigarette vapour extract, neutrophils exhibited a diminished ability to produce ROS which coincided with the reduced ability to migrate through a membrane towards a chemoattractant after exposure to e-cigarettes (Corriden et al., 2020). Phagocytosis of *E. coli* and *S. aureus* by circulating neutrophils was significantly reduced by 30 minutes of e-cigarette vapour extract and e-liquid exposure independently of nicotine; indicating that e-cigarette use may limit the control and elimination of bacterial infections (Clapp et al., 2017, Corriden et al., 2020). After just 20 minutes of e-cigarette vapour extract treatment, neutrophil migration through transwells to fMLP has been shown to be significantly diminished compared to UTC (Corriden et al., 2020). E-liquids have been shown to not affect neutrophil spontaneous or PMA-induced NET generation (Clapp et al., 2017) while e-cigarette extract did not induce spontaneous NET generation, but suppressed PMA-induced NET generation (Corriden et al., 2020). This highlights that different e-cigarette vapour exposure models can produce different results. In a report examining neutrophils from BAL from e-cigarette users, neutrophils were more sensitive to NET-stimulating PMA than

controls (Reidel et al., 2018), indicating there could be systemic alterations caused by e-cigarette use, affecting circulating neutrophils.

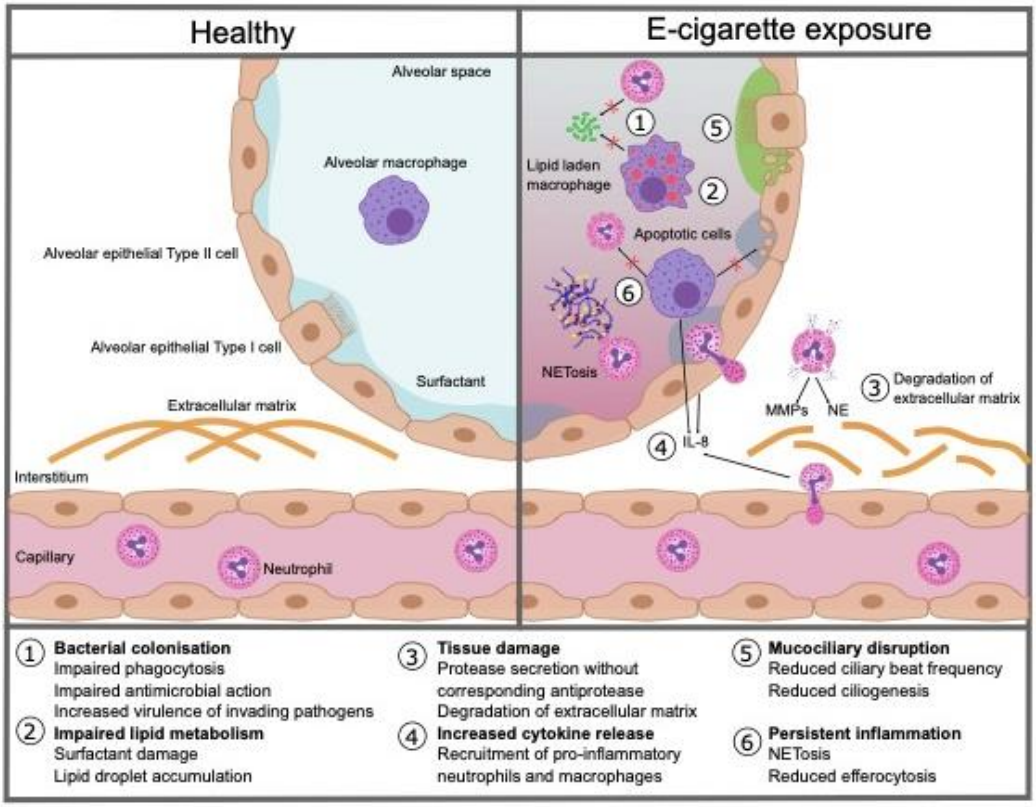


Figure 1.7: A summary of the effects of e-cigarette vapour exposure on lung homeostasis driven by alterations in important lung cells.
In response to e-cigarette exposure, functional changes in a range of cell types, and subsequent dysfunctional interactions lead to changes characteristic of oxidative stress: 1) bacterial colonisation is driven by impaired phagocytosis and bacterial killing by alveolar macrophages and neutrophils, exacerbated by evidence of increased virulence by invading pathogens, 2) impaired lipid metabolism by alveolar macrophages and alveolar type II epithelial cells leads to damaged surfactant as well as the formation of lipid laden macrophages which exhibit abnormal processing of both endogenous and exogenous lipids, 3) tissue damage to the interstitium and epithelial cell layer is caused by recruitment of neutrophils and their subsequent degranulation of proteases such as MMPs and NE without a corresponding increase in antiproteases such as alpha 1 antitrypsin, leading to degradation of the extracellular matrix, 4) increased cytokine release by alveolar macrophages and epithelial cells recruits neutrophils and monocytes to the airspaces, causing tissue destruction as they transmigrate, 5) Mucociliary disruption causes accumulation of mucus due to reduced ciliogenesis and ciliary beat frequency, 6) persistent inflammation is driven by reduced efferocytosis by alveolar macrophages, subsequent accumulation of apoptotic cells and neutrophil NETosis. These substantial changes are driven by functional changes in neutrophils, alveolar macrophages, and epithelial cells as a result of e-cigarette exposure. Consequently, the alveolar spaces become inflamed and changes, some irreversible, occur which can lead to the development of a range of respiratory diseases including bronchiectasis, chronic obstructive pulmonary disease and emphysema. Abbreviations: IL-8 = Interleukin 8, MMPs = Matrix metalloproteases, NE = Neutrophil elastase, NET = Neutrophil extracellular trap

1.6.4 Parallels between e-cigarette and cigarette studies

The effects of cigarette smoke are well established, whilst e-cigarette vapour effects remain exploratory. However, there are parallels emerging between the two, which suggest e-cigarette vapour could drive similar effects to those of cigarette smoke. As mentioned in section 1.2.1, there are many overlapping toxicants between cigarette smoke and e-cigarette vapour including formaldehyde, acetaldehyde and acrolein (Kosmider et al., 2014, Jensen et al., 2015, Ogunwale et al., 2017, Goniewicz et al., 2014), indicating the potential for parallels in the effects of cigarette smoke and e-cigarette vapour on respiratory health. In addition, there is potential for exaggerated nicotine driven effects due to higher nicotine delivery by e-cigarettes as e-liquids can have as much as 20 mg/mL nicotine (in the UK) (MHRA, 2022) while cigarettes contain 6-12 mg nicotine (Taghavi et al., 2012). Smoking is associated with upregulation in inflammatory cytokines CXCL8, LTB_4 and IL-6 release (Amin et al., 2003) and e-cigarette studies have replicated these findings *in vitro* (Lerner et al., 2015, Scott et al., 2018, Ween et al., 2020) and *in vivo* (murine models) (Vlahos et al., 2006, Lerner et al., 2015, Phillips et al., 2015). Substantial transcriptome changes have been described (in murine and human studies) due to cigarette smoke (Brody, 2012) which are now being uncovered in e-cigarette studies (Ghosh et al., 2018, Park et al., 2019, Shen et al., 2016). Studies have shown NE activity to be elevated in smoker's plasma (Weitz et al., 1987) and BALF (Harris et al., 1975) and has been associated with smoking-related lung damage in animal models (Shapiro et al., 2003, Churg et al., 2008). Increases in NE, PR3, MPO, MMP-2 and MMP-9 have already been detected in the BALF of e-cigarette users (Ghosh et al., 2019, Reidel et al., 2018), indicating the potential for the development of similar features of cigarette-induced emphysema.

Together, these are just some of the similarities between the findings of cigarette and e-cigarette research to date, representing the potential dangers of long-term e-cigarette use to respiratory health. The dangers associated with cigarette smoking took decades to uncover, but ignoring the similarities between cigarette smoke and e-cigarette vapour effects may mean history repeats itself.

1.7 Gap in knowledge and the importance of this work

To date, there is a lack of comprehensive studies of neutrophil functions after direct exposure to e-cigarette vapour – many studies have treated neutrophils with e-cigarette vapour extract, condensate, or directly with e-liquids. For the first time here, a novel vapour chamber was established with well-characterised and physiological parameters. Major neutrophil effector functions including migration, phagocytosis, NET generation, degranulation, and oxidative burst were assessed. Uniquely, second generation e-cigarette devices were used alongside higher powered-fourth generation e-cigarette device, enabling a direct comparison of device generation on neutrophil functions. In addition, devices were refilled with nicotine-free and nicotine-containing e-liquid to delineate the contribution of nicotine and the functional implications of vehicle molecules alone. Finally, an investigation into the mechanism of action was pursued to unpick drivers of dysfunction and attempt to restore function.

1.8 Hypothesis and aims

Hypothesis: Neutrophil function is impaired by e-cigarette vapour exposure, which is exaggerated by the presence of nicotine in e-liquids and higher device power.

To assess this hypothesis the following aims will be addressed:

1. To validate the application of a novel e-cigarette vapour exposure system (Chapter 3).
2. To validate and optimise existing protocols to ensure they accurately address functional questions in the e-cigarette vapour exposure model here (Chapter 3).
3. To investigate the impact of e-cigarette vapour exposure on neutrophil functions: chemotaxis, transmigration, phagocytosis, degranulation, oxidative burst, NET generation (Chapter 4).
4. To investigate the contribution of nicotine to the neutrophil functions detailed above (Chapter 4).
5. To investigate the contribution of e-cigarette device power to the neutrophil functions detailed above (Chapter 4).
6. To investigate the mechanistic drivers of e-cigarette-induced neutrophil dysfunction (Chapter 5).

Chapter 2 -

MATERIALS AND METHODS

2.1 Ethical approval

Ethical approval for this study was granted by the University of Birmingham Research Ethics Committee (approval number: ERN 12-1185R2). Written informed consent was obtained from all participants prior to the collection of biological samples.

2.2 Subject recruitment

Volunteers aged 19-63 years old were recruited from members of staff in and around the University of Birmingham Research Laboratories in the Queen Elizabeth Hospital Birmingham. All participants were self-reported non-smokers, non-vapers, and otherwise healthy.

2.3 Blood sample collection

Trained phlebotomists collected peripheral venous blood samples from healthy volunteers using the vacutainer systems into 6 mL lithium heparin (BD biosciences, Berkshire, UK product no. 367886) coated tubes.

2.4 Neutrophil isolation

2.4.1 Percoll™ density gradient separation

Neutrophils were isolated as described previously (Jepsen and Skottun, 1982). Lithium heparin anticoagulated whole blood was transferred to 50 mL centrifuge tubes (Appleton woods, Birmingham, UK product no. BF034) and gently mixed with sterile 2% Dextran (Sigma-Aldrich, Poole, UK product no. 31392) in 0.154 M NaCl (Sigma-Aldrich, Poole, UK product no. S9888) in a 6:1 whole blood to dextran ratio. Blood was left to stand for 30 minutes, or until the erythrocytes had sedimented (maximum of 45

minutes). Percoll (Sigma-Aldrich, Poole, UK product no. P4937) was diluted 9:1 (v/v) in 1.54 M NaCl to produce an isotonic stock solution. This was further diluted 14:11 in 0.154 M NaCl to produce a 56% percoll solution or 4:1 in 0.154 M NaCl to produce an 80% Percoll solution. Percoll solutions were prepared fresh on the day of neutrophil isolation and allowed to come to room temperature prior to layering. Using a sterile fine-tipped pipette (Alpha Labs, Eastleigh, UK product no. LW4238), 2.5 mL 80% percoll was layer beneath 5 mL 56% percoll in a 15 mL centrifuge tube (Appleton woods, Birmingham, UK product no. BF032) to form a discontinuous percoll density gradient. Immediately after preparation of the density gradient, the buffy coat from the erythrocyte sedimented whole blood was gently layered on top of the percoll gradient using a sterile fine-tipped pipette. Gradients were centrifuged at 470 x *g* for 20 minutes at room temperature, with no brake or acceleration. Following centrifugation, the plasma and peripheral blood mononuclear cell (PBMC) layers were removed and discarded, and the neutrophil layer (see Figure 2.1) was aspirated using a sterile fine tipped pipette and transferred into a fresh, sterile phosphate buffered saline (PBS)-containing 15 mL centrifuge tube. Cells were centrifuged at 250 x *g* for 10 minutes at room temperature with full brake and acceleration to form a pellet. Supernatants were discarded and pellets gently resuspended in RPMI 1640 (Sigma-Aldrich, Poole, UK product no. R8758) containing 2 mM L-glutamine and supplemented with penicillin-streptomycin (1% w/w, Sigma-Aldrich, Poole, UK product no. P4333). A Fast Read 102® (Biosigma, Cona, Italy product no. BVS100) slide was used to assess neutrophil yield and cells were diluted to the appropriate concentration for downstream experiments in the same RPMI 1640, or assay specific media as specified.

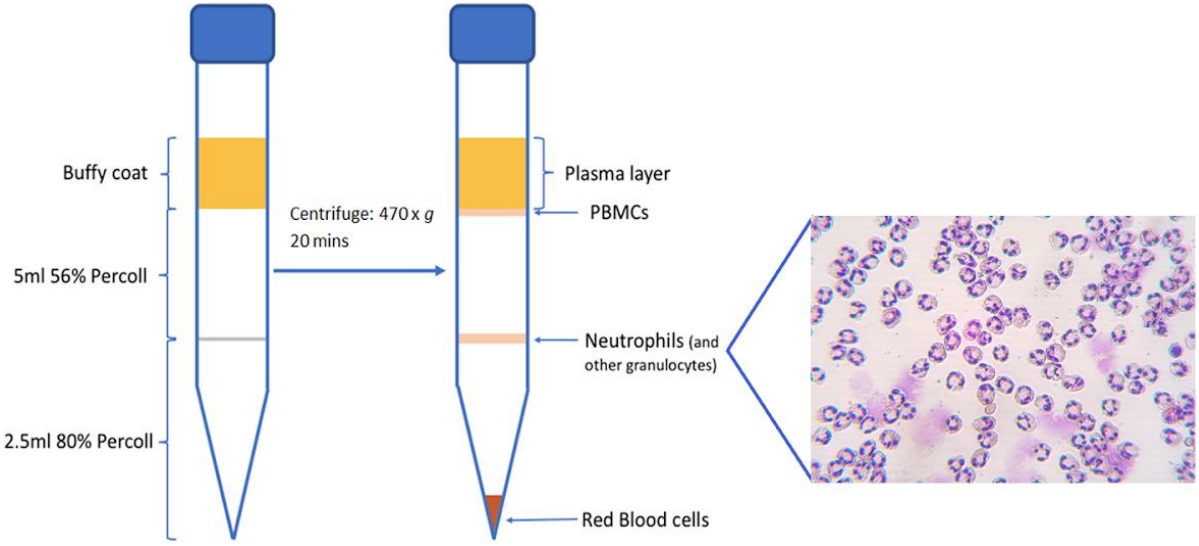


Figure 2.1: A schematic diagram of the percoll gradient neutrophil isolation method.
Blood samples were treated with Dextran to allow for erythrocyte sedimentation before the buffy coat was layered on the 56%/80% percoll gradient and centrifuged at 470 x g for 20 minutes with no brake or acceleration at room temperature. The plasma layer and PBMCs were discarded and neutrophils isolated from the gradient interface, as indicated.

2.4.2 Assessing neutrophil purity by cytospin

Neutrophil purity was assessed by cytospin (Shandon). Cells were resuspended to a concentration of $1x10^5$ in a total volume of 100 µL. Suspensions were carefully transferred to cytospin funnels which were clamped to frosted microscope slides (Fisher Scientific, Loughborough, UK product no. 12362098) and centrifuged at 300 rpm for 5 minutes at room temperature with maximum brake and acceleration. Slides were fixed by immersion in 100% methanol for approximately 30 seconds followed by staining using the REASTAIN® Quick-Diff Kit (REAGENA, Finland product no. 102164) red (cytoplasmic) and blue (nuclear) stains for approximately 30 seconds each. Once dried, slides were observed under a light microscope (45x magnification) and cell isolation purities were determined by differential cell count, assessed in 4 fields of vision (see Figure 2.2). Only preparations with a neutrophil purity >90% were used for subsequent assays.

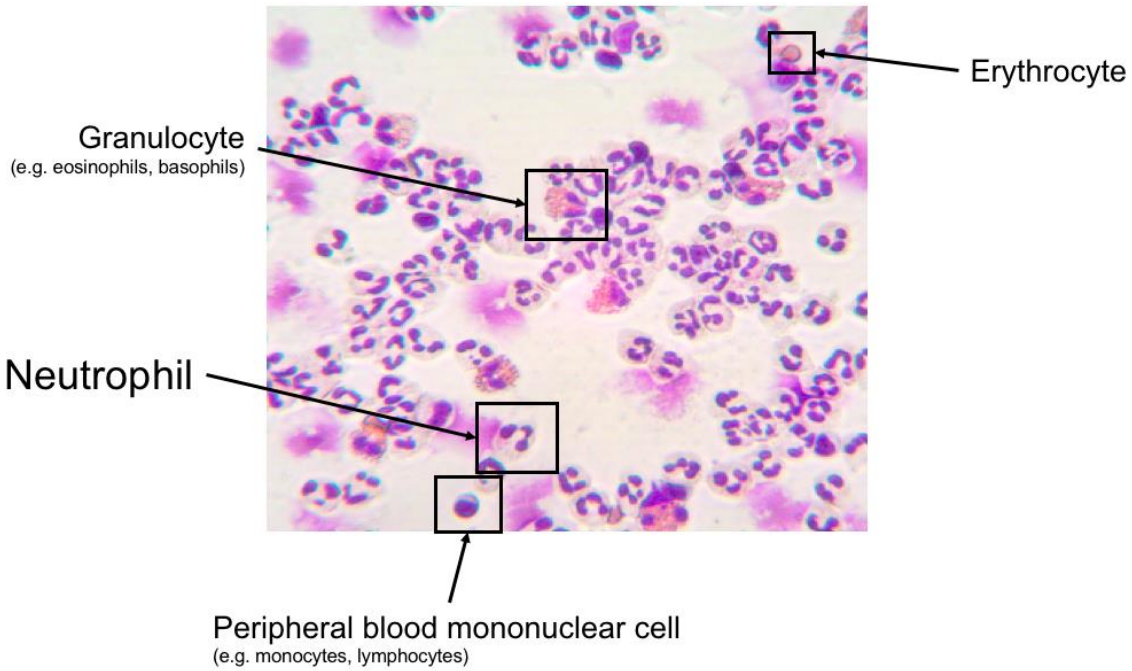


Figure 2.2: Cytospin slide photograph after Quick-Diff staining to allow identification of blood cell subtypes.
1 x 10^5 cells were centrifuged onto a frosted microscope slide (300 rpm, 5 minutes, maximum brake and acceleration). Slides were fixed in methanol and then stained with the cytoplasmic REASTAIN® Quick-Diff red stain followed by the nuclear REASTAIN® Quick-Diff blue stain. This produced a slide which could be visualised under a light microscope to distinguish between cell types to assess the purity of a neutrophil isolation. The multi-lobed nucleus of a neutrophil was clearly distinguishable in dark purple while peripheral blood mononuclear cells appeared as round, single nucleated cells with little cytoplasm. Erythrocytes appear small with no purple nucleus, and granulocytes have a highly red-stained nucleus and often multinucleated purple nucleus.

2.5 E-cigarette devices

KangerTech® TOP EVOD (2nd generation) and TOPBOX mini (4th generation devices) e-cigarette starter kits (KangerTech®, Shenzhen, China product no. B076X43TCV and B018ZSDP6O respectively) were purchased from Amazon UK. KangerTech® replacement atomisers were also purchased from Amazon UK (KangerTech®, Shenzhen, China product no. B00NP0ZLTM). At the time of project conception, larger tank models were referred to generally as 3rd generation and those with larger batteries and more modifications as 4th generation. With time, 3rd and 4th generation devices have become more difficult to define and the advent of pod-based systems, some have moved to describe these as 4th generation devices. In this study, we have retained 4th generation to describe the KangerTech® TOPBOX mini device which consists of a large tank model with modifiable features. KangerTech® are a commercially available global vaping brand, and 2nd and 4th generation devices were chosen to enable comparison between the impact of high vs low power devices on neutrophil functions.

Unflavoured e-liquid (50:50 PG:VG) containing 0 or 36 mg/mL nicotine were purchased from American e-liquid. Separate devices were refilled with nicotine-containing e-liquid or nicotine-free e-liquid to ensure there was no cross contamination in this study. E-liquids without flavour were used here with the project focus remaining on the fundamental effects of e-cigarettes on neutrophils. 36 mg/mL was the maximum nicotine strength of e-liquid that could be purchased on American e-liquid, and this was used to achieve a maximal nicotine-dependent response. The 2nd generation device had the following fixed parameters: 1.8 Ω, 7.6 W with rechargeable 650 mAh battery, while the 4th generation device loaded with a rechargeable 3000 mAh, 3.7 V battery

and manually set to the parameters: 315 ºC, 0.2 Ω, 75 W, representing the maximum temperature and power settings of the device. E-cigarette tanks were filled with e-liquid and allowed to saturate the wick before use, to prevent dry-puff generation. A fully charged battery and filled tank was used for both devices each time they were used, and atomisers were changed approximately every week.

2.6 E-cigarette vapour exposure system

A modified hypoxia chamber with a total volume of 5.5 L was used as an e-cigarette vapour exposure system to model exposure of neutrophils migrated into the lung lumen (see Figure 2.3). E-cigarette devices were attached to the chamber via a short piece of piping, which was sealed to the mouthpiece using Parafilm® (Sigma-Aldrich, Poole, UK product no. P6543) to prevent leakage. The chamber was attached to a vacuum pump via piping and Parafilm®, which created a closed circuit, generating the suction required for full e-cigarette activation. Every 30 seconds, the e-cigarette was activated manually via the activating switch, at the same time as the vacuum starting. This created a puff in the chamber lasting 4 seconds (duration based on topography studies, as discussed in section 1.2.2 (Hua et al., 2013, Robinson et al., 2015, Farsalinos et al., 2013, Dautzenberg and Bricard, 2015)). A 30 second inter-puff interval allowed the device to cool between puffs, to prevent overheating. A total of 40 puffs were generated for one condition at a time over a 20 minute period. Neutrophils were plated in a 96 well flexi plate pre-coated with 1% bovine serum albumin (BSA)-PBS (Corning, Loughborough, UK product no. 2797) at 1 x 10^5 cells/well and placed in the centre of the chamber (except where functional assay did not allow for this). Neutrophils from

each donor were exposed to the conditions displayed in Table 2.1, with UTC neutrophils being included for each functional assay and every individual donor.

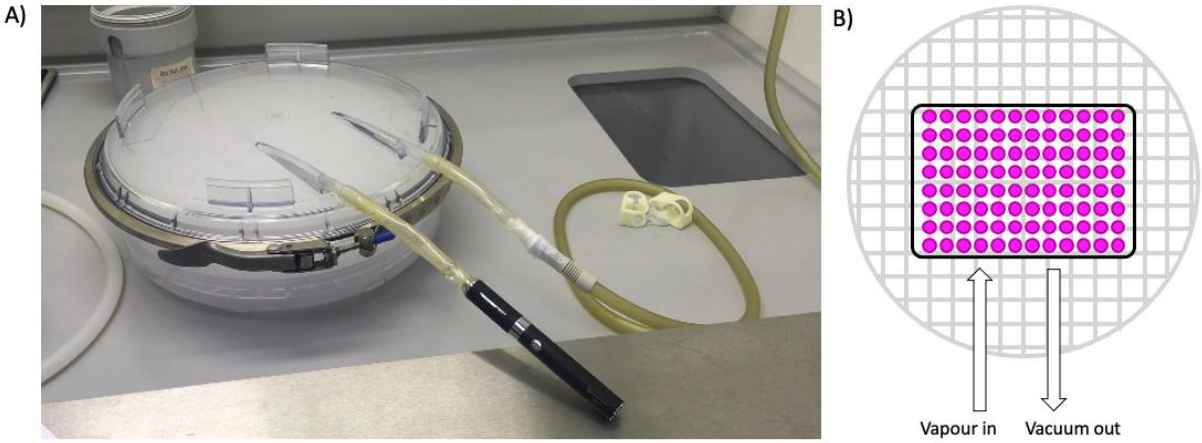


Figure 2.3: The e-cigarette vapour exposure system developed to expose cells directly to e-cigarette vapour.
The system used to generate e-cigarette vapour is photographed in A) and schematically represented in B). The system was clamped shut with a tight seal, and the piping was sealed using parafilm. One pipe was attached to the e-cigarette white the other was attached to a vacuum. When the e-cigarette device and vacuum were activated simultaneously, a cloud of vapour as generated in the chamber, as pictured. E-cigarette exposures took place over a 20 minute period with a 4 second puff of e-cigarette vapour produced every 30 seconds (total 40 puffs). A 96 well plate containing neutrophils was placed in the centre of the chamber during exposures.

Treatment condition	E-cigarette device	Device settings	E-liquid flavour	Nicotine concentration	Number of 4s puffs	Total exposure time (minutes)	Plating method
UTC	None	N/a	N/a	N/a	N/a	N/a	100 μL of 1 x 10^6 neutrophil//mL solution per well of a 96 well flexi plate (1 x 10^5 cells/well)
2GECV	KangerTech® TOP EVOD (2nd generation device)	1.8 Ω 7.6 W	None	36 mg/mL	40	20	
4GECV	KangerTech® TOPBOX nano (4th generation device)	315 ºC 0.2 Ω 75 W	None	36 mg/mL	40	20	
2GNF	KangerTech® TOP EVOD (2nd generation device)	1.8 Ω 7.6 W	None	0 mg/mL	40	20	
4GNF	KangerTech® TOPBOX nano (4th generation device)	315 ºC 0.2 Ω 75 W	None	0 mg/mL	40	20	

Table 2.1: Group definitions for each e-cigarette vapour exposure method.
Neutrophils were isolated from the venous whole blood of participants as described in section 2.3. Neutrophils were plated in a 96 well flexi plate with 1 x 10^5 neutrophils per well. The plates were placed in the centre of the exposure system described in section 2.6 and puffs of e-cigarette vapour generated as described. These group definitions will be used throughout this thesis. Abbreviations used: UTC: untreated control, 2GECV: 2nd generation e-cigarette vapour (with nicotine), 4GECV: 4th generation e-cigarette vapour (with nicotine), 2GNF: 2nd generation nicotine free (e-cigarette vapour), 4GNF: 4th generation nicotine free (e-cigarette vapour).

2.7 Neutrophil viability

Neutrophils were resuspended to 1 x 10^6/mL in annexin V binding buffer (produced by diluting a 10 X concentrated buffer solution consisting of 0.2 µM sterile filtered 0.1 M 4-(2-hydroxyethyl)-1-piperazineethanesulfonic acid (HEPES) (pH 7.4), 1.4 M NaCl and 25 mM $CaCl_2$ with distilled water 1:10) and transferred to ice. Annexin V-FITC stain (BD Bioscience, Berkshire, UK product no. 556420) was added (1:100 dilution) and the cells were left in on ice, protected from light, for 20 minutes. Neutrophils were centrifuged at 250 x *g* for 5 minutes at 4 °C with full brake and acceleration, supernatants discarded and resuspended in annexin V binding buffer. Neutrophils were washed twice more before resuspension in 200 µL of annexin V binding buffer. Immediately prior to running, propidium iodide (PI) (Sigma-Aldrich, Poole UK, product no. P4864) was added to the sample 1:100 (v/v). Samples were read on a BD FACSvia flow cytometer. The fluidics were set to medium speed and 10,000 neutrophil events (gated on FSC-A and SSC-A channels) were collected. Gates for Annexin V (FL-1 channel) and PI (FL-2 channel) positivity respectively, were plotted based and compared to unstained control neutrophils for each donor to account for variations in autofluorescence between individuals. Proportions of live (viable) (FL-1^{low}, FL-2^{low}), early apoptotic (FL-1^{high}, FL-2^{low}), late apoptotic (FL-1^{high}, FL-2^{high}) and necrotic (FL-1^{low}, FL-2^{high}) neutrophils were determined as shown in Figure 2.4.

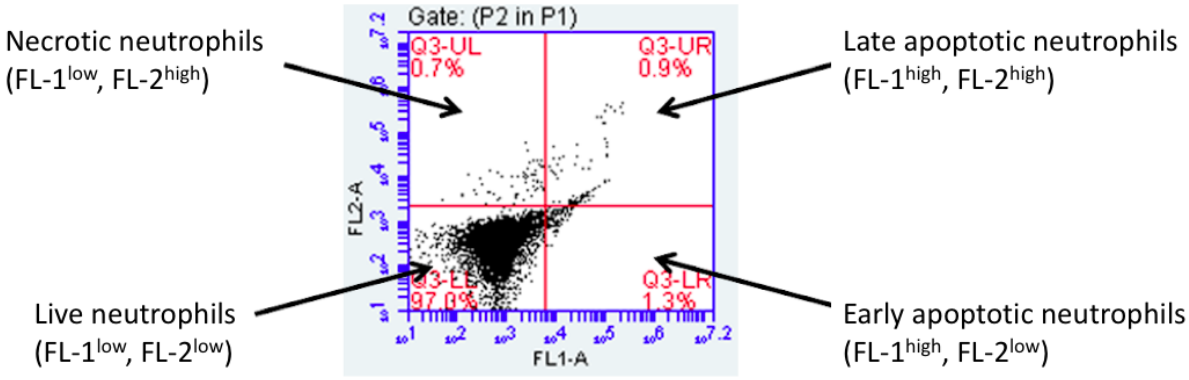


Figure 2.4*:* An example of flow cytometry analysis plots used to assess cell viability.
Annexin V-FITC positivity is read in the FL1-A channel, while Propidium Iodide positivity is read in the FL2-A channel. Displayed is a plot generated by flow cytometric analysis of the neutrophil population. Gates are plotted based on unstained neutrophil autofluorescence and adjusted between individuals. Quadrants represent different stages of neutrophil viability, as labelled.

2.8 Neutrophil migration assays

2.8.1 Insall chamber – chemotaxis

The neutrophil chemotaxis assay was performed using a modified Dunn chamber (Muinonen-Martin et al., 2010) which has been applied extensively to published literature (Sapey et al., 2010, Sapey et al., 2011, Sapey et al., 2014, Sapey et al., 2017, Patel et al., 2018, Sapey et al., 2019). Neutrophils were resuspended at 2 x 10^6/mL in RPMI 1640. 22x22 mm glass coverslips (Surgipath® premier cover glass, Leica Biosystems, Wetzlar, Germany product no. 3800106G) were handled using inverted forceps (Sigma-Aldrich, Poole, UK product no. Z168769) and sterilised by submersion in 0.4 M H_2SO_4 followed by twice in distilled water before being left to air dry on filter paper covered by a petri dish. Sterilised coverslips were coated in 400 µL 7.5% BSA (Sigma-Aldrich, Poole, UK product no. A8412) which was discarded before 8 x 10^5 neutrophils (in 400 µL volume) were added to the coverslip. Control neutrophils were left on the benchtop covered by a petri dish for 20 minutes to adhere to the coverslip, while e-cigarette vapour exposed neutrophils were transferred to the vaping chamber on a petri dish lid and exposed to 40 puffs of e-cigarette vapour during the 20 minute adherence phase. The chemoattractant wells of the Insall chamber were washed with RPMI 1640 and left filled with RPMI 1640. After 20 minute incubation, the excess fluid was discarded, coverslip inverted, and placed on the Insall chamber slide (as shown in Figure 2.5). The RPMI was removed from the chemoattractant wells and replaced with 70 µL of 100 nM CXCL8 (R&D Systems, Bio-Techne, Oxfordshire, UK product no. 208-IL). A vehicle control substituting CXCL8 with fresh RPMI in the chemoattractant well was performed for each sample. Ensuring the coverslip on the underside, and the large viewing field was at the top, the Insall chamber with coverslip was placed onto a

Leica DMI 6000B microscope with fitted DFL350 FX camera. The microscope was focussed using the 20X lens, and a field of vision in the large viewing field containing at least 10 non-touching neutrophils was selected. The field of vision was filmed for 12 minutes, with an image captured every 20 seconds, yielding a total of 37 films per condition. If necessary, the microscope recording was paused (with automatic continuation to prevent delay between images), refocussed and resumed to ensure high quality images were captured. Films were analysed using the manual tracking plugin on FIJI Image J before using a pre-formulated excel template to generate values for speed, velocity, persistence, and chemotactic index, as defined in

Table 2.2.

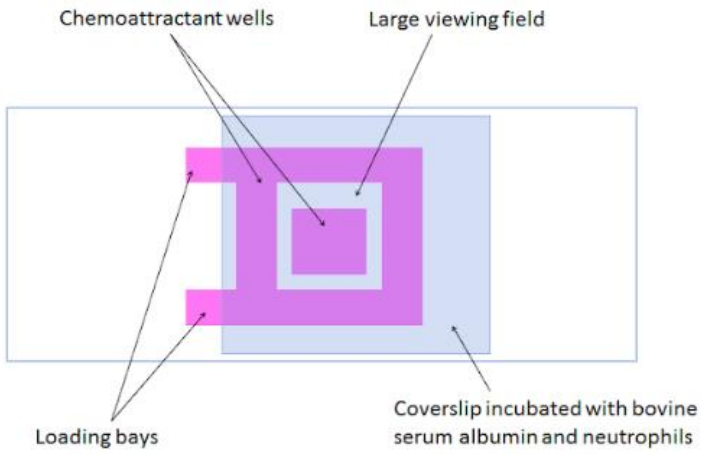


Figure 2.5: A schematic diagram of the Insall chamber used to assess neutrophil chemotaxis.
Neutrophils were incubated on a bovine serum albumin (BSA)-coated coverslip and allowed to adhere before being inverted onto the Insall chamber slide where the neutrophils were exposed to a chemoattractant gradient across the large viewing field, indicated in the diagram. Using a Leica DMI 6000B microscope with fitted DFL350 FX camera, an image was captured every 20 seconds, yielding a total of 36 films per condition. The films were then analysed using the manual tracking plugin and the results transferred to a pre-formatted template which was used to generate values for speed, velocity, persistence, and chemotactic index as described in Table 2.2.

Parameter	Definition
Speed	The average of speed of movement (or chemokinesis) in any direction over time. (µm/minute)
Velocity	The average speed of migration in a consistent direction relative to the orientation of the chemotactic gradient (the y direction). (µm/minute)
Persistence	The cellular orientation with reference to the orientation of the chemotactic gradient. Expressed as a score between 0 and 1. 1 is the highest persistence which would represent a neutrophil that moves in a straight line towards the chemoattractant, while 0 would represent a randomly moving neutrophil which rapidly changes direction.
Chemotactic index	The accuracy of neutrophil migration towards the chemotactic gradient for the duration of the film. Expressed on a scale of -1 to 1 where 1 represents movement directly towards the chemoattractant in all frames, and -1 represents movement directly away from the chemoattractant in all frames.

Table 2.2 Definitions of parameters used to assess neutrophil migration as defined by Greenwood et al in 2014 (Greenwood, 2014).
A video microscope was used to film neutrophil migration towards CXCL8 over 12 minutes, as described in section 2.8.1. For each exposure group, 10 random neutrophils were tracked using the Manual tracking plugin on ImageJ, and the data generated used to calculate average values for speed, velocity, persistence and chemotactic index as defined above. These parameters were used for comparison between groups, to address the aims of the present study.

2.8.2 Transwell migration

Neutrophils were resuspended at 1 x 10^6/mL in RPMI 1640 before e-cigarette exposure to allow for consistency in vaping steps. Following vaping, neutrophils were centrifuged at 250 x *g*, 10 minutes, room temperature, brake and acceleration maximum and resuspended in RPMI (phenol red free, + L-glutamine, penicillin, and streptomycin (GPS) + 10% Fetal calf serum (FCS)) at 1x10^7/ml. Meanwhile, 600 µL RPMI (phenol red free + GPS + 10% FCS) was added to required wells of a 24-well plate (Fisher Scientific, Loughborough, UK product no. 10021863) which was transferred to an incubator (37°C, 5% CO_2). 100 nM CXCL8 (R&D, 208-IL) was added to relevant wells before Nunc™ transwell inserts (Fisher Scientific, Loughborough, UK product no. 40627) were placed in the wells. 100 µL of neutrophils at 1 x 10^7/mL was transferred to the inserts, and the plate incubated (37°C, 5% CO_2) for 90 minutes. After 90 minutes, the inserts were removed, the well supernatants transferred to fluorescence activated cell sort (FACS) tubes and the number of cells in 100 µL of the supernatant measured on a BD FACSvia machine on fast fluidics setting, with a gate set around the neutrophil population according to forward and side scatter (FSC/SSC). The number of neutrophils in the gate represents the number of neutrophils in 100 µL of the supernatant, 1/6 of the total well volume. Therefore, each neutrophil count was multiplied by 6 to calculate total number of neutrophils which had migrated through the transwell insert.

2.9 Neutrophil phagocytosis of *E. coli* and *S. aureus*

Neutrophil phagocytosis was assessed using the pHrodo™ bioparticle assay which incorporates a pH-sensitive fluorescent conjugate, only fluorescing when subjected to

a pH drop such as that during the acidification of a phagosome when bacteria are phagocytosed. Neutrophils were resuspended at 1 x 10^6/mL in RPMI 1640. 1 x 10^5 neutrophils were added to each of the required wells of a 96 well flexi-plate which had been precoated with 1% PBS-BSA. Cytochalasin D (Sigma-Aldrich, Poole, UK product no. PHZ1063) (final concentration 20 μM) was added to negative control neutrophils for 20 minutes; meanwhile experimental neutrophils were exposed to 40 e-cigarette vapour puffs via the vaping chamber. *S. aureus* and *E. coli* pHrodo™ green bioparticles (Fisher Scientific, Loughborough, UK product no. P35361 and A10010 respectively) were resuspended in pHrodo™ buffer (Hanks' Balanced Salt Solution (HBSS), with additional 20 mM HEPES (476.6 mg HEPES in 100 mL HBSS) pH adjusted to 7.4 with NaOH to minimise background signal from uningested particles) (made up to 1 mg/mL) and sonicated for 10 minutes to ensure an even suspension. 50 µL of pHrodo™ bioparticles were added to required neutrophil wells for 30 and 60 minutes and left to incubate at 37°C, 5% CO_2. Negative control neutrophils were incubated with pHrodo™ bioparticles for 60 minutes. After incubation was complete, plates were transferred to ice to quench phagocytosis before wells were topped up with ice cold 2% PBS-BSA. Plates were centrifuged at 250 x *g* for 5 min at 4°C applying maximum brake and acceleration and resuspended in ice cold 2% PBS-BSA. Plates were centrifuged (250 x *g* for 5 min at 4°C, maximum brake and acceleration) and washed in ice cold 2% PBS-BSA twice before being resuspended in 2% PBS-BSA and transferred to FACS tubes ready for analysis. BD Accuri C6 plus (BD Biosciences, Berkshire, UK) was used for flow cytometry analysis. Neutrophils were gated according to forward scatter and side scatter on unstained control samples. 10,000 neutrophil events were collected per

condition for each analysis. Median fluorescence intensity (MFI) values were recorded for entire neutrophil population in the FL2 channel for each condition.

2.10 Neutrophil NETosis assays

2.10.1 Immunofluorescence staining for NETs

2 x 10^5 neutrophils were seeded onto glass coverslips (Surgipath® Premier Cover Glass, Leica Biosystems, Wetzlar, Germany product no. 3800106G) in a 6 well plate (Sigma-Aldrich, Poole, UK product no. CLS3516) and incubated at 37°C, 5% CO_2 for 30 minutes. Coverslips were then flooded with RPMI 1640 and PMA (Sigma-Aldrich, Poole, UK product no. P1585) was added at a final concentration of 25 nM. Plates were returned to the incubator (37°C, 5% CO_2) for 3 hours. Post-incubation, 4% PFA (Sigma-Aldrich, Poole, UK product no. 47608) was added to fix the cells and the plate was incubated (37°C, 5% CO_2) for a further 30 minutes. Coverslips were washed 3 times in PBS (5 minutes per wash) at room temperature followed by one 1 minute wash with 0.1% triton x-100 (Sigma-Aldrich, Poole, UK product no: T8787) made up in PBS. Coverslips were washed again with PBS for 5 minutes before blocking using PBS containing 5% BSA and 5% goat serum (Fisher Scientific, Loughborough, UK, product no.11530526) for 30 minutes. Slides were incubated at room temperature in a humidified environment with 1 µg/mL primary antibody: rabbit anti-histone H3 (Abcam, Cambridge, UK, product no. ab5103) made up in PBS + 5% BSA + 5% goat serum for 1 hour. Post-incubation, slides were washed 3 times for 5 minutes with PBS and stained using the secondary antibody Goat Anti-Rabbit Alexa Fluor 350 (Fisher Scientific, Loughborough, UK, product no. 10347212) made up to 10 µg/mL in PBS containing 5% BSA and 5% goat serum for 1 hour in a humidified environment.

Coverslips were washed again 3 times with PBS for 5 minutes each before staining with 1 μM SYTOX® green (Fisher Scientific, Loughborough, UK product no. S7020) made up in PBS. Coverslips were washed for a final time with PBS for 5 minutes before being mounted onto microscope slides (Fisher Scientific, Loughborough, UK product no.17244884) using fluoromount medium (Fisher Scientific, Loughborough, UK product no.00-4958-02) and visualised using the Leica DMI 6000B microscope.

2.10.2 Quantification of NET release

2 x 10^5 neutrophils were added to each well of a 96 well flat-bottomed clear plate (Sigma-Aldrich, Poole, UK product no. CLS3997). Cells were stimulated with 25 nM PMA (or vehicle control) for 3 hours in an incubator (37°C, 5% CO_2). Post stimulation, supernatants were transferred to eppendorfs (Sigma-Aldrich, Poole, UK product no. AXYMCT150CS) and centrifuged at 2,200 x *g* for 10 minutes at 4°C. 100 μL of supernatant was transferred to a flat bottomed 96 well black plate and stained with 1 μM SYTOX® green made up in PBS for 10 minutes at room temperature in the dark. Fluorescence was measured using the BioTek Synergy 2 fluorometric plate reader with excitation and emission set at 485/20 nm and 528/20 nm respectively.

2.11 Neutrophil degranulation - protein release

To measure neutrophil degranulation/protease release, cells were exposed to e-cigarette vapour as described previously (section 2.6). Plates were centrifuged (250 x *g* for 5 minutes at 4°C) and the supernatants transferred to 1.5 mL microtubes. Supernatants were centrifuged at 400 x *g* for 5 minutes at room temperature with full brake and acceleration before being transferred to fresh 1.5 mL microtubes and stored

at -20 °C until assays were run. Quantikine® enzyme-linked immunosorbent assay (ELISA) kits (R&D Systems, Bio-Techne, Oxfordshire, UK) as detailed in table 2.3. ELISAs were performed as per the manufacturer's protocols. Briefly, samples were thawed, reagents and working standards prepared as per the kit-specific instructions. Assay diluent was added to each well, followed by appropriate amounts of standard, sample, or control in duplicate. Plates were sealed with adhesive strips provided and incubated for 2 hours at room temperature on a horizontal orbital microplate shaker set at 500 ± 50 rpm. Post-incubation, wells were washed four times using wash buffer provided and conjugate was added to each well. A new adhesive strip was used to seal the plate, and it was returned to the horizontal orbital microplate shaker for a further 2 hour incubation at room temperature. The wash steps were repeated, and substrate solution added to each well. The plates were incubated at room temperature on the benchtop, protected from light. Stop solution was added to each well, and the optical density determined using BioTek Synergy HT absorbance plate reader with wavelength set to 450 nm. A standard curve was generated, and the quantification of protein release extrapolated from the standard curve, accounting for the sample dilution factor (

Table *2.3*).

Name of protein	Product type	Manufacturer	Product number	LOT number	Top standard	Sample dilution factor
MPO	Quantikine ELISA kit	R&D Systems, Bio-techne	DMYE00B	P287906	10 ng/mL	1:2
MMP-2	Quantikine ELISA kit	R&D Systems, Bio-techne	MMP200	P281663	16 ng/mL	Neat
MMP-8	Quantikine ELISA kit	R&D Systems, Bio-techne	DMP800B	P268284 P262204	10 ng/mL	Neat
MMP-9	Quantikine ELISA kit	R&D Systems, Bio-techne	DMP900	P269601	10 ng/mL	1:10

Table 2.3: ELISA kits used to measure protein release by e-cigarette treated neutrophils.
Protein release into supernatants by e-cigarette treated neutrophils was measured using Quantikine ELISA kits by manufacturer Bio-techne. 4 proteins were measured; myeloperoxidase (MPO), matrixmetalloproteinase (MMP)-2, MMP-8 and MMP-9 and two plates were used per protein. Each sample was run in duplicate with the dilution factor indicated. Dilution factors were determined by performing Luminex analysis prior to running ELISAs.

2.12 Neutrophil metabolic assay

Agilent Seahorse XF96 analysers were used to perform two metabolic tests: the glyco stress test and oxidative burst test. Two metabolic tests were performed: the glyco stress test and the oxidative burst test. On the day preceding an assay, Seahorse XF96 cell culture microplates (Agilent, California, USA product no. 101085-004) were coated with Corning® CellTak (Fisher Scientific, Loughborough, UK product no. 10317081) (22.4 µg/mL diluted in 0.1 M $NaHCO_3$ (pH 8.0)) by applying 25 µL to each well, leaving for 20 minutes at room temperature before washing each well twice with 200 µL distilled water. The plates were stored at 4°C overnight and warmed to 37°C in a non-CO_2 incubator on the morning of the assay. In addition, on the day before assays, Seahorse XFe96 sensor cartridges (Agilent, California, USA product no. 102416-100) were hydrated by adding 200 µL distilled water to the utility plate and lowering the sensory cartridge into the wells. The assembled sensor cartridge was placed in a non-CO_2, 37°C incubator overnight. Finally, the Agilent Seahorse XF96 analyser was switched on and allowed to warm up to 37°C overnight.

On the day of the assay, human peripheral blood neutrophils were isolated as described in section 2.4 and resuspended to 4 x 10^6/ml in pre-warmed phenol red free RPMI (Sigma-Aldrich, Poole, UK product no. R8755) dissolved in 1 L distilled water, supplemented with L-glutamine (2 mM), sodium pyruvate (1 mM), glucose (10 mM) and HEPES (5 mM), pH 7.4, filter sterilised), which will be referred to as Seahorse media. Water was discarded from the utility plate and replaced with 200 µL pre-warmed Seahorse XF calibrant solution (Agilent, California, USA product no. 100840-000). The sensor cartridge was replaced into the calibrant and incubated in a non-CO_2, 37°C

incubator for 45-60 minutes. Meanwhile, 50 µL neutrophil solution was loaded into experimental wells of the CellTak-coated plate, and 50 µL Seahorse media into background/control wells. The plate was centrifuged at 200 x *g* for 1 minute with maximum acceleration but no brake at room temperature before incubation in a non-CO_2, 37°C incubator for 25-30 minutes. 130 µL warm Seahorse media was gently added down the side of each well, taking care to avoid disturbing the cells. The base of the plate was observed under a light microscope to ensure cells were still adherent, and the plate was transferred back to the non-CO_2, 37°C incubator for a further 15-25 minutes. Meanwhile, 25 µL of each inhibitor/stimulant outlined in Table 2.4 was added to the injection ports A-C of the sensor cartridge, following the loading strategy outlined in Figure 2.6. The sensor cartridge and utility plate were then placed on the tray of the Seahorse XFe96 analyser and allowed to undergo equilibration and automated calibration. Once this was completed, the utility plate was replaced with the cell plate and the assay was run using the protocol: 4 baseline measurements: 2 min 30 sec mix, 30 sec wait, 3 min measure, Port A injection, 3 measurements: 2 min 30 sec mix, 30 sec wait, 3 min measure, Port B injection, 3 measurements: 2 min 30 sec mix, 30 sec wait, 3 min measure, Port C injection, 20 measurements: 2 min 30 sec mix, 30 sec wait, 3 min measure. The procedure steps were pre-set on the protocol template made using the Seahorse Wave Desktop software version 2.6.

The oxygen consumption rate (OCR) and extracellular acidification rate (ECAR) were recorded for both metabolic tests. To analyse glyco stress test data, a pre-formatted template was used to generate values for non-glycolytic acidification, glycolysis, glycolytic capacity and glycolytic reserve from the ECAR traces, as shown in Figure

2.7A. To analyse oxidative burst test data, area under the curve analysis was performed using GraphPad Prism to generate values for time to max OCR, maximum OCR and total oxygen consumption, as shown in Figure 2.7B.

Compound	Action	Working conc.	Injection port (A-C)		Final conc.
			Glyco Stress Test	Oxidative Burst Test	
Oligomycin	Inhibits mitochondrial complex V	16 mM	B	-	2 µM
Antimycin A	Inhibits mitochondrial complex III	20 µM	-	B	2 µM
Rotenone	Inhibits mitochondrial complex I	20 µM	-	B	2 µM
2-DG	Glycolysis inhibitor	500 mM	C	-	50 mM
PMA	Activator of neutrophils via NOX2	1.6 µM	A	C	160 nM
Seahorse media	N/a	N/a	-	A	N/a

Table 2.4: Inhibitors and stimulants used in the Agilent Seahorse XF96 neutrophil metabolism protocol.

Neutrophils were isolated as described in section 2.4 before being 2 x 10^5 were added to required wells of a CellTak-coated Seahorse XF96 microplate. 2 metabolic tests: glyco stress and oxidative burst to PMA stimulation were performed. 25 µL of each inhibitor/stimulant outlined in the table were added to injection ports A-C for each test, as indicated. Upon injection into the well, inhibitors and stimulants were diluted approximately 10 times. Inhibitors and stimulants were reconstituted in Seahorse media. A schematic diagram of the injection ports referred to is shown in Figure 2.6. Abbreviations: PMA: phorbol 12-myristate 13-acetate, 2-DG: 2-Deoxy-d-glucose

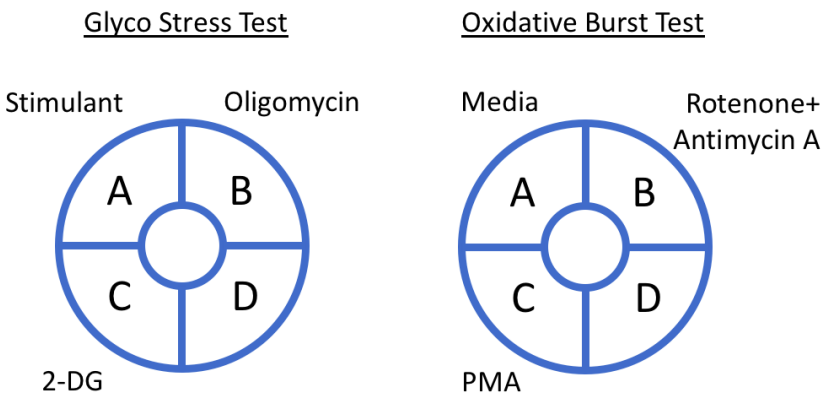


Figure 2.6: A schematic diagram of the injection ports of the Agilent Seahorse XF96 sensor cartridge.

The injection strategy for each metabolic test is outlined by the labels. 25 µL of stimulant/inhibitor was added to each port and injected into the well beneath during the procedure by the analyser. The injection/mix/wait/measure cycles are pre-programmed into the Wave software protocol template.

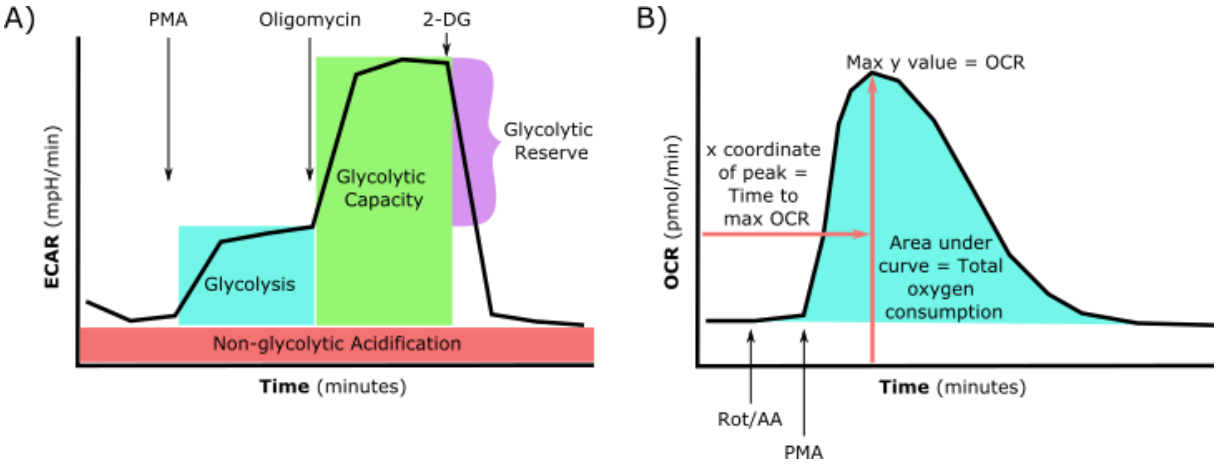


Figure 2.7: Schematic diagrams of ECAR and OCR traces generated during the glyco stress test and oxidative burst test.
A) The extracellular acidification rate (ECAR) was measured over time, while 160 nM phorbol 12-myristate 13-acetate (PMA), 2 µM oligomycin and 50 mM 2-Deoxy-d-glucose (2-DG) were injected sequentially to push the glycolytic system to its maximum. The results were exported to a pre-formatted analysis template which calculated the glycolytic parameters: non-glycolytic acidification, glycolysis, glycolytic capacity, and glycolytic reserve, as indicated. B) The oxygen consumption rate (OCR) was measured over time, while 2 µM rotenone/2 µM antimycin A (Rot/AA) then 160 nM PMA were injected sequentially to induce an oxidative burst response. The OCR trace was exported to GraphPad Prism, where an area under the curve analysis was performed to determine the maximum OCR, time to reach maximum OCR and total oxygen consumption over the duration of the test for each sample. Adapted from (Swain et al., 2018)

2.13 Calcium signalling assay

Calcium signalling was measured using the Fluo-4 Direct™ calcium assay kit (Thermo Fisher Scientific, Loughborough, UK product no. F1071) following the manufacturer's protocol. Briefly, neutrophils were resuspended in Fluo-4 Direct™ calcium assay buffer and 5 x 10^4 neutrophils were added to each well of a flat bottomed 96 well black plate and incubated at 37°C and 5% CO_2 for 60 minutes. A 2X Fluo-4 Direct™ calcium reagent solution was reconstituted, containing 5 mM probenecid and an equal volume as the cells was added to each well. The plate was incubated at 37°C and 5% CO_2 for 45 minutes and then 15 minutes at 21°C in the BioTek Synergy 2 fluorometric plate reader with excitation and emission set at 485/20 nm and 528/20 nm respectively. A reading was taken every minute for 3 minutes, before a 2 minute interval to add 0.6 or 3 μM nicotine or 2.5 μM thapsigargin (Sigma-Aldrich, Poole, UK product no. T9033). The plate was returned to the plate reader for 12 further measurements, 1 minute apart. There was a significant time delay between e-cigarette exposure and measurement of cytoplasmic calcium signal (approx. 2 hours), which should be noted.

2.14 Graph and figure generation

All graphs were generated using GraphPad prism (Version 9.0.2 for Mac, GraphPad Software, San Diego, California USA). Except where data presentation by a different graph type was preferable, data is presented as tukey box and whisker diagrams where the box represents median and interquartile range (IQR) values, and whiskers represent the minimum/maximum points. Outlier values are automatically displayed as separate points using GraphPad prism. For data with replicate values of less than 6, data is presented as aligned dot plots, with dots representing biological replicates with

median and IQR values indicated. Schematic diagrams and other figures were produced using Inkscape (Version 1.1 for Mac, Inkscape.org).

2.15 Statistical analysis

All statistical analysis was performed using GraphPad prism (Version 9.0.2 for Mac, GraphPad Software, San Diego, California USA). Descriptive statistics were used to deduce basic parameters of the data sets including averages and interquartile ranges. Shapiro-Wilk test of normality was performed to determine whether data was normally distributed. Data containing less than six replicates were considered not normally distributed. Where all groups in a dataset were normally distributed according to the Shapiro-Wilk test ($p > 0.05$), parametric tests were used to assess statistical difference. Where one or more groups were not normally distributed ($p < 0.05$), non-parametric tests were used to assess statistical significance. Paired and unpaired t-tests, one and two way ANOVA, Wilcoxon matched-pairs signed rank tests and Mann-Whitney tests were performed where appropriate to determine if there were differences between control and treatment groups, and between treatment groups. A p value less than 0.05 was considered to be statistically significant, and is marked by an asterisks on data graphs. This workflow is summarised in Figure 2.8.

2.15.1 Power calculations

Where differences were seen between treatment groups, but the results were not statistically significant, power calculations were performed. https://clincalc.com/stats/samplesize.aspx was used to calculate the sample size

required to reach statistical significance. Mean and standard deviation values were input to the website, applying a power of 80% and an alpha value of 0.05.

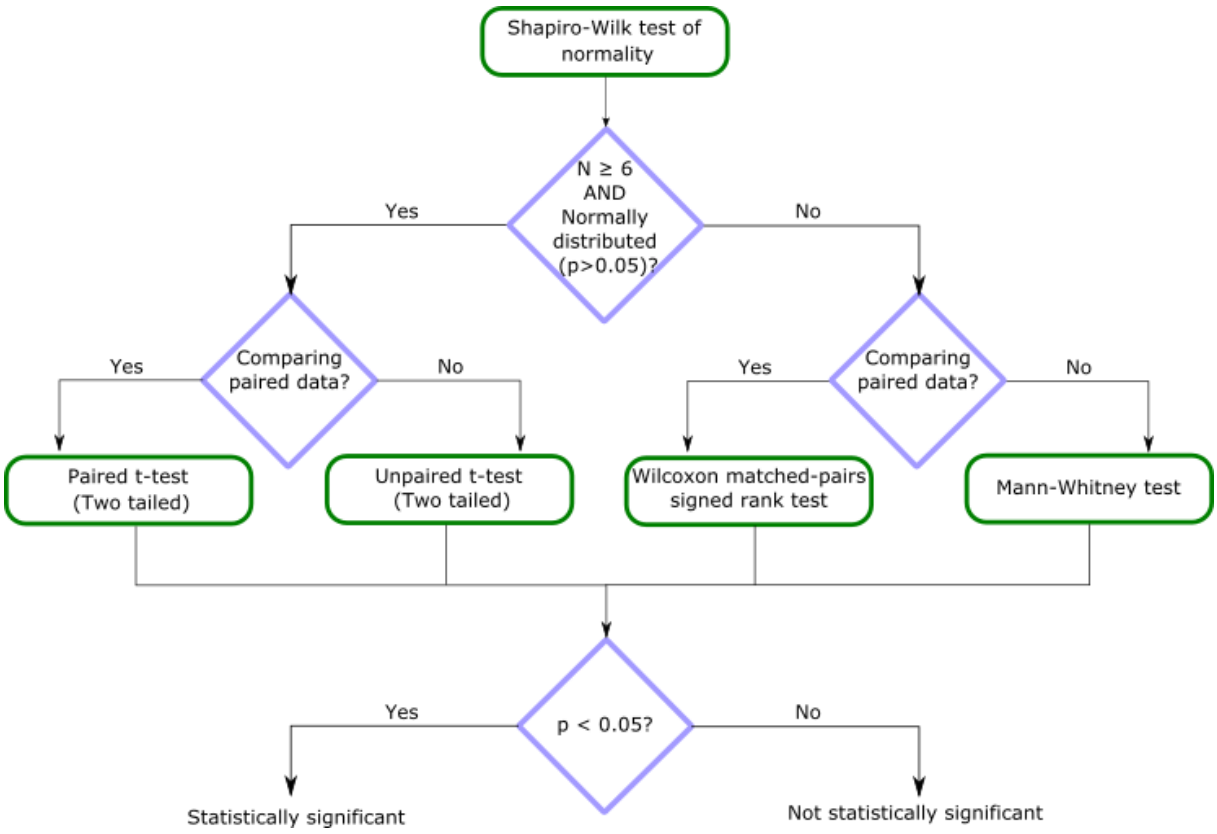


Figure 2.8*: An overview of the approach to statistical analysis used in this thesis* Data was tested for normality using the Shapiro-Wilk test. If data was normally distributed (Shapiro-Wilk, $p > 0.05$ AND $n \geq 6$), a Wilcoxon matched-pairs signed rank test or paired t-test (two tailed) was performed, depending on whether the comparison was between paired or unpaired data. If data was not normally distributed (Shapiro-Wilk, $p < 0.05$ or $n \leq 6$), a Mann-Whitney test or unpaired t-test (two tailed) was performed, depending on whether the comparison was between paired or unpaired data. All statistical tests were performed using GraphPad Prism Version 9.0.2 for Mac

Chapter 3 - ASSAY OPTIMISATION AND VALIDATION

Foreword: Chemical analysis of samples in section 3.4.2.1 was performed by colleagues in the school of Chemistry at the University of Birmingham. Validation of metabolic assay protocols by Seahorse, in section 3.4.6 was performed in collaboration with Dr. Frances Grudzinska and with advice from Dr Jonathan Barlow. Ribonucleic acid (RNA) yield analysis by Tapestation in section 3.4.9 was performed by colleagues at Genomics Birmingham.

3.1 Chapter 3 introduction

Assay optimisation and validation are essential steps in the set-up of a study, even when using commercially available kits or pre-designed protocols. Optimisation is defined as a set of experiments that determines how a range of assay elements effects the assay outcomes or performance. This includes, for example, the number of cells used in an assay and reagent concentrations. Validation is defined as a set of experiments that quantify the performance, reproducibility, or detection range of an assay. For example, ensuring there is a detectable difference between negative and positive controls in an assay. Together, these steps build confidence in results and add robustness to conclusions drawn from resulting experiments.

Work in the e-cigarette field has used a range of exposure models, from extract to condensate (Hwang et al., 2016, Scott et al., 2018, Corriden et al., 2020). This study is the first to use a novel e-cigarette vapour model developed to assess neutrophil functions. Therefore, it was essential to optimise protocols to ensure they would work correctly in this context, and that the results presented, were caused by the effect of e-cigarette vapour on neutrophils, not an artefact of vaping itself. Although much of this

work was based on previously validated protocols and procedures, validation and optimisation were required to ensure the main aims of this thesis were being answered by the experimental design.

3.2 Aims of chapter 3

1. To establish and validate a novel e-cigarette vapour exposure model.

2. To perform validation and optimisation experiments to ensure protocols work effectively and consistently to address the aims of this thesis.

3.3 Materials and Methods linked to chapter 3

3.3.1 Nicotine deposition - Gas chromatography with flame ionization detector

100 μL RPMI 1640 was added to each well of a 96 well flexi plate. 40 puffs of 2nd generation and 4th generation e-cigarette vapour generated were using unflavoured, 36 mg/mL nicotine e-liquid by the system described in section 2.7. The plate was divided into 8 sections and 12 wells in each section were combined to produce 1.2 mL of vaped media corresponding to different areas of the plate. The solutions were stored in a -20°C freezer for 24 hours before being sent to colleagues at the analytic facility in the University of Birmingham chemistry department where gas chromatography with flame ionisation detection (GC-FID) analysis was performed as described previously (Scott et al., 2018) to determine the nicotine concentration.

3.3.2 Calcein AM staining for transwell migration

Neutrophils were resuspended at 1 x 10^{7}/mL in HEPES buffer with 1 mM Ca^{2+} and calcein AM (Life technologies, product no. C1430) was added at a concentration of 3

µg/mL. Cells were incubated in a water bath at 37ºC for 30 minutes before being centrifuged at 250 x g for 10 minutes at room temperature (maximum brake and acceleration) and resuspended at 1 x 10^7/mL in phenol red-free RPMI + GPS + 10% FCS. 100 µL of stained neutrophils (total 1 x 10^6) was added to the transwell inserts and the plate transferred to a 37ºC, 5% CO_2 incubator for 90 minutes. Transwell inserts were removed and a standard curve of 0-1 x 10^6 calcein AM-stained neutrophils was added to the plate and the fluorescence intensity measured on a Synergy 2 plate reader set to excitation: 485/20 nm and emission: 528/20 nm. The number of neutrophils migrated was determined by producing a standard curve of fluorescence and determining the fluorescence intensity of each well.

3.3.3 Measuring pHrodo™ bioparticle fluorescence

100 µL RPMI (pH 8.0, 7.4, 6.0, 5.0, 4.0 (± 0.05)) or pHrodo™ buffer (pH 7.2) was added to each well of a 96 well clear bottom black sided plate (Sigma Aldrich, product no. CLS3603). 50 µL *E. coli* or *S. aureus* pHrodo™ bioparticles (ThermoFisher Scientific, product no. P35366 and P35367) was added to each well and incubated for 90, 60, 45, 30, 15 or 0 minutes at room temperature protected from light. Fluorescence was measured using the Synergy 2 plate reader set to 485/20 nm excitation and 528/20 nm emission.

3.3.4 Validation of cytochalasin D concentration for inhibition of phagocytosis.

Isolated human peripheral blood neutrophils were resuspended to 1 x 10^6/mL in RPMI 1640 and 1 x 10^5 were added to each well of a 96 well flexi plate. Cells were incubated with 0, 20 nM, 200 nM, 2 µM, 20 µM, 40 µM or 200 µM cytochalasin D (CytD) for 20

minutes before addition of red or green *E. coli* or *S. aureus* pHrodo™ bioparticles for 60 minutes. The percentage of cells in the pHrodo™ positive population was recorded, as well as the MFI of the whole plot using a BD Accuri flow cytometer.

3.3.5 Assessing the effect of CellTak on neutrophil viability

Neutrophils were resuspended at 1 x 10^6/mL in Seahorse media. 4 wells of an 8 well chamber culture slide (Corning Life Sciences, Amsterdam, The Netherlands, product number: 354118) were coated with 100 µL CellTak (22.4 µg/mL in 0.1 M NaOH) for 20 minutes at room temperature before being washed twice with sterile water. Four wells were coated with 2% BSA-PBS for 20 minutes (and not washed off). 1 x 10^5 neutrophils were added per well, including some heat killed (70°C, 2 minutes 15 seconds). The chamber slide was centrifuged at 200 x *g*, RT, for 1 minute with no brake before being incubated for 1 hour at 37°C. Cells were stained with Annexin V-FITC (Miltneyi Biotec Ltd, Surrey, UK product no. 130-097-928) diluted 1:400 in annexin binding buffer for 20 minutes, protected from the light. Each well was gently washed 3 times with annexin binding buffer (centrifuged for 5 mins at 300 x *g*, RT, in between each wash) before suspending in 200 µL annexin buffer. 2 µL PI was added just before imaging. Imaging was performed using the Leica DM6000 microscope. A 20x brightfield image was captured and overlayed with two images generated using the FCr2, L5 and FCr3, N3 lenses.

3.4 Chapter 3 results

3.4.1 Donor demographics

72 healthy volunteers were recruited for blood donations from staff, students and visitors at the Institute of Inflammation and Ageing at the Queen Elizabeth Hospital Birmingham. The average age of donors was 30 years (19-63). 54.1% of volunteers were female and 75.0% Caucasian. Further details can be found in

Table *3.1*. All volunteers were self-reported non-smokers and non-vapers. Some volunteers were bled multiple times over the duration of the project for the purposes of performing different functional tests however, n numbers for each experiment represent the number of individual donors used to generate the data shown, unless stated otherwise. The median age reported in the demographics table accounts for multiple bleeds over time and their age at the time of bleeding.

Total number of donors		72
Age, median (range)		30 (19-63) years
Sex, % Female		54.1%
Ethnicity	Caucasian	75.0%
	Asian	13.9%
	African	2.8%
	Other/unknown	8.3%

Table 3.1*:* The demographics of study participants who donated blood for the purposes of this project.
All participants were otherwise healthy staff, students and visitors to the Institute of Inflammation and Ageing who were self-reported non-smokers and non-vapers. Some donors were bled on multiple occasions during the duration of this project, and their neutrophils used for different functional and mechanistic experiments. The median age accounts for age on each occasion they were bled.

3.4.2 E-cigarette vapour model validation

As discussed in section 1.3, a range of e-cigarette vapour exposure models have been developed for studying their effects *in vitro*. Each have advantages and disadvantages of their use. More recently, studies have employed the use of automated vaping robots to ensure consistency in e-cigarette vapour exposure. Here, we developed an in-house version of this exposure system, employing a modified hypoxia chamber, the set up of which is described in section 2.6.

3.4.2.1 GC-FID results

It was essential to quantify the amount of nicotine depositing into cell media, representing the amount of nicotine neutrophils will be exposed to during treatments. RPMI 1640 was exposed to e-cigarette vapour, as in the treatments, and the nicotine content analysed by GC-FID. Kentucky research cigarettes averaged 94 µg/mL (87-114 µg/mL) (0.58 µM) nicotine over 20 minutes of exposure as shown in Figure 3.1A. 2nd generation e-cigarette vapour treatment generated an average nicotine deposition of 97.5 µg/mL (87-118 µg/mL, Figure 3.1B) (0.6 µM), similar to the research cigarettes in this setting. 4th generation e-cigarette vapour deposited an average of 494.9 µg/mL (447-641 µg/mL) (3 µM) nicotine as shown in Figure 3.1C.

Overall, this data suggested higher power, higher temperature 4th generation devices have a greater nicotine deposition into media than 2nd generation devices. Nicotine deposition was starkly increased in the 4th generation device compared to Kentucky research cigarettes.

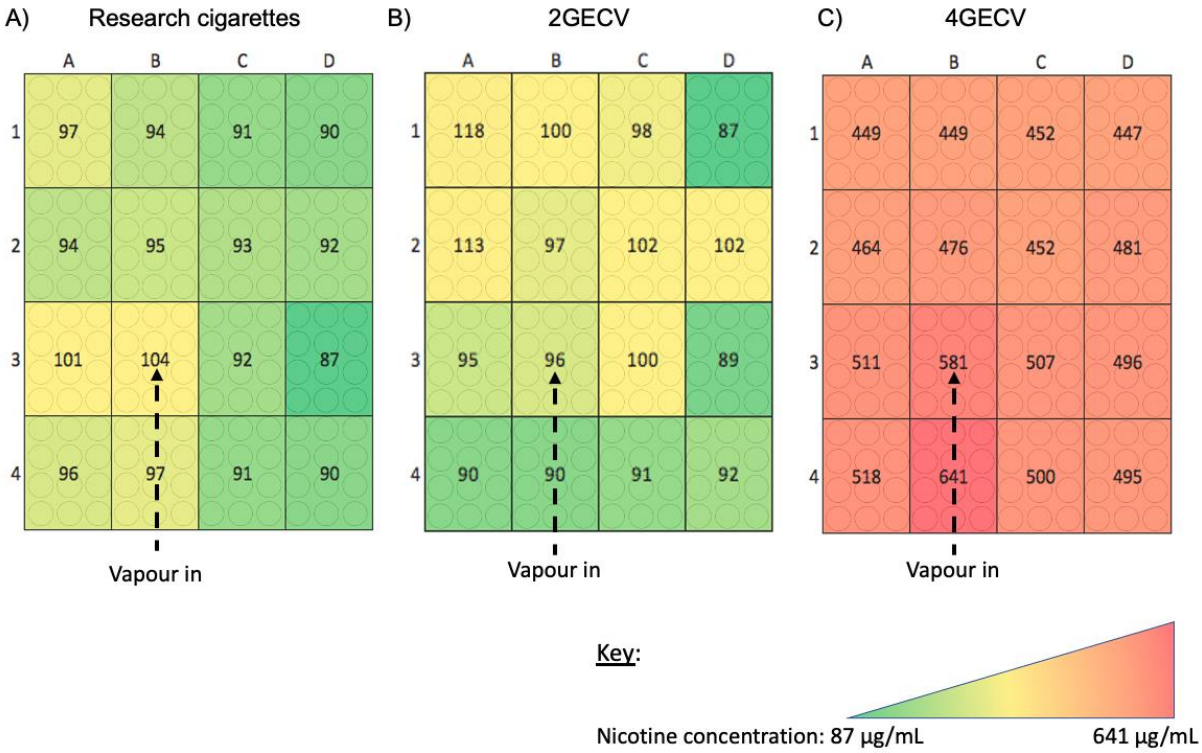


Figure 3.1: Heat maps showing the distribution of nicotine across the e-cigarette vaping chamber used in this study.
2 x 96 well plates were loaded with 100 µL per well of RPMI-1640, placed into the e-cigarette vaping chamber and exposed to 40 puffs of a) Kentucky research cigarettes, b) 2nd generation e-cigarette vapour (2GECV), c) 4th generation e-cigarette vapour (4GECV) over a 20-minute period. The samples were analysed for nicotine content by gas chromatography with flame ionization detection (GC-FID). Numbers represent the nicotine content in µg/mL for that area of the plate. In total, 8 Kentucky research cigarettes were used, and the e-cigarettes were filled with unflavoured 36 mg/mL nicotine containing e-cigarette liquid (50/50 PG/VG).

3.4.2.2 Neutrophil viability after e-cigarette exposure

Previous work carried out in our laboratory showed low levels of e-cigarette vapour condensate can be toxic to macrophages (Scott et al., 2018), highlighting the need to test the potentially toxic effects of direct vapour exposure on neutrophils.

Annexin V-FITC and PI staining were used to assess stages of viability. Figure 3.2 shows the gating strategy used to gather viability data. Figure 3.3 shows the proportion of live, apoptotic and necrotic cells in untreated and e-cigarette vapour exposed neutrophils. E-cigarette treatments did not affect neutrophil viability compared to UTC, see Figure 3.3. On average, 93.3% (median) of UTC neutrophils were live and viable (2GNF: 92.1%, 2GECV: 96.7%, 4GNF: 89.2%, 4GECV: 86.2% (median)). There were no significant differences in the percentage of live neutrophils between treatment groups and UTC, or between e-cigarette treatment groups. The majority of cells which weren't live were apoptotic (UTC: 7.3%, 2GNF: 4.7%, 2GECV: 4.8%, 4GNF: 11.4%, 4GECV: 7.6% (all median values). There were no significant differences between the proportion of apoptotic cells in e-cigarette treatment groups compared to UTC or compared to other treatment groups. There were minimal necrotic cells in all groups, with no significant differences between any of the groups, as shown in Figure 3.3.

This data showed there was no significant impact on neutrophil viability caused by the e-cigarette vapour exposure system used in this project. It was essential to categories the impact of this model on neutrophil viability to ensure any functional changes were not just a result of impacted viability.

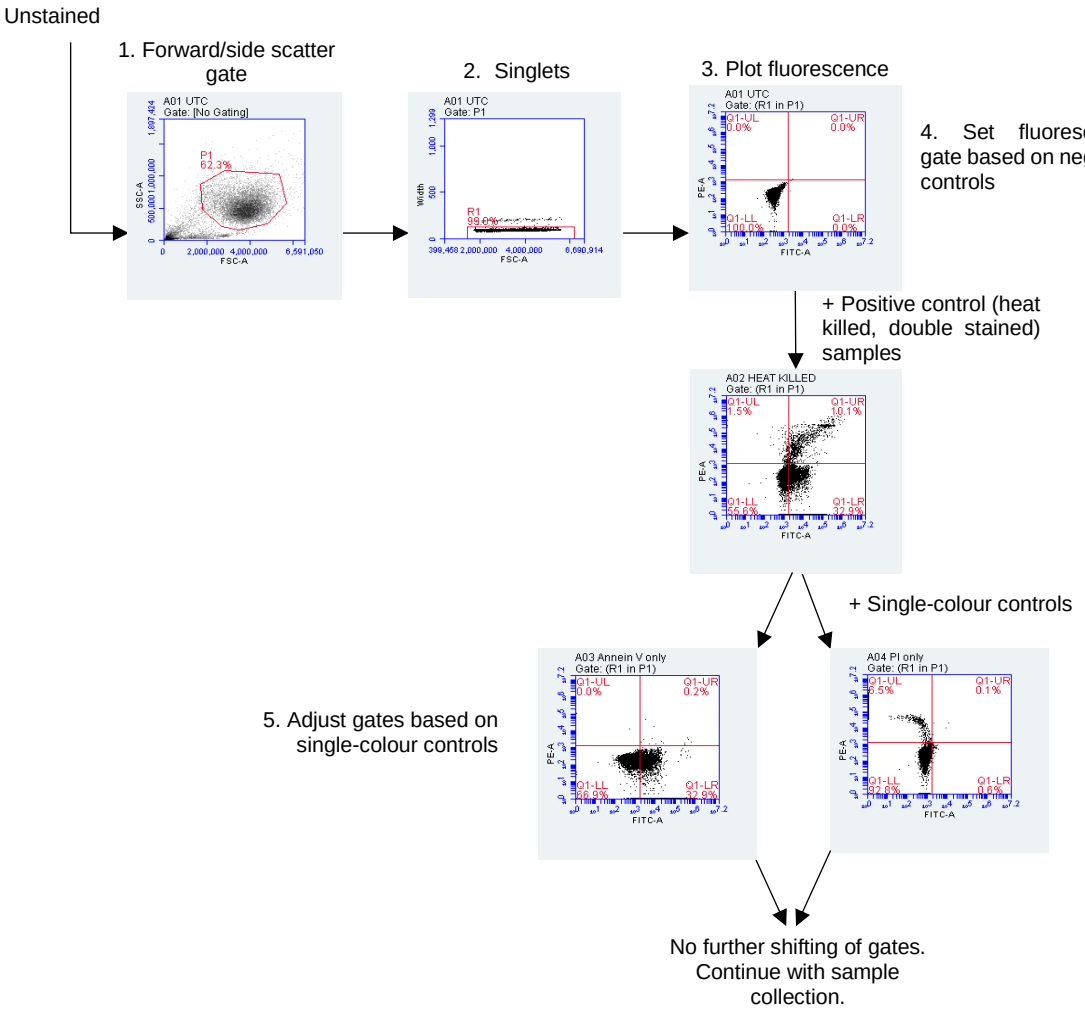


Figure 3.2: The gating strategy used to assess neutrophil viability.
1) Unstained cells were run through the FACSvia, and the neutrophil population was gated (gate P1) according to forward scatter (FSC-A) (size) and side scatter (SSC-A) (granularity). 2) Neutrophils in the P1 gate were carried over to a second plot, where singlets were gated (gate R1) according to forward scatter and width, as shown. 3) Cells meeting the requirements of P1 and R1 were plotted on a final plot of FITC-A (Annexin V positivity) vs. PE-A (Propidium iodide (PI) positivity). 4) The gate was set based on the double negative unstained control cells. 5) Single stain controls - stained with Annexin V only or PI only - were run, and the gates shifted minimally to ensure they were placed correctly, and were not shifted again during sample collection. A heat killed (70 °C for 1 minute 15 seconds) was included to ensure both stains were working correctly. Cells appearing in the lower left quadrant (Annexin V^{low}, PI^{low}) were considered live cells. Cells in the lower right quadrant (Annexin V^{high}, PI^{low}) were considered early apoptotic cells while those in the upper right quadrant (Annexin V^{high}, PI^{high}) were considered late apoptotic. Cells in the upper left quadrant (Annexin V^{low}, PI^{high}) were considered necrotic.

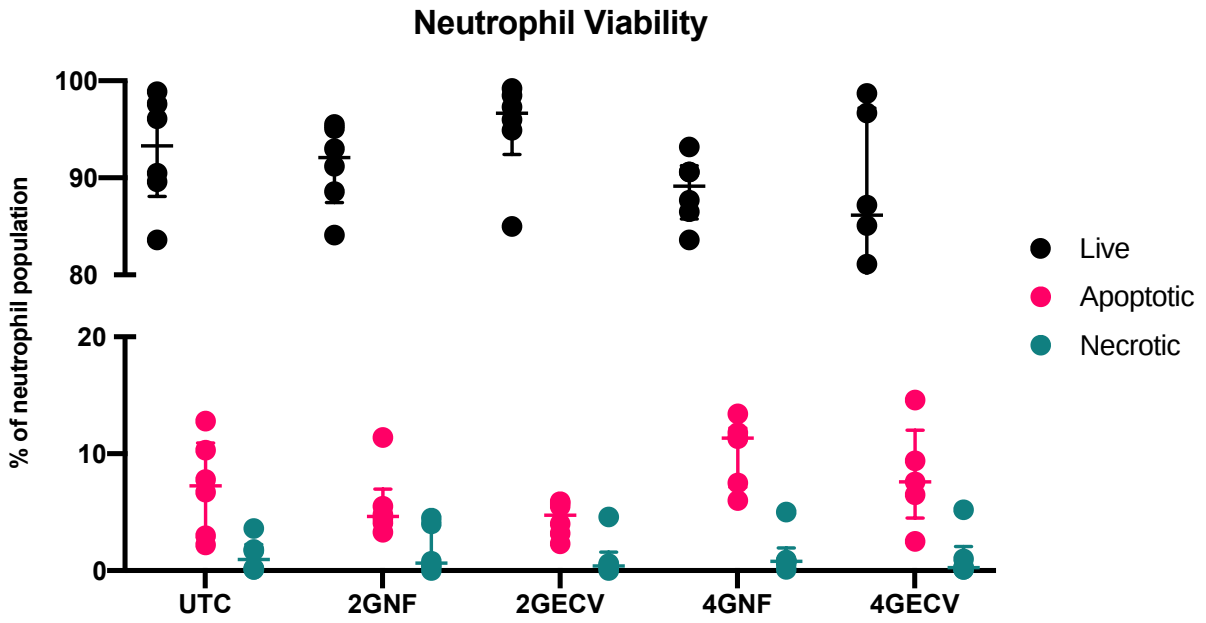


Figure 3.3: The effect of e-cigarette vapour exposure on neutrophil viability at baseline.
Neutrophils were exposed to 40 puffs of e-cigarette vapour over 20 minutes before being stained using annexin V-FITC and propidium iodide. The gating strategy outlined in Figure 3.2 was applied and the percentage of cells falling into each quadrant was recorded to determine the percentage of live cells, apoptotic cells and necrotic cells. Bars represent the mean and error bars represent the standard deviation from the mean. Data was not normally distributed (shapiro – wilk) and mann-whitney tests were performed. There were no significant differences between e-cigarette treatments compared to baseline, or between e-cigarette groups. N = 6 per group. UTC = untreated control, 2GNF = 2nd generation nicotine free e-cigarette vapour, 2GECV = 2nd generation nicotine-containing e-cigarette vapour, 4GNF = 4th generation nicotine free e-cigarette vapour, 4GECV = 4th generation nicotine-containing e-cigarette vapour.

3.4.3 CXCL8 as a chemoattractant for neutrophil chemotaxis in the Insall chamber model

To ensure the Insall chamber system was operating as previously (Sapey et al., 2011, Sapey et al., 2014, Sapey et al., 2017), validation experiments comparing migration of UTC neutrophils to 100 nM CXCL8 (positive control) and RPMI (negative control, no chemoattractant gradient) were performed. Figure 3.4A and B are representative traces of neutrophil migration in these presence and absence of a chemoattractant gradient. Traces, such as those shown in Figure 3.4A and B were used to generate values for chemotactic parameters in Figure 3.4C-F. 100 nM CXCL8 significantly upregulated neutrophil chemotactic parameters: velocity ($p = 0.0026$, Figure 3.4C), speed ($p = 0.0310$, Figure 3.4D), and chemotactic index ($p = 0.0029$, Figure 3.4F). There was no change in persistence of neutrophil chemotaxis, as shown in Figure 3.4E.

Overall, this data suggested 100 nM CXCL8 is a robust chemoattractant, supporting previous findings. By using the same concentration and chemoattractant as existing work, subsequent chemotaxis data can be compared to chemotactic parameters of neutrophils in age, pneumonia, sepsis and COPD (Sapey et al., 2011, Sapey et al., 2014, Sapey et al., 2017, Sapey et al., 2019, Wilson et al., 2020). Here, 100 nM CXCL8 upregulates neutrophil chemotaxis parameters compared to baseline in the Insall chamber system, and these increases are consistent with previous data using the same chemoattractant and Insall chamber methods.

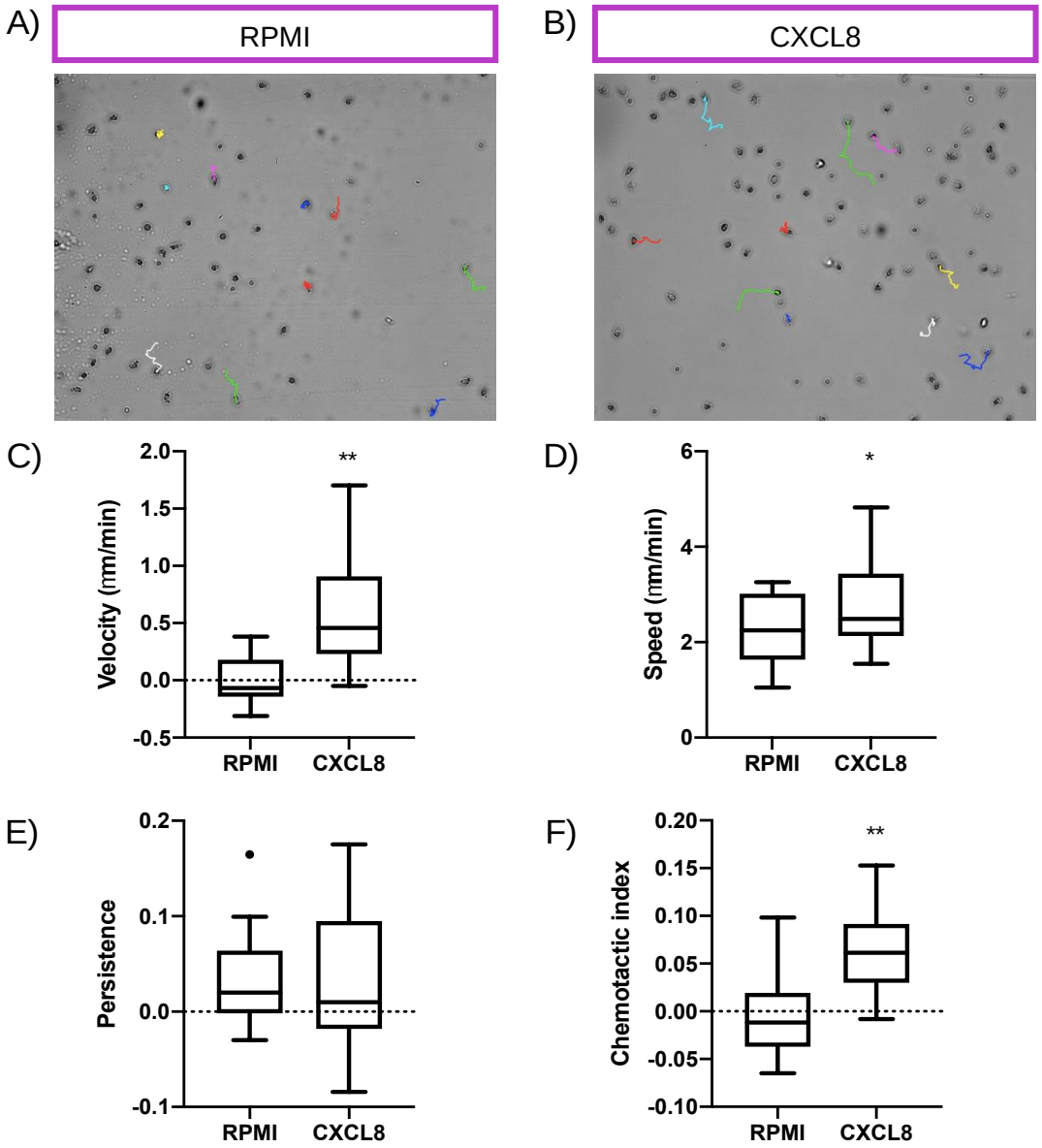


Figure 3.4: Neutrophil chemotaxis is upregulated in response to 100 nM CXCL8 using the Insall chamber.
Neutrophil chemotaxis was measured using the Insall chamber, as described in section 2.10.1. RPMI was used as a control, whereby no chemotactic gradient was generated across the chamber slide. Here, RPMI was compared directly to 100 nM CXCL8. 10 random neutrophils were tracked using the manual tracking plugin on FIJI Image J. A and B are representative images of tracked neutrophils migrating in the absence (A) and presence (B) of the chemoattractant CXCL8. The chemoattractant well is above the field of view, as indicated. The traces are used to generate measurements for the chemotaxis parameters: C) velocity, D) speed, E) persistence and F) chemotactic index (as defined in Table 2.2). Data was normally distributed (shapiro-wilk test of normality) and paired t-tests were performed to test for differences between the groups. A significant difference between chemoattractants is indicated by an asterix. * = $p \leq 0.05$, ** = $p \leq 0.01$, *** = $p \leq 0.001$, **** = $p \leq 0.0001$, n = 13.

3.4.4 Transwell migration validation work

Previously, the transwell migration protocol applied to this project had quantified neutrophil transmigration by staining with 3 µg/mL calcein AM, and then measuring fluorescence intensity on a plate reader. Next, the fluorescence intensity of each well was compared to a standard curve to deduce the number of neutrophils which had transmigrated. Despite previous success, this method of measuring transwell migration lacks precision due to limitations of plate reader readouts.

3.4.4.1 Measuring migration by fluorescence

To determine whether the existing calcein AM staining protocol could be used in the application of e-cigarette vapour, neutrophils were stained with calcein AM and then exposed to e-cigarette vapour before generating a standard curve of 0-1 x 10^6 neutrophils per well, as described in section 3.3.2. Neutrophils exposed to e-cigarette vapour exhibited lower baseline calcein AM fluorescence, as shown by the standard curves in Figure 3.5. This was a significant barrier to continuing with this method, as reduced fluorescence at baseline could result in artefactually low neutrophil readouts.

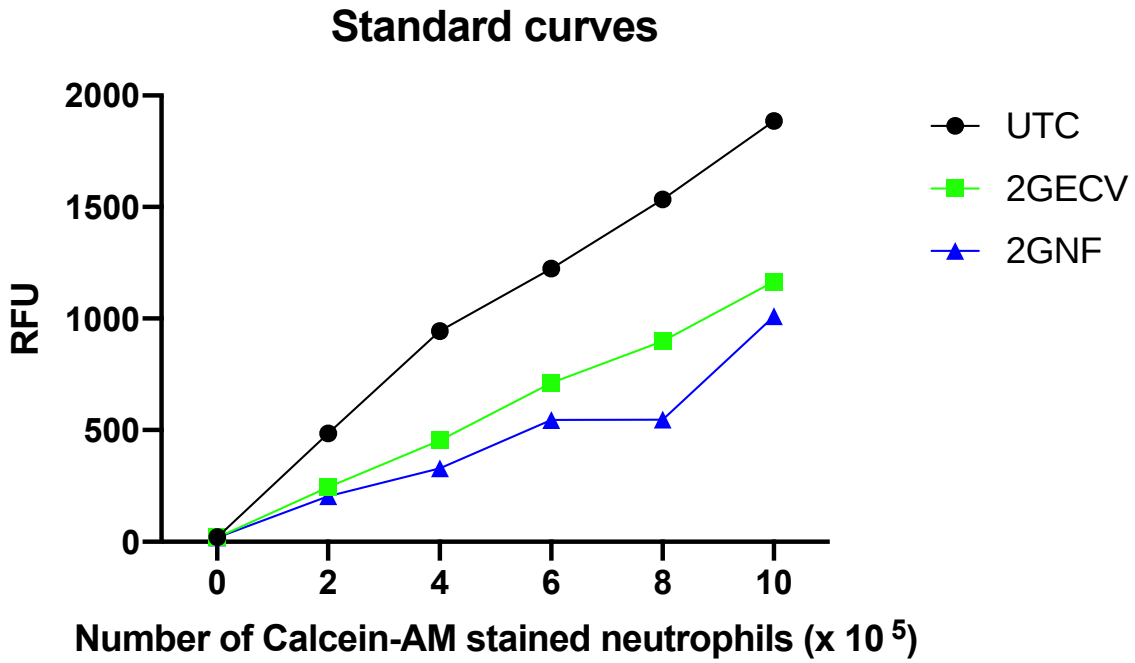


Figure 3.5: Fluorescence intensity of neutrophils stained with calcein AM before and after e-cigarette vapour exposure.
Neutrophils were stained with 3 µg/ml calcein AM and exposed to 2nd generation e-cigarette vapour (with and without nicotine) or untreated (UTC). 0-1 x 10^6 neutrophils added to each well before the fluorescence intensity was measured using the Synergy 2 plate reader set to excitation: 485 nm and emission: 528 nm. Standard curves represent the median relative fluorescence unit of n = 2 individual experiments for each condition.

3.4.4.2 Measuring migration by FACS

To measure neutrophil transmigration in a way that would not be affected by e-cigarette vapour exposure and with greater precision, methods that count individual migrated cells were investigated. Figure 3.1A&B shows one example of an experiment comparing the number of cells counted on a plate reader compared to on the flow cytometer. The plate reader overestimated the cell count in the lower range, but underestimated the cell count in the higher range. This is often the case with standard curve- based assays as a range of, in this case, a range of 0 to 1 x 10^6 cells is compressed into a 0-1500 scale, reducing the accuracy of the reading. The plate reader produced a significantly different cell count readout than the flow cytometer method ($p = 0.0210$, Figure 3.6B). On average, the plate reader method of measuring transwell migration by fluorescence estimated an 8.9-fold higher cell count readout than when the number of cells was counted by FACS (see Figure 3.6D).

Together, this data shows transwell migration readouts were different between FACS and plate reader methods. Due to the ability to detect smaller iterations means counting via flow cytometry, cell counting using flow cytometry was the method used for subsequent transwell migration experiments.

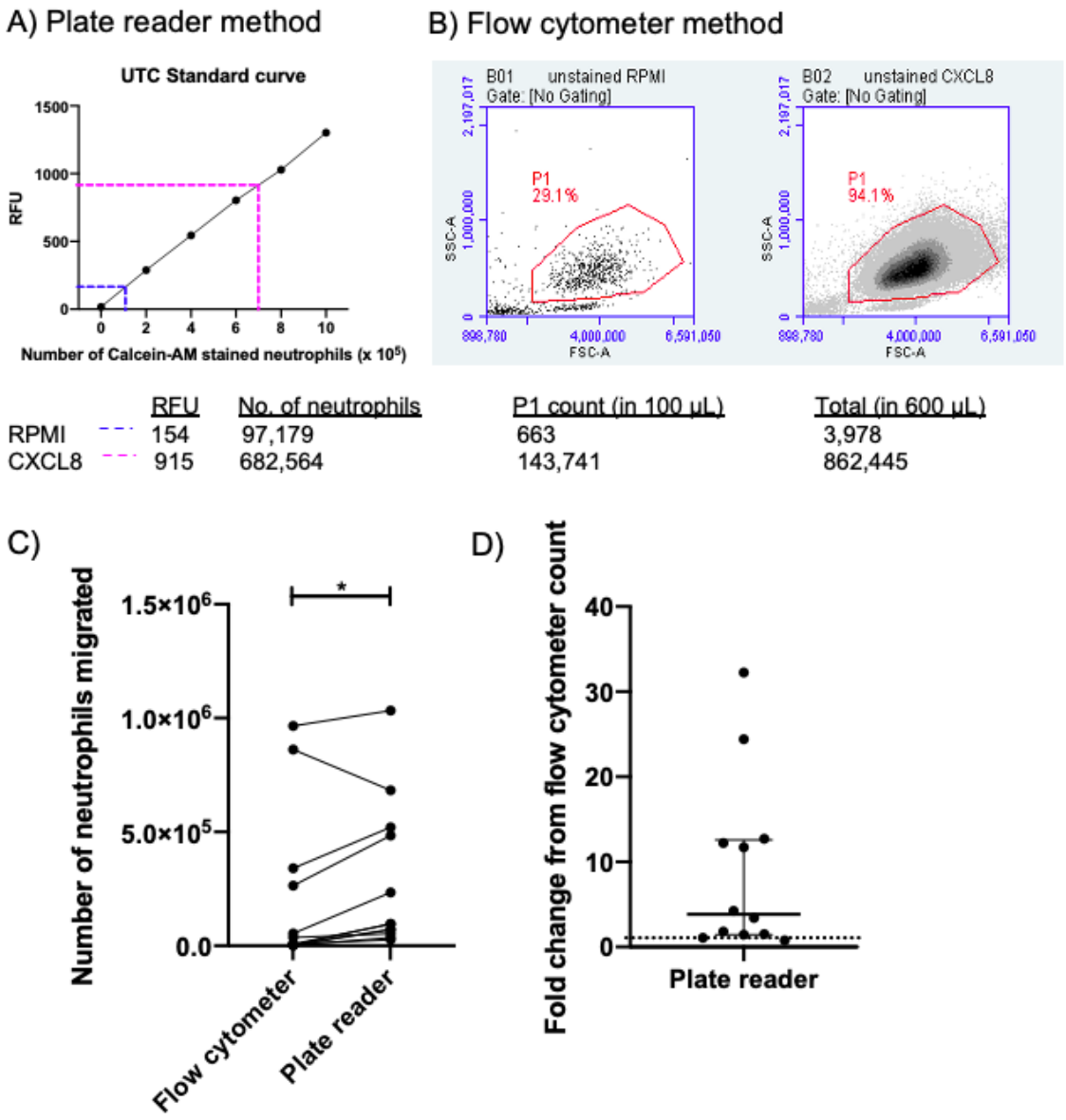


Figure 3.6: Comparing plate reader to flow cytometer methods of measuring neutrophil transmigration.
A and B represent the same experiment performed on neutrophils isolated from the same individual at the same time on the same day, with the cells migrating at the same time however A) shows the cell count when it was measured by counting using a flow cytometer, and B) shows the cell count when measured using the plate reader method. C) combines 12 experiments where the same comparison between counting techniques has been compared. The data was not normally distributed, so a wilcoxon matched-pairs signed rank test was performed to test for significant differences between the measuring techniques. A significant difference between counting techniques is indicated by an asterisks above a capped line. * = $p \leq 0.05$, ** = $p \leq 0.01$, *** = $p \leq 0.001$, **** = $p \leq 0.0001$. D) represents the fold change in the number of cells counted by the plate reader method compared to the flow cytometer count. The dotted line represents a fold change of 1 (indicating the results were the same across the techniques). Error bars represent the median and IQR of the data. N = 12.

3.4.4.3 CXCL8 as a chemoattractant for neutrophil transmigration in the transwell model

To ensure that 100 nM CXCL8 also produced a significant upregulation in transmigration in the transwell model, RPMI was compared to CXCL8 as chemoattractants. 100 nM CXCL8 significantly increased the number of cells migrating through the transwell over a 90 minute period ($p = 0.0002$, Figure 3.7).

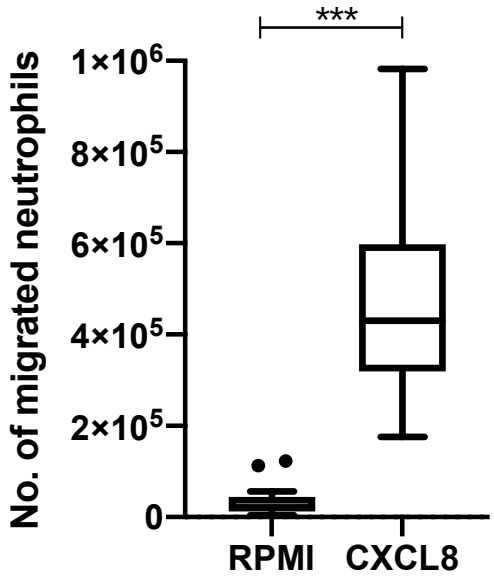


Figure 3.7: Neutrophil transmigration is upregulated in response to 100 nM CXCL8 using the transwell migration model.
Neutrophil transmigration was measured using transwell inserts, as described in section 2.10.2. RPMI was used as a control, whereby no chemotactic gradient was generated across the transwell. The number of cells migrating through the transwell was measured after 90 minute incubation on the transwell inserts. Here, RPMI is compared directly to 100 nM CXCL8. Data was not normally distributed (shapiro-wilk test of normality) and therefore wilcoxon matched pairs tests were performed to test for differences between the groups. A significant difference between chemoattractants is indicated by an asterix. * = $p \leq 0.05$, ** = $p \leq 0.01$, *** = $p \leq 0.001$, **** = $p \leq 0.0001$, n = 13.

3.4.5 pHrodo™ bioparticle assay validation

To assess neutrophil phagocytosis, the use of *E. coli* and *S. aureus* pHrodo™ bioparticles was validated. pHrodo™ uniquely exploits the pH drop associated with ingestion of bacteria into the phagosome, meaning the bacteria only fluoresce when they have been phagocytosed, reducing background fluorescence signals. By using both *E. coli* and *S. aureus*, we can also determine if there is a differential response to gram-positive and gram-negative bacteria. However, extensive validation to determine the most robust combination of bioparticle colour, incubation timecourse and negative control was performed.

3.4.5.1 Inter -batch variation and pHrodo™ bioparticle colour consideration

Green pHrodo™ bioparticles had a higher fluorescence intensity than red bioparticles, allowing discrimination of smaller changes in phagocytosis. In addition, when a new batch of red pHrodo™ bioparticles was used, there was no fluorescent separation of pHrodo™-negative and pHrodo™-positive populations, as had previously been seen, Figure 3.8. Confocal imaging (see Figure 3.8C) revealed neutrophils were phagocytosing the bioparticles and the bioparticles were fluorescing; they were just dimmer than the previous batch so the flow cytometer was less able to detect a difference in fluorescence between pHrodo™-positive and pHrodo™-negative neutrophils. This was a batch-specific effect which wasn't seen with another lot number, but was particularly apparent in *E. coli* bioparticles. Therefore, the consistent brightness of green pHrodo™ bioparticles meant they were a more reliable choice. For consistency, a single lot number for both *E. coli* and *S. aureus* was used for all experiments in this project.

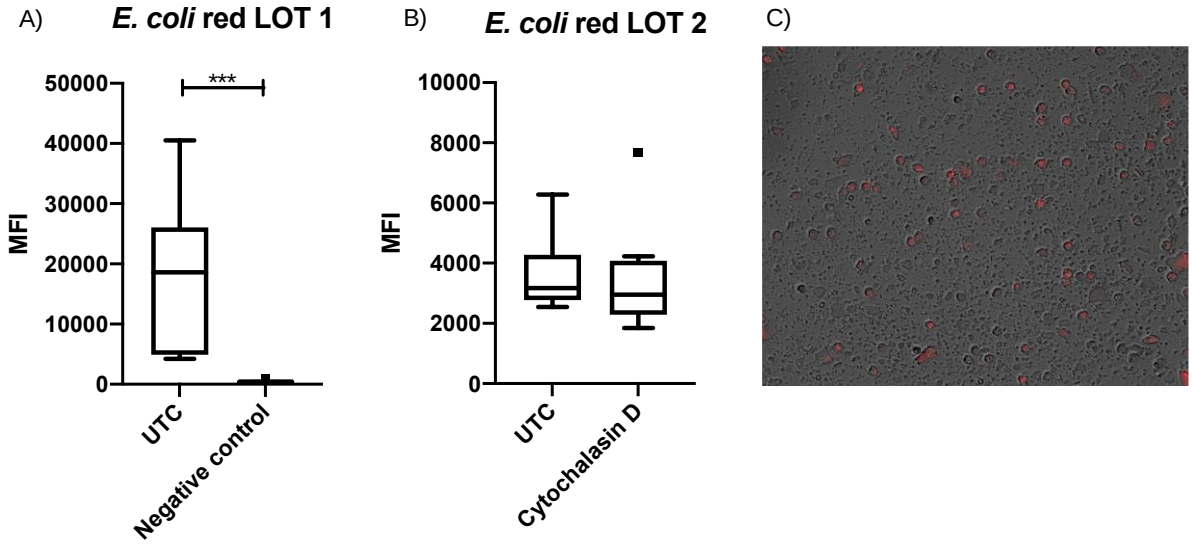


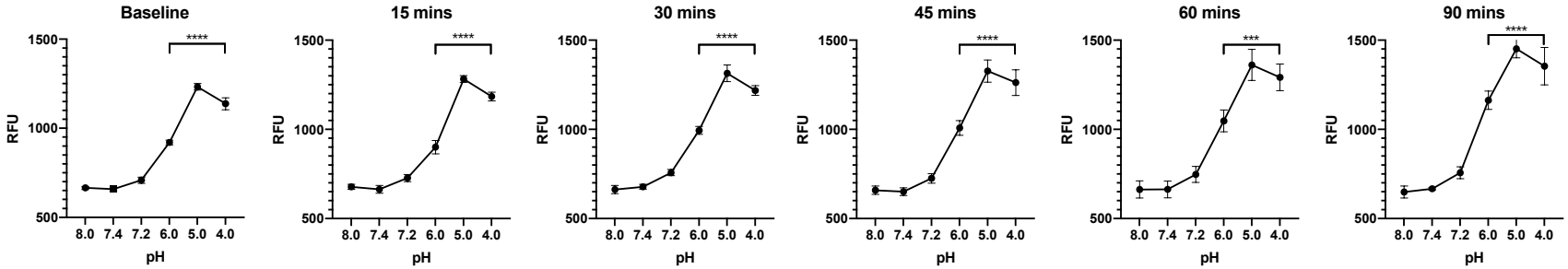
Figure 3.8: Inter-batch variation in pHrodo™ red *E. coli* bioparticles.
2 batches (lot 1 and lot 2) of pHrodo™ red *E. coli* bioparticles were compared. A) shows data previously collected by the group using LOT 1 of pHrodo™ red bioparticles, where pHrodo™-positive neutrophils were highly fluorescent and there was a significant shift ($p = 0.0006$) from the negative control. B) shows the data produced using a new lot (LOT 2) of pHrodo™ red bioparticles and analysing data on the same flow cytometer, BD Accuri c6, however there was no shift from the negative control of cytochalasin D. C) is a confocal image of neutrophils phagocytosing lot 2 pHrodo™ bioparticles, showing the neutrophils were capable of phagocytosing them, and the bioparticles fluoresced once in the phagosome. Note: Negative control neutrophils in A) were not treated with cytochalasin D, but immediately run on the BC accuri C6 after addition of pHrodo™ (incubation time = 0 mins) A: n = 7, B: n = 8.

3.4.5.2 Fluorescence intensity

To ensure pHrodo™ bioparticles would fluoresce only when exposed to a drop in pH, and would sustain a fluorescence signal for the duration of the assay, pHrodo™ bioparticle fluorescence was assessed as described previously (section 3.3.3). Both *E. coli* and *S. aureus* bioparticles peaked in fluorescence at pH 5.0 across all time points. There was a significant increase in RFU from pH 8.0, 7.4 and 7.2 to 6.0, 5.0 and 4.0 across all time points (multiple comparisons by one-way ANOVA revealed $p \leq 0.001$ between all neutral and low pHs at all time points measured, see Figure 3.9). The bioparticles fluoresced immediately when exposed to lowering pH and sustained this fluorescent signal over a 90 minute period. There were no significant differences (tested for by one-way ANOVA with multiple comparisons) in the fluorescence intensity of *E. coli* or *S. aureus* bioparticles at any pH level at 30 minutes or 60 minutes, the two time points used in this study.

This set of experiments suggested the fluorescence signal could be maintained over the duration of the timecourse and a fading in fluorescence intensity at the later time points would not be seen.

A) *E. coli*



B) *S. aureus*

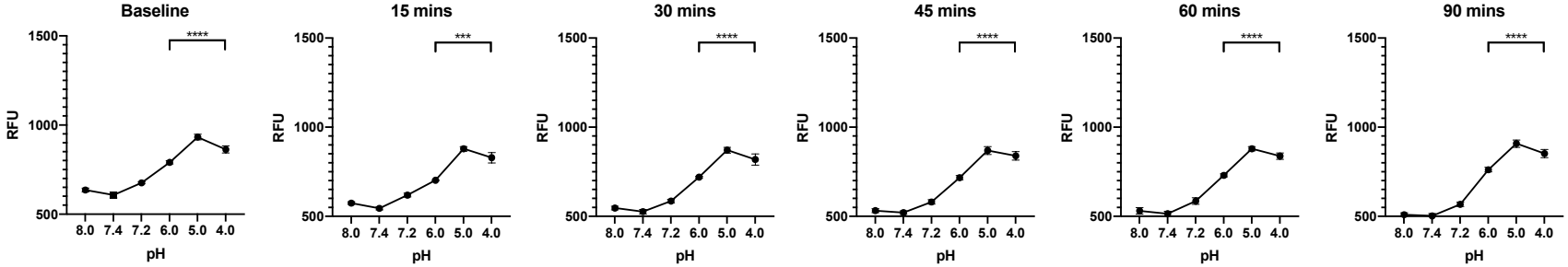


Figure 3.9: pHrodo™ bioparticle fluorescence over time.
E. coli and S. aureus pHrodo™ bioparticles were exposed to RPMI of pH 8.0, 7.4, 7.2, 6.0, 5.0 or 4.0. Bioparticles were allowed to incubate at room temperature in the dark for 0, 15, 30, 45, 60 or 90 minutes before being read on the Synergy 2 plate reader at 485/20 nm excitation 528/20 nm emission. Data was normally distributed, and a one-way ANOVA was used for multiple comparisons of the means of each group (defined as each pH). A statistically significant difference between pHs 8.0, 7.4, 7.2 and pHs 6.0, 5.0, 4.0 is represented by an asterisks above an n-zigzag line. * = $p \leq 0.05$, ** = $p \leq 0.01$, *** = $p \leq 0.001$, **** = $p \leq 0.0001$, n = 3.

3.4.5.3 pHrodo™ assay gating strategy

Phagocytosis was assessed with a flow cytometer using pHrodo™ bioparticles, as described previously (section 2.11). Measuring phagocytosis readouts on a flow cytometer provides the advantage of being able to assess the percentage of cells that had phagocytosed pHrodo™ bioparticles, deduce the amount of bioparticles ingested and account for any cellular autofluorescence. Figure 3.10 details the gating strategy used to assess phagocytosis. Neutrophils were first gated based on forward scatter (size) and side scatter (granularity). Cells falling into this first gate were carried over into the second plot where forward scatter was plotted against cell width, to select only the singlets. Singlets were carried over into the final plot where a histogram of FITC fluorescence was plotted. The final gate was placed against the histogram of the negative control neutrophils treated with cytochalasin D, meaning any FITC fluorescence greater than this value represents positive phagocytosis. Neutrophils phagocytosing a large amount of pHrodo™ bioparticles can change in size and granularity to shift out of the initial cell gate. Therefore, the first forward scatter/side scatter gate must be enlarged to accommodate the change in size, which can be seen in Figure 3.10.

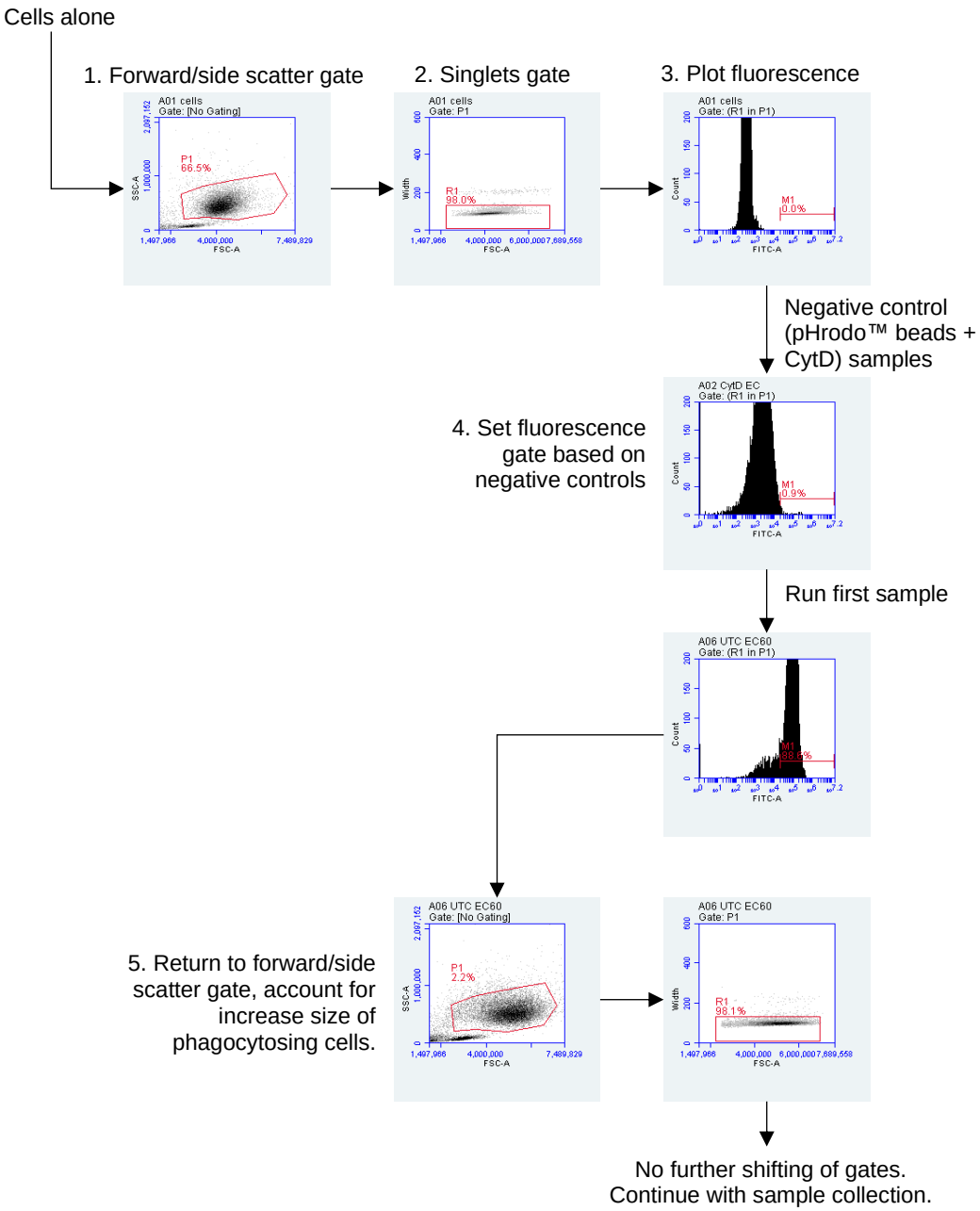


Figure 3.10: Representative flow cytometry plots to describe the gating strategy for phagocytosis assays.
Firstly, neutrophils were gated (P1) based on forward scatter (FSC-A) and side scatter (SSC-A) which show up as a distinct granular population. This population was carried over to the next plot to select only the singlets (gate R1) by plotting forward scatter against width. The singlet neutrophil population (R1 in P1) was carried over to plot fluorescence in the FL1 channel, representative of FITC fluorescence. To decide which cells represented pHrodo™ positive cells, the M1 gate was set based on the FITC fluorescence intensity of cytochalasin D negative control cells. Subsequently, the median fluorescence intensity (MFI) of the whole FITC plot and the % positive cells (In M1 gate) were recorded.

3.4.5.4 Timecourse

To determine the optimal sampling time points for this phagocytosis assay, neutrophils were incubated with *E. coli* or *S. aureus* bioparticles for 15, 30, 45, 60 or 90 minutes, time points consistent with previously published work (Corriden et al., 2020, Tortorella et al., 1992) and recommended by the manufacturer (Invitrogen, 2020). There appeared to be an increase in the amount of *E. coli* pHrodo™ bioparticle uptake at 45, 60 and 90 minutes (Figure 3.11A). There also appeared to be a notable increase in *E. coli* phagocytosis between 30 and 60 minutes (Figure 3.11A) but not between any other time points. The proportion of cells phagocytosing appeared greater than cytochalasin D controls at 30, 45, 60 and 90 minutes (Figure 3.11B), but not at 15 minutes. To avoid a negative effect on neutrophil viability, and to coincide with published literature, 60 minutes was chosen as the maximum incubation time.

This work aided the decision to choose two time points: 30 minutes and 60 minutes which would enable the resulting data to decipher phagocytosis dynamics, and to discuss whether any alterations in phagocytosis recover, or sustain.

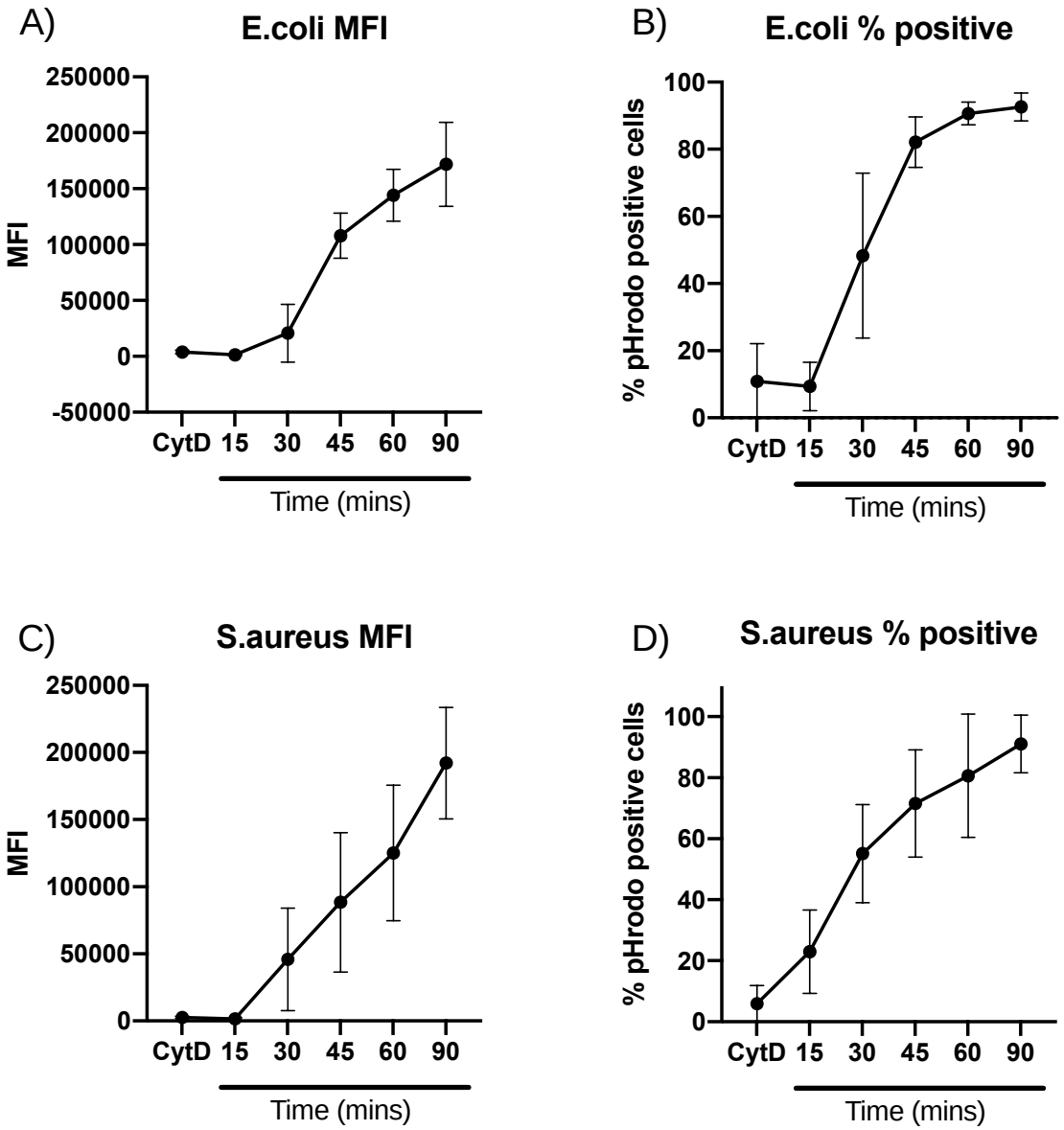


Figure 3.11: Neutrophil phagocytosis of *E. coli* and *S. aureus* bioparticles over time.

Neutrophils were incubated with *E. coli* or *S. aureus* pHrodo™ bioparticles for 15-90 minutes. The amount of pHrodo™ bioparticles phagocytosed (MFI) was measured (A, C) as well as the percentage of cells phagocytosing the bioparticles (B, D) as described in section 2.11. Negative control cells were treated for 20 minutes with 20 μM cytochalasin D (Cyt D) and incubated with pHrodo™ bioparticles for the longest time point (90 minutes). Data is presented as the mean and standard deviation of 3 independent donors (n = 3) for each phagocytic parameter. Data was considered not normally distributed due to low n numbers. To test for statistical difference, wilcoxon matched-pairs test were performed. There were no statistical differences between any of the time points.

3.4.5.5 Cytochalasin D concentration

To determine the optimal cytochalasin D concentration for use in the phagocytosis assay, 6 concentrations were tested against UTC for both red and green *E. coli* and *S. aureus* pHrodo™ bioparticles. Cytochalasin D is a robust inhibitor of actin polymerisation, a process necessary for neutrophil phagocytosis. Previous work has used 10 µM cytochalasin D to inhibit macrophage efferocytosis (Mahida et al., 2021). In the present study, cytochalasin D concentrations far below and far exceeding these values were trialled to determine the optimal cytochalasin D concentration for phagocytosis inhibition in neutrophils. Figure 3.12A-C shows the amount of phagocytosis and the proportion of phagocytosing cells at each Cytochalasin D concentration. At 20 µM there was a large drop in total phagocytosis and the percentage of neutrophils phagocytosing pHrodo™ bioparticles. This was particularly apparent in the green bioparticles (see Figure 3.12A-C). Further validation showed a significant increase in the amount of *E. coli* bioparticle phagocytosis (MFI) at both 30 and 60 minutes ($p = 0.0084$, < 0.0001 respectively, Figure 3.12D) compared to 20 µM cytochalasin D control. Further, a cumulative increase in fluorescence intensity with time (30 mins vs 60 mins: $p = 0.0004$, Figure 3.12D) proves the assay was not saturated at 30 minutes. Similarly, the percentage of cells phagocytosing green *E. coli* was significantly higher than cytochalasin D controls at 30 minutes ($p = 0.0010$) and 60 minutes ($p = 0.0010$) and significantly different across time points ($p = 0.0010$, Figure 3.12E). There was also a significant increase in the amount of *S. aureus* bioparticle phagocytosis at 30 and 60 minutes ($p = 0.0020$, 0.0010 respectively, Figure 3.12F) compared to cytochalasin D control, as well as a significant difference between the two time points ($p = 0.0010$, Figure 3.12F). Similarly, the percentage of cells

phagocytosing green *S. aureus* was significantly higher than cytochalasin D controls at 30 minutes ($p = 0.0010$) and 60 minutes ($p = 0.0010$) and significantly different across time points ($p = 0.0010$, Figure 3.12G).

Overall, the validation work described here supports the use of green pHrodo™ bioparticles, incubating with neutrophils for 30 and 60 minutes with a negative control of 20 µM cytochalasin D to assess neutrophil phagocytosis over time of gram-positive and gram-negative bacteria. This fluorophore-bioparticle combination was used for subsequent experiments.

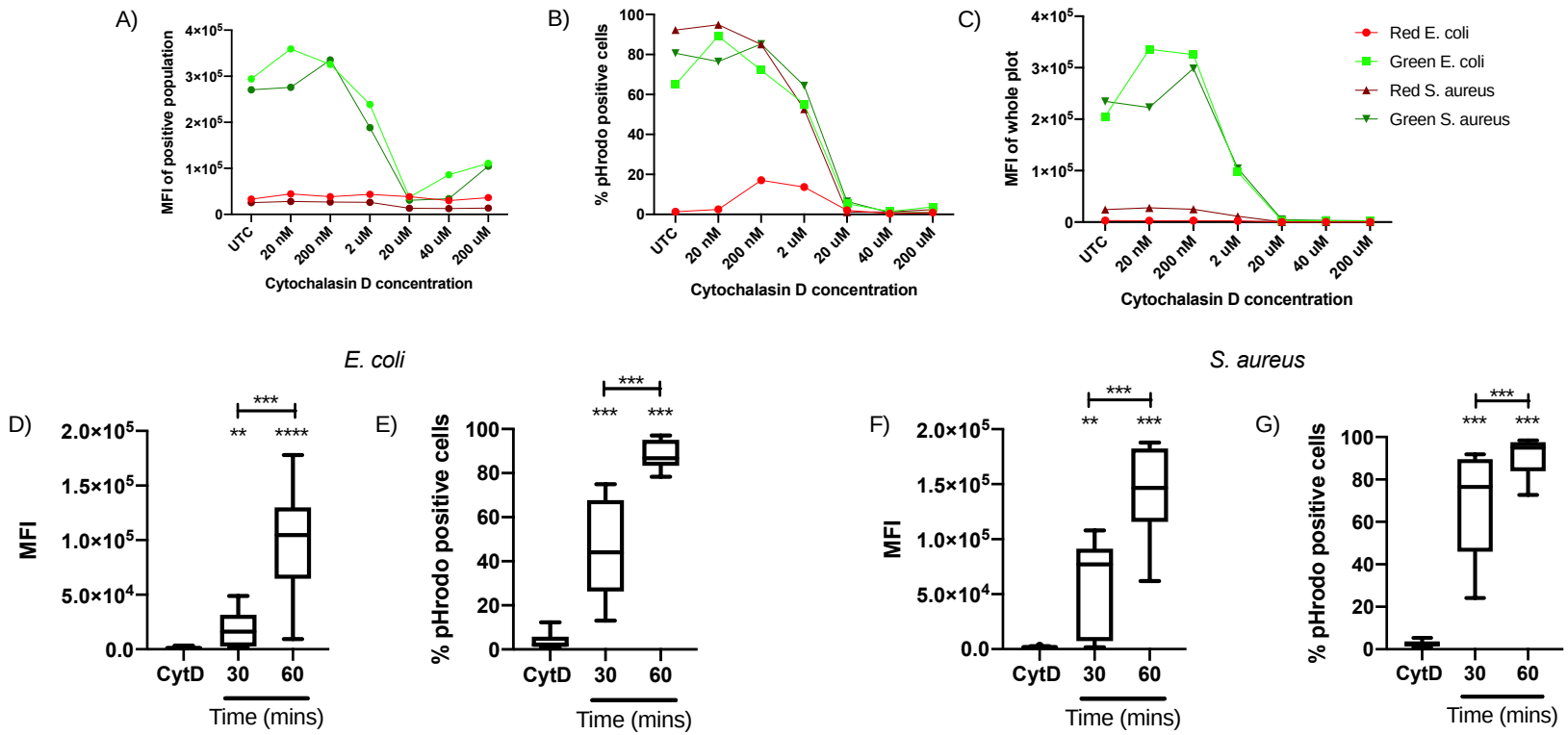


Figure 3.12: Validation of cytochalasin D concentration for inhibition of phagocytosis.
Isolated human peripheral blood neutrophils were incubated with 0, 20 nM, 200 nM, 2 µM, 20 µM, 40 µM or 200 µM cytochalasin D (CytD) for 20 minutes before addition of red or green *E. coli* or *S. aureus* pHrodo™ bioparticles for 60 minutes. The MFI (A) and percentage of cells (B) in the pHrodo™ positive population was recorded as well as the MFI of the whole plot (C) using a BD Accuri flow cytometer. N = 1 for dose response experiments. After deciding to use a combination of 20 µM CytD and green pHrodo™ bioparticles, the MFI of the whole plot and percentage of pHrodo™ positive cells at 30 and 60 minutes was recorded and compared to 20 µM CytD to ensure that there was a significant inhibition of phagocytosis in the assay setting. Data was normally distributed for *E. coli* MFI (D), but not normally distributed for the other data (E-G). To test for statistical difference, a paired t-test was used for *E. coli* MFI and Wilcoxon matched-pairs test for data in E-G. An asterisks represents a statistically significant difference between the group and CytD group, and a difference between phagocytosis time points is represented by an Asterisks above a capped line. * = $p \leq 0.05$, ** = $p \leq 0.01$, *** = $p \leq 0.001$, **** = $p \leq 0.0001$, A-C: n = 1, D-G: n = 11.

3.4.6 Seahorse validation

Agilent Seahorse technology is commonly used to assess cellular metabolism in cell lines. More recently, researchers have adapted the existing protocols to assess bioenergetic patterns in neutrophils to answer important scientific questions (Forrest et al., 2018, Del Arroyo et al., 2019, Reyes et al., 2021, Swain et al., 2018, Porter et al., 2018). This work had not previously been done in our group, so extensive validation was required to set up the systems and protocols to work as they are in the existing literature.

3.4.6.1 Cell-Tak and neutrophil viability

To successfully carry out a Seahorse metabolism experiment, cells must be adhered to the bottom of the well to allow the sensors to accurately detect changes in pH and oxygen content. Adherent cells can be cultured in the plates, but neutrophils are non-adherent cells which cannot be cultured and therefore Cell-Tak is used to adhere neutrophils to the base of the wells to maximise sensitivity. Plates were coated with Cell-Tak before neutrophils are added. Cell-Tak does not interfere with the Seahorse protocol and has been previously shown to have very little impact on neutrophil oxidative burst (Porter et al., 2018). Figure 3.13 shows the minimal impact on neutrophil viability by fluorescently imaging neutrophils adhered to the well by Cell-Tak.

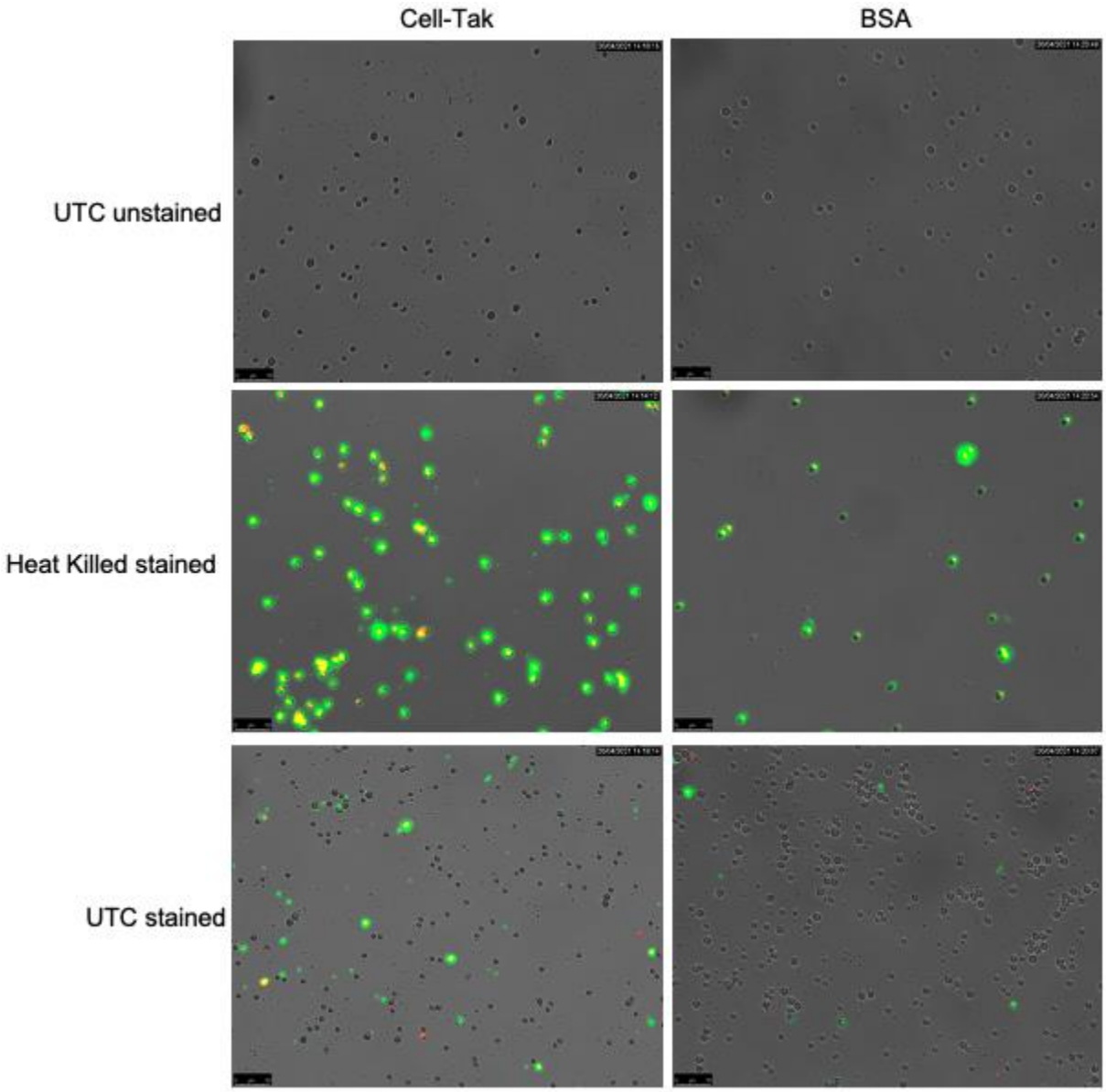


Figure 3.13: Viability staining for neutrophils adhered to a well via Cell-Tak and BSA.
Neutrophils were stained using Annexin V-FITC and PI after being allowed to adhere to the slide via BSA or Cell-Tak, as described in section 3.3.5. Images were captured on the Leica DM6000 and an overlay of the 3 channels (brightfield, FCr2, L5 and FCr3, N3 lenses) to generate the images presented.

3.4.6.2 Cell seeding density

Agilent recommend a confluence of 50-90% when performing seahorse experiments to maximise specificity and enable accurate detection by the probes in the system. Figure 3.14 shows microscopic images of the base of a seahorse plate seeded with 1 x 10^4-5 x 10^5 neutrophils/well. Around 2 x 10^5 neutrophils/well, approximately 90% confluence was achieved. At higher cell seeding densities, the base of the well was densely packed, and the resulting metabolic tests were disrupted as there was not a monolayer of cells. A range of cell seeding densities in both the glyco stress test and oxidative burst test were trialled to determine the optimal density for each. There was an increase in magnitude of oxidative burst response from 1-5 x 10^4 neutrophils/well, however, with higher cell seeding concentrations there were inconsistencies in response, see Figure 3.15. Therefore, 5 x 10^4 neutrophils/well were used as the cell seeding density for the oxidative burst test. However, in the glyco stress test, 5 x 10^4 neutrophils/well produced a very small response, which was concentrated in the lower level of machine detection. Higher cell seeding densities – up to 5 x 10^5 neutrophils/well were tested, and it was found that for this test, 2 x 10^5 neutrophils/well produced a robust response without overcrowding the well (see Figure 3.14 and Figure 3.16). A higher number of neutrophils was required to produce a response in the glyco stress test as this utilises the pH probe, and a response must overcome the buffering capacity of the seahorse media to be detected.

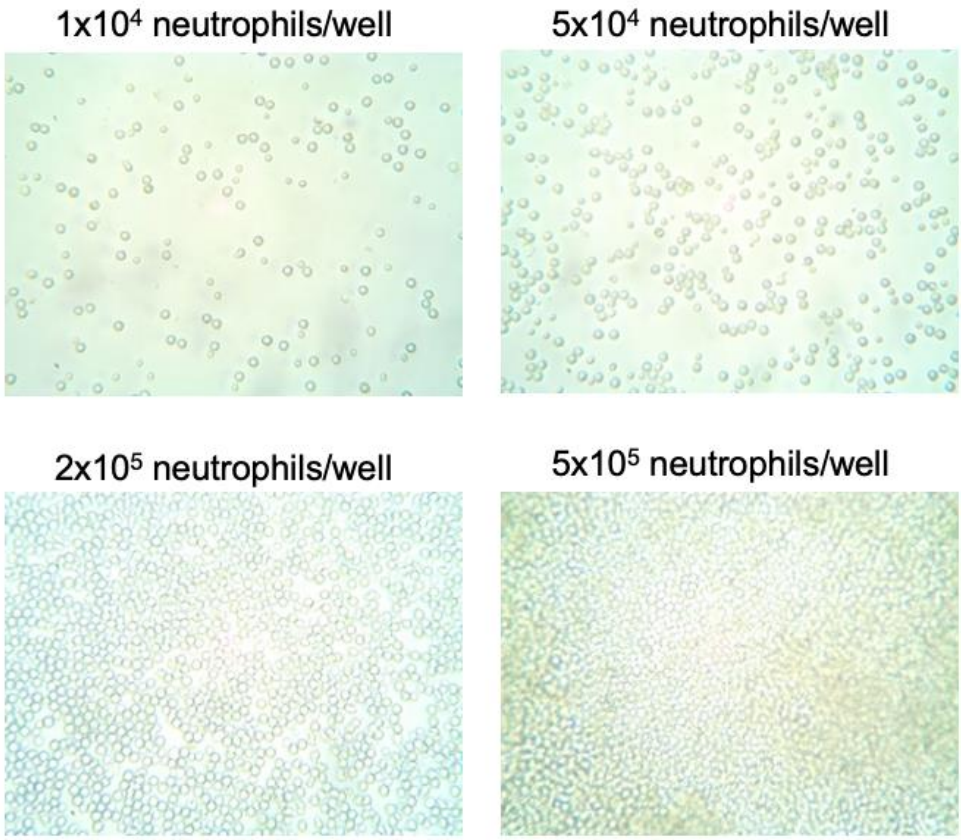


Figure 3.14: Representative photographs of the cell seeding densities of neutrophils used in the Seahorse assay.
1 x 10^4 – 5 x 10^5 neutrophils were adhered to the base of each well of a Seahorse assay plate using Cell-Tak, as described in section 2.13. The base of the wells were imaged under a light microscope (45x magnification) and the confluence assessed by eye. The manufacturer recommends a confluence of 50-90% for assays. Confluence assessments were combined with experimental data to achieve the optimal number of neutrophils per well which achieved the correct confluence and consistent data output.

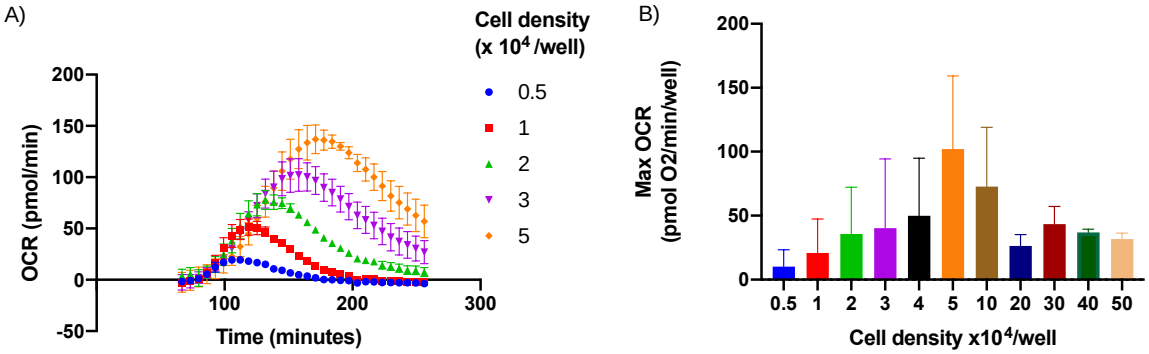


Figure 3.15*:* Neutrophil oxidative burst test cell seeding densities.
Neutrophils were seeded at 0.5 - 50 x 10^4 neutrophils/well before undergoing the oxidative burst test using the Agilent Seahorse XF96, as described in section 2.13. The oxygen consumption rate (OCR) over the duration of the test was measured, and the peak OCR reached (max OCR) was measured. A) is a representative OCR trace of the cell seeding density experiments performed, on a single sample (n = 1). B) is the combined max OCR data for all cell seeding densities tested. N = 3 per group.

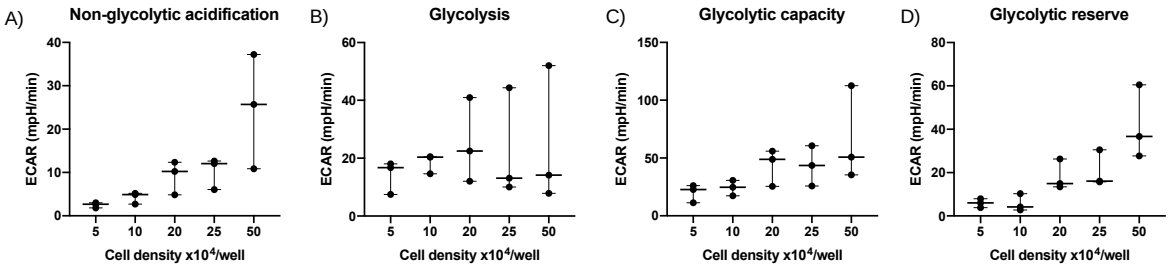


Figure 3.16: Neutrophil glyco stress test parameters and cell seeding densities.
Neutrophils were seeded at 5 - 50 x 10^4 neutrophils/well before undergoing the glyco stress test, as assessed using the Agilent Seahorse XF96, as described in section 2.13. The ECAR (extracellular acidification rate) trace was used to extrapolate glycolysis parameters: a) non-glycolytic acidification, B) glycolysis, C) glycolytic capacity and D) glycolytic reserve. 5 cell seeding densities were assessed: 5, 10, 20, 25 and 50 x 10^4 cells/well. N = 3.

3.4.6.3 PMA concentration validation

To determine the optimal concentration of PMA needed to produce a robust oxidative burst response, a dose response with 9 PMA concentrations (640, 320, 160, 80, 40, 20, 10, 5 and 2.5 nM PMA) was performed, consistent with method validation work previously published (Swain et al., 2018). Figure 3.17A shows the time from start of the seahorse run for peak OCR to be reached. Only 160, 320 and 640 nM PMA consistently peaked after PMA injection (indicated by the dotted line in Figure 3.17A). The other concentrations of PMA investigated produced only a small increase in OCR below the limit of reliable measurement. 160, 320 and 640 nM PMA produced an increase in OCR compared to unstimulated control wells, which could be reliably discriminated (Figure 3.17B). Similarly, total oxygen consumption over the course of the procedure was only increased from baseline when using 160, 320 and 640 nM doses of PMA. 160 nM PMA was selected for subsequent oxidative burst experiments, consistent with published literature (Hickman et al., 2019, Chen and Junger, 2012, Swain et al., 2018).

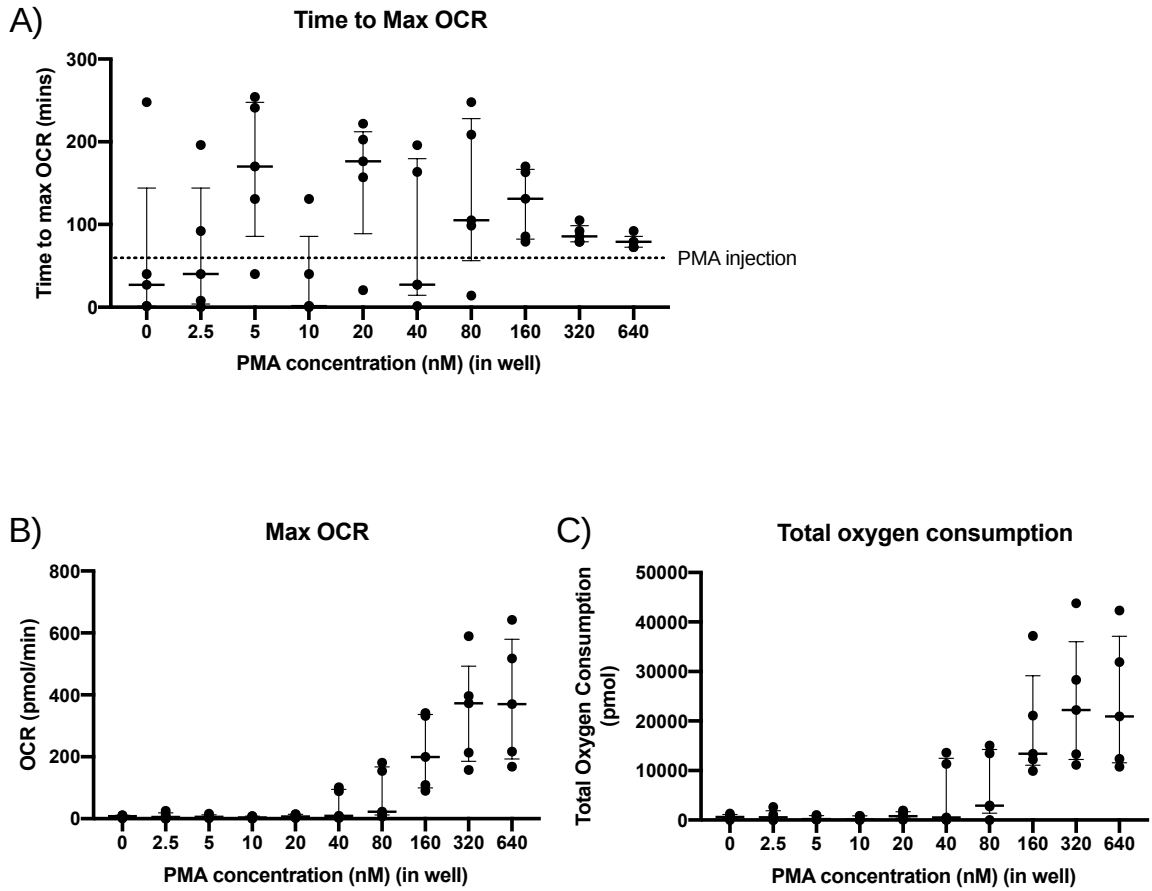


Figure 3.17: PMA induced-oxidative burst dose responses.
5 x 10^4 isolated human peripheral blood neutrophils were seeded per well onto a CellTak coated Seahorse XF96 plate. The oxidative burst protocol was followed where neutrophils are injected with media followed by PMA. 640, 320, 160, 80, 40, 20, 10, 5 and 2.5 nM PMA were used as the key concentrations. PMA concentrations represent the amount of PMA neutrophils were exposed to in the well, accounting for the dilution into the well. The time to max oxygen consumption rate (OCR) (A), Maximum OCR (B) and Total oxygen consumption (C) were calculated from area under the curve analysis. Data was not normally distributed so statistical difference was tested for using Wilcoxon matched-pairs test. N = 5.

3.4.7 SYTOX® green / anti-histone H3 NET co-staining

SYTOX® green is a robust nucleic acid stain, however, to ensure SYTOX® green localises to NETs, immunofluorescent imaging was performed with co-staining using an anti-histone H3 antibody to show co-localisation of the two molecules to the NETs, as shown in Figure 3.18. These microscopy images demonstrated SYTOX® green was accurate for staining NETs and suggests there were not off-target effects in this model.

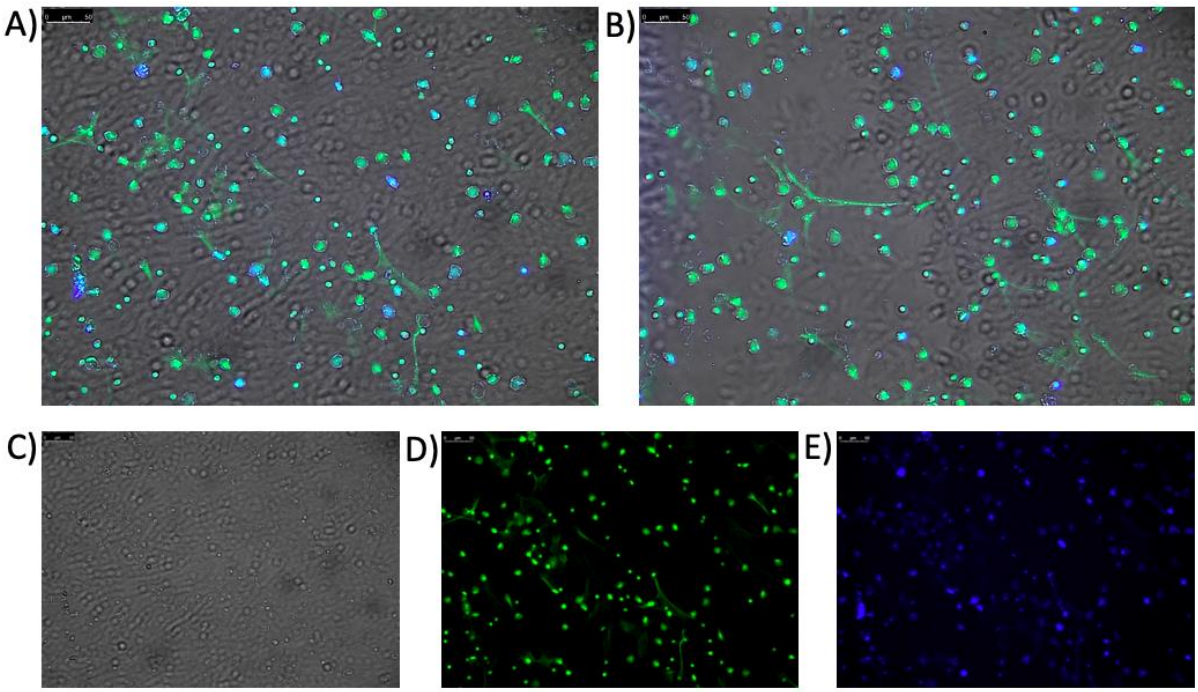


Figure 3.18: Neutrophil extracellular traps co-stained with SYTOX® green and Anti-Histone H3 antibody.
Neutrophils were stimulated with 25 nM PMA for 3 hours on coverslips. Following neutrophil extracellular trap (NET) stimulation, neutrophils were fixed and stained, firstly with a primary rabbit polyclonal anti-histone H3 antibody, then a secondary goat anti-rabbit antibody and finally SYTOX® green, as described in section 2.11.1. Images were captured using the Leica DMI 6000 B microscope. A and B are representative overlay images of C) Brightfield, D) SYTOX green and E) Alexa Fluor 350 channels.

3.4.8 Calcium assay validation

Previous studies have uncovered the link between nicotine, increases in intracellular calcium signalling and subsequent protease release (Ghosh et al., 2019). To determine if calcium signalling is a driver molecule in our model, the Fluo-4 direct intracellular calcium signalling kit was used. There is no fixed requirement for cell density according to the kit manufacturer's protocol, so 5 cell concentrations (2.5×10^4 - 2.5×10^5) and 3 concentrations of the positive control, thapsigargin, were validated. 2.5 µM thapsigargin caused a significant increase in calcium signal at all cell concentrations, except 2×10^5 neutrophils/well (Figure 3.19). 5 µM and 10 µM thapsigargin did produce a significant signal in some cell concentrations, however there were no significant differences in the signal produced between the thapsigargin concentrations at any cell seeding densities, suggesting a depletion of calcium stores and subsequent maximal signal had been reached.

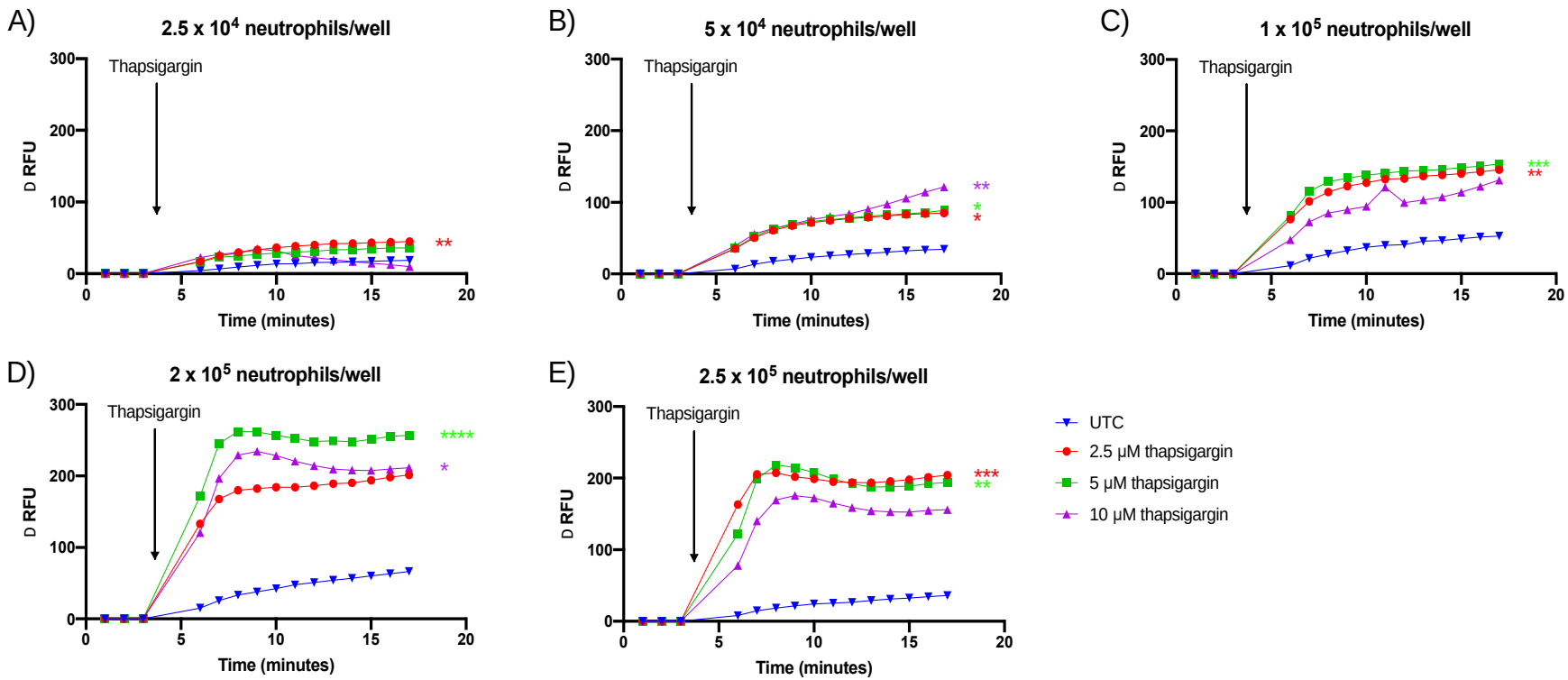


Figure 3.19: Neutrophil treatment with thapsigargin increases cytoplasmic calcium.
Neutrophils were seeded at 2.5 x 10^4-2.5 x 10^5 neutrophils/well before incubation with the calcium indicator Fluo-4 direct. Baseline readings (time: 1, 2, 3 minutes) were taken before thapsigargin (2.5, 5 or 10 µM thapsigargin was added) and a further 12 readings taken. The fluorescence is expressed as ΔRFU, whereby the final RFU reading before addition of thapsigargin is subtracted from the subsequent RFU values. Data was not normally distributed so a kruskal-wallis test with multiple comparisons was used to test for significant difference between groups. A statistically significant difference between thapsigargin and UTC is represented by an asterisks at the end of the corresponding trace (in the same colour as the trace). A statistically significant difference between groups is indicated by an asterisks with a capped line. * = p≤0.05, ** = p≤0.01, *** = p≤0.001, **** = p≤0.0001, n = 2

3.4.9 RNA extraction validation

Neutrophils have relatively low levels of mRNA as they are not as transcriptionally active as some other myeloid cells. Compounded with this, stored cellular components can lead to reactive species and enzymatic damage to transcripts during cell lysis and isolation. RNAqueous™-Micro total RNA isolation kit was used based on previous successful application to neutrophil RNA isolation. RNA concentration and RNA integrity number (RIN) were assessed by Qubit and Tapestation respectively, as described in section 5.4.3. Median RNA concentration yielded from 5×10^6 neutrophils was 86.7 ng/µL (IQR 35.9 - 248.9 ng/µL). Median RIN score was 8.3 (IQR 2.9 - 9.5). Further analysis revealed that commonly in these samples there was an inverse relationship between RNA concentration and RIN score. Colleagues at Genomics Birmingham advised maximal output from these samples could be achieved using the Lexogen QuantSeq 3' mRNA-sequencing protocol with altered incubation times to account for low input (<10ng) samples. Samples marked in red in Figure 3.20 indicate those which were carried over to sequencing which met the minimum requirements for this the Lexogen QuantSeq 3' mRNA-sequencing library prep.

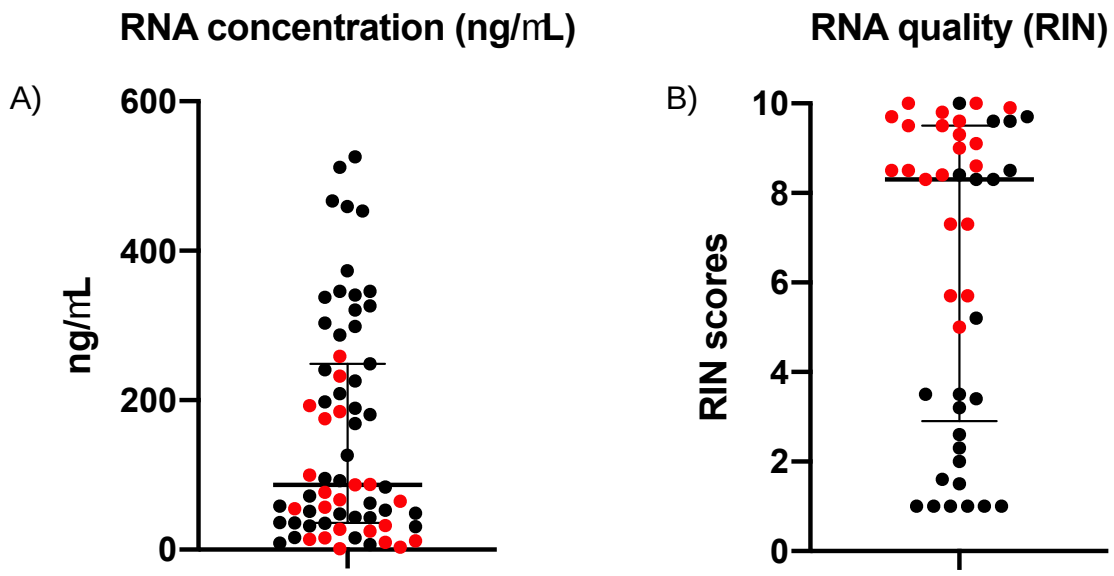


Figure 3.20: Extracted RNA yield (concentration) and quality (RNA integrity number).
RNA lysates from 5 x 10^6 neutrophils for various treatment conditions were collected and stored. Extraction was performed before analysis of yield including concentration and RNA integrity using Qubit High Sensitivity RNA assay and an RNA tape on the Agilent TapeStation. Samples in red represent those which were carried through to sequencing as analysis revealed they had the optimal combination of concentration and RNA integrity for Lexogen QuantSeq 3'. Each point represents the analysis of an individual extracted RNA sample, but some points represent the same lysis sample extracted into multiple collection tubes. It was not possible to get a RIN score for every sample analysed, which is reflected in the lower n numbers for the quality (B) graph compared to the concentration (A). RNA concentration: n = 67, RNA quality: n = 45. N numbers represent individual RNA extraction samples, some of which are replicate extraction repeats of the same sample to maximise RNA collection. These do not represent individual donors.

3.5 Chapter 3 discussion

To ensure existing protocols were working optimally and able to address the research aims of this project sufficiently, validation work was required for many of the experimental procedures. The work outlined here aided decision making, as will be discussed, for finalisation of protocol steps.

3.5.1 E-cigarette vapour chamber model

The first aim of this chapter was to set up and validate a novel e-cigarette vapour exposure system. The e-cigarette exposure chamber used in the current study is a modified hypoxia chamber which allows cells to be exposed directly to vapour constituents. As this was the first instance of usage for these experiments it was essential to characterise the nature of the exposure when e-cigarette vapour was produced in the chamber. As previously described in section 2.6 a puffing-based system was used to replicate user exposure. This importantly prevented device overheating which could lead to toxic substances not normally produced under natural usage conditions. In each exposure experiment laid out in this chapter and in subsequent data chapters, a 40-puff exposure system was employed using a unflavoured e-liquid loaded into second generation or fourth generation devices. In this exposure system neutrophils, suspended at 1 x 10^6/mL in 100 µL of media in a tissue culture plate were exposed to e-cigarette vapour. Whilst this is a more direct system there must also be an element of dissolution in the media.

The total volume of the chamber was 5.5 L, similar to the average total lung capacity of an adult human, which is approximately 6 L (Delgado BJ, 2021). This gave our

system distinct advantage, as it doesn't compress a puff into a smaller, more condensed area than in the lung, preventing concentration of the exposure. GC-FID analysis revealed neutrophils were exposed to an average of 0.6 µM or 3 µM nicotine (2GECV, 4GECV, respectively) across a 20-minute exposure time. According to recent data, sputum nicotine after a 1 hour vaping session is approximately 45 µM, with an exposure range from 1 µM to 300 µM (Ghosh et al., 2019), (compared to 33.6 µM after a full cigarette was smoked (Clunes et al., 2008)) so our e-cigarette vapour exposure is not super-physiological.

To ensure any differences detected in neutrophil effector function downstream were not the result of simple cell death we assessed viability after 40 puffs. Data here suggests there were no significant effects of e-cigarette vapour exposure in our model. Previous macrophage studies in our lab showed toxic responses however these studies differ in fundamental ways. Our previous studies used longer term (24h) exposure using a vapour condensate, meaning the challenge was maintained throughout the time course. Our shorter, vapour exposure (20 minutes) used a puff-based system after which the challenge is not maintained. This is consistent with other work examining the effects of e-cigarettes on neutrophils using an extract-based system, in which no effect on viability was detected (Higham et al., 2016).

Together, we have a model of e-cigarette exposure which is physiologically relevant, simulates real life e-cigarette use and does not compromise the viability of neutrophils, allowing continuation of downstream effector function analysis.

3.5.2 Neutrophil migration assays

CXCL8 is a potent neutrophil chemoattractant which is produced by endothelial cells, fibroblasts, and alveolar macrophages and is found to be elevated in the BALF of COPD patients (Hollander et al., 2007, Strieter et al., 1989, Schröder et al., 1990). Previous work has demonstrated in dose-response experiments that CXCL8 is neutrophil chemotactic to concentrations up to 100 nM, where responses plateau (Sapey et al., 2010). In addition, CXCL8 concentration in sputum from COPD patients has been shown to be up to 58 nM (Sapey et al., 2010), indicating 100 nM is a reasonable pathological concentration. Validation work detailed here revealed in both the Insall chamber and transwell migration models, neutrophil chemotaxis and transmigration were significantly upregulated in response to 100 nM CXCL8 compared to RPMI, similar in magnitude to previously published work (Sapey et al., 2011).

Validation experiments revealed that measuring transmigration by calcein-AM fluorescence of e-cigarette exposed neutrophils was an unreliable method due to the e-cigarette vapour exposed neutrophils having a lower baseline level of fluorescence. In addition, work such as that by Davis et al has shown deposition from e-cigarette vapour is autofluorescent, indicating there is further capacity for e-cigarette vapour to disrupt this measurement (Davis et al., 2017). Calcein AM is a cell-permeant dye which is metabolised by cells which converts it to a green-fluorescent calcein. Lower baseline fluorescence of neutrophils stained with calcein AM and then exposed to e-cigarette vapour could be due to a variety of reasons: increasing neutrophil metabolism leading to break down of the fluorescent element, decreasing neutrophil metabolism causing lower amounts of fluorescent calcein to be produced or an effect on neutrophil viability.

Whichever mechanism is causing the decrease in fluorescence, the results will be skewed negatively so that neutrophils exposed to e-cigarettes appear to be migrating less. To prevent artefacts, this assay protocol was altered to direct counting of migrated cells in the lower transwell chamber by FACS. This method proved more reliable and is not affected by e-cigarette exposure.

Combining use of the Insall chamber and transwell migration models provides detailed insight into neutrophil migratory parameters after e-cigarette use. Transwell models provide an end-stage read out of total neutrophil migration over a time course while Insall chamber allows real-time dynamics of chemotaxis to be analysed (Muinonen-Martin et al., 2010). Together, determining the ability of neutrophils to migrate through pores as well as directionality, speed and velocity, allows the assessment of neutrophil migratory dynamics to help predict the potential for excess tissue damage.

3.5.3 Neutrophil phagocytosis model

Neutrophil phagocytosis of *E. coli* and *S. aureus* was assessed using pHrodo™ bioparticles. The pHrodo™ system of staining means that uniquely, the bacteria fluoresce more brightly in response to a pH drop associated with ingestion into the phagosome (Miksa et al., 2009). Therefore, background signal associated with pHrodo™ bioparticles bound to the neutrophil membrane is minimal. Data presented in this chapter showed a significant increase in pHrodo fluorescence from pH 6.0 and below compared to pH 8.0-7.2. This corresponds with the drop in phagolysosomal pH observed in neutrophils, as discussed previously in section 1.4.5. Bacterial lung infections are most commonly caused by *Streptococcus pneumoniae (S.*

pneumoniae), *Haemophilus influenza (H. influenza)*, *S. aureus* and *Mycobacterial tuberculosis (M. tuberculosis)* (Speert, 2006). The range of pHrodo™ products available during this project were pHrodo™ bioparticles (available in *E. coli, S. aureus* and zymosan conjugates) or pHrodo™ dye itself. Previously in our group, work to stain *H. influenza* and *S. pneumoniae* bacteria with pHrodo™ dye has failed to create a reliable and consistent model, and therefore, assessing both gram-positive and gram-negative bacterial phagocytosis using a highly reliable and sophisticated bioparticle system was preferable.

Here, green bioparticles produced a substantially brighter fluorescent signal than red bioparticles in both *E. coli* and *S. aureus*. This is important to allow finer discrimination of differences caused by more subtle changes in phagocytic capacity. Cytochalasin D is a potent inhibitor of cytoskeletal rearrangement, a process which phagocytosis is entirely dependent upon (Schliwa, 1982, May and Machesky, 2001). 20 µM cytochalasin D was shown to robustly inhibit phagocytosis, appropriately for use as a negative control.

Two time points were chosen for measuring phagocytosis: 60 minutes- whereby phagocytosis was plateauing and 30 minutes – where intermediate-phase phagocytosis level could be assessed. By choosing to investigate two phagocytosis time points, any e-cigarette-induced changes to intermediate and late-phase phagocytosis could be assessed. Around 60 minutes, phagocytosis was plateauing to saturation, representing close to maximal phagocytosis, meaning any later time points would be detrimental to neutrophil viability, but would not achieve any higher

phagocytosis levels. 30 and 60 minute time points are consistent with published literature and manufacturer suggestions (Corriden et al., 2020, Tortorella et al., 1992, Invitrogen, 2020).

The assay validation and optimisation detailed here supports the present protocol to assess gram-positive and gram-negative bacterial phagocytosis by neutrophils, over time.

3.5.4 Neutrophil bioenergetics – seahorse assay

Agilent Seahorse analysers provide the technology to perform a variety of metabolic tests on any cell type to answer research questions. For the purposes of this project, we only needed to perform two tests: oxidative burst and glycolysis stress test, however, this technology has great scope to be able to delve further into neutrophil bioenergetics particularly in the context of e-cigarettes. Validation and optimisation experiments were necessary to ensure robust operating procedures and accurate data interpretation.

Cell-Tak is a commonly used adhesive in seahorse assays to force suspended cells into a monolayer on the base of a well, as is required for seahorse experiments. Previous studies found a minimal effect of Cell-Tak on neutrophil oxidative burst (Porter et al., 2018), supporting the current findings of a minimal effect on cell viability. Here, it has been shown that 5×10^4 neutrophils/well for the oxidative burst response and 2×10^5 neutrophils/well for the glyco stress test produce robust, consistent responses while meeting the protocol requirements. Validation work was performed to

determine the optimal PMA concentration required to produce a robust oxidative burst response. At 320 nM PMA, the neutrophil response was plateauing at maximum oxidative burst response. As e-cigarette vapour exposure has the potential to either increase or decrease oxidative burst response from UTC, using a concentration of PMA that produced a robust, but not maximal response, in this case 160 nM, was required. Furthermore, 160 nM PMA is consistent with the manufacturer's recommended concentration to use in the neutrophil oxidative burst test and previous studies which have assessed the effect of e-liquid flavourants on neutrophil oxidative burst (Swain et al., 2018, Hickman et al., 2019).

Therefore, real time neutrophil oxidative burst and glycolytic parameters can be assessed using Agilent Seahorse technology. For this project, these tests could be applied to e-cigarette vapour exposure to determine the effect of vaping on oxidative burst and neutrophil glycolysis.

3.5.5 Staining for NETs using SYTOX® green

Published work has applied the use of SYTOX® green fluorescent DNA dye to the analysis of NETs (Hazeldine et al., 2019, Hampson et al., 2017, Hazeldine et al., 2014, Sapey et al., 2019). However, SYTOX® green is a non-specific DNA dye which will stain all intracellular, extracellular, nucleus derived, or mitochondria derived nucleic acid. One protein which decorates the nuclear DNA backbone of NETs is citrullinated histone H3 (Cit H3) (Liu et al., 2012). Analysis of the presence of Cit H3 has previously been used to validate NET assays and confirm their presence in samples (Dinsdale, 2017, Hazeldine et al., 2017). Here, detection of Cit H3 and co-localisation with

SYTOX® green confirms analysis of NET generation using SYTOX® green staining accurately stains for NETs in isolated neutrophil populations.

3.5.6 Neutrophil intracellular calcium signalling assay

Previous studies have shown nicotine acting on nAChRs induce calcium signalling in neutrophils which, in turn, acts as a messenger to cause protease secretion (Ghosh et al., 2019). To ensure our work is comparable to this existing literature, we have again used the same calcium assay for comparison. The Fluo-4 direct calcium assay kit provides a valuable opportunity to investigate intracellular calcium signalling in live cells without the need to remove excess reagent. The calcium assay kit does not require a specific number of cells per well, therefore, 5 cell concentrations (2.5×10^4 - 2.5×10^5) were trialled along with 3 concentrations (2.5, 5 and 10 µM) of thapsigargin – a non-competitive inhibitor of the sarco/endoplasmic reticulum Ca^{2+} ATPase (SERCA) (Sehgal et al., 2017, Antigny et al., 2011) which results in the emptying the intracellular calcium stores into the cytoplasm. 2.5 µM thapsigargin produced a robust calcium signal and is consistent with previous work (Ghosh et al., 2019). Neutrophils were exposed to e-cigarette vapour at a concentration of 1×10^6/mL, and the use of 5×10^4 neutrophils/well in the calcium assay maintains this concentration, meaning the amplitude of the calcium signal is directly representative of that in the e-cigarette vapour model used in this study.

3.5.7 Limitations

Due to limitations in the exposure model set up, we were unable to quantify the temperature of vapour flowing into the e-cigarette chamber or the air flow speed. If

these factors could have been monitored, puff-to-puff validation could have been performed to ensure there was consistency in exposures over time. Validation on the number of uses of atomiser before replacement was not performed, but measuring cytotoxicity over time, and e-liquid usage over time work could have informed replacement schedules for this study. In addition, during vapour exposure, neutrophils were sealed in the chamber so real time parameters such as calcium signalling or bioenergetics could not be measured. Therefore, all subsequent functional tests were performed after vapour exposure. This limits the results, as immediate responses, and potentially key signals, may be missed. Finally, only one e-cigarette exposure could be performed at a time so, to prevent time-related differences, the order of vaping conditions was randomised, and to prevent neutrophils sitting on the bench for extended periods of time, only a maximum of 2 vaping conditions were performed at a time.

3.5.8 Conclusion

The validation and optimisation work detailed here demonstrates the neutrophil assays used in this thesis worked sufficiently to address the research questions of this project. Where necessary, assays were modified to ensure effector function experiments were a consequence of direct effect on function not simply due to cell death in either untreated or e-cigarette exposed neutrophils, allowing the detection of an increase and decrease from baseline measurements induced by e-cigarette vapour exposure. Therefore, the conclusions drawn from subsequent experiments are as robust and true as possible.

Chapter 4 - IMPACT OF E-CIGARETTE VAPOUR EXPOSURE ON NEUTROPHIL FUNCTIONS

Foreword: Content in section 4.1 draws heavily on work which has been published in a peer-reviewed review article (Jasper et al., 2021) and adapted for the purpose of this thesis.

4.1 Chapter 4 introduction

As discussed previously (section 1.4.9.1), neutrophils are central contributors to the chronic lung inflammation associated with COPD and it is thought that their recruitment, accumulation and degranulation drives tissue damage and their dysregulation in stable disease contributes to increased inflammation and impaired bacterial clearance (Stockley et al., 2013). Neutrophil dysfunction has been reported in a range of disease states including COPD, bronchiectasis and asthma (Patel et al., 2018, Sapey et al., 2014, Jasper et al., 2019, Liew and Kubes, 2019). These diseases are also associated with cigarette smoking.

Cigarette smoking upregulates neutrophil numbers in BAL, hinders normal neutrophil function and promotes a pro-inflammatory phenotype (Karimi et al., 2012, Xu et al., 2013, Guzik et al., 2011). Speed, velocity and directionality of neutrophil chemotaxis to fMLP and CXCL8 are significantly reduced after exposure to cigarette smoke extract (White et al., 2018). In addition, cigarette smoke extract inhibits PMA-induced NET generation (White et al., 2018) and neutrophil cell death (Guzik et al., 2011), leading to persistent inflammation and increased tissue damage which can drive early changes in the lung associated with progression to COPD.

Here, the impact of direct e-cigarette vapour exposure on human neutrophil functions was investigated. For the first time, 2nd generation and 4th generation e-cigarettes from the same manufacturer are directly compared to determine the effect of device power on neutrophil functions.In addition, nicotine-free e-cigarette vapour has been tested alongside nicotine-containing e-cigarette vapour to understand the effects of vapourised vehicle molecules as well as the contribution of nicotine to functional changes in neutrophils.

4.2 Aims of chapter 4

1. To investigate the effect of e-cigarette vapour exposure on neutrophil chemotaxis and transmigration to CXCL8.

2. To investigate the effect of e-cigarette vapour exposure on neutrophil phagocytosis of *E. coli* and *S. aureus* bioparticles.

3. To investigate the effect of e-cigarette vapour exposure on neutrophil degranulation/protein secretion.

4. To investigate the effect of e-cigarette vapour exposure on neutrophil basal metabolism.

5. To investigate the effect of e-cigarette vapour exposure on neutrophil oxidative burst response.

6. To investigate the effect of e-cigarette vapour exposure on neutrophil spontaneous and stimulated NET generation.

7. To understand the contribution of nicotine and e-cigarette device power on the above functions.

4.3 Materials and methods linked to chapter 4

4.3.1 Transwell staining and visualisation

After the neutrophil transwell migration procedure as described in section 2.9.2, transwell inserts were removed and stained with CD16-FITC (BD Bioscience, product no. 555406) diluted 1:100 in PBS containing 2% BSA for 20 minutes in the dark. Membranes were then washed twice in PBS containing 2% BSA before being visualised under the Leica DM6000. A brightfield image (20X magnification) and FLUO FCr2 image (using the L5 lens) were taken simultaneously and overlaid.

4.3.2 Nicotine treatment

Neutrophils were resuspended to 1 x 10^6/mL in RPMI 1640 and treated directly (not vaped) with 0.6 or 3 μM nicotine (L-isomer) (Sigma-Aldrich, Poole, UK product no. N0267) (based on GC-FID (see section 3.2.1) results) for 20 minutes before functional assays were performed. 20 minutes was chosen to represent e-cigarette treatments used in this study.

4.4 Chapter 4 results

4.4.1 Neutrophil migratory parameters

4.4.1.1 E-cigarette vapour exposure and neutrophil chemotaxis to CXCL8

Neutrophil chemotaxis to CXCL8 was assessed using the Insall chamber. 2GECV significantly impaired neutrophil chemotactic parameters: velocity ($p = 0.0039$, Figure 4.1A), speed ($p = 0.0029$, Figure 4.1B) and chemotactic index ($p = 0.0195$, Figure 4.1) compared to UTC. 4GECV significantly impaired velocity ($p = 0.0059$, Figure 4.1A), speed ($p = 0.0003$, Figure 4.1B), chemotactic index ($p = 0.0391$, Figure 4.1D) of neutrophil chemotaxis compared to UTC. There was a statistically significant reduction in chemokinesis (speed of chemotaxis) by 4GNF treated neutrophils ($p = 0.0324$, Figure 4.1B) compared to UTC but no other parameters measured were affected by this e-cigarette treatment. No e-cigarette treatments affected persistence of neutrophil chemotaxis, see Figure 4.1C. There were no nicotine-dependent effects of e-cigarette vapour on neutrophil chemotaxis parameters. According to power calculations, a replicate number of 24 would be required to achieve statistical difference between chemokinesis of 2GNF and 2GECV-treated neutrophils. In addition, there appeared to be e-cigarette device power-dependent effects on neutrophil chemotaxis parameters, but there was not a statistical difference. Power calculations revealed a replicate number of 13 would be needed to achieve a statistically significant difference in chemokinesis between 2GECV and 4GECV treated neutrophils.

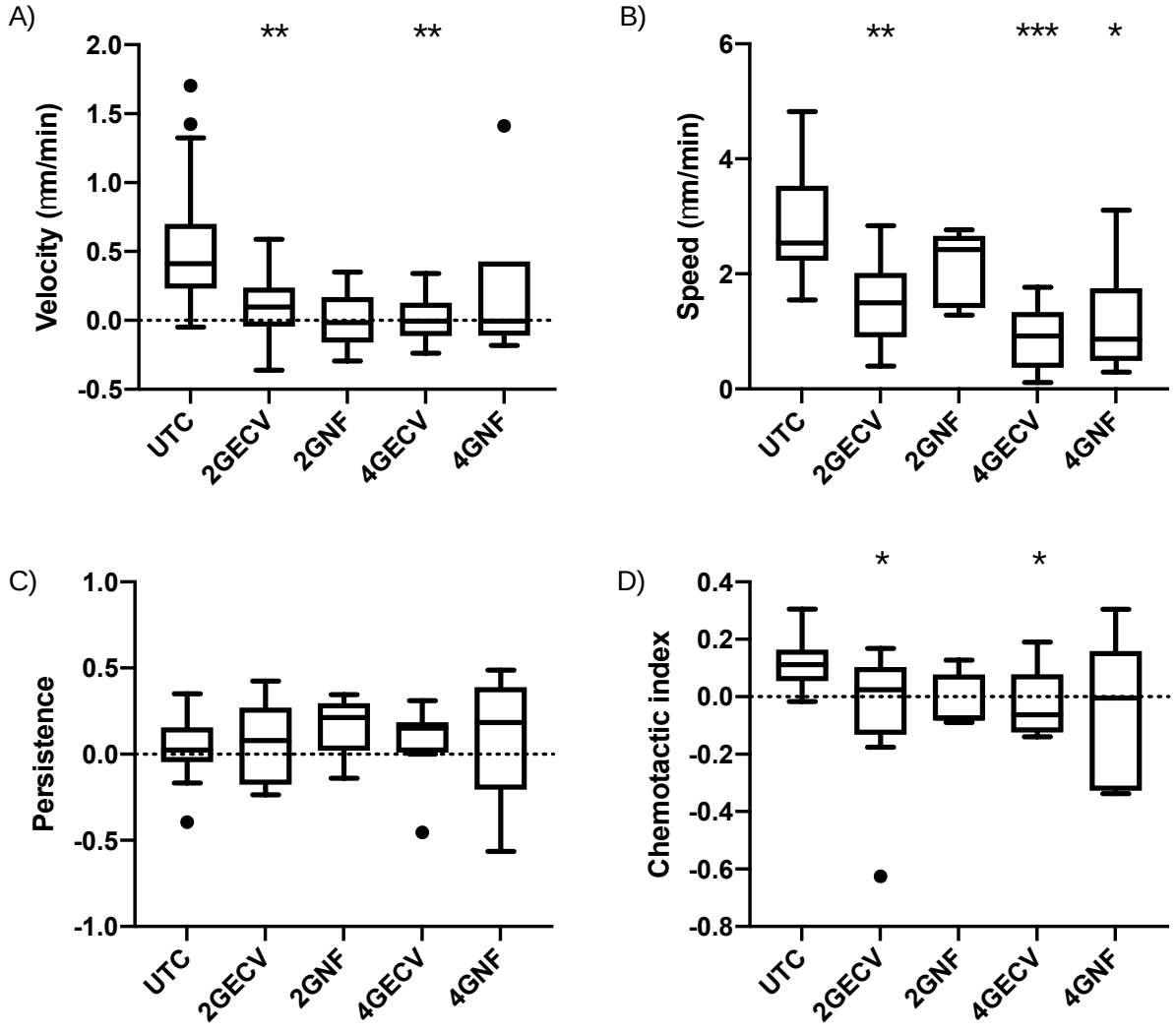


Figure 4.1: The effect of e-cigarette vapour exposure on neutrophil chemotaxis to CXCL8.

Neutrophils were treated with e-cigarette vapour while on coverslips. Insall chambers were used to assess live chemotaxis to 100nM CXCL8. Images were captured every 20 seconds for a total of 12 minutes using the Leica DM6000 microscope. Using FIJI Image J, 10 neutrophils were tracked over 12 minutes and the data imported into a pre-formatted template which gave (A) velocity, (B) speed, (C) persistence and (D) chemotactic index output values. Data was normally distributed for speed so paired and unpaired t tests were used to assess statistical significance. All other data was not normally distributed so wilcoxon matched-pairs signed rank and Mann Whitney tests were used to assess statistical difference. Statistical significance is indicated by an asterisks above each group, corresponding to a significant difference from untreated control (UTC). A significant difference between treatment groups is indicated by an asterisks above a capped line between the two significantly different groups. * = $p \leq 0.05$, ** = $p \leq 0.01$, *** = $p \leq 0.001$, **** = $p \leq 0.0001$, n = 5 (2GNF), n = 6 (4GNF) and n = 10 per nicotine-containing e-cigarette vapour groups.

4.4.1.2 E-cigarette vapour exposure and neutrophil transmigration to CXCL8

To further investigate the effect of e-cigarette vapour exposure on neutrophil migration, a transwell system was used to measure neutrophil transmigration across a membrane towards the chemoattractant CXCL8. All e-cigarette treatments significantly impaired neutrophil transmigration to CXCL8 compared to UTC (2GECV: $p = 0.0488$, 2GNF: $p = 0.0273$, 4GECV $p = 0.0020$, 4GNF $p = 0.0020$), as shown in Figure 4.2A. There was a device-power dependent effect on neutrophil transmigration, with significantly fewer migrating neutrophils in 4th generation e-cigarette vapour exposed neutrophils compared to 2nd generation (2GECV vs 4GECV: $p = 0.0159$, 2GNF vs 4GNF: $p = 0.0418$). There were no nicotine-dependent effects in neutrophil transmigration, with no significant differences between 2GECV & 2GNF and 4GECV & 4GNF.

Furthermore, the transwell membranes were stained for the neutrophil cell surface marker CD16 and visualised under the Leica DMI 6000B microscope. 4GECV-exposed neutrophils were seen to be aggregated in the membrane, which was not seen in the UTC or 2GECV transwells (Figure 4.2B-D).

Overall, this data suggested neutrophil migration as impaired by e-cigarette vapour exposure, exaggerated by higher power devices, in a nicotine-independent manner. Both speed and velocity of chemotaxis towards the chemoattractant were impaired, and neutrophils appeared to aggregate in the transwell membrane, together potentially driving this dysfunction.

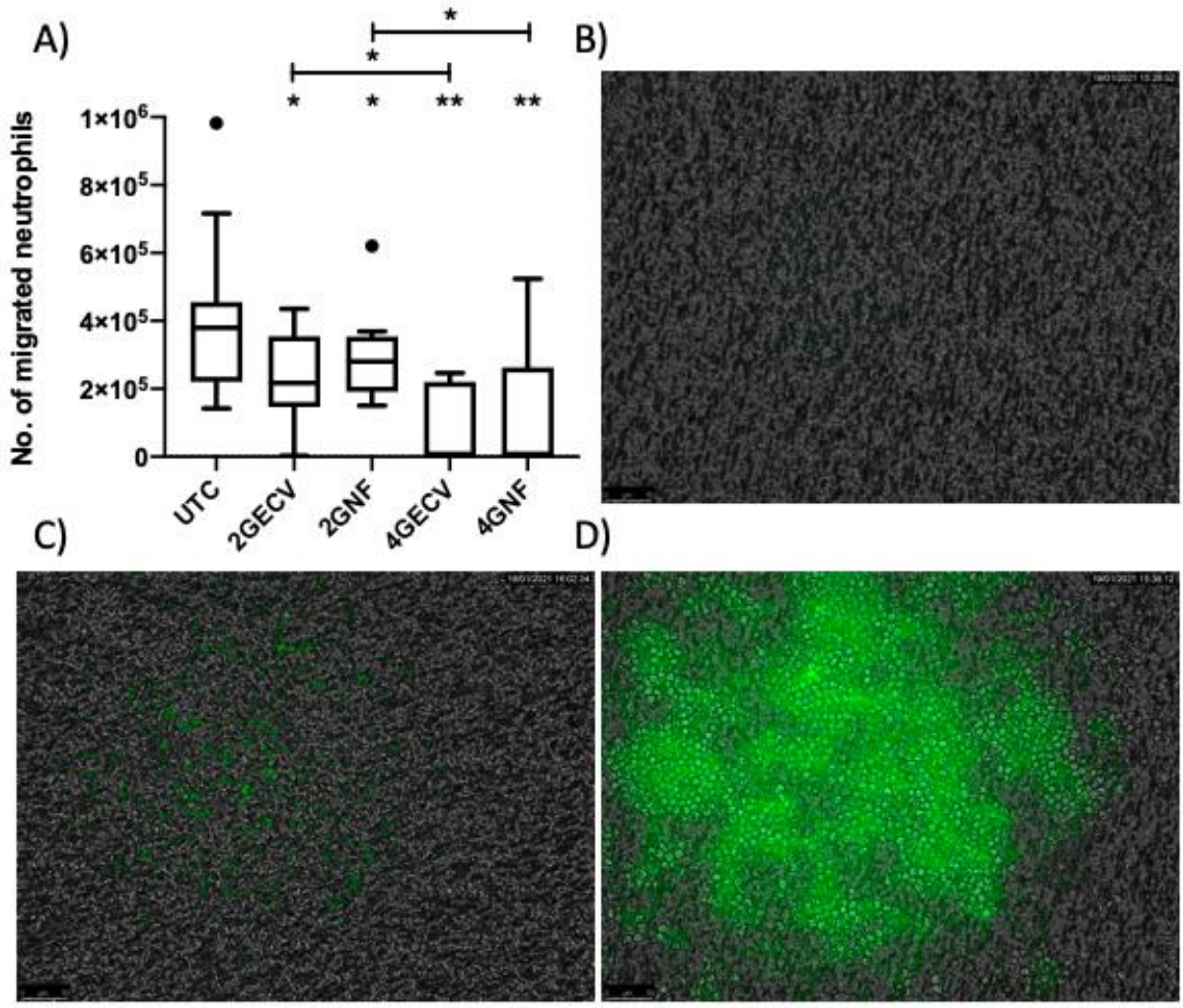


Figure 4.2: The effect of e-cigarette vapour exposure on neutrophil transwell migration.

Neutrophils were exposed to e-cigarette vapour before being added to the transwell containing 100 nM CXCL8 in the bottom well. After 90 minutes, the transwells were removed and disposed of and the supernatant was collected. 100 μL of the supernatant was run through the BD FACSvia and the number of neutrophils counted. This was scaled up to the total volume of the supernatant to get the total number of cells which migrated through the transwell in each condition (A). In addition, transwells were removed from the supernatant and stained with CD16-APC (1:100 in 1% PBS-BSA) before being visualised under the Leica DMI 6000B to observe whether there were cells unable to detach from the transwell the pictures are displayed in B (UTC), C (2GECV) and D (4GECV). Data was not normally distributed so statistical significance was assessed using wilcoxon matched-pairs signed rank test and Mann-Whitney tests. Statistical significance is indicated by asterisks above each group, corresponding to a significant difference from untreated control (UTC). A significant difference between treatment groups is indicated by an asterisks above a capped line between the two statistically different groups. * = $p \leq 0.05$, ** = $p \leq 0.01$, *** = $p \leq 0.001$, **** = $p \leq 0.0001$, n = 10 per group.

4.4.2 E-cigarette vapour exposure and neutrophil phagocytosis of *E. coli* and *S. aureus*

To examine the effects of e-cigarette vapour exposure on neutrophil phagocytosis, *E. coli* and *S. aureus* pHrodo™ bioparticles were used to determine whether there are differences in ability to clear gram-positive and gram-negative bacteria. Two time points, 30 minutes and 60 minutes time points were measured to assess phagocytic dynamics over time.

4.4.2.1 *E. coli*

At 30 minutes, there was a significant reduction in the amount of *E. coli* pHrodo™ bioparticles phagocytosed (MFI) by 4GECV and 4GNF treated neutrophils compared to UTC ($p = 0.0093$, 0.0078 respectively, Figure 4.3A). However, there was a significant decrease in the percentage of pHrodo™ -positive cells in all e-cigarette treatment groups ($p = 0.0312$ (2GNF), 0.0049 (2GECV), 0.0039 (4GNF), 0.0007 (4GECV), Figure 4.3B).

At 60 minutes, there was a significant decrease in the MFI of neutrophils treated with 2GNF ($p = 0.0078$), 4GNF ($p = 0.0078$) and 4GECV ($p = 0.0093$) compared to UTC but not 2GECV as shown by Figure 4.3E. The difference between the amount of bioparticles ingested between UTC and 2nd generation e-cigarette exposed neutrophils appears greater at 30 minutes than 60 minutes, but in 4th generation e-cigarette exposed neutrophils, phagocytosis was more different from UTC at 60 minutes than 30 minutes. However, there remained a significant reduction in the percentage of

pHrodo™ positive cells in all treatment groups at 60 minutes (p = 0.0234 (2GNF), 0.0068 (2GECV), 0.0078 (4GNF), 0.0005 (4GECV), Figure 4.3F).

4.4.2.2 *S. aureus*

At 30 minutes, all 4 e-cigarette treatment groups: 2GNF, 2GECV, 4GNF and 4GECV induced a reduction in the amount of *S. aureus* pHrodo™ bioparticles ingested by neutrophils compared to UTC (p = 0.0078, 0.0024, 0.0156, 0.0010 respectively, Figure 4.3C). In addition, the percentage of pHrodo™ positive neutrophils was significantly reduced compared to UTC in all treatment groups (p = 0.0078, 0.0024, 0.0078, 0.0010 respectively, Figure 4.3D).

At 60 minutes, there remained significant reductions in the amount of pHrodo™ bioparticles phagocytosed by all 4 treatment groups (2GNF p = 0.0078, 2GECV p = 0.0210, 4GNF p = 0.0078, 4GECV p = 0.0010, Figure 4.3G). Finally, at 60 minutes there was also a reduction in the percentage of pHrodo™ positive neutrophils in all 4 treatment groups (2GNF p = 0.0078, 2GECV p = 0.0029, 4GNF p = 0.0078, 4GECV p = 0.0005, Figure 4.3H).

4.4.2.3 Nicotine-dependent effects on neutrophil phagocytosis of *E. coli* and *S. aureus*

A nicotine-dependent reduction in the amount of pHrodo™ bioparticles ingested by neutrophils was observed in 2GECV treated neutrophils compared to 2GNF when incubated with *E. coli* for 30 minutes (p = 0.0391, Figure 4.3A). Conversely, after 30 minutes of incubation with *S. aureus* bioparticles, there was a lower uptake by 2GNF

treated neutrophils compared to 2GECV treated neutrophils (p = 0.0391, Figure 4.3C). However, these effects were no longer present at 60 minutes (see Figure 4.3E&G). There were no nicotine dependent differences in 4th generation device exposed groups in any conditions measured.

4.4.2.4 Device power-dependent effects on neutrophil phagocytosis of *E. coli* and *S. aureus*

A significant reduction from controls in the percentage of pHrodo™ positive neutrophils was observed between the 2GECV and 4GECV groups (p = 0.0469, Figure 4.3D) when incubated with *S. aureus* bioparticles for 30 minutes. This difference was not seen at the 60 minute time point (see Figure 4.3H). However, again there was a significant reduction in the percentage of pHrodo™ positive neutrophils between the 2GECV and 4GECV groups (p = 0.0312, Figure 4.3F) when incubated with *E. coli* for 60 minutes, but this difference was not observed at the earlier time point. This can be seen in Figure 4.4.

Together, these data demonstrate neutrophil phagocytosis of *E. coli* and *S. aureus* was significantly impaired by e-cigarette vapour exposure, however, the dynamics of the impairments are different between the two bacterial bioparticles. Lower phagocytosis caused by e-cigarette exposure are seen at the intermediate phase of phagocytosis and persist to 60 minutes.

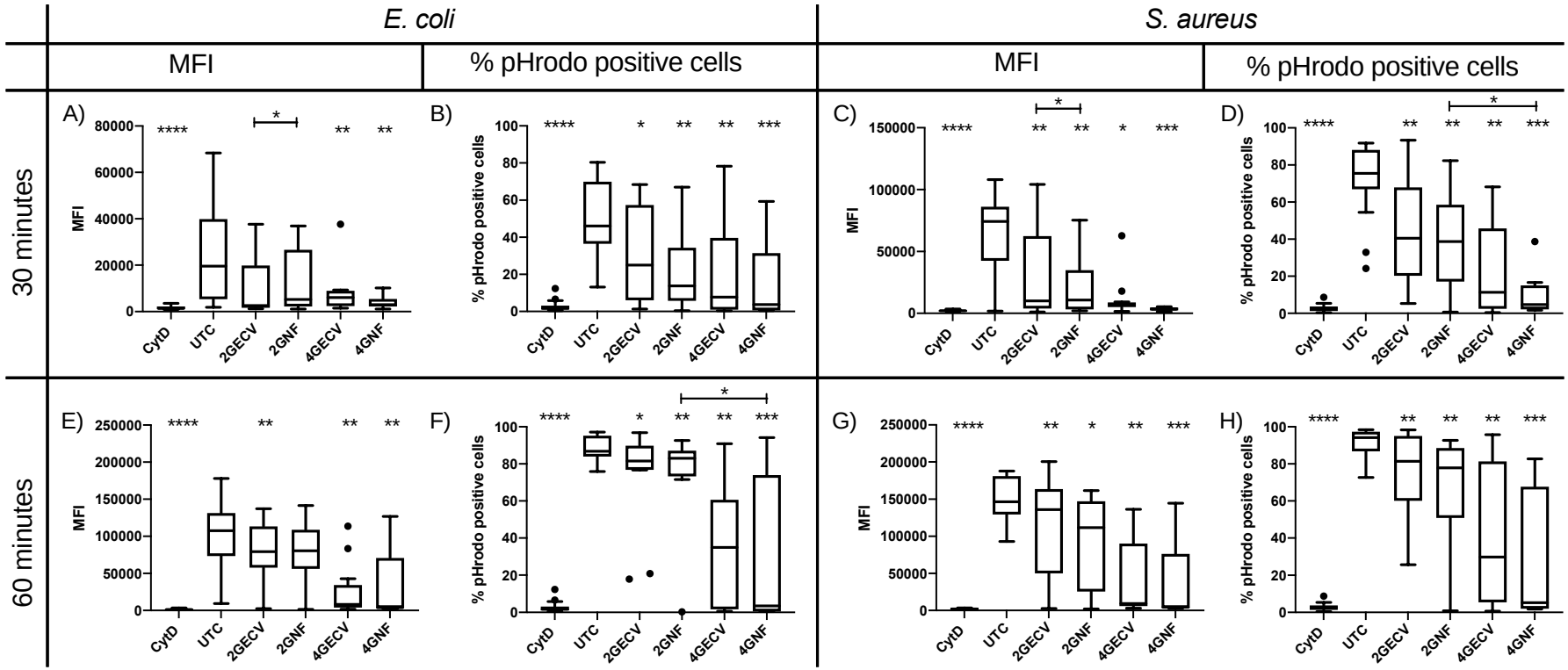


Figure 4.3: The effect of e-cigarette vapour exposure on neutrophil phagocytosis of *E. coli* and *S. aureus* pHrodo™ bioparticles.

Neutrophils were treated with relevant e-cigarette vapour before incubation with *E. coli* or *S. aureus* pHrodo™ bioparticles for 30 or 60 minutes. Negative control cells were incubated with 20 μM Cytochalasin D (CytD) for 20 minutes prior to the addition of bioparticles for the longest time point (60 minutes). The median fluorescence intensity (MFI) of the FL1 channel for the whole population was recorded, corresponding to the amount of pHrodo™ bioparticles ingested (A, C, E, G). In addition, the percentage of pHrodo™ positive cells in the population was recorded (based on CytD control samples) (B, D, F, H). Data was not normally distributed so statistical significance was assessed using a wilcoxon matched-pairs signed rank test. Statistical significance is indicated by asterisks above each group, corresponding to a significant difference from untreated control (UTC). A significant difference between treatment groups is indicated by an asterisks above a capped line between the two statistically different groups. * = $p \leq 0.05$, ** = $p \leq 0.01$, *** = $p \leq 0.001$, **** = $p \leq 0.0001$, n = 8 per 2GNF and 4GNF treatment groups, n = 12 per 2GECV and 4GECV treatment groups.

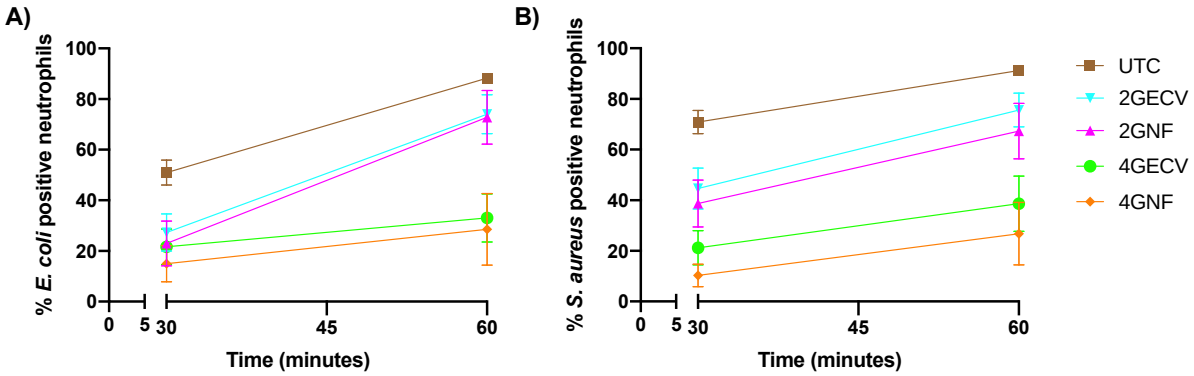


Figure 4.4: Neutrophil phagocytosis of *E. coli* and *S. aureus* pHrodo™ bioparticles over time

Neutrophils were treated with relevant e-cigarette vapour before incubation with E. coli or S. aureus pHrodo™ bioparticles for 30 or 60 minutes. The percentage of pHrodo™ positive cells in the population was recorded (based on CytD control samples). A) represents the *E. coli*-positive neutrophils after 30 and 60 minutes, and B) represents the *S. aureus*-positive neutrophils after 30 and 60 minutes. Data is expressed as mean and SEM of biological repeats. N = 8 per 2GNF and 4GNF treatment groups, n = 12 per 2GECV and 4GECV treatment groups.

4.4.3 Neutrophil protein secretion in response to e-cigarette vapour exposure

To assess neutrophil degranulation, supernatants of e-cigarette vapour treated neutrophils were examined using Quantikine ELISA kits. Markers of each category of neutrophil granule: MPO (primary azurophilic granule), MMP-8 (secondary specific granule) and MMP-9 (tertiary gelatinase granule) were measured for each sample (Völs et al., 2017). In addition, MMP-2 was measured as preliminary Luminex data indicated detectable levels in neutrophil supernatants, and this had previously been investigated in BALF of e-cigarette users (Ghosh et al., 2019).

MMP-2 was significantly higher in 2GNF e-cigarette-exposed samples compared to UTC ($p = 0.0226$). There were no other significant differences in MMP-2 secretion between UTC and treatment groups (Figure 4.5A). There were no significant differences in MMP-8 secretion between UTC and treatment groups (Figure 4.5B). There were no significant differences in MMP-8 secretion between any of the e-cigarette treatment groups. There were no significant differences in MMP-9 secretion between UTC and e-cigarette treatment groups, but there was a trend towards significance between UTC and 4GECV-exposed neutrophils ($p = 0.0533$). According to power calculations, 51 repeats would be needed to achieve statistical significance between these groups. There were no significant differences in MMP-9 secretion between any of the e-cigarette vapour exposure groups, as shown in Figure 4.5C. There was significantly lower MPO secretion in 4GECV-exposed neutrophils compared to UTC ($p = 0.0449$, Figure 4.5D). There were no other significant differences in MPO secretion between any of the groups.

Overall, there are some changes in neutrophil degranulation shown here. MMP-2 secretion into supernatants was higher in 2GNF-exposed neutrophils compared to UTC and MPO secretion was inhibited by 4GECV-exposure compared to UTC. However, the extent to which these results have biological significance is not clear without futher replicates, and positive controls for degranulation. This is also an acute response and may not represent in vivo effects.

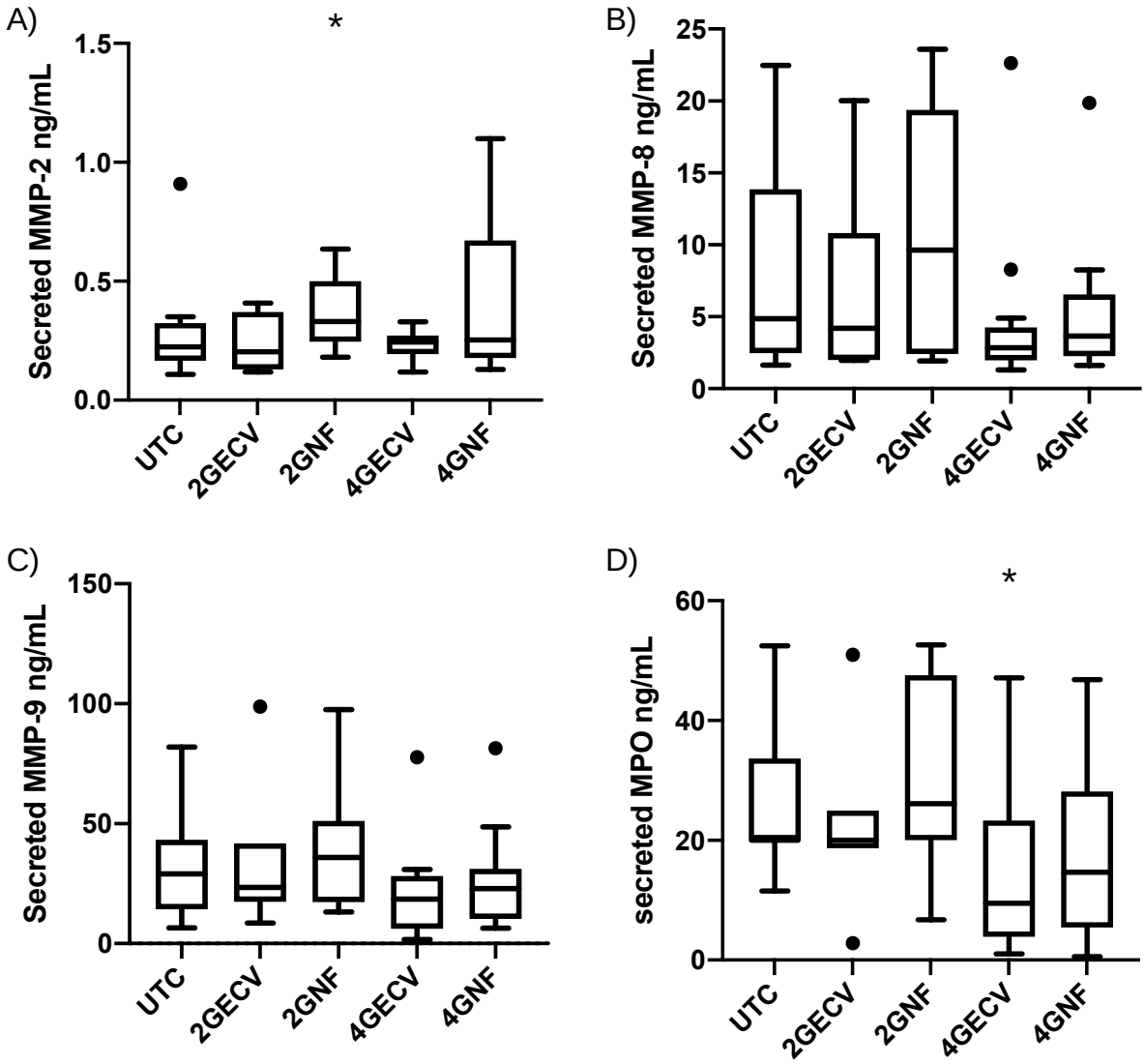


Figure 4.5: Neutrophil secretion of MMP-2, MMP-8, MMP-9 and MPO in response to e-cigarette vapour exposure.

Neutrophil supernatants were sampled using Bio-techne Quantikine ELISA kits for MMP-2, MMP-8, MMP-9 and MPO content. Details of the kits used and dilution factors can be found in table 2.3. Data was not normally distributed (shapiro-wilk), so statistical differences were assessed used mann-whitney tests. Statistical significance is indicated by asterisks above each group, corresponding to a significant difference from untreated control (UTC). A significant difference between treatment groups is indicated by an asterisks above a capped line between the two statistically different groups. * = $p \leq 0.05$, ** = $p \leq 0.01$, *** = $p \leq 0.001$, **** = $p \leq 0.0001$, N = 7 (2GNF), n = 10 (2GECV), n = 13 (4GECV), n = 15 (4GNF), including paired UTC sample per treated sample.

4.4.4 Neutrophil bioenergetics

4.4.4.1 E-cigarette vapour exposure and basal neutrophil metabolism

The Agilent Seahorse XF96 analyser was used to test glycolysis and oxidative burst responses of treated and untreated neutrophils. During these tests, it was possible to determine baseline metabolic parameters by examining OCR and ECAR before the addition of any stimulants/inhibitors. Figure 4.6A&B show these traces, representing the OCR and ECAR over time before the addition of any compounds. There were no significant differences in the OCR or ECAR of neutrophils at baseline between any of the groups (Figure 4.6A&B). Mitochondrial acidification, shown in Figure 4.6C, was based on the ECAR data, but accounting for the buffer factor of the media and the OCR of the test, allowing a calculation of the contribution of proton efflux rate (PER) attributable to the mitochondria. There were no differences in mitochondrial acidification between UTC and any of the e-cigarette treatment groups, nor between the treatment groups themselves.

There were no differences between UTC and treatment groups when comparing basal ECAR (Figure 4.6D). There was, however, significantly higher basal glycolysis and non-glycolytic acidification rates in the 4GECV treatment group compared to 2GECV (Basal glycolysis: $p = 0.0391$, non-glycolytic acidification: $p = 0.0391$). There were no further differences in baseline metabolism between any of the groups.

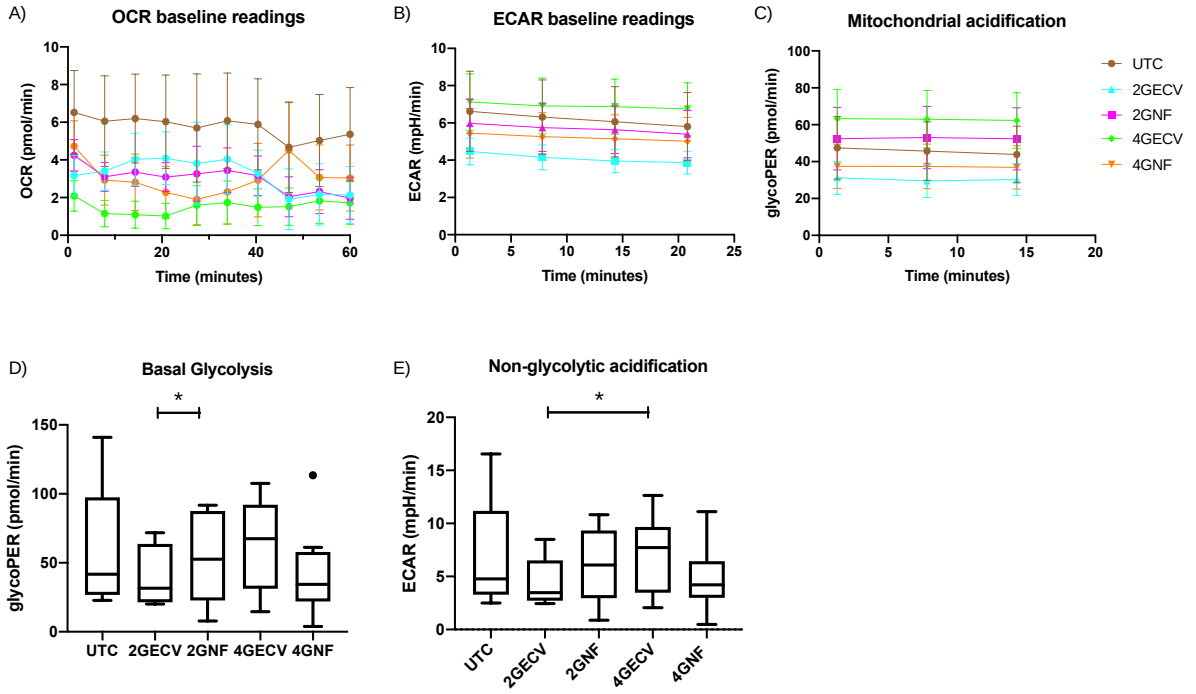


Figure 4.6: Baseline metabolism of neutrophils treated with e-cigarette vapour. A) and B) represent the oxygen consumption rate (OCR) and extracellular acidification rate (ECAR) of neutrophils treated or untreated with e-cigarette vapour when the Seahorse protocol begins, up until the first injection of a stimulant/inhibitor. Traces represent the mean and SEM of this time period for all 5 groups performed on neutrophils from 7 distinct volunteers. Measurements were taken in quadruplicate, and the average (mean) OCR and ECAR calculated for each sample before combining to form traces A and B. C) is the mitochondrial acidification of the treated/untreated neutrophils based on the ECAR accounting for the buffer factor of the media and the OCR of the test, allowing a calculation of the contribution of proton efflux rate (PER) attributable to the mitochondria. D) represents basal glycolysis which is the final glycoPER reading before injection of inhibitors and E) is the non-glycolytic acidification of the cells, deduced as shown in Figure 2.7. Data was not normally distributed so two-way ANOVA (A-C) and Wilcoxon matched pairs signed rank tests (D-E) were performed to test for statistical differences. Statistical significance is indicated by asterisks above/adjacent to each group, corresponding to a significant difference from untreated control (UTC). A significant difference between treatment groups is indicated by an asterisks with a capped line between the two statistically different groups. * = $p \leq 0.05$, ** = $p \leq 0.01$, *** = $p \leq 0.001$, **** = $p \leq 0.0001$, n = 7 per group.

4.4.4.2 E-cigarette vapour exposure and neutrophil oxidative burst response

Neutrophil oxidative burst response to 160 nM PMA was investigated using the Agilent Seahorse XF96 analyser. Figure 4.7A shows the combined trace of 7 distinct neutrophil donors and the oxidative burst response in all treatment groups. A two-way ANOVA with multiple comparisons revealed a significant difference in oxidative burst response in 4GECV compared to UTC ($p = 0.0211$). There were no differences between 2GECV, 2GNF or 4GNF and UTC groups in any of the comparisons. There were significant differences between device generations (2GECV vs. 4GECV $p = 0.0263$, 2GNF vs. 4GNF $p = 0.0419$) with 4th generation treated groups exhibiting lower oxidative burst response to PMA than 2nd generation treated groups. There were no nicotine-dependent effects on oxidative burst response to PMA (2GECV vs. 2GNF not significant, 4GECV vs 4GNF not significant). Area under the curve analysis revealed there were no differences between the time to reach peak OCR in any of the groups (Figure 4.7B). There was a significant reduction in maximum OCR reached by 4GECV treated neutrophils ($p= 0.002$, Figure 4.7C). There was a trend towards a significant difference in maximum OCR of 4GNF treated neutrophils compared to UTC ($p = 0.0716$). Power calculations on maximum OCR data revealed a replicate value of 7 should have achieved statistical significance between UTC and 4GNF, indicating this data was on the close to significance. Furthermore, there was a significant reduction in maximum OCR in 4th generation treated groups compared to their 2nd generation device counterparts (2GNF vs. 4GNF $p = 0.0135$, 2GECV vs. 4GECV $p = 0.009$, Figure 4.7C). No e-cigarette vapour treatment, device power or nicotine presence had a significant impact on the total oxygen consumption over the duration of the oxidative burst test (Figure 4.7D). There was a trend towards a reduction in total oxygen

consumption in multiple comparisons tested (4GECV vs 2GECV p = 0.0625, 4GNF vs 2GNF p = 0.0625, 4GECV vs UTC p = 0.0625, 4GNF vs UTC p = 0.0625). Power calculations revealed only low numbers (1-6 replicates) were needed to achieve significance in total oxygen consumption between UTC and treatment groups, however it is likely that due to the nature of the non-parametric test performed, statistical significance would not be confirmed until larger replicate numbers were reached.

Data presented here showed baseline metabolism was higher in 4th generation e-cigarette vapour exposed neutrophils, suggesting they may be more activated at baseline than 2nd generation-exposed neutrophils. The significant inability of neutrophils exposed to 4th generation e-cigarette vapour to amount an oxidative burst response to PMA has consequences for neutrophil antimicrobial activity, chemotaxis and apoptosis (Nordenfelt and Tapper, 2011, Dupré-Crochet et al., 2013). This was a nicotine-independent effect and highly device power-dependent.

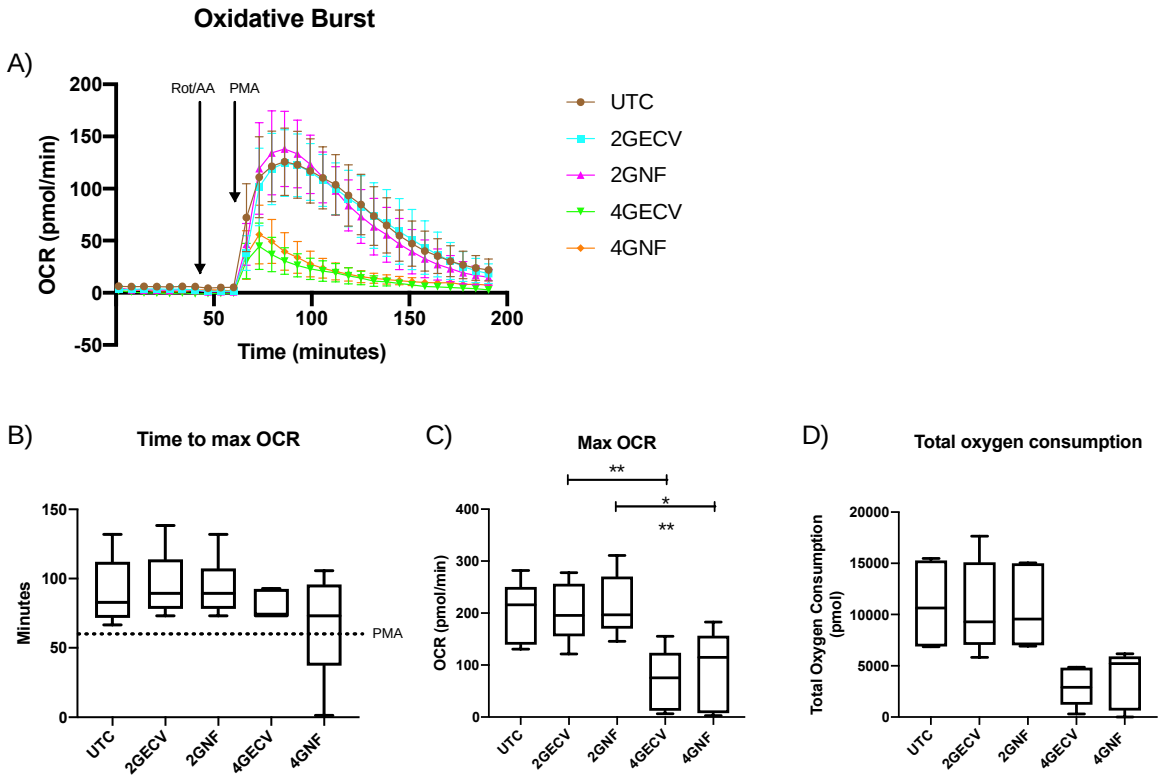


Figure 4.7: The effect of e-cigarette vapour exposure on neutrophil oxidative burst response to 160 nM PMA.

Neutrophil oxidative burst response to 160 nM PMA was assessed using the Agilent Seahorse XF96 and corresponding application note protocol was followed. A) shows the combined oxygen consumption rate (OCR) trace for the duration of the metabolic test for all 5 treatment groups performed on neutrophils from 7 distinct volunteers. Measurements were taken in quadruplicate, and the average (mean) OCR calculated for each individual. The trace represents the mean and SEM of 7 distinct donors. Area under the curve analysis was performed on the trace for each individual and the time to max OCR (B), maximum OCR (C) and total oxygen consumption (D) were established. Time to max OCR and Total oxygen consumption data was not normally distributed so statistical significance was assessed using awWilcoxon matched-pairs signed rank test. Max OCR data was normally distributed so differences were assessed using a paired two tailed t-test. Statistical significance is indicated by asterisks above each group, corresponding to a significant difference from untreated control (UTC). A significant difference between treatment groups is indicated by an asterisks above a capped line between the two statistically different groups. * = $p \leq 0.05$, ** = $p \leq 0.01$, *** = $p \leq 0.001$, **** = $p \leq 0.0001$, n = 7 per group for all data.

4.4.5 E-cigarette vapour exposure and NET generation

NETosis can be triggered by a range of stimuli including microorganisms, proinflammatory cytokines, activated endothelial cells and nitric oxide, but drivers of NETs are still being uncovered (Vorobjeva and Chernyak, 2020, Kaplan and Radic, 2012). It was important to assess both spontaneous NET generation after e-cigarette vapour exposure and stimulated NET generation. From this data, it was possible to determine whether e-cigarette exposure triggers NET release alone and the ability of neutrophils to amount a NET response when stimulated with PMA after e-cigarette vapour exposure.

4.4.5.1 Spontaneous NET generation

Spontaneous NET generation was measured to assess whether e-cigarette vapour exposure causes induction or suppression of baseline NETosis alone. **Error! Reference source not found.**A shows the fluorescence intensity of neutrophil supernatants stained with the nucleic acid stain SYTOX® green. E-cigarette vapour did not statistically effect spontaneous NET generation from UTC. There was a trend towards a statistically significant increase in spontaneous NET generation in neutrophils exposed to 2GNF e-cigarette vapour ($p = 0.0625$) compared to UTC. To reach statistical significance between UTC and 2GNF, this would have required a total of 150 repeats, however, there was a less statistically significant difference between UTC and 2GECV ($p = 0.1250$), but this would have required only 20 repeats to achieve statistical significance. There were no differences in spontaneous NET generation between any of the e-cigarette treatment groups.

4.4.5.2 PMA-stimulated NET generation

Neutrophils were stimulated with PMA as a robust stimulator of NETosis and the effect of e-cigarette vapour exposure on this process was investigated. Compared to UTC, there were no differences in the NET response to PMA in any of the e-cigarette vapour treatment groups, see **Error! Reference source not found.**B. There was a trend towards a reduction in NET generation in 4GECV treated neutrophils compared to UTC ($p = 0.0625$) this difference did not reach statistical significance. According to power calculations, a replicate number of 7 would have achieved a statistically significant difference between UTC and 4GECV and a replicate number of 20 between UTC and 2GECV when examining PMA-stimulated NET response, indicating there may be differences but this data was underpowered.

It was possible to calculate the size of the NET response amounted (Δ RFU) to PMA, as shown in **Error! Reference source not found.**C. No e-cigarette vapour treatments induced a significant change in size of PMA-induced NET response amounted, however, there was a trend towards reduction in 4GNF and 4GECV treated neutrophils compared to UTC ($p = 0.0625$). According to power calculations, smaller sample sizes than those presented here would be needed to produce a statistically significant difference, suggesting this type of statistical test used was not likely not to produce a statistically significant difference with a sample size as small as 5. There were no significant differences between e-cigarette treatment groups, but there was a trend towards significance between 2GECV and 4GECV ($p = 0.0625$). A sample size of 10 or more would be required to produce a statistically significant difference in this test, based on the data presented.

It has been shown previously that e-cigarette vapour exposure alone does not stimulate NET generation in our model. In addition, there was no change in the PMA NET response in any of the e-cigarette treatment groups. However, it appears that the ability of neutrophils to amount a NET response to PMA was reduced after e-cigarette vapour exposure, but this cannot be concluded due to underpowered data.

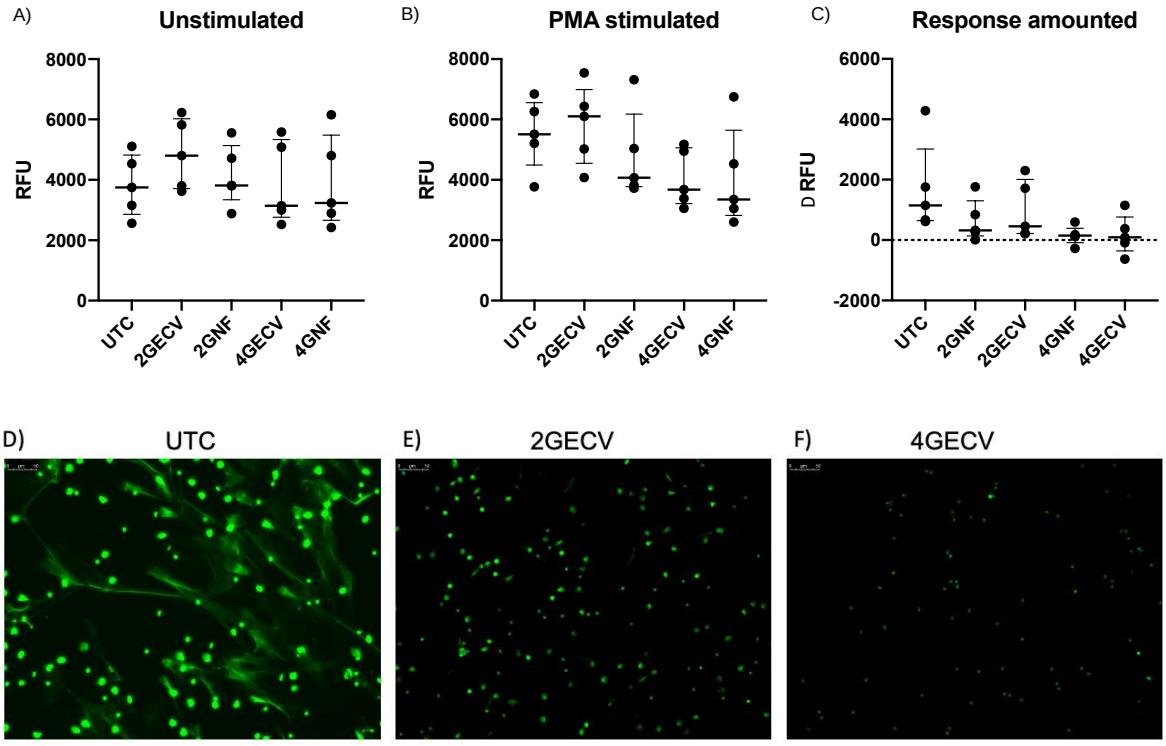


Figure 4.8: The effect of e-cigarette vapour exposure on neutrophil NETosis. Neutrophil NETosis was measured by assessing fluorescence after staining supernatants with SYTOX® Green, as described in section 2.11.2. Fluorescence was measured using a plate reader, and the relative fluorescence unit (RFU) readout correlates with NET generation. NETosis was assessed after exposure to e-cigarette vapour, with or without stimulation with 25 nM PMA. This allowed the assessment of both A) unstimulated and B) PMA stimulated NETosis. From these data, the size of NET response to PMA (C: PMA stimulated – unstimulated = ∆ RFU) was calculated. Data was treated as not normally distributed due to low n numbers so wilcoxon matched-pairs signed rank tests were performed to assess statistical differences. There were no statistically significant differences between any of the groups. n = 5 per group.

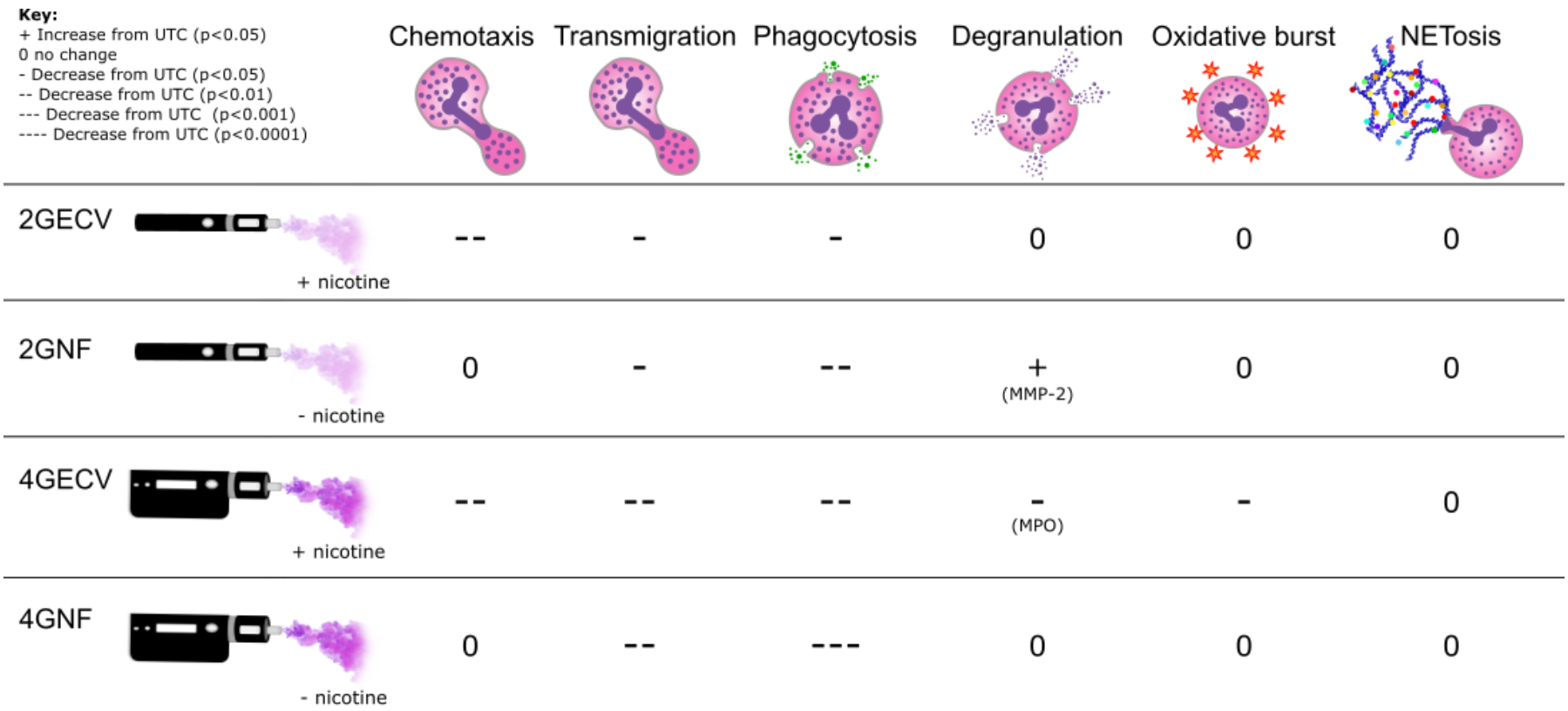


Figure 4.9: Infographic summary of the effects of e-cigarette vapour on key neutrophil effector functions studied in chapter 4.

Neutrophil effector functions studied in this chapter include migration, phagocytosis, degranulation, oxidative burst and NET generation. The effect of each e-cigarette vapour treatment on neutrophils functions is indicated. 2GECV is the vapour generated using a 2nd generation device loaded with e-liquid containing nicotine. 2GNF represents the vapour generated using a 2nd generation device loaded with nicotine free e-liquid. 4GECV is the vapour generated using a 4th generation device loaded with e-liquid containing nicotine. 4GNF represents the vapour generated using a 4th generation device loaded with nicotine free e-liquid. +, 0 and – represent changes from UTC, as indicated by the key.

4.4.6 Direct treatment of neutrophils with nicotine

To determine the contribution of nicotine to neutrophil dysfunction seen in e-cigarette vapour exposure, nicotine was added directly to neutrophils in media and the effects on viability, phagocytosis, NET generation and transwell migration were assessed. Nicotine concentrations were matched with those determined by GC-FID analysis that neutrophils are exposed to during 2GECV (0.6 μM) and 4GECV (3 μM) exposure in our model.

4.4.6.1 Nicotine treatment and neutrophil viability

Neutrophils were treated for 20 minutes with 0.6 μM or 3 μM nicotine based on GC-FID results. Neutrophil viability was unaffected by this treatment (Figure 4.10). On average, 85.13% of UTC neutrophils were live, compared to 88.83% of neutrophils treated with 0.6 μM nicotine and 83.93 of neutrophils treated with 3 μM nicotine.

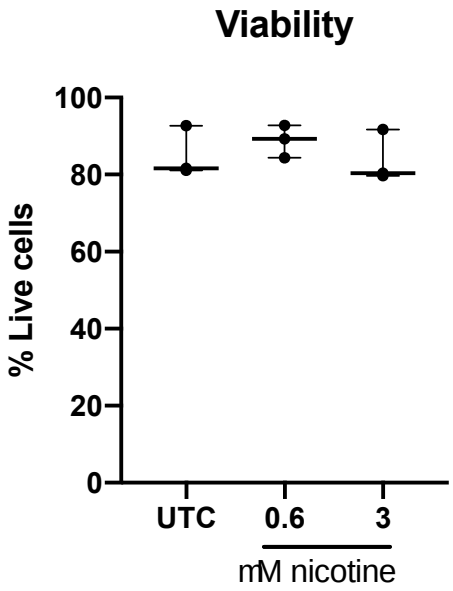


Figure 4.10: The effect of nicotine treatment on neutrophil viability.
Neutrophils were treated with 0.6 or 3 µM nicotine (based on GC-FID results) for 20 minutes before viability was assessed by annexin V/PI co-staining. Data was treated as non-parametric due to low n numbers. Wilcoxon matched-pairs signed rank tests were used to assess statistical difference between the groups, there were no differences between any of the groups. N = 3.

4.4.6.2 Nicotine treatment and neutrophil transwell migration

There was a trend towards a reduction in neutrophil transwell migration by treatment with 0.6 μM nicotine and 3 μM nicotine ($p = 0.0625$) compared to UTC, as shown in Figure 4.11. There was no difference in the number of neutrophils migrating through a transwell to CXCL8 between the two nicotine-treatment groups. Power calculations revealed a sample size of 11 would be necessary to achieve a statistically significant difference from UTC caused by 3 μM nicotine treatment.

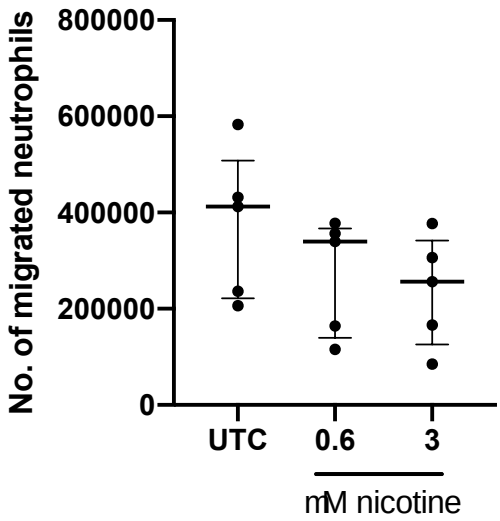


Figure 4.11: The effect of nicotine treatment on neutrophil transwell migration. Neutrophils were treated with 0.6 or 3 μM nicotine (based on GC-FID results) for 20 minutes before incubating on a transwell with 100 nM CXCL8 in the bottom well. Cell migration was measured by counting the number of cells in the supernatant using a flow cytometer. Data was treated as non-parametric due to low n numbers. Wilcoxon matched-pairs signed rank tests were used to assess statistical difference between the groups. There were no statistically significant differences between any of the groups. N = 5.

4.4.6.3 Nicotine treatment and NET generation

There was no change in NET generation compared to UTC at baseline caused by either nicotine treatment, see Figure 4.12A. There was also no effect of 0.6 μM nicotine compared to 3 μM nicotine with no further stimulation. Upon stimulation, there was no difference in the RFU between nicotine treatment groups or when they were compared to UTC, as shown in Figure 4.12B. In response to PMA stimulation, both nicotine treatments appeared to reduce the size of the NET response generated (Figure 4.12C), however this affect was not statistically significant and would require a sample size of at least 4 to have reached significance. There was also no difference in NET response amounted between the nicotine treatment groups at the concentrations of nicotine used in the exposure.

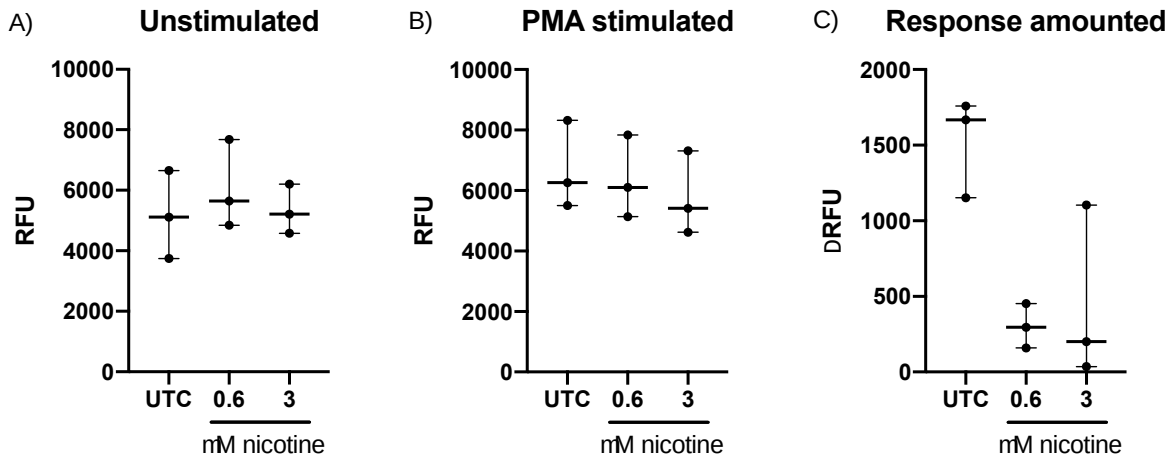


Figure 4.12*:* The effect of nicotine treatment on neutrophil NET generation. Neutrophils were treated with 0.6 or 3 µM nicotine (based on GC-FID results) for 20 minutes before stimulating with 25 nM PMA for 3 hours. SYTOX® green was used to stain cell supernatants for DNA, correlating with the number of NETs generated. A) is the unstimulated NET generation, where cells were only treated with nicotine and NET generation measured. B) is the level of NET generation in response to PMA stimulation and C) is the difference between the fluorescence intensity of A and B, representing the size of the NET response. Data was treated as non-parametric due to low n numbers. Wilcoxon matched-pairs signed rank tests were used to assess statistical difference between the groups. There were no significant differences between any of the groups. N = 3.

4.4.6.4 Nicotine treatment and neutrophil phagocytosis of *E. coli* and *S. aureus* bioparticles

Nicotine treatment did not affect neutrophil phagocytosis to a statistically significant extent due to low replicate numbers. At 60 minutes, there was a trend towards a reduction in the percentage of *E. coli* pHrodo™ -positive neutrophils by 3 μM nicotine ($p = 0.0625$, Figure 4.13F) compared to UTC and 0.6 μM nicotine ($p = 0.0625$, Figure 4.13F) however there was no difference in the amount of pHrodo™ beads ingested (MFI) (Figure 4.13E). To achieve a statistical difference between UTC and 3 μM nicotine in this case, a replicate number of 9 would be required according to power calculations. There was only a trend towards a significant reduction in the amount of *E. coli* pHrodo™ bioparticles ingested by 3 μM nicotine treated neutrophils compared to UTC at 60 minutes, see Figure 4.13A&E, not in the amount of bioparticles phagocytosed. There were no changes in any *E. coli* phagocytosis parameters at 30 minutes, Figure 4.13A&B.

At 30 minutes, there was a trend towards a reduction in the amount of *S. aureus* pHrodo™ bioparticles ingested as well as the percentage of pHrodo™-positive neutrophils caused by 3 μM nicotine treatment ($p = 0.0625$, Figure 4.13C&D) compared to UTC. This trend towards a difference in the percentage of *S. aureus* pHrodo™-positive neutrophils persisted at the 60 minute time point ($p = 0.0625$, Figure 4.13H) but not the amount of *S. aureus* pHrodo™ bioparticles ingested (MFI). Comparing UTC to 0.6 μM nicotine treatment, there was a trend towards an increase in the amount of *S. aureus* pHrodo™ bioparticles ingested at 60 minutes ($p = 0.0625$, Figure 4.13G). There was a consistent trend towards a reduction in phagocytosis

parameters (% positive cells and MFI) at both time points between 0.6 μM and 3 μM nicotine treated neutrophils ($p = 0.0625$). For some of these parameters, power calculations revealed samples sizes less than 5 (the size of the data presented) should be required to achieve statistical difference. It is likely that the type of non-parametric tests performed would not result in p values < 0.05 with datasets of this size.

Overall, this data shows there was a trend towards impairment of normal neutrophil function caused by treatment with nicotine but that a larger sample size would be necessary to confirm this.

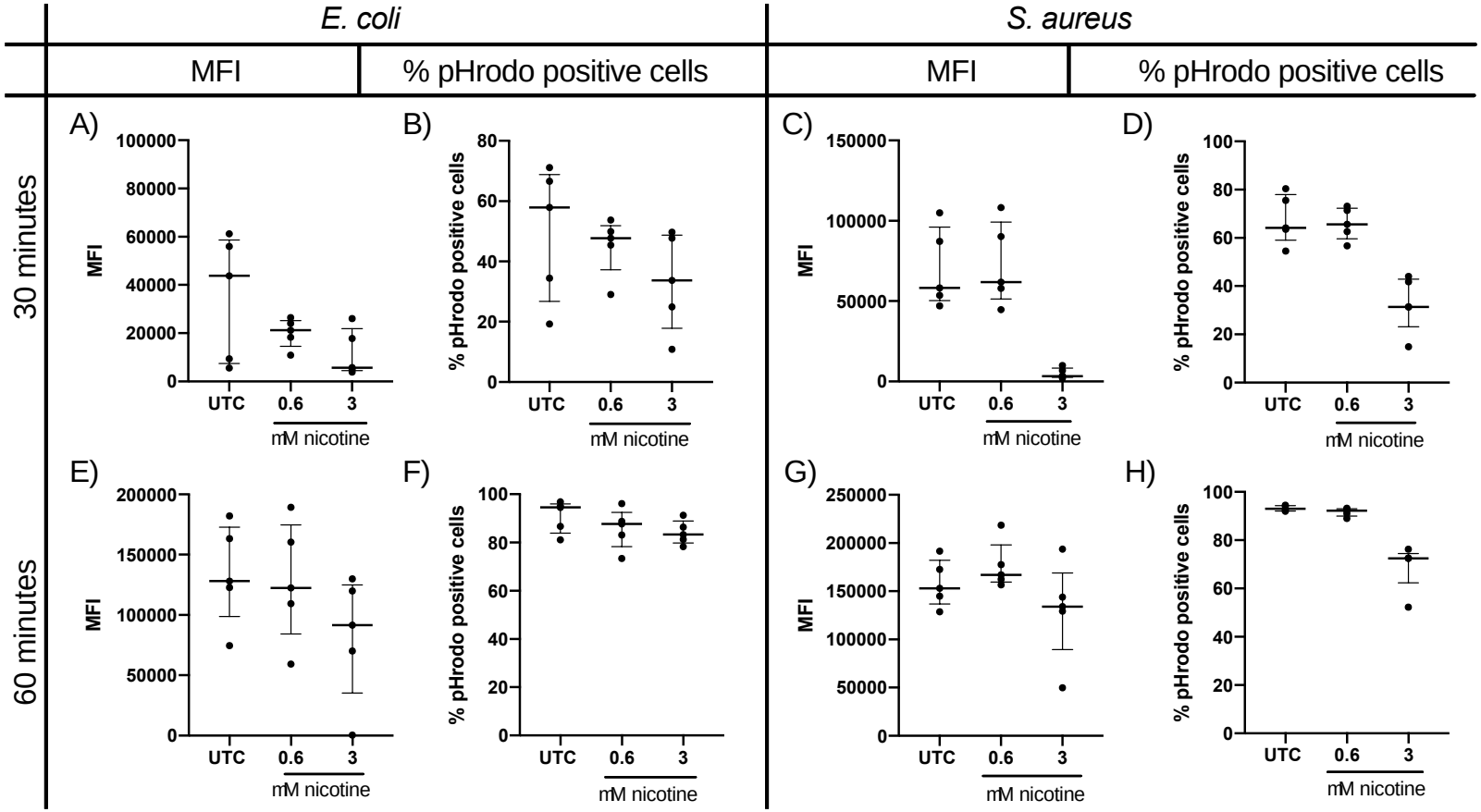


Figure 4.13: The effect of direct nicotine treatment on neutrophil phagocytosis.
Neutrophils were treated for 20 minutes with 0.6 μM or 3 μM nicotine before assessing phagocytosis of E. coli and S. aureus pHrodo™ bioparticles. Phagocytosis of both E. coli and S. aureus was assessed at 30 minutes and 60 minutes and the MFI (amount of bacteria ingested) and % pHrodo™ positive neutrophils is expressed. Data was treated as non-parametric due to low n numbers. Wilcoxon matched-pairs signed rank tests were used to assess statistical difference between the groups. There were no statistically significant differences between the groups. N = 5 per group.

4.5 Chapter 4 discussion

This chapter aimed to assess the impact of e-cigarette vapour on neutrophil chemotaxis, transmigration, phagocytosis, degranulation, oxidative burst and NET generation. In addition, the contribution of nicotine to these functions and the impact of device power on these key functions were assessed.

4.5.1 Neutrophil migratory parameters

E-cigarette vapour exposure induced significant reductions in in velocity, speed, and chemotactic index of neutrophils migrating toward CXCL8. Similarly, transmigration to CXCL8 was also significantly impaired by all e-cigarette vapour treatment groups, consistent with findings from Corriden et al. (Corriden et al., 2020). In both the Insall chamber and transwell models, there was a significant power-dependent effect, with more exaggerated inhibition of chemotaxis and transmigration by high power, 4th generation devices. 2nd generation e-cigarette devices appeared to provide a nicotine-dependent effect of e-cigarette vapour on neutrophil chemotaxis in this setting, as 2GNF treatment did not affect chemotactic parameters compared to baseline while 2GECV did. However, according to transmigration data, there were no nicotine-dependent effects exhibited, suggesting RCS (derived from thermal and oxidative degradation of PG and VG) are driving this impairment.

Neutrophils play an important role as rapid responders to sites of injury and infection and triggering activation of the immune cell cascade (Kobayashi et al., 2018, Borregaard, 2010). If neutrophils are unable to migrate to sites of insult and injury, response by the rest of the immune system will be slower and injury or infection will be

more severe before a full immune response is amounted. This is likely to increase obligate tissue damage, result in more severe tissue infections and cause sustained inflammation due to a longer clearance time.

Together, these data show neutrophil migration was significantly impaired by e-cigarette vapour, but that this effect was driven by impairments in velocity and speed of chemotaxis to CXCL8. This finding provides scope for the future application of a signalling molecule inhibitor which can correct neutrophil chemoattractant sensing and responding, to investigate if migration can be restored.

4.5.2 Neutrophil phagocytosis

The percentage of *E. coli* and *S. aureus* pHrodo™ -positive neutrophils was significantly impaired by all e-cigarette treatment groups, at both 30 and 60 minutes. The amount of *S. aureus* pHrodo™ beads ingested (MFI) was significantly impaired by all e-cigarette treatment groups at both time points, but 2nd generation e-cigarette vapour (nicotine-containing and nicotine-free) did not inhibit the amount of *E. coli* bioparticle phagocytosis at 30 minutes. By 60 minutes, 2GECV treatment significantly inhibited *E. coli* pHrodo™ bioparticle phagocytosis, but this was not the case in nicotine free vapour. At 30 minutes (but not 60 minutes) there was a nicotine-dependent effect on the amount of *E. coli* and *S. aureus* pHrodo™ bioparticle phagocytosis in 2nd generation e-cigarette vapour groups, however, nicotine-containing vapour inhibited phagocytosis of *E. coli* more than nicotine-free vapour, but inhibited phagocytosis of *S. aureus* less than nicotine-free vapour. The difference in findings between *E. coli* and *S. aureus* phagocytosis suggests gram-positive bacterial phagocytosis was more

significantly impaired than gram-negative bacterial phagocytosis after exposure to vapour from lower power e-cigarette devices. Neutrophils express TLR2 and TLR4, which are PRRs for Lipoteichoic acid (LTA) (expressed in the cell wall of gram-positive bacteria including *S. aureus*) and LPS (expressed on the surface of gram-negative bacteria including *E. coli*) respectively (Sabroe et al., 2005). Engagement of TLR2 or TLR4 with their ligands allows neutrophils to directly phagocytose bacteria without the need for opsonisation by complement and antibodies. Alterations in TLR signalling and expression on alveolar macrophages and epithelial cells have been reported in the context of cigarette smoking (Metcalfe et al., 2014, Pace et al., 2008, Mortaz et al., 2011), but this has not been investigated in neutrophils or with e-cigarette vapour exposure to date. This a potential avenue to investigate in future neutrophil studies, to determine whether aberrant neutrophil phagocytosis is a TLR-driven response to e-cigarette vapour.

In most cases in this study, the inhibition of phagocytosis by e-cigarettes was observed at both time points indicating an early inhibition and an inability to recover function over time. Conversely, neutrophils treated directly with nicotine, only tended to only show significantly impaired phagocytosis at one time point, suggesting the sustained inhibition was driven by RCS in e-cigarette vapour. Inhibition of phagocytosis reported here was consistent with previous findings in the field, even when using different exposure models and bacteria (Corriden et al., 2020, Clapp et al., 2017). For the first time, the dynamics of phagocytosis over time, a comparison between gram-positive and gram negative bacteria and the contribution of device power and nicotine content on neutrophil phagocytosis after e-cigarette exposure have been detailed here.

Neutrophil impairments in phagocytosis after e-cigarette exposure have been reported previously (Clapp et al., 2017, Corriden et al., 2020). This will have consequences for lung health including severe and frequent lung infections, sustained inflammation, and increased tissue damage.

4.5.3 Neutrophil degranulation

Significant degranulation caused by e-cigarette vapour could indicate increased tissue damage *in vivo.* Previous studies have reported significant increases in MMP-9 (content and activity) and NE content in supernatants from neutrophils treated with e-cigarette vapour extract for 6 hours (Higham et al., 2016). In addition, elevated NE, MMP-2, and MMP-9 was found in BALF of e-cigarette users, with an unchanged corresponding antiproteinase levels (Ghosh et al., 2019, Reidel et al., 2018). BALF is a complex biological milieu where inflammation from epithelial cells drives activation of neutrophils and subsequent degranulation. This is exaggerated by the priming and activation steps a neutrophil must undergo to reach the airspaces which may result in a greater inflammatory response to e-cigarette vapour exposure and may explain the differences in results demonstrated here. Application of e-cigarette vapour to primed neutrophils is an area which should be investigated in the future.

Here, there were no changes in MMP-9 or MMP-8 levels in neutrophil supernatants after e-cigarette vapour exposure. Analysis of BALF from both smokers and vapers has reported elevated levels of MMP-9 (Sivaraman et al., 2014, Ghosh et al., 2019, Reidel et al., 2018). This contrasts with the findings presented here, but other sources of MMP-9 and MMP-8 include alveolar macrophages. Macrophages are a potent

source of MMP-9, and work from our group has shown significantly increased MMP-9 from e-cigarette vapour condensate treated alveolar macrophages (Scott et al., 2018), representing a potential alternative source of this proteinase. Published literature has found that MMP-9 was secreted by neutrophils exposed to e-cigarette vapour extract, but only at mid-range concentration (0.001-0.01 OD), not at low or high e-cigarette vapour extract concentrations, and this varied between e-liquid brands (Higham et al., 2016). This suggests there is an optimal dose of e-cigarette vapour exposure, for which our model may not have reached or may have surpassed. Increased MMP-9 could be an effect seen with longer exposure times, different nicotine content in e-liquid or more e-cigarette puffs, but was not seen in this model.

Neutrophils exposed to 2GNF vapour exhibited significantly increased MMP-2 secretion however, the levels were still very low so this may be statistically significant but not clinically significant. This effect was not consistent across all e-cigarette vapour treatments tested, and power calculations revealed sample sizes of 46 or more would be required to reach significance for the other e-cigarette vapour treatments. The presence of nicotine appeared to have a slightly suppressive effect, with slightly lower levels of secretion compared to nicotine-free vapour from equivalent devices. Elevated MMP-2 has been reported in BALF of e-cigarette users (Ghosh et al., 2019) and smokers (Sivaraman et al., 2014). The target molecules for MMP-2 are collagen and elastin, the breakdown of which would have significant implications for lung tissue structure. In smokers BALF, the levels of MMP-2 were around 900 ng/mL (Sivaraman et al., 2014) while here, in isolated neutrophils, MMP-2 levels are less than 1 ng/mL,

suggesting the key source of MMP-2 detected in smokers and vapers BALF is likely epithelial cells or other immune cells, rather than neutrophils.

MPO content was analysed as an azurophilic granule member and was found to be significantly lower in supernatants from 4GECV-exposed neutrophils compared to UTC. Previously, MPO has been reported to be elevated in the serum of cigarette smokers (Andelid et al., 2007), but in e-cigarette users, serum MPO levels have been shown to be lower, albeit not reaching statistical significance compared to normal subjects (Singh et al., 2019). However, proteomic analysis of induced sputum samples revealed increased MPO in samples from e-cigarette users compared to healthy controls (Reidel et al., 2018). MPO is involved in the formation of reactive oxygen intermediates and the oxidation of lipids. The effects of e-cigarette vapour on MPO abundance and activity remain to be fully elucidated.

Unlike other key neutrophil effector functions studied here, there were not consistent patterns of degranulation in any groups. For example, no e-cigarette treatment group displayed increased or decreased protein secretion across all proteins tested, and there were no nicotine-dependent or device power-dependent effects. Neutrophil granule release is a calcium-dependent effect, with each granule differentially sensitive to intracellular calcium levels (Perez et al., 1987). The effect of e-cigarette vapour on neutrophil calcium signalling will be investigated in chapter 5. Despite showing statistically significant changes in protein secretion by some treatments here, it is likely this is does not represent a biologically significant effect.

4.5.4 Neutrophil oxidative burst

Neutrophils did not exhibit changes in baseline OCR or ECAR as a result of e-cigarette vapour exposure compared to UTC. 4GECV treated neutrophils did, however, exhibit higher basal glycolysis and non-glycolytic acidification compared to 2GECV treated neutrophils. This could represent a higher state of priming or activation by 4GECV-treated neutrophils compared to 2GECV-treated neutrophils, but if this were the case, a significant difference from UTC would be expected. This may have been achieved with greater sample size, but power calculations suggested a sample of nearly 1000 would be required to detect a difference between these groups, which is unachievable for any study. It should be noted that both parameters are very low compared to other cell types, and the levels reached during active metabolic tests. Therefore, these differences may be statistically significant but not clinically significant. To investigate this further, incorporating priming agents into the metabolic tests and monitoring how a primed or activated neutrophil behaves without stimulants and examining basal metabolism of neutrophils from e-cigarette users and smokers would help to understand this effect further.

Neutrophils exhibited a significantly diminished ability to produce a robust oxidative burst response to PMA when exposed to e-cigarette vapour generated from high-powered 4th generation e-cigarette devices (in the presence of nicotine), but not from 2nd generation devices. Neutrophil oxidative burst responses involve the generation of ROS by NADPH oxidase (Chen and Junger, 2012). In this model, OCR directly correlates with the activity of the NADPH oxidase complex, with total oxygen consumption representing the amount of ROS generated in response to PMA

stimulation (Hickman et al., 2019, Swain et al., 2018). Previous work performing the same oxidative burst response test uncovered neutrophil oxidative burst was diminished in response to treatment with e-liquid flavouring components (Hickman et al., 2019). Here we add that e-cigarette vapour, in the absence of any flavourings, also significantly diminishes neutrophil oxidative burst responses, but only after 4GECV treatment. The inability of neutrophils to amount an oxidative burst response has consequences for bacterial killing and NET generation, which can be seen in the genetic disease chronic granulomatous disease (CGD) where patients have a genetic inability to assemble NADPH oxidase and amount an oxidative burst response (Bianchi et al., 2009). Impairments of neutrophil phagocytosis, and the apparent reduction in NET response to PMA has been demonstrated in this chapter. This could be driven by an inability to amount an oxidative burst response, however, neutrophils exposed to vapour from 2nd generation e-cigarette devices exhibited diminished phagocytic ability, but not oxidative burst generation. This suggests there are further drivers of this dysfunction to be uncovered. In the work presented here, impaired oxidative burst response could be driven by interference in NADPH oxidase assembly, inhibition of glucose uptake or inhibition of glycolysis enzymes, as has previously been hypothesised (Hickman et al., 2019). Glycolysis and glucose uptake will be further investigated in chapter 5.

4.5.5 Neutrophil NET generation

E-cigarette vapour does not induce spontaneous NET generation, which supports previous findings (Corriden et al., 2020, Clapp et al., 2017). There was no change in PMA-stimulated NET generation after e-cigarette vapour exposure, however, when the

size of the NET response amounted was calculated, neutrophils exposed to e-cigarette vapour appeared less able to amount a response to PMA, but this result was underpowered, requiring 7 or more repeats to achieve statistical significance. Neutrophils isolated from the blood of e-cigarette users have previously been shown to be more sensitive to the NET stimulant PMA (Reidel et al., 2018). This could represent the effect of vapour constituents, such as nicotine, in the blood priming neutrophils ready for action. This would have widespread implications, not only for respiratory health. Nicotine has previously been shown to be a NET stimulator and enhance neutrophil NET responses (Lee et al., 2017, Hosseinzadeh et al., 2016). However, e-cigarette vapour extract has been shown suppressed NET response to PMA (Corriden et al., 2020), similarly to the results presented here. It should be noted that PMA is a commonly used NET-inducer but does not occur physiologically and the same study found no effect of e-cigarette vapour extract on NET generation stimulated by nigericin, a microbial toxin which causes non-canonical NET generation. This highlights the need to test physiological stimuli of NETs alongside PMA. Together, research suggests that in e-cigarette users, there could be systemic activation of neutrophils caused by e-cigarette usage *in vivo*, priming them for a NET response and increasing their sensitivity to stimuli, but that direct exposure suppresses responses. oxidative burst is required for NETosis (Fuchs et al., 2007), and therefore suppression of NET response to PMA could be linked to the earlier findings of a suppressed oxidative burst response to PMA.

4.5.6 Impact of device generation on neutrophil functions

By performing this investigation using 2 different generations of e-cigarette devices in parallel, for the first time, we can comment on the impact of device power on neutrophil functions. 4th generation devices had a consistently more inhibitory effect on neutrophil transmigration, phagocytosis, and oxidative burst compared to 2nd generation e-cigarettes. Baseline glycolysis and non-glycolytic acidification are significantly higher in 4th generation-exposed neutrophils compared to 2nd generation, suggesting a potential priming/activation associated with higher powered devices or a need to scale up redox defence (reduced glutathione: oxidised glutathione) when exposed to high levels of RCS (Owen and Butterfield, 2010). High power e-cigarette devices have the ability to reach higher temperatures and produce denser clouds of vapour therefore increasing the RCS load (Zelinkova and Wenzl, 2020). In the 4th generation device treatment groups, there were often no differences to the impact on neutrophil function made when nicotine was present. This suggests that RCS contributes to neutrophil dysfunction which may be a receptor driven pathway or a total switch to withstand the oxidative insult, resulting in a shutdown of other functions.

4.5.7 Nicotine-dependent neutrophil dysfunction

Comparisons between nicotine-free and nicotine-containing e-cigarette exposed neutrophils from the same device generation revealed few statistically significant differences. There were significantly fewer *E. coli* pHrodo™ bioparticles ingested at 30 minutes in neutrophils exposed to 2GECV compared to 2GNF, but this effect did not persist to 60 minutes, therefore this could be a rate-dependent effect. Continuing the experiments to a later time point may have showed this. Contrastingly, there were

significantly fewer *S. aureus* pHrodo™ bioparticles ingested at 30 minutes by neutrophils exposed to 2GNF compared to 2GECV, but again this effect didn't last to 60 minutes. No further significant differences in any other functions between nicotine-free and nicotine-containing e-cigarette vapour treated neutrophils, were observed. However according to power calculations a sample size of 18 would have achieved a statistically significant difference in speed of chemotaxis to CXCL8 between 2GECV and 2GNF treated neutrophils.

GC-FID analysis revealed neutrophils were exposed to 0.6 µM nicotine when exposed to 2GECV for 20 minutes in our model, and 3 µM nicotine when exposed to 4GECV. Sputum nicotine after a 1 hour vaping session is between 1 µM to 300 µM, with an average of 45 µM (Ghosh et al., 2019), (compared to 33.6 µM after smoking (Clunes et al., 2008)), indicating the nicotine exposure of our model is not out of physiological range.

Neutrophils were treated directly with 0.6 µM or 3 µM nicotine (unvaped) before transmigration, phagocytosis and NET generation were examined. There was a trend towards ($p = 0.0625$) significantly reduced *S. aureus* and *E. coli* phagocytosis and transmigration to CXCL8 caused by both nicotine treatments. These did not reach statistical significance due to low replicate numbers. Power calculations revealed sample sizes of 15 and 11 for phagocytosis and transmigration respectively were required to reach statistical significance. Nicotine appears to influence neutrophil functions, but this cannot be determined from the work presented here. Previous work has demonstrated nicotine-treated neutrophils exhibit dose-dependent increased

CXCL8 secretion at nicotine concentrations of 100 μM or greater (Iho et al., 2003). Nicotine has been shown to induce NETosis at concentrations 10 μM or more (Hosseinzadeh et al., 2016), which was not seen here but could be due to the lower nicotine doses. Both Akt and NF-κB pathways have been implemented in cigarette smoke extract and nicotine-induced neutrophil dysfunctions (Hosseinzadeh et al., 2016, Xu et al., 2013, Iho et al., 2003, Matthews et al., 2011, Stringer et al., 2007) however, NF-κB pathway was not induced by e-cigarette vapour extract (Higham et al., 2016), indicating the potential for different drivers of dysfunction in e-cigarettes compared to traditional cigarettes.

4.5.8 Nicotine-independent neutrophil dysfunction

Investigating the impact of nicotine-free e-cigarette vapour has revealed that the functional impact cannot be assumed to be only due to nicotine. Speed of chemotaxis to CXCL8, transmigration and phagocytosis were significantly inhibited by nicotine-free e-cigarette vapour, while MMP-2 secretion and spontaneous NET generation were significantly increased, indicating a nicotine-independent functional defect. This must be driven by the vehicles PG and VG, and the resulting chemicals caused by their thermal decomposition into vapour form. Here we have shown the fundamental effects of base e-liquid chemicals on neutrophil functions, however, flavours are likely to have an additive effect as they have already been shown to be harmful to neutrophils (Hickman et al., 2019).

As well as examining nicotine-containing and nicotine-free vaped e-liquid, we have also examined direct nicotine treatment on neutrophil viability, transmigration, NET

generation and phagocytosis. Doses of 0.6 μM and 3 μM nicotine were chosen to match the concentrations of nicotine that neutrophils are exposed to during a vapour exposure in our model. It is difficult to determine the impact of direct nicotine treatment on these functions due to underpowering meaning statistical difference could not be detected. However, both nicotine treatments did appear to alter neutrophil functions, but this cannot be fully determined due to low replicate values.

Evidence of nicotine-independent neutrophil dysfunction contrasts with previous work from our group where a nicotine dependent impairment of function was observed in alveolar macrophages (Scott et al., 2018). Published literature demonstrates there is a difference in nicotinic acetylcholine receptor (nAChR) subunit expression between neutrophils and alveolar macrophages (Ghosh et al., 2019), which may explain this difference. Additionally, the model of direct vapour exposure developed in this thesis may deliver a higher RCS load to cells, which isn't recapitulated in e-cigarette vapour condensate models, having a greater impact on function than nicotine in this context. To investigate this hypothesis, gas chromatography mass spectrometry analysis of e-cigarette vapour condensate could be performed to identify and quantify RCS components, and compared to e-cigarette vapour.

Overall, the findings presented here indicate there was a contribution of direct nicotine treatment to neutrophil dysfunction, but there were other significant impairments when the same dosage of nicotine is delivered as a component of vapour, likely due to contributions of other e-cigarette vapour constituents such as RCS formed from the vapourisation of PG and VG.

4.5.9 Limitations

The most significant limitation to the work presented in this chapter is the statistical power to back up the data. Many of the experiments are underpowered due to time constraints exacerbated by the COVID-19 pandemic, and a statistical difference may have been achieved had more replicates been possible. This is exacerbated by the natural inter-person differences increasing the variability of the effects of e-cigarette vapour on neutrophils. Due to factors such as age, infection status, ethnicity and lifestyle, the response of neutrophils to an external challenge can be different. As far as possible this has been controlled for in the experimental conditions, but some elements could not be accounted for in the scope of this project. In addition, e-cigarette devices can be temperamental in their operation, particularly due to the lack of regulation surrounding device quality control. The output may have changed from one use to the next, altering the RCS load, temperature output and puff volume, despite controlling for these changes as much as possible. Here, a 20 minute exposure (of 40 puffs) was chosen based on topography literature, however, some e-cigarette users vape much more daily. Further investigations into the effect of the number of puffs on neutrophil functions would help to address this.

During chemotaxis experiments, e-cigarette vapour exposure reduced the number of neutrophils adhering to the coverslip. Therefore, this may have negatively skewed the data as there were fewer adhered neutrophils to track. The transwell migration assay detects neutrophils in the supernatant after the end of the assay and therefore depends upon the ability of neutrophils to migrate through the transmembrane but also detach

from the underside. Imaging of the underside of the transmembrane revealed that neutrophils treated with 4th generation nicotine-containing e-cigarette vapour appeared to have migrated partially through the membrane but were unable to complete this and detach from the underside (Figure 4.2A).

The choice of *E. coli* for phagocytosis was not the most physiologically relevant and that use of *H. influenzae* or *S. pneumoniae* would have better represented colonisation in respiratory health and chronic disease (Weinreich and Korsgaard, 2008). However, by using the pHrodo™ bioparticle procedure the validity of the results presented was maximised by capitalising on the unique ability of the dye to only fluoresce after a pH drop associated by encapsulation in a phagolysosome. Work by our group has found the pHrodo™ beads to be far more stable and consistent than bacteria stained with pHrodo™ dye, and a reliable method was needed for the purposes of this thesis.

Here, markers of neutrophil degranulation were assessed by measuring secreted proteins into neutrophil supernatants using the highly validated Quantikine ELISA kits. In this data, UTC values for MMP-8, MMP-9 and MPO appear high, and variable at baseline. This could be caused by processing, inter-person variability or assay-specific artefacts. Preliminary data using Luminex kits was performed to determine the correct dilution facts for analysis of each protein. However, for some samples, this did not translate between the kits and they were very high or very low on the standard curve. A positive control for degranulation, such as calcium ionophore, may have helped understand the pattern of responses here, but these samples were not collected. Production of NE, PR3 or anti-proteinases were not analysed due to limitations in

freeze-thaw cycles and volume of samples remaining, but these would be interesting next steps as well as the activity footprint of these molecules.

Agilent Seahorse technology can monitor real-time metabolic responses of neutrophils to a variety of stimuli and inhibitors. Current technological limitations in the setup of the Seahorse XF96 analyser and the e-cigarette chamber mean it is not possible to look at real-time metabolic response to e-cigarette vapour. This means that the readings are taken at least 1 hour after vapour exposure, due to protocol requirements, and so metabolic profiles may be missed.

While measuring NET generation, the plate reader used may not have the sensitivity to detect low level or small changes in fluorescence intensity. Instead, more advanced machinery such as uScope would be preferable, but was not available for this project. In addition, RFU levels reached by unstimulated UTC neutrophils appeared high. This doesn't translate to high levels of NETosis necessarily, as unstained media and empty wells exhibit RFU values of approximately 1000 on the plate reader used for these experiments. To rectify this, baseline correction can be done for future experiments. When comparing the raw data collected here to raw data presented in published literature, the same high baseline values are present (Corriden et al., 2020), suggesting this is an equipment limitation as opposed to experimental flaw.

Finally, a dose response of nicotine may have been valuable to this study, but the aim was to directly investigate the impact of nicotine in this exposure system.

4.5.10 Conclusion

This chapter details the significant detrimental effect of e-cigarette vapour exposure on important neutrophil functions. These results highlight the impact of high-power devices having a more significant effect on neutrophil functions than lower power devices which reach lower temperatures. By including nicotine-free e-cigarette vapour we have ruled out the possibility that neutrophil dysfunction after e-cigarette vapour exposure is only due to nicotine. Describing the clinical relevance of these *ex vivo* functional defects is challenging without further cohort studies. However, the findings presented are unlike previously reported neutrophil behaviours in ageing, pneumonia, sepsis, ARDS, asthma, or COPD. Instead, neutrophils appear to be in an almost paralysed state – unable to perform key effector functions but with little or no effect on viability. This combination of dysfunction in the acute setting is concerning and whilst this does not inform us on long-term effects, if this paralysis persists with chronic exposure it suggest e-cigarette usage could compromise neutrophil mediated innate immune defence.

Chapter 5 -

MECHANISTIC

WORK

Foreword: RNA quality check and sequencing was performed by colleagues at Genomics Birmingham. Advice on RNA data analysis was kindly provided by Professor Mark Lindsay and Lauren Davis. Some work in the discussion has been published in a peer-reviewed literature review (Jasper et al., 2021) and adapted for the purposes of this thesis.

5.1 Chapter 5 introduction

Results presented in Chapter 4 demonstrated significant effects of e-cigarette vapour on neutrophils, impairing key effector functions. These dysfunctions cannot be addressed without defining the mediation of these effects, therefore the results presented in this chapter will detail studies to unpick the mechanism of action causing e-cigarette driven neutrophil dysfunction.

5.1.1 Neutrophil transcriptome

Neutrophils have long been thought of as transcriptionally inactive due to their short-lived nature and high turnover (Kumar and Dikshit, 2019). However, research has revealed altered transcriptomes in mature neutrophils are associated with modified neutrophil functions including NETosis (Khan and Palaniyar, 2017) and transmigration into inflamed tissues (Lakschevitz et al., 2015). Neutrophil messenger RNA (mRNA) expression has been shown to be upregulated within 2-4 hours of exposure to bacteria (Subrahmanyam et al., 2001, Sukumaran et al., 2005) and up to 4 hours of LPS treatment (Malcolm et al., 2003, Tsukahara et al., 2003). A study of bronchial epithelial cell proteomes revealed 113 uniquely altered proteins expressed in vapers compared to non-smokers and smokers, including MUC5AC and CYP1B1 (Ghosh et al., 2018).

Previous work has found that nasal epithelial cells from e-cigarette users demonstrate downregulation of 305 genes (Martin et al., 2016). This provided rationale for investigating the transcriptome of neutrophils exposed to e-cigarette vapour via our model.

5.1.2 Neutrophil metabolism

Similarly to the paradigm of transcriptional inactivity, neutrophils were thought to depend only on glycolytic metabolism. However, research has revealed metabolic shifts associated with neutrophil activation, functions and roles in disease (Kumar and Dikshit, 2019). The role of mitochondria in neutrophils has been debated since the 1950s and extensively reviewed (Kumar and Dikshit, 2019, Injarabian et al., 2019) however remains a topic of question. Electron microscopy revealed relatively few mitochondria per neutrophil, only 5-6 per cell (Peachman et al., 2001), and functional tests showed no effect on neutrophil respiration when mitochondria were inhibited (Reiss and Roos, 1978). Furthermore, neutrophil functions such as NET formation and phagocytosis were shown to be dependent on glycolysis rather than mitochondrial ATP generation, suggesting the dispensability of mitochondria to the neutrophil (Fossati et al., 2003, Rodriguez-Espinosa et al., 2015). However, further investigations revealed extensive networks of mitochondria across the neutrophil cytoplasm (Fossati et al., 2003, Maianski et al., 2002), and the role of mitochondria in apoptosis and chemotaxis (Maianski et al., 2004, Bao et al., 2015). The adaptation of neutrophils to produce their ATP in a largely oxygen-independent manner is beneficial in inflammatory states where oxygen supply is limited (Fossati et al., 2003, Silver, 1977, Edwards et al., 1984). Despite these findings indicating an overlooked role for mitochondria, glycolytic

inhibitors have been shown to completely abolish ATP levels, stopping all effector functions (Sbarra and Karnovsky, 1959, Borregaard and Herlin, 1982) while oxidative phosphorylation inhibitors have minimal effects on neutrophil respiration (Reiss and Roos, 1978). Glycolysis remains the predominant source of ATP in neutrophils and leading metabolic pathway for phagocytosis and NETosis (Kumar and Dikshit, 2019). Given the importance of glycolytic capacity in mediating neutrophil function, this presents a critical point at which e-cigarettes could mediate negative effects.

5.1.3 Nicotine receptors

5.1.3.1 Nicotine receptor signalling

The main components of e-cigarette vapour common to all e-liquids are PG, VG and nicotine. Current literature suggests nicotine can impact neutrophil function in a receptor-driven manner (Lee et al., 2017). For example, NE secretion and gene expression is induced by nicotine in neutrophils (Ghosh et al., 2019, Armstrong et al., 1996) and chemotaxis and phagocytosis are suppressed by nicotine in a dose-dependent manner (Seow et al., 1994). NAChRs are ligand-gated ion channels, with a pentameric structure, composed from a combination of twelve neuronal nAChR subunits (Hogg et al., 2003). The combination of nAChR subunits expressed by human neutrophils is still poorly understood. Neutrophils have been shown to express subunits: α5, α6 and β1 via qPCR (Ghosh et al., 2019) and selective inhibitor studies suggests the absence of α4 and α7 subunits (Iho et al., 2003). However, RT-PCR accompanied by southern blot analysis revealed presence of α3, α4, α7, β2 and β4 but with variable signals between donors, suggesting heterogeneity in the population (Benhammou et al., 2000, De Rosa et al., 2005) and confocal imaging revealed the

presence of α7 subunits on the surface of human neutrophils (Lee et al., 2017). Furthermore, α7 subunit inhibitors have been shown to mediate nicotine-induced delay in neutrophil cell death and NET generation (Xu et al., 2013, Lee et al., 2017) and α3 and possibly α1 subunits have been implemented in nicotine-induced IL8 production from neutrophils (Iho et al., 2003). Without consistent evidence of which nAChR subunits are present in human neutrophils, choosing a receptor inhibitor is challenging. In this study, Benzethonium chloride, a potent inhibitor of α4β2 and α7 nAChRs (Coates and Flood, 2001) was used due to its multiple targets as opposed to other broad-spectrum or single subunit- specific alternative inhibitors available at the time of these experiments and due to previous evidence of α4β2 and α7 nAChRs subunits at both transcript and protein level (Lee et al., 2017, Benhammou et al., 2000).

5.1.3.2 Calcium signalling

Changes in cytoplasmic Ca^{2+} levels are caused by depletion of intracellular calcium stores or influx of extracellular Ca^{2+} via Calcium release-activated channels (CRAC) or in the process of endoplasmic reticulum Ca^{2+} depletion termed store operated calcium entry (SOCE) (Immler et al., 2018). SOCE can be initiated by ligand-gated receptors including nAChRs (Zia et al., 1997), G-protein coupled receptors (GPCRs) (Jiang et al., 1997) and interaction of E-selectin with L-selectin (Schaff et al., 2008, Immler et al., 2018). Neutrophils depend on Ca^{2+} signalling for activation, phagocytosis, degranulation, integrin activation, ROS production, migration, and cytoskeletal rearrangement (Immler et al., 2018, Jiang et al., 1997, Schaff et al., 2008). Stimulation nicotine treatment is followed by an increase in cytosolic Ca^{2+} levels in human neutrophils (Ghosh et al., 2019, Carlisle et al., 2004). It has previously been shown

that nicotine causes a dose-dependent increase in cytoplasmic Ca^{2+} and induces subsequent protease release by neutrophils (Ghosh et al., 2019). In lung epithelial cells, e-liquids and the PG/VG alone elevate cytosolic Ca^{2+} (Rowell et al., 2019). The full extent to which e-cigarette vapour affects Ca^{2+} signalling in neutrophils is not fully understood. However, the importance of Ca^{2+} signalling in neutrophil functions highlights the importance of understanding the relationship between calcium signalling effect of e-cigarette vapour exposure on human neutrophils.

5.1.4 Restoration of function – Pi3K signalling

Previous studies have shown neutrophil dysfunction caused by inflammatory disease processes (Patel et al., 2018, Sapey et al., 2017, Scott et al., 2021) and in ageing (Sapey et al., 2014, Hazeldine et al., 2014, Wilson et al., 2020) sharing a common signalling molecule of interest. Phosphoinositide 3-kinase (Pi3K) is a key intracellular signalling molecule which regulates a range of cellular functions and has been implicated in the formation of pseudopods in human neutrophils. Following activation of tyrosine kinase or G-protein coupled receptors, Pi3K converts $PI(4,5)P_2$ to $PI(4,5)P_3$ which activates downstream signalling molecules resulting in F-actin polymerisation allowing the formation of a pseudopod in the leading edge of the neutrophil (Charest and Firtel, 2007). This is complemented by RhoA activation in the trailing edge which drives myosin contraction and inhibits F-actin polymerisation via PTEN, causing the propulsion of the neutrophil towards the chemoattractant (Mocsai et al., 2015). Pi3K signalling is also important in neutrophil phagocytosis due to its role in assembling NADPH oxidase, with Pi3K inhibition reducing neutrophil phagocytosis (Rossi and Lord, 2013). Pi3K exists in many isoforms, with neutrophils expressing the class I Pi3K

subunits: alpha (Pi3Kα), delta (Pi3Kδ) and gamma (Pi3Kγ) (Martin et al., 2015). Studies have shown inhibition of Pi3Kδ activates RhoA and restores neutrophil phagocytosis, which is impaired in critically ill patients (Scott et al., 2021, Morris et al., 2011). Pi3Kδ has also been implicated in neutrophil chemotaxis, with evidence it is involved in neutrophil polarisation and directional migration (Sadhu et al., 2003). However, constitutive activation of Pi3K in neutrophils from healthy older adults, leads to less accurate migration towards chemoattractants that can be resolved by Pi3Kγ and Pi3Kδ inhibition (Sapey et al., 2014). This indicates that a fine balance of activation levels of Pi3K is required for normal neutrophil function. Pan- and alpha Pi3K inhibition have previously been shown to attenuate the negative implications of e-cigarette vapour condensate on alveolar macrophages and partially restore phagocytic ability of alveolar macrophages after e-cigarette vapour condensate treatment (Scott et al., 2018). However, Pi3K has not been investigated in the context of e-cigarettes and human neutrophils. With previous success in restoring impaired neutrophil migration and phagocytosis, the application of Pi3Kγ and Pi3Kδ inhibition to these e-cigarette-induced dysfunctions was trialled.

5.1.5 Restoration of function – antioxidants

RCS such as formaldehyde, acetaldehyde, acrolein, acetone, methylglyoxal and glyoxal are produced from thermal decomposition of PG and VG, which make up 70-80% of all e-liquids (Kosmider et al., 2014, de Falco et al., 2020, Jensen et al., 2015, Sussan et al., 2015). E-cigarette vapour has also been shown to contain 1.2-8.9 nmol/puff H_2O_2 as well as ROS precursors which have the potential to generate additional ROS when deposited in the lung (Zhao et al., 2018). RCS and ROS are

known drivers of cigarette smoke (Valavanidis et al., 2009) and e-cigarette related cellular harm (Anderson et al., 2016). Antioxidants have been shown to ameliorate the effect of these reactive species, restoring function in e-cigarette exposed vascular endothelial cells and alveolar macrophages (Anderson et al., 2016, Scott et al., 2018) and preventing e-cigarette induced autophagy in Beas2B cells (Shivalingappa et al., 2016). N-acetyl cysteine (NAC) is an antioxidant and anti-aldehyde that has been previously used to prevent cytotoxicity and restore phagocytosis of alveolar macrophages treated with e-cigarette vapour condensate (Scott et al., 2018). NAC is a precursor of L-cysteine, needed with ATP for cells to produce glutathione, a the most abundant naturally occurring antioxidant (Sansone and Sansone, 2011). Glutathione exists in a reduced or oxidised state, the ratio between which is an indicator of cellular health (Mokhtari et al., 2017). Reduced phagocytic capacity of neutrophils affected by changes in glutathione levels have been reported (Boxer et al., 1979) and chemotaxis has been shown to be affected by exogenous ROS, although this effect has been attributed to an induction of apoptosis (Splettstoesser and Schuff-Werner, 2002). The impact of antioxidant treatment on neutrophils exposed to e-cigarette vapour has not been investigated prior to this study. The effect of NAC on neutrophil viability and function has been studied, finding only high concentrations (>10 mM) of NAC have a detrimental effect on viability, IL-8 and elastase release (Sadowska et al., 2006a). Similarly, it has been reported that 30 mM is the cytotoxic dose for neutrophils *in vitro*, and that any detrimental effects on chemotaxis are due to cytotoxicity (Kharazmi et al., 1988). Therefore, the application of a sub cytotoxic dose of NAC to the pre-treatment of neutrophils may be able to mitigate the effects of the RCS-driven element of neutrophil dysfunction after e-cigarette vapour exposure.

5.2 Aims of Chapter 5

1. To investigate the impact of e-cigarette vapour exposure on neutrophil RNA expression.

2. To investigate the impact of e-cigarette vapour exposure on neutrophil glycolytic metabolism.

3. To investigate whether nicotine receptor inhibition restores neutrophil dysfunction caused by e-cigarette vapour exposure.

4. To investigate the impact of e-cigarette vapour exposure on neutrophil intracellular calcium signalling.

5. To investigate whether phosphoinositide 3-kinase inhibition restores neutrophil dysfunction caused by e-cigarette vapour exposure.

6. To investigate whether antioxidant treatment restores neutrophil dysfunction caused by e-cigarette vapour exposure

5.3 Materials and methods linked to chapter 5

5.3.1 RNAseq

5.3.1.1 Sample collection, storage, and extraction

Neutrophils isolated from heparinised whole blood via percoll gradient separation were exposed to e-cigarette vapour as described in chapter 2, before they were lysed and stored for RNA isolation. A treatment of only 20 minutes was applied to determine if transcriptional changes were responsible for the functional deficits reported in chapter 4. 5 x 10^6 neutrophils were taken for RNA isolation per condition, and RNA was isolated using the Invitrogen™ RNAqueous™-Micro Total RNA Isolation Kit (Fisher Scientific, Loughborough, UK product no. AM1931). Briefly, neutrophils were centrifuged at 250 x *g* for 10 minutes at room temperature with maximum brake and acceleration. The supernatant was discarded, the neutrophil pellet resuspended in 1 mL Lysis solution and transferred to 1.5 mL DNAse-free, RNAse-free microfuge tubes (Fisher Scientific, Loughborough, UK product no. AM12400) before being stored in a -80°C freezer until RNA isolation.

5.3.1.2 RNA extraction

The manufacturer's protocol for RNA isolation using the RNAqueous™-micro kit was followed. Briefly, one-half volume of 100% ethanol was added to the lysate and mixed using a vortex. The lysate was passed through a micro filter cartridge assembly, 150 µL at a time. The filter was washed with 180 µL of wash solution 1, followed by wash solution 2 and wash solution 3 (all provided in the kit). The flow-through was discarded and the filter centrifuged for 1 minute at maximum speed at room temperature with maximum brake and acceleration. The RNA was removed from the filter by transferring

it into a micro elution tube and then applying 10 µL elution solution (preheated to 75 ºC) twice.

5.3.1.3 DNase I treatment and DNase inactivation

The manufacturer's protocol for DNase treatment and inactivation using the RNAqueous™-Micro Kit was followed. Briefly, 1/10 volume of 10X DNase buffer and 1 µL of DNase I was added to the eluted RNA. The reaction was incubated for 20 minutes at 37°C, 5% CO_2. 2 µL (or 1/10 volume) DNase inactivation reagent was added to the reaction, vortexed (2 seconds, max speed) and left at room temperature for 2 minutes. The reaction was centrifuged for 1.5 minutes at 14,100 x *g* and the RNA transferred to an RNAse-free microfuge tube (Invitrogen, product no.: AM12400) and stored at -20°C.

5.3.1.4 RNA purity check

RNA quality was checked initially using NanoDrop™ 2000 spectrophotometer (ThermoFisher Scientific, product no.: ND-2000). 1.5 µL RNase-free water was used to blank calibrate the machine 3 times before use. 1.5 µL per RNA sample was used to assess concentration (ng/µL) and 260/280 ratios of extracted RNA. Further quality check was performed by Birmingham genomics service using the Qubit High Sensitivity RNA assay and an RNA tape on the Agilent TapeStation to assess concentration and RIN quality scores.

5.3.1.5 RNA sequencing

Sequencing data was generated using the Lexogen QuantSeq 3' mRNA-Seq library prep kit FWD for Illumina by the Birmingham genomics service. Briefly, RNA was normalised to 0.5 ng/µL and 2.25 ng was input for the prep. The protocol for low input (<10 ng) samples was followed including alterations to incubation times to account for lower input of total RNA. 0.5 µL SIRV set 3 was spiked into each sample to allow technical evaluation of library prep and sequencing performance. More information on this can be found at: https://www.lexogen.com/sirvs/. 5 µL was taken of the normalised sample + SIRV through to the library prep. Mouse RNA was used as a library prep control. 22 cycles of PCR were performed in total. Library QC was performed using DNA high sensitivity Qubit assay and sized with a high sensitivity D1000 tape. Libraries were bought down to 2 nM and pooled in equal 5 µL volumes. These were then quality checked using the Agilent TapeStation DNA 1000 tape and DNA high sensitivity Qubit. The pool was taken into sequencing at 3 nM and was loaded on the NextSeq at 1.6 pM.

5.3.1.6 RNA sequencing data analysis

Project data was transferred via Illumina BaseSpace (https://basespace.illumina.com) from which the FASTQ files were downloaded and uploaded to Galaxy (https://usegalaxy.org/), along with the gencode human genome reference file (hg38 downloaded from: http://hgdownload.soe.ucsc.edu/downloads.html#human). The four FASTQ files per sample were concatenated on Galaxy before running a FASTQC to check the quality of the RNA. The files were run through HISAT2 function on galaxy, and converted to counts per gene htseq files. DeSeq2 analysis was performed,

comparing UTC samples to paired e-cigarette treated samples. A text transformation (s/\.[0-9]+//) was performed on the gene IDs before join two datasets function was applied, to allow compatibility with the annotatemyIDs function giving gene names per hit. Results were run through the volcano plot function or were filtered by $log_2fc > 1$ (fold change > 2) and p values < 0.05, sorted by highest significance for gene reads and the top 20 lines selected (representing the top 20 differentially expressed genes). This workflow is summarised in Figure 5.1.

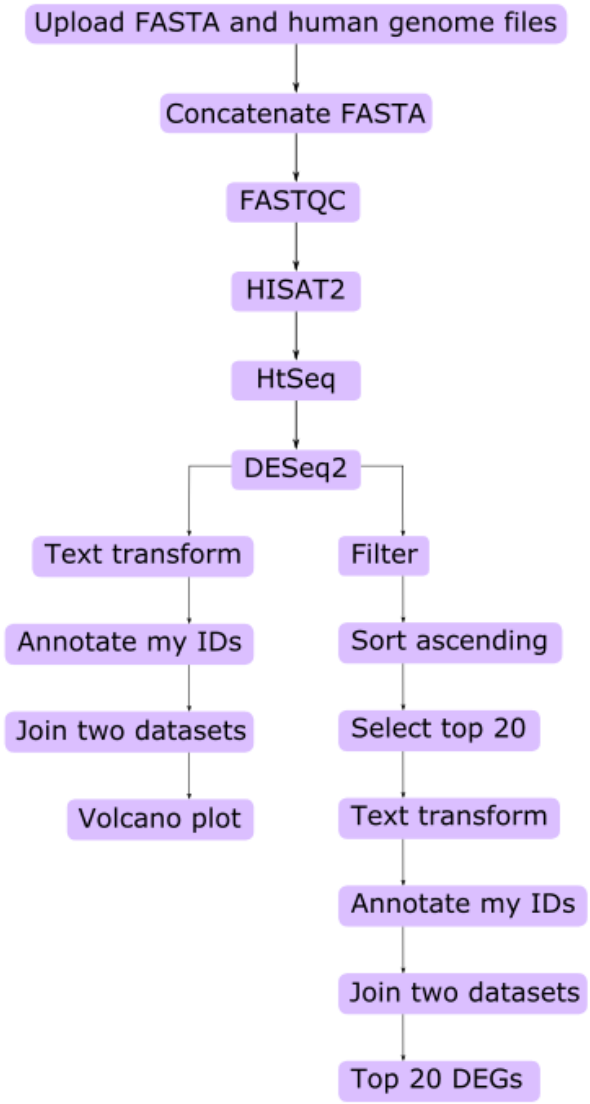


Figure 5.1*:* A summary of the RNA analysis workflow described in section 5.3.1.6.
All steps were performed on https://usegalaxy.org/. DeSeq2 analysis was performed once per e-cigarette treatment group, comparing UTC samples to paired e-cigarette treated samples. Text transformation involved the code s/\.[0-9]+//. Filters: $\log_2$fc > 1 (fold change > 2) and p values <0.05 were applied. DEGs = differentially expressed genes.

5.3.2 6NBDG glucose uptake assay

Neutrophils were resuspended to 1 x 10^6/mL in glucose-free RPMI (Sigma, product no.: R1383) + penicillin-streptomycin (1% w/w). Cells were exposed to e-cigarette vapour before being centrifuged at 250 x *g* for 5 minutes, at room temperature with full brake and acceleration and resuspended at 2.5 x 10^6/mL. 5 x 10^5 neutrophils were added to each well of a 96 well black sided plate. Cells were incubated at 37 °C, 5% CO_2 for 1 hour. 25 nM PMA was added to required wells and put on the plate shaker for 30 seconds before incubating at 37 °C, 5% CO_2 for a further 1 hour and 50 minutes. 200 µM 6NBDG was added to wells, shaken for 30 seconds on the plate shaker and incubated at 37 °C, 5% CO_2 for a further 10 minutes. The plate was centrifuged at 300 x *g* for 5 minutes, at room temperature with full brake and acceleration before the supernatant was discarded. 200 µL PBS was added to each well and the plate analysed on Synergy 2 plate reader at excitation: 485/20 nm and emission: 528/20 nm.

5.3.3 Inhibitor treatment

Neutrophils were resuspended to 1 x 10^6/mL in RPMI before being treated with the following inhibitors for 20 minutes at room temperature: 49 nM benzethonium chloride (α4, α7, β2 nAChR subunit inhibitor) (Selleck chem product no. S4162), 33 nM AS252424 (Pi3Kγ inhibitor) (Selleck chem product no. S2671), 75 nM CAL101 (Pi3Kδ inhibitor) (Selleck chem product no. S2226). Previous work has used the same Pi3K inhibitor concentrations and despite them being only the IC50 (partial inhibition), they have been shown to provide benefit (Sapey et al., 2014). Post-incubation, viability, phagocytosis, and/or transwell protocols were followed, as described in Chapter 2.

5.3.4 Antioxidant treatment

Neutrophils were resuspended to 1 x 10^6/mL in RPMI before being treated with 600 µM NAC (reconstituted in ddH_2O and diluted in RPMI) (Sigma-Aldrich, Poole UK, product no. A7250) for 20 minutes at room temperature. Post-incubation, viability, phagocytosis and/or transwell protocols were followed, as described in Chapter 2.

5.4 Chapter 5 results

5.4.1 E-cigarette vapour and the neutrophil transcriptome

In turn, each e-cigarette vapour treatment was examined for a change in transcriptome caused by e-cigarette vapour. Paired samples were used in the analysis to directly determine the effects.

To begin with, DESeq2 analysis was performed on paired treated/untreated samples to determine the effect of each e-cigarette treatment group on neutrophil transcriptional responses. From here, the differentially expressed genes (DEGs) between UTC and treatment conditions were identified. The DEGs were used to generate volcano plots to show up/down regulation and statistical significance of these genes. Figure 5.2A-D show that when UTC gene expression was compared to paired treated samples, there were no statistically significant DEGs caused by any e-cigarette vapour treatment. To avoid over-interpreting insignificant results, heatmaps have not been included in this thesis. To understand whether statistical significance was not reached due to small sample sizes in this analysis, DESeq2 analysis was repeated, comparing all UTC samples to all e-cigarette treated samples, regardless of which e-cigarette vapour they were exposed to. Figure 5.3 shows the results in the form of a volcano plot, where there were still not any statistically significant DEGs even when all the samples were combined. In addition, pathways associated with the DEGs for each treatment are displayed in Figure 5.4.

The list of all DEGs in each e-cigarette treatment was sorted, according to significance, into ascending order and the top 20 selected, representing the 20 most significantly

DEGs, as shown in Table 5.1. As part of DESeq2 analysis, p values are adjusted using the Benjamini-Hochberg procedure which controls false discovery rate (Love et al., 2014). The adjusted p value associated with the top 20 most highly DEGs can be seen in Table 5.1, all of which remained insignificant..

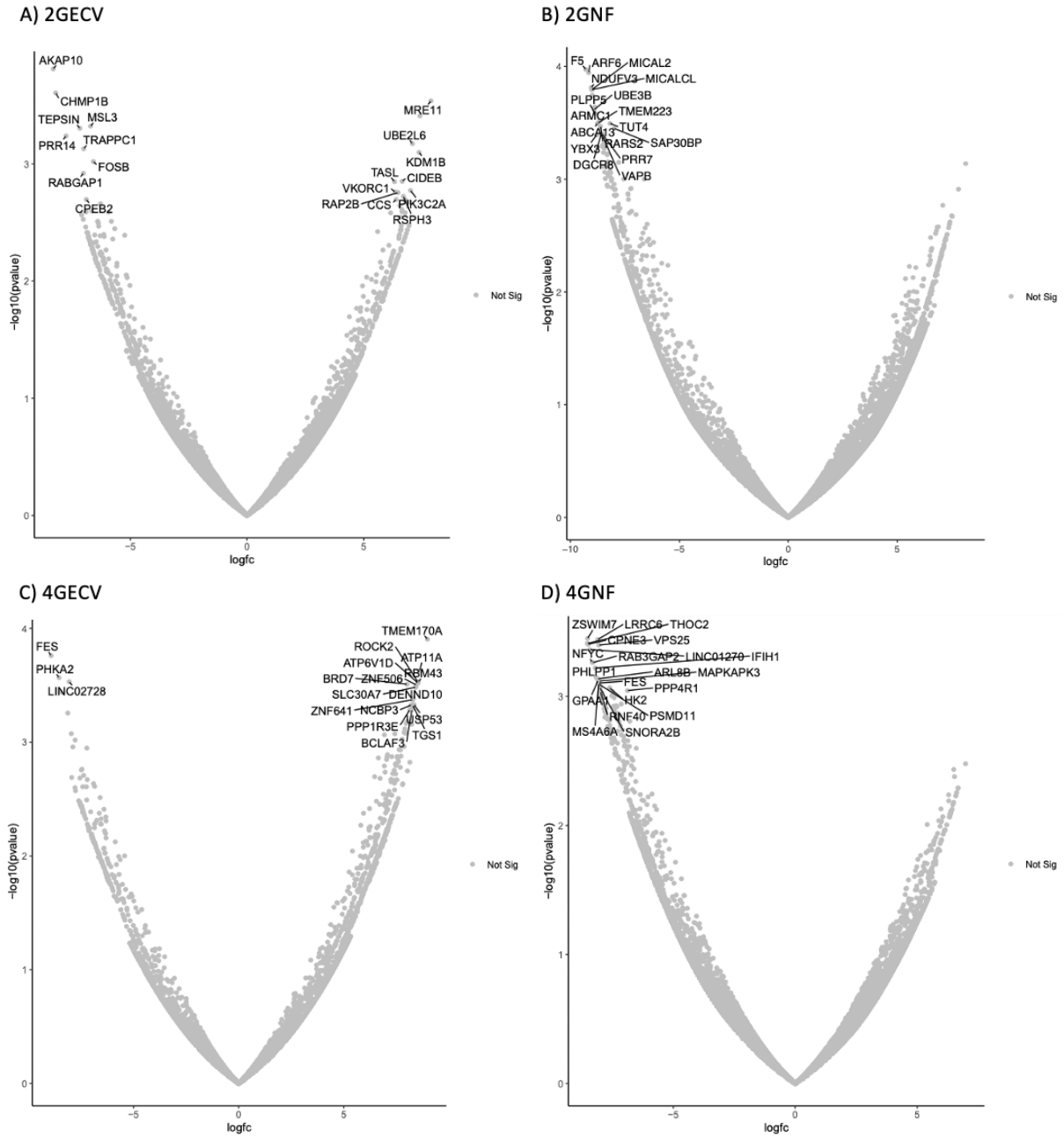


Figure 5.2: Volcano plots generated from DESeq2 analysis of gene counts comparing UTC to paired treated samples.

Each gene of the human genome is plotted as a point on the graphs. Genes on the right-hand side (log(fc) > 0) represent upregulation compared to UTC. Genes on the left-hand side (log(fc) < 0) represent downregulated genes caused by e-cigarette treatment, compared to UTC. Y axis height represents the significance of up/down gene regulation (-log10(p value)); the higher on the axis the gene is plotted, the more significant it is. Each graph represents a different e-cigarette treatment: A) 2GECV (n = 3, paired), B) 2GNF (n = 2, paired), C) 4GECV (n = 3, paired), D) 4GNF (n = 2, paired). The top 20 most significantly differentially expressed genes are labelled. Grey points represent genes which are not statistically significantly different between the treatments and UTC.

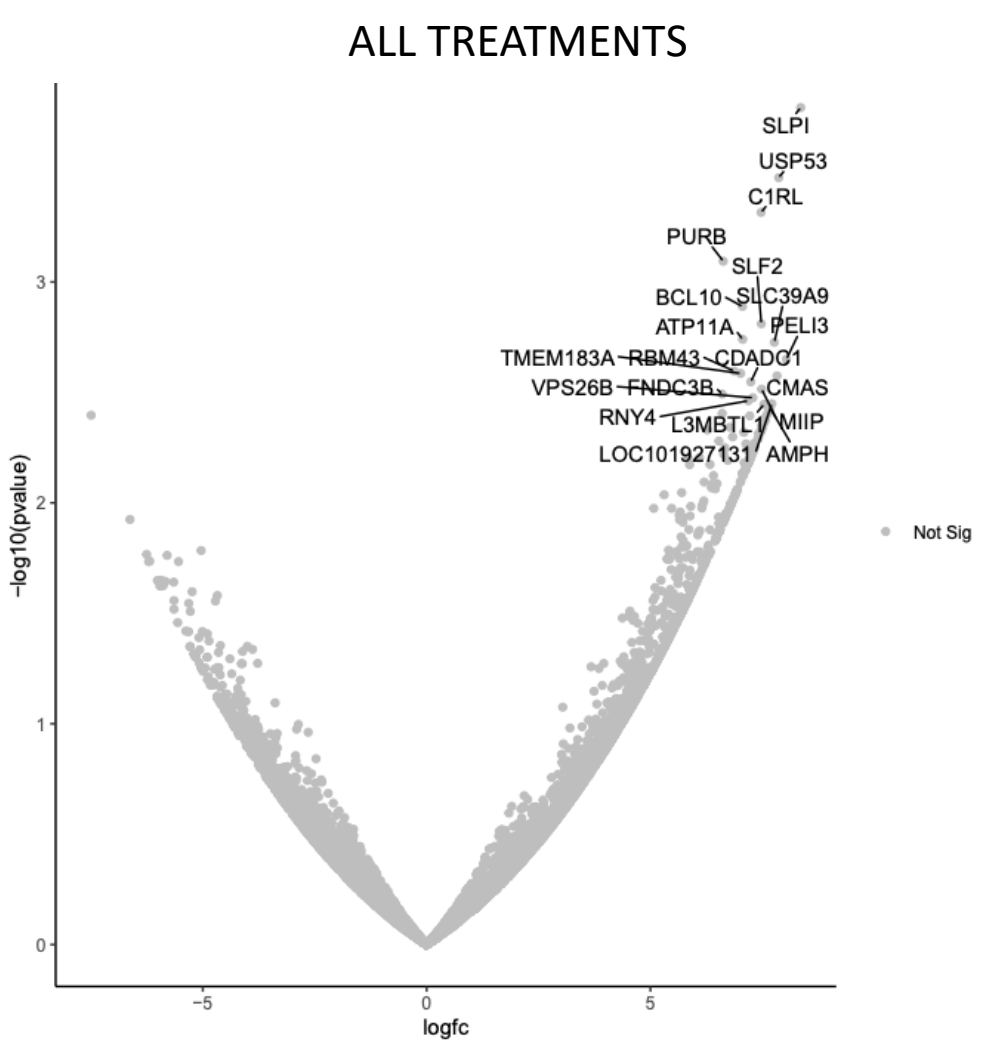


Figure 5.3: Volcano plots generated from DESeq2 analysis of gene counts comparing all UTC samples to all treated samples, regardless of which e-cigarette vapour condition was used.

Each gene of the human genome is plotted as a point on the graph. Genes on the right-hand side (log(fc) > 0) represent upregulation caused by e-cigarette vapour compared to UTC. Genes on the left-hand side (log(fc) < 0) represent downregulated genes caused by e-cigarette treatment, compared to UTC. Y axis height represents the significance of up/down gene regulation (-log10(p value)); the higher on the axis the gene is plotted, the more significant the p value is. The top 20 most significantly differentially expressed genes are labelled. Grey points represent genes which are not statistically significantly different between UTC and e-cigarette treated neutrophils. N = 5, with paired treatments.

	Gene symbol	q-value		Gene symbol	q-value		Gene symbol	q-value		Gene symbol	q-value
2GECV	PIK3C2A	0.4635	2GNF	AKAP11	0.0812	4GECV	ATP11A	0.0871	4GNF	ZNF506	0.1127
	MRE11	0.4635		ZNF506	0.0831		NCBP3	0.0871		ZNF445	0.1183
	PMM1	0.4635		NOL4L	0.0934		ZNF506	0.0871		ESCO1	0.1288
	USP42	0.4635		LIG4	0.0934		ATP6V1D	0.0871		RRP7A	0.1497
	TASL	0.4635		CCDC88C	0.0934		DENND10	0.0871		LATS1	0.1497
	ELOF1	0.4635		PALM2AKAP2	0.0934		ROCK2	0.0871		SNRNP48	0.1563
	RSPH3	0.4635		CALCOCO1	0.0934		TGS1	0.0871		INTS6	0.1604
	CEMIP2	0.4635		ZNF507	0.0934		USP53	0.0871		TOPBP1	0.1609
	CIDEB	0.4635		ZNF407	0.0934		SLC30A7	0.0871		N/A	0.1609
	ZNF185	0.4635		R3HDM1	0.0934		BRD7	0.0871		KDM4A	0.1615
	SCN3A	0.4635		RBM6	0.0934		TMEM170A	0.0871		TMOD2	0.1615
	UBE2L6	0.4635		JADE2	0.0934		ZNF641	0.0871		UNC45A	0.1615
	MTMR14	0.4635		ZNF160	0.0934		BCLAF3	0.0871		ZNF609	0.1615
	KDM1B	0.4635		PROSER3	0.0934		RBM43	0.0871		SLC16A7	0.1615
	VKORC1	0.4635		FCRL3	0.0934		N/A	0.0871		RTCA	0.1615
	ZNF641	0.4635		VPS53	0.0940		PPP1R3E	0.0871		SPEF2	0.1615
	CCS	0.4635		TMOD2	0.0941		FNDC3B	0.0902		PCED1A	0.1615
	RAP2B	0.4635		ZBTB10	0.0941		ABCC5	0.0902		TRIM52	0.1615
	N/A	0.4635		AXIN2	0.0941		EMG1	0.0902		N/A	0.1615
	N/A	0.4635		SLC25A28	0.0950		BAG5	0.0902		PROSER3	0.1615

Table 5.1: The top 20 differentially expressed genes associated with each e-cigarette vapour treatment, and the corresponding statistical significance.

DESeq2 analysis was performed comparing UTC to paired treated samples for each e-cigarette vapour treatment. The top 20 most significantly differentially expressed genes in each condition are listed, with the adjusted p value (q-value), applying the Benjamini-Hochberg procedure to control for false discovery rate. No genes in any of the treatment groups were statistically significant between UTC and treatments.

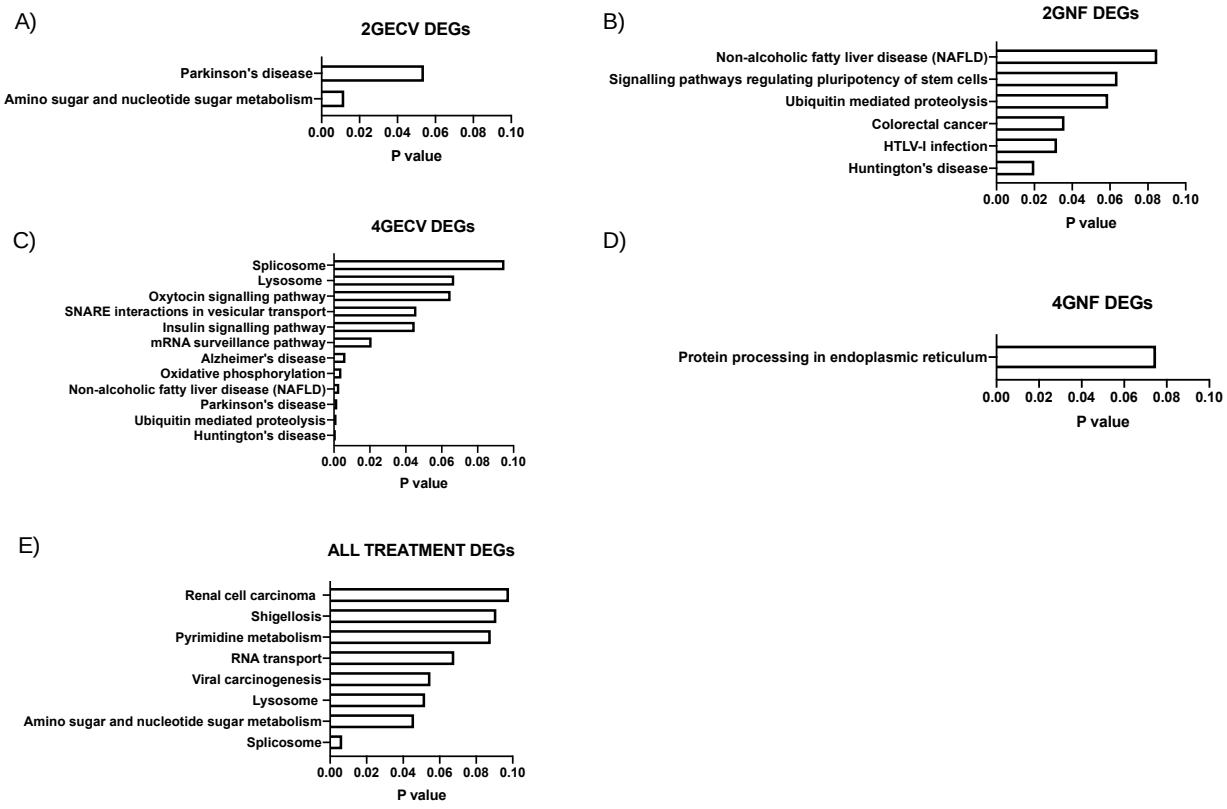


Figure 5.4 KEGG pathway analysis of all DEGs caused by e-cigarette treatments.

Pathway analysis was performed on all differentially expressed genes (DEGs) associated with each e-cigarette treatment. Pathway analysis was performed using DAVID bioinformatics resource at https://david.ncifcrf.gov/home.jsp. KEGG pathways were analysed and the associated p values plotted. It should be noted that although some pathways are significantly represented ($p < 0.05$), no genes were significantly differentially expressed.

5.4.2 E-cigarette vapour and neutrophil glycolysis

Glycolysis is a key metabolic process in neutrophils, providing the majority of ATP to perform their array of functions and adapt to their surroundings (Kumar and Dikshit, 2019, Borregaard and Herlin, 1982). Here, the impact of e-cigarette vapour on neutrophil glycolysis was investigated to determine if this could be a potential driver of neutrophil dysfunction caused by e-cigarette vapour exposure. To complement this work, glucose uptake before and after e-cigarette vapour exposure was assessed to determine whether neutrophils can both take up glucose and process it by glycolysis after e-cigarette vapour challenge.

5.4.2.1 Glycolytic parameters

To investigate whether e-cigarette vapour treatment suppresses neutrophil metabolism of glucose, the Agilent Seahorse XF96 analyser was used to inject defined stimulants and inhibitors into the cell media to perform the glyco stress test. Figure 5.5A shows the combined PER trace of 7 distinct neutrophil donors and the glyco stress test in all treatment groups. A two-way ANOVA with multiple comparisons revealed a significant difference in glycolytic response between 4GECV and UTC ($p = 0.0007 – 0.0336$) wells from 40 to 66 minutes (Oligomycin injection – 2-DG injection). Despite a trend towards a reduction, there were no further significant differences between treatment and UTC groups during the test. There was a significant difference between 4GECV and 2GNF ($p = 0.0467$) treated cells during one reading at peak glycolytic rate, however this was not sustained for the full duration of the test. There were no significant differences between nicotine-free and nicotine-containing groups in either 2nd generation or 4th generation devices (2GECV vs. 2GNF not significant,

4GECV vs 4GNF not significant). Figure 5.5B shows the measure of glycolysis after stimulation. Neutrophils were in a glucose-rich media, which was catabolised upon stimulation by 160 nM PMA. The pre-formatted analysis template calculated glycolysis of the cells based on the increase in ECAR upon PMA stimulation. There was a significant reduction in neutrophil glycolysis in 4GECV treated cells compared to UTC ($p = 0.0156$). No other treatments produced a significant difference in glycolysis compared to UTC. There were no further device-related or nicotine-related differences in this measurement of glycolysis.

Non-glycolytic acidification refers to the ECAR prior to any injections which is caused by processes other than glycolysis. There were no significant differences between UTC and any of the treatment groups, or any nicotine-related differences in treatment groups. However, there was a significant difference in non-glycolytic acidification between 4GECV and 2GECV treated cells ($p = 0.0391$) as shown in Figure 5.5C.

Glycolytic capacity measures the maximum, or peak ECAR the cells reach in each group when metabolism is switched entirely to glycolysis. 2nd generation devices with or without nicotine did not produce a significant difference in glycolytic capacity compared to UTC. However, compared to UTC both 4GECV ($p = 0.0078$) and 4GNF ($p = 0.0156$) treated neutrophils had significantly lower glycolytic capacity, as shown in Figure 5.5D. In addition, the glycolytic capacity of 4GECV treated neutrophils was significantly lower than that of 2GECV ($p = 0.0156$) indicating device power-related differences but this was not the case in 2GNF vs 4GNF (not significant). There were no nicotine-related differences in glycolytic capacity.

Glycolytic reserve refers to the difference between glycolytic capacity and glycolysis rate and represents the ability of cells to upregulate glycolysis. Compared to UTC, glycolytic reserve was significantly reduced by 4GECV ($p = 0.0391$) and 4GNF ($p = 0.0156$) treatment. There were no significant differences between nicotine-containing and nicotine-free groups exposed to the same power devices.

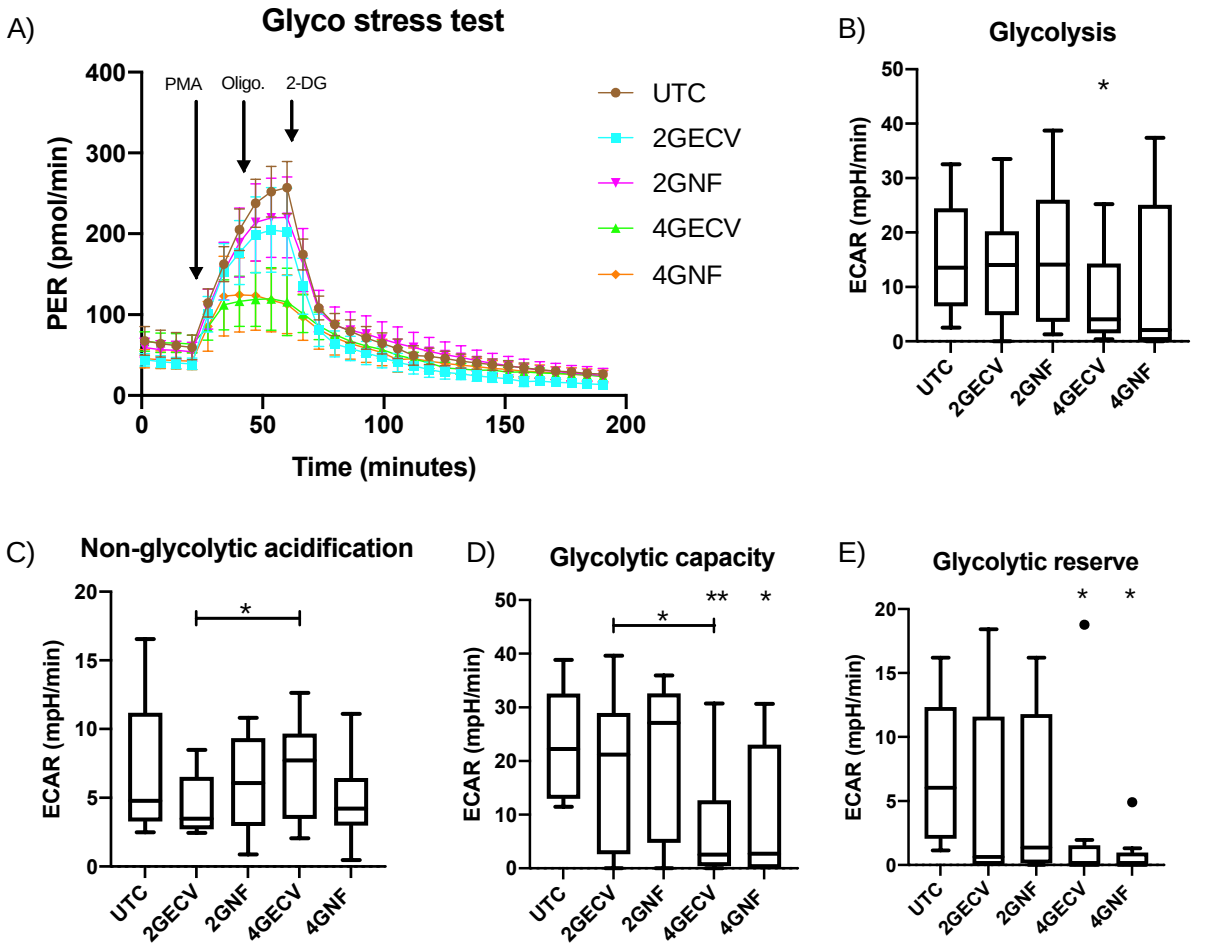


Figure 5.5: The effect of e-cigarette vapour exposure on neutrophil glycolysis. Using the Agilent Seahorse XF96, human neutrophils from 7 unique donors were tested using the glyco stress test designed to push cells to their maximal glycolysis rates. A) shows the combined proton efflux rate (PER) trace for the duration of the metabolic test for all 5 e-cigarette treatment groups. The trace represents the mean and standard error of the mean (SEM) for each treatment. Injections of 160 nM PMA, 2 µM oligomycin (Oligo.) and 50 mM 2-DG are indicated by the corresponding arrows. This pattern of stimulant/inhibitor injections allows the extrapolation of B) glycolysis C) non-glycolytic acidification, D) glycolytic capacity and E) glycolytic reserve) using a pre-formatted analysis template. Data was not normally distributed so statistical significance was assessed using wilcoxon matched-pairs signed rank tests. Statistical significance is indicated by asterisks above each group, corresponding to a significant difference from untreated control (UTC). A significant difference between treatment groups is indicated by an asterisks above a capped line between the two statistically different groups. * = p≤0.05, ** = p≤0.01, *** = p≤0.001, **** = p≤0.0001, n = 7 per group for all data.

5.4.2.2 Glucose uptake

After a reduction in glycolysis was demonstrated, the next aim was to determine whether the glycolytic defect was driven by inability to uptake or process glucose. To test this, the fluorescently-labelled glucose analogue, 6-(*N*-(7-Nitrobenz-2-oxa-1,3-diazol-4-yl)amino)-6-Deoxyglucose (6NBDG) was incubated with neutrophils after a period of glucose starvation and its uptake measured. At baseline, there were no significant differences in glucose uptake in any treatment group compared to UTC, as shown in Figure 5.6A. When 25 nM PMA was added, glucose uptake reduced but there were still no differences between the groups, see Figure 5.6B & C. There were no differences between the 2nd generation and 4th generation device groups, or between nicotine-containing and nicotine-free e-cigarette vapour in any of the glucose uptake experiments.

Taken together, this data indicated there was not a change in glucose uptake caused by e-cigarette vapour exposure, but a deficit in glucose processing which results in an overall reduction in the glycolytic ability of neutrophils exposed to e-cigarette vapour compared to UTC.

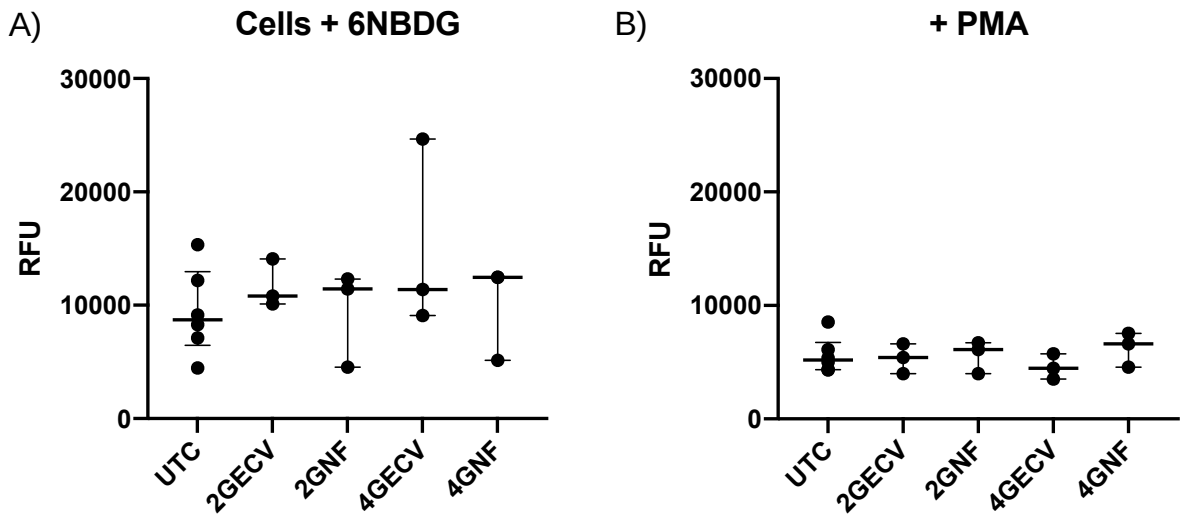


Figure 5.6: The effect of e-cigarette vapour exposure on neutrophil uptake of fluorescent 6NBDG analogue of glucose.
Neutrophils were glucose-starved for 3 hours before 6NBDG (6-(*N*-(7-Nitrobenz-2-oxa-1,3-diazol-4-yl)amino)-6-Deoxyglucose) was added and the fluorescence intensity measured on a plate reader. Relative fluorescence unit (RFU) was associated with the amount of glucose uptake. A) shows the baseline glucose uptake by cells in each treatment group. B) glucose uptake after addition of 25 nM PMA (phorbol 12-myristate 13-acetate) Data was considered not normally distributed due to low n numbers. To test for statistical difference, wilcoxon matched-pairs test were performed. There were no statistical differences between any of the time points. N = 3 per group.

5.4.3 Pre-treatment of neutrophils exposed to e-cigarette vapour with α4β2 and α7 nAChR inhibitor

The functional data presented in chapter 4 suggests nicotine was not a major driver of neutrophil dysfunction in response to e-cigarette vapour. However, to confirm this finding, investigating the impact of nicotine receptor inhibition was an essential step. The nicotine receptor inhibitor benzethonium chloride, an α7 nAChRs competitive antagonist and non-competitive inhibitor of α4β2 nAChRs (Coates and Flood, 2001) was used to treat neutrophils for 20 minutes before e-cigarette vapour exposure.

5.4.3.1 Phagocytosis

Neutrophils exposed to 4GECV showed a trend toward a significant reduction from UTC in phagocytosis of *E. coli* ($p = 0.0625$) and *S. aureus* ($p = 0.0625$) (Figure 5.7A&B). When neutrophils had been pre-treated with 49 nM benzethonium chloride (4GECV + BC), neutrophil phagocytosis of both *E. coli* and *S. aureus* appeared less impacted by 4GECV treatment. Mean fold change of phagocytosis when treated with 4GECV alone was 46.83 ± 41.58% (*E. coli*) and 44.53 ± 35.23 % (*S. aureus*) compared to 86.63 ± 95.01% (*E.* coli) and 72.04 ± 37.19% (*S.* aureus) with 49 nM benzethonium chloride pre-treatment. When neutrophils were exposed to 4GNF vapour, mean phagocytosis was 6.48 ± 5.80% (*E. coli*) and 18.73 ± 15.14% (*S. aureus*) compared to UTC (100%) (see Figure 5.7C&D). 49 nM benzethonium chloride pre-treatment had no effect on phagocytosis levels compared to 4GNF exposure alone: 9.00 ± 11.08% (*E. coli*) and 21.53 ± 18.90% (*S. aureus*). Benzethonium chloride only appeared to restore function to neutrophils exposed to nicotine-containing e-cigarette vapour,

suggesting that benzethonium chloride was acting specifically on neutrophil nicotine receptors, and not just providing an overall protective effect from non-specific binding.

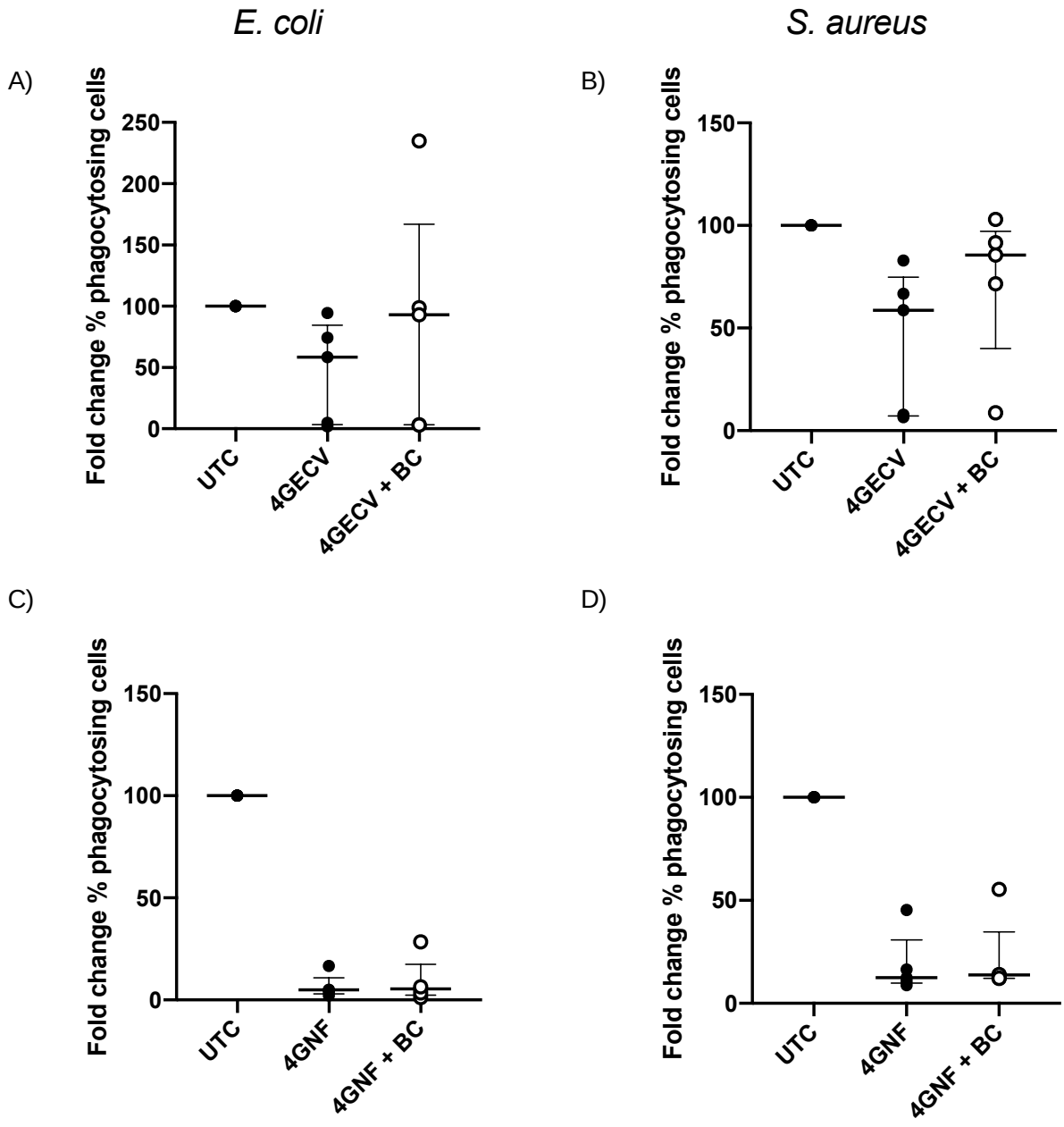


Figure 5.7: The effect of nicotine receptor inhibition prior to 4th generation e-cigarette exposure on neutrophil phagocytosis of *E. coli* and *S. aureus* bioparticles.

Neutrophils were treated with 49 nM benzethonium chloride (BC) (α4, α7, β2 nAChR subunit inhibitor) for 20 minutes prior to 4GNF/4GECV exposure. Neutrophils were then incubated with *E. coli* and *S. aureus* pHrodo™ bioparticles for 60 minutes before the percentage of pHrodo™-positive cells was measured. To assess the ability of BC to restore phagocytosis to baseline levels, UTC values were normalised to 100%, and a fold change calculated for the other groups. n = 5 per group for all data. Data was considered not normally distributed due to low n numbers. To test for statistical difference, wilcoxon matched-pairs test were performed. There were no statistical differences between any of the time points.

5.4.3.2 Transwell migration

Neutrophils exposed to 4GECV exhibited mean transwell migration to 100 nM CXCL8 of 36.28 ± 33.41% which appeared to be restored to 67.85 ± 59.32% of baseline value (UTC = 100%) with pre-treatment of 49 nM benzethonium chloride, as shown in Figure 5.8A. Neutrophils exposed to 4GNF e-cigarette vapour had mean transwell migration to 100 nM CXCL8 of 0.38 ± 0.59% of UTC value which did not improve with pre-treatment of 49 nM benzethonium chloride (0.91 ± 1.51% of baseline, see Figure 5.8B). According to power calculations, 4 repeats would be needed to detect a significant difference between 4GECV-treated neutrophils and UTC and a sample size of 55 repeats would be needed to produce a statistically significant difference between 4GECV and 4GECV + benzethonium chloride, indicating this test was underpowered.

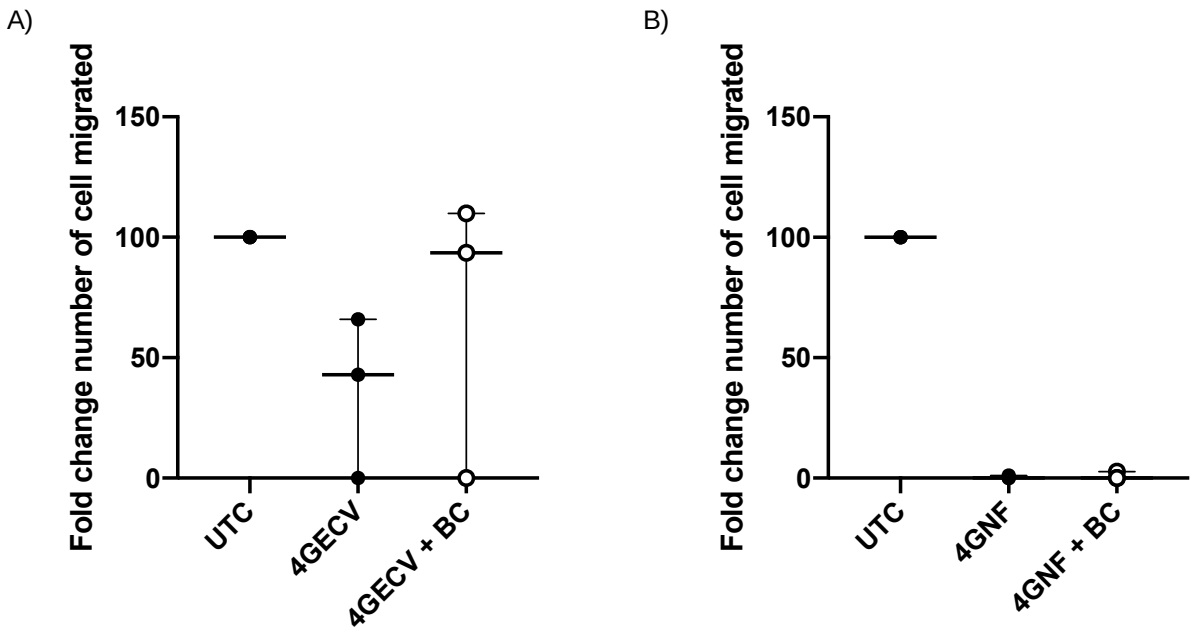


Figure 5.8: The effect of nicotine receptor inhibition prior to 4th generation e-cigarette exposure on neutrophil transmigration to 100 nM CXCL8.
Neutrophils were treated with 49 nM benzethonium chloride (BC) (α4, α7, β2 nAChR subunit inhibitor) for 20 minutes prior to 4GNF/4GECV exposure. Neutrophils were then incubated on transwells with 100 nM CXCL8 in the well, for 90 minutes. To assess the ability of BC to restore transwell migration to baseline levels, UTC values have been normalised to 100%, and a fold change calculated for the other groups. N = 3 per group for all data. Data was considered not normally distributed due to low n numbers. To test for statistical difference, wilcoxon matched-pairs test were performed. There were no statistical differences between any of the time points.

5.4.4 E-cigarette vapour and calcium signalling

Studies in the field have suggested elevated intracellular Ca^{2+} signalling is a major cellular event caused by e-cigarette exposure which can drive functional changes in neutrophils (Ghosh et al., 2019). To investigate whether e-cigarette vapour exposure caused aberrant intracellular Ca^{2+} signalling in this model, the Fluo-4 Direct™ Calcium assay kit was used to assess intracellular Ca^{2+} signalling. 4GNF e-cigarette vapour treated neutrophils had significantly lower Ca^{2+} signalling compared to UTC ($p = 0.0007$), 0.6 µM nicotine ($p = 0.0010$) and 2GNF ($p = 0.0203$) groups, see Figure 5.9. There were no further differences in Ca^{2+} signalling between any of the groups.

Overall, this preliminary data suggested treatment of neutrophils with 49 nM Benzethonium chloride prior to 4th generation e-cigarette vapour exposure appeared to increase phagocytosis of *E. coli* and *S. aureus* bioparticles and transwell migration to 100 nM CXCL8. Benzethonium chloride pre-treatment seemed to have had no effect on neutrophil exposed to nicotine-free e-cigarette vapour; indicating a nicotine-receptor specific protective effect. This provided further evidence that human peripheral blood neutrophils express the nAChR subunits α7, α4 and β2. In addition, there was no significant increase in intracellular calcium signalling caused by e-cigarette vapour exposure, or 0.6/3 µM nicotine treatment in this setting. However, neutrophils treated with nicotine-free e-cigarette vapour generated by 4th generation devices did exhibit significantly lower intracellular calcium signalling. Further work is required to understand the full contribution of nicotine, nicotine receptors and their association with calcium to e-cigarette induced harm in human neutrophils.

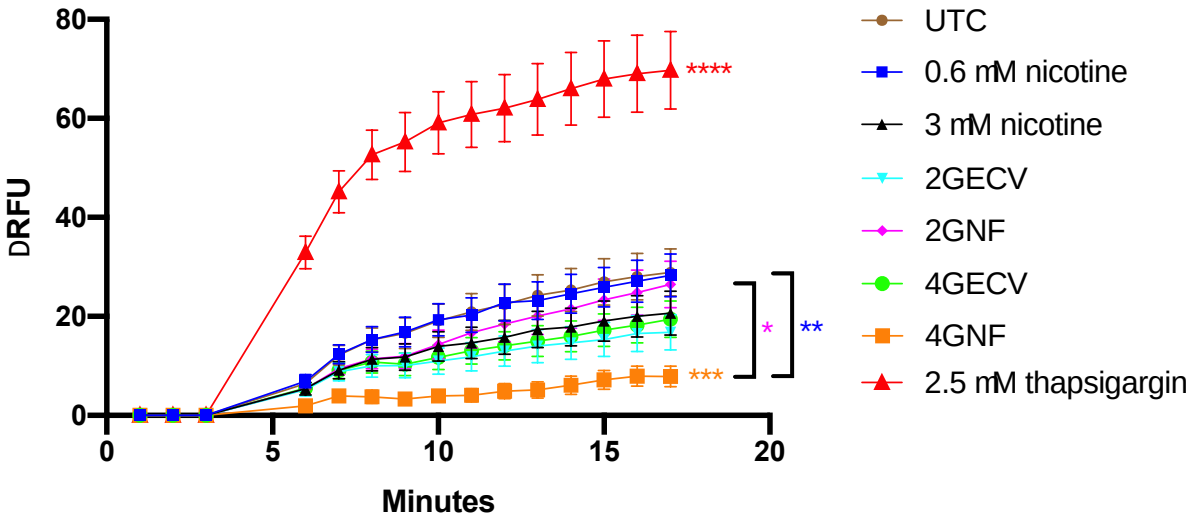


Figure 5.9: The effect of e-cigarette and nicotine treatment on neutrophil intracellular calcium signalling

After 20 minutes of e-cigarette vapour or nicotine treatment, 5 x 10^5 neutrophils were added per well to a black 96-well plate before being incubated for 60 minutes. FLuo-4 Direct calcium reagent was added before a further 45 minutes of. The plate was transferred to the plate reader and incubated for a further 15 minutes in the plate reader. Fluorescent readings were taken every minute for 17 minutes (with a 2-minute interval to add 2.5µM thapsigargin- the positive control) at excitation: 485/20 nm and emission: 528/20 nm. The graph shows a trace of the change in relative fluorescence units (RFU) over time for the duration of the experiment, expressed as the change in RFU from the final baseline reading before addition of thapsigargin. Traces represent the mean and SEM of each group, made up of experiments from 4 distinct neutrophil donors (N = 4). Statistical significance was assessed using an ordinary one-way ANOVA with multiple comparisons. Statistical significance is indicated by an asterisks at the end of a trace of the corresponding group, representing a significant difference from untreated control (UTC). A significant difference between treatment groups is indicated by an asterisks beside a capped line between the two statistically significant groups. * = $p \leq 0.05$, ** = $p \leq 0.01$, *** = $p \leq 0.001$, **** = $p \leq 0.0001$.

5.4.5 Pre-treatment of neutrophils exposed to e-cigarette vapour with Pi3K inhibitors

Previous published work has demonstrated the restorative effect of Pi3K inhibition on neutrophil function in older adults, pneumonia, and critical care patients (Sapey et al., 2014, Scott et al., 2021, Wilson et al., 2020). To investigate whether PI3K inhibition can conserve neutrophil function after exposure to e-cigarette vapour, CAL101, a selective Pi3Kδ inhibitor and AS252424, a selective Pi3Kγ inhibitor, were used to treat neutrophils prior to e-cigarette vapour exposure. Here, we focussed on the highest power 4th generation devices which showed the largest effect on neutrophil phagocytosis and transmigration.

5.4.5.1 Phagocytosis

Neutrophils exposed to 4GECV demonstrated a trend towards a significant reduction from UTC in phagocytosis of *E. coli* ($p = 0.0625$) and *S. aureus* ($p = 0.0625$) (Figure 5.10A&B). Pre-treatment with 75 nM CAL101 (Pi3Kδ inhibitor) (4GECV + Pi3Kδ), appeared to reduce the impact of 4GECV treatment on neutrophil phagocytosis of *E. coli*, albeit modestly. Conversely, neutrophils exposed to 4GECV appeared to exhibit lower *S. aureus* phagocytosis when pre-treated with CAL101. Mean fold change of *E. coli* phagocytosis when treated with 4GECV alone was 46.83 ± 41.58% vs 59.79 ± 52.25% of baseline when treated with Pi3Kδ inhibitor. Mean fold change of *S. aureus* phagocytosis when treated with 4GECV alone was 44.53 ± 35.23% compared to 34.07 ± 31.35% of baseline when pre-treated with Pi3Kδ inhibitor. There was no effect of Pi3Kδ inhibition on the impact of 4GNF exposure on phagocytosis of *E. coli* or *S. aureus* (see Figure 5.10C&D). *E. coli* phagocytosis did not change from mean fold

change 6.48 ± 5.80% of baseline with 4GNF exposure alone to 8.37 ± 7.92% of baseline when pre-treated with 75nM Pi3Kδ inhibitor. *S. aureus* phagocytosis was also unaffected, from 4GNF exposure values of 18.73 ± 15.14% of baseline phagocytosis to 18.80 ± 15.43% of baseline after Pi3Kδ inhibition.

When pre-treated with 33 nM AS252424 (Pi3Kγ inhibitor) (4GECV + Pi3Kγ), phagocytosis of *E. coli* by 4GECV treated neutrophils appeared to increase while *S. aureus* was unaffected (see Figure 5.10A&B). On average, the amount of *E. coli* phagocytosed by 4GECV treated neutrophils was 46.83 ± 41.58% of baseline value, but when pre-treated with Pi3Kγ inhibitor, this appeared to increase to 70.00 ± 65.22% of baseline. Whereas *S. aureus* phagocytosis did not change from 44.53 ± 35.23% of baseline to 45.85 ± 33.18% of baseline when Pi3Kγ inhibitor pre-treatment was applied. There appeared to be a minimal effect of Pi3Kγ inhibition on 4GNF-exposed neutrophils, with mean fold change of *E. coli* phagocytosis without inhibition at 6.48 ± 5.80% and with Pi3Kγ inhibition 11.91 ± 15.38% of baseline values. Pi3Kγ inhibition did not affect *S. aureus* phagocytosis after 4GNF e-cigarette vapour treatment, with levels remaining unchanged from before pre-treatment (18.73 ± 15.14% of UTC values) to after pre-treatment (21.42 ± 18.73% of UTC values), as shown in Figure 5.10C&D.

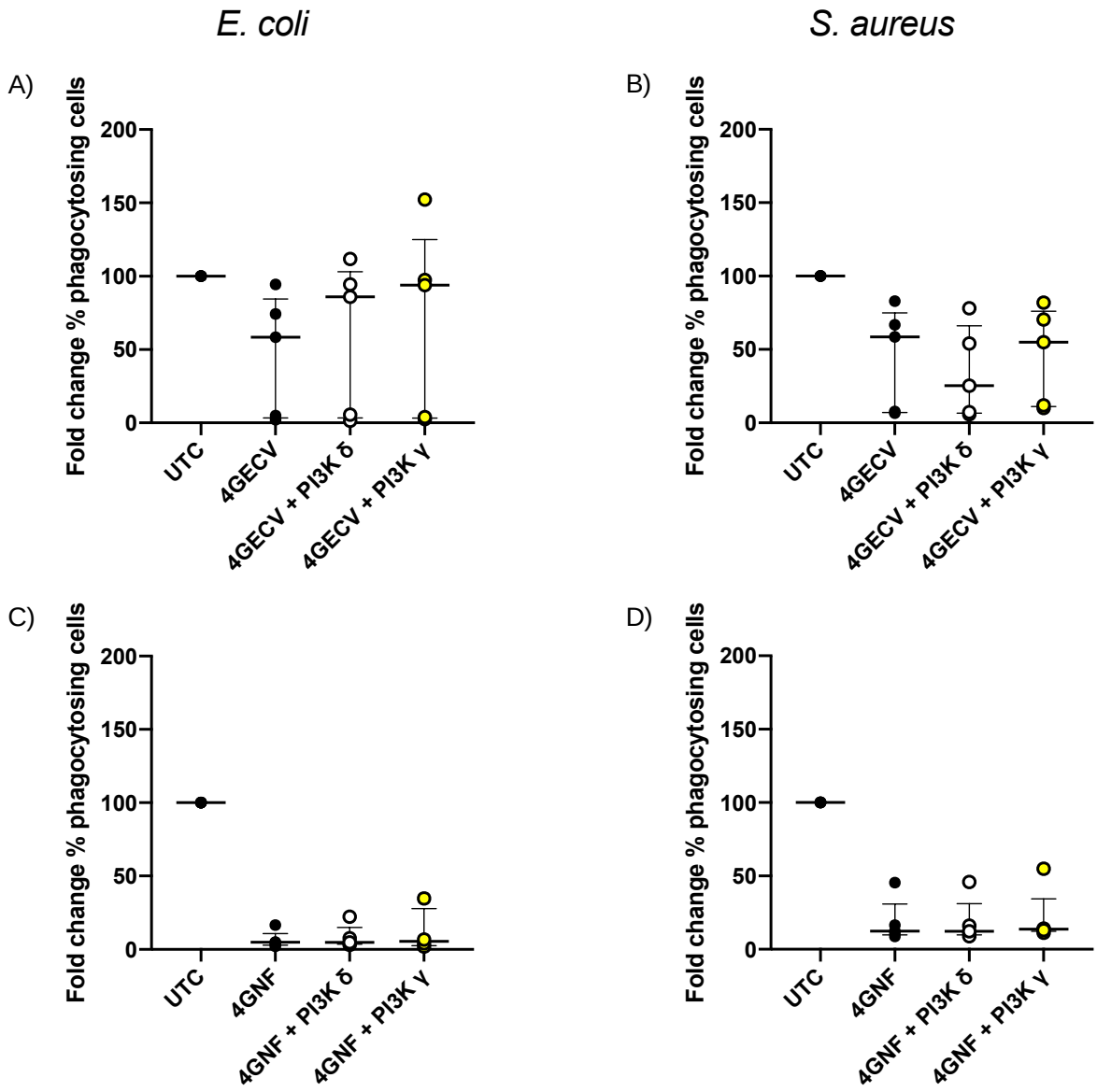


Figure 5.10: The effect of Pi3Kδ and γ inhibition prior to 4th generation e-cigarette exposure on neutrophil phagocytosis of *E. coli* and *S. aureus* bioparticles.
Neutrophils were treated with 33 nM AS252424 (Pi3Kγ inhibitor), 75 nM CAL101 (Pi3Kδ inhibitor) for 20 minutes prior to 4GNF/4GECV exposure. Neutrophils were then incubated with *E. coli* and *S. aureus* pHrodo™ bioparticles for 60 minutes before the percentage of pHrodo™-positive cells was measured. To assess the ability of Pi3K inhibitors to restore phagocytosis to baseline levels, UTC values were normalised to 100%, and a fold change calculated for the other groups. n = 5 per group for all data. Data was considered not normally distributed due to low n numbers. To test for statistical difference, wilcoxon matched-pairs test were performed. There were no statistical differences between any of the time points.

5.4.5.2 Transwell migration

Figure 5.11A shows the effect of 4GECV exposure with and without Pi3Kδ and Pi3Kγ inhibition on neutrophil transmigration. There appeared to be a slight increase in the fold change from baseline of neutrophils transmigrating to 100 nM CXCL8 after 4GECV exposure when Pi3Kδ was inhibited by 75 nM CAL101. The mean proportion of neutrophils migrating was 36.28 ± 33.41% of baseline when neutrophils were exposed to 4GECV which appeared to increase, albeit modestly, to 43.04 ± 37.27% after Pi3Kδ inhibition. Similarly, there was very little difference between the fold change of the number of neutrophils migrating after 4GNF exposure 0.38 ± 0.59% of baseline vs 0.70 ± 1.38% of baseline after Pi3Kδ inhibition, as shown in Figure 5.11B.

Inhibition of Pi3Kγ using 33 nM AS252424 also had minimal impact on neutrophil transmigration. Pre-treatment with Pi3Kγ inhibitor appeared to modestly increase transmigration from baseline neutrophil transmigration (mean: 47.48 ± 41.40% from UTC levels) compared to 4GECV treatment alone (mean: 36.28 ± 33.41% from UTC levels). Pi3Kγ inhibition appeared to have a slightly greater effect on 4GNF-treated neutrophils compared to Pi3Kδ inhibition, but there was effectively no difference between any of the groups. Mean fold change in neutrophils transmigrating compared to UTC was 0.38 ± 0.59% of baseline in 4GNF-exposed neutrophils and 1.27 ± 2.52% of baseline with pre-treatment Pi3Kγ inhibition.

Power calculations revealed a replicate number of 4 should have achieved a statistically significant difference between UTC and 4GECV-treated neutrophils, indicating a potential for improvement in transwell migration by Pi3K inhibition could

have been shown with further repeats. However, Figure 5.11B appeared to show no beneficial effect of Pi3K inhibition in 4GNF exposed neutrophils and power calculations suggested over 70 repeats would have been required to show statistical significance.

In conclusion, the preliminary data presented here revealed partial Pi3Kδ and Pi3Kγ did not appear to provide a restorative effect on 4th generation e-cigarette vapour treated neutrophil phagocytic or transmigration functions. Therefore, it is unlikely aberrant activation of Pi3K is driving neutrophil dysfunction of phagocytosis of *E. coli* and *S. aureus* bioparticles or transmigration to CXCL8 in this model, but more work would be needed to determine this.

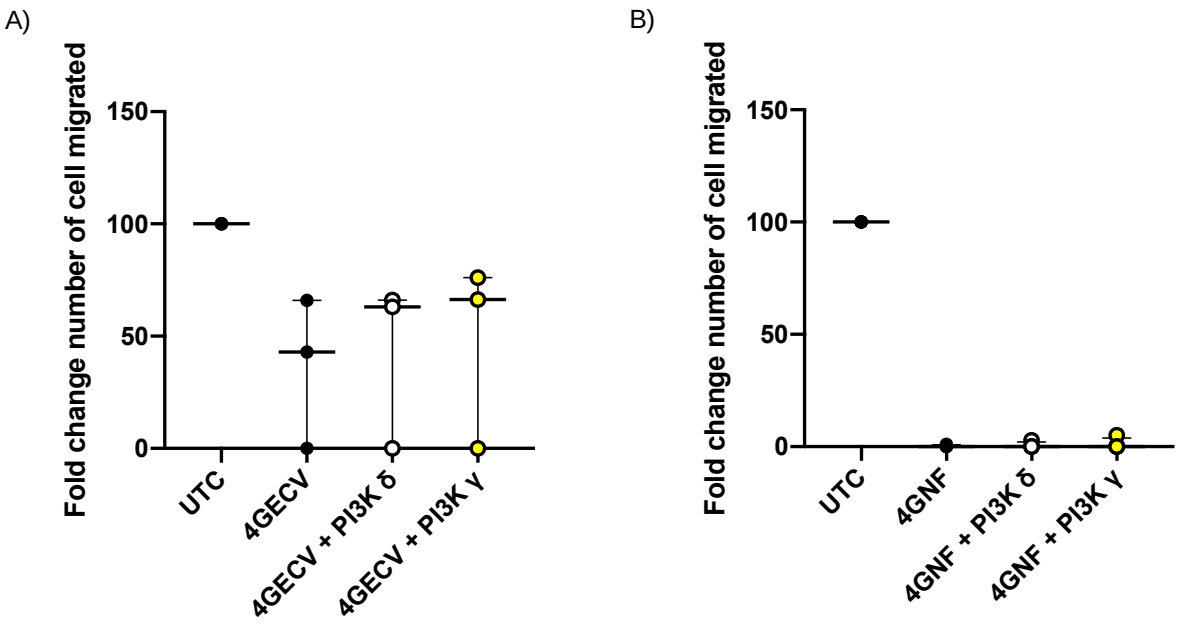


Figure 5.11: The effect of Pi3Kδ and γ inhibition prior to 4th generation e-cigarette exposure on neutrophil transmigration to 100 nM CXCL8.
Neutrophils were treated with 33 nM AS252424 (Pi3Kγ inhibitor), 75 nM CAL101 (Pi3Kδ inhibitor) for 20 minutes prior to 4GNF/4GECV exposure. Neutrophils were then incubated on transwells with 100 nM CXCL8 in the bottom well, for 90 minutes. To assess the ability of Pi3K inhibitors to restore transwell migration to baseline levels, UTC values have been normalised to 100%, and a fold change calculated for the other groups. N = 3 per group for all data. Data was considered not normally distributed due to low n numbers. To test for statistical difference, wilcoxon matched-pairs test were performed. There were no statistical differences between any of the time points.

5.4.6 Pre-treatment of neutrophils exposed to e-cigarette vapour with NAC

The data in Chapter 4 suggest ROS and RCS may be the major drivers of neutrophil dysfunction after e-cigarette vapour exposure with a limited or minor role attributed to nicotine-dependent effects. Therefore, the ability of the antioxidant NAC to ameliorate the harmful effects of e-cigarette vapour on neutrophil phagocytosis and transmigration were investigated.

5.4.6.1 Phagocytosis

Neutrophils exposed to 4GECV exhibited a reduction in phagocytosis of *E. coli* to 46.83 ± 41.58% of UTC values, which appeared to increase to 80.66 ± 71.85% of UTC values with 600 µM NAC treatment prior to e-cigarette vapour exposure, as shown in Figure 5.12A. Similarly, phagocytosis of *S. aureus* bioparticles after 4GECV treatment appeared less impacted with NAC pre-treatment (68.95 ± 30.25% of UTC values) than without (44.53 ± 35.23% of UTC values) (see Figure 5.12B). 4GNF-treated neutrophils only achieved 6.48 ± 5.80% of UTC *E. coli* phagocytosis levels; but with pre-treatment of 600 µM NAC, this appeared to improve to 21.71 ± 29.49% of UTC phagocytosis levels for *E. coli* (see Figure 5.12C). NAC also had a beneficial effect on *S. aureus* phagocytosis, improving response from 18.73 ± 15.14% after 4GNF treatment alone to 41.27 ± 28.32% of UTC values after NAC pre-treatment. A replicate number of at least 25 repeats would have been needed to provide sufficient power to the statistics, according to power calculations for this work.

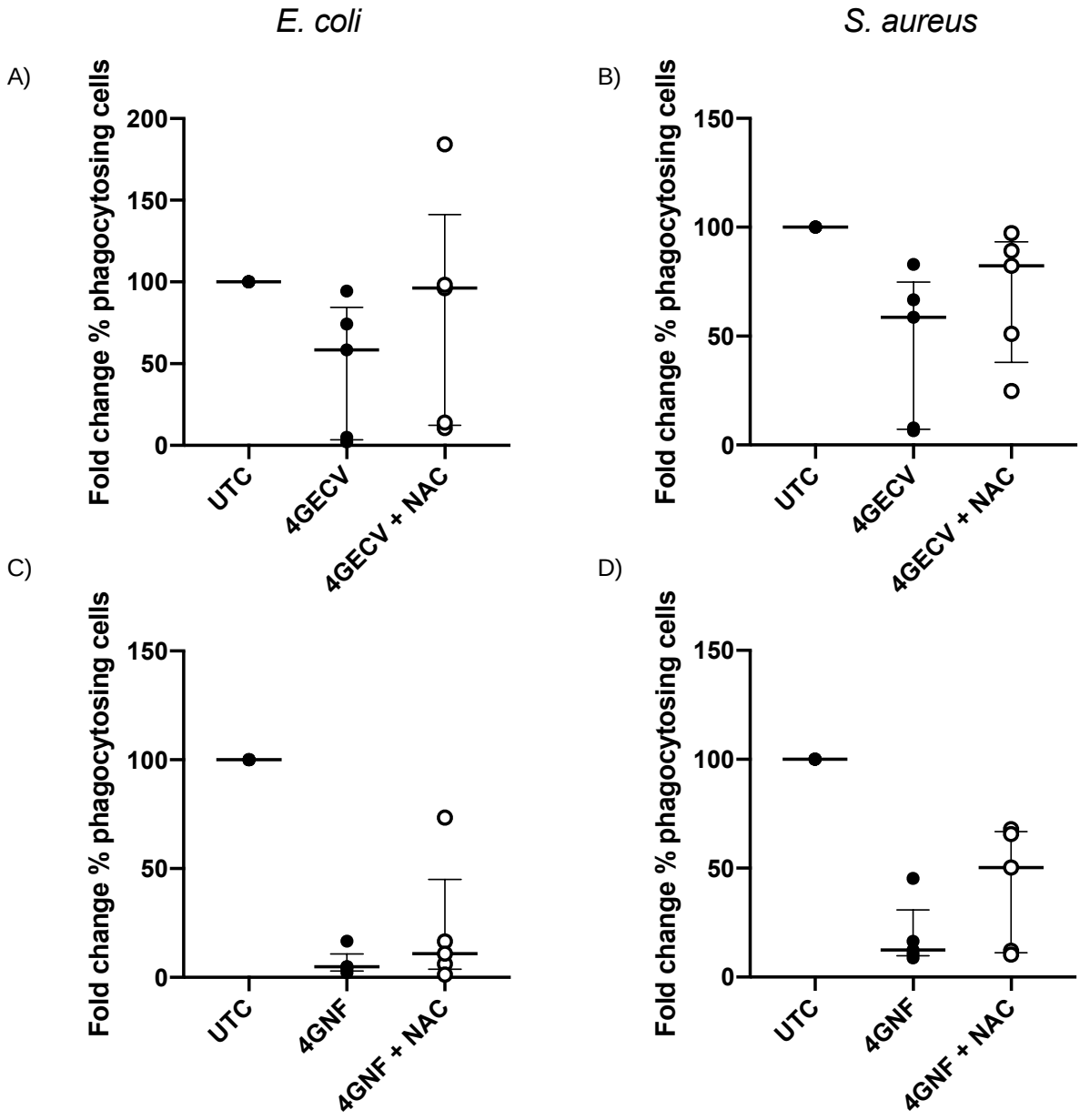


Figure 5.12: The effect of antioxidant treatment prior to 4th generation e-cigarette exposure on neutrophil phagocytosis of *E. coli* and *S. aureus* bioparticles.
Neutrophils were treated with 600 µM N-acetyl-cystine (NAC) for 20 minutes prior to 4GNF/4GECV exposure. Neutrophils were incubated with *E. coli* and *S. aureus* pHrodo™ bioparticles for 60 minutes before the percentage of pHrodo™ positive cells was measured. To assess the ability of NAC to restore phagocytosis to baseline levels, UTC values have been normalised to 100%, and a fold change calculated for the other groups. n = 5 per group for all data. Data was considered not normally distributed due to low n numbers. To test for statistical difference, wilcoxon matched-pairs test were performed. There were no statistical differences between any of the time points.

5.4.6.2 Transwell migration

Next, the effect of NAC on neutrophil transwell migration was assessed. After 4GECV treatment, neutrophil transmigration to CXCL8 was 36.28 ± 33.41% UTC levels. This appeared to increase to 67.23 ± 53.66% of UTC levels after pre-treatment with 600 µM NAC before being exposed to e-cigarette vapour, as shown in Figure 5.13A. The biggest apparent improvement was seen in transmigration of neutrophils treated with 4GNF. Prior to antioxidant treatment, neutrophils exposed to 4GNF migrated at 0.38 ± 0.59% of UTC levels, which appeared to improve to 51.13 ± 44.28% when a pre-treatment of 600 µM NAC was given, as shown in Figure 5.13B. Power calculations suggested a replicate number of 12 would have been required to show sufficient statistical difference between the groups using this preliminary data.

Overall, this work suggested pre-treating neutrophils with NAC prior to e-cigarette vapour exposure appeared to reduce the negative impact on both phagocytosis of *E. coli* and *S. aureus* and transwell migration to CXCL8. NAC treatment appeared to show the greatest potential for preservation of function out of all the pre-treatments trialled. This work indicated a potential for a protective effect of antioxidant treatment on neutrophils before exposure to e-cigarette vapour, even when generated by the highest-powered devices. However, further work would be required to determine the full potential of NAC as a protective agent against negative e-cigarette induced effects.

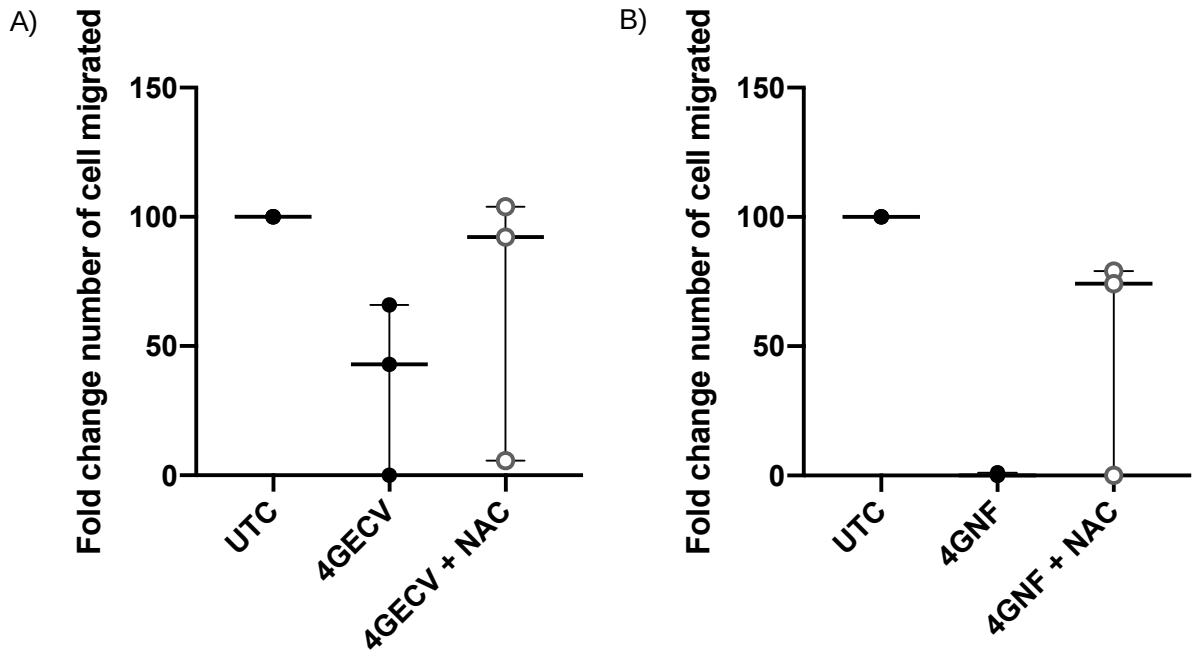


Figure 5.13: The effect of N-acetyl-cystine pre-treatment on neutrophil transwell migration prior to e-cigarette vapour exposure.
Neutrophils were exposed to 600 µM N-acetyl-cysteine (NAC) for 20 minutes prior to e-cigarette vapour exposure. The transwell migration assay was performed and the number of cells migrated counted. To assess whether NAC treatment can restore transmigration to baseline levels, graphs A and B represent the number of neutrophils migrating, normalised to the individual's baseline levels (UTC). N = 3 for all groups. Data was considered not normally distributed due to low n numbers. To test for statistical difference, wilcoxon matched-pairs test were performed. There were no statistical differences between any of the time points.

5.5 Chapter 5 discussion

5.5.1 Neutrophil transcriptome

To address the first aim of this chapter, the work presented here showed neutrophil dysfunction was not driven by a transcriptional response in our model. There were no significantly DEGs in the samples. A list of genes of interest was constructed which was going to be used to investigate the link between neutrophil dysfunction shown in Chapter 4, and translational changes. However, the lack of statistical significance in any DEGs signalled this would not be a fruitful investigation. Potentially, transcriptional changes were induced by e-cigarette vapour exposure in neutrophils, however, longer exposures and larger sample sizes would be needed to detect these changes. Previous work has shown neutrophil mRNA expression is significantly altered after 2-4 hour treatment with bacteria (Sukumaran et al., 2005) and as little as 30 minutes of high dose LPS stimulation (Tsukahara et al., 2003). This indicates transcriptomic changes caused by e-cigarette vapour exposure in the present model had the potential to be detected after only 20 minutes of vapour exposure followed by RNA harvesting. However, in the Tsukahara study, neutrophils were harvested 90 minutes after the 30 minute LPS stimulation, allowing time for gene expression to change (Tsukahara et al., 2003). Other reasons for the lack of detectable changes include intra-donor variability in response exacerbated by low replicate numbers, meaning DEGs did not reach statistical significance. Follow-up western blots and qPCR experiments have not been performed due to the findings that no genes were significantly differentially expressed after e-cigarette treatment. It was not possible to determine a mechanism of action from RNA sequencing data; instead, signalling molecule and receptor inhibitor

investigations were pursued to investigate if other mechanistic drivers could be identified.

5.5.2 Neutrophil glycolytic metabolism

Work addressing the second aim of this chapter, revealed 4th generation e-cigarette vapour significantly reduced the ability of neutrophils to upregulate glycolysis when stimulated. This was a nicotine-independent effect and device power-dependent as it was not seen in the lower power 2nd generation devices. However, this was not due to a reduction in the ability of neutrophils to take up glucose, rather in the processing of that glucose. It has been shown that epithelial cells exhibit a reduction in glucose uptake after exposure to PG/VG (55:45) (Woodall et al., 2020) however, this did not translate to neutrophils in this study. Glucose uptake decreased after addition of 25 nM PMA. This is likely due to the 2 hour incubation after addition of PMA, which would allow the cells to generate NETs, missing the initial glucose uptake response, a methodological limitation.

Total glycolysis has been shown to be reduced in neutrophils exposed to e-liquid flavouring agents, particularly cinnamaldehyde and ethyl vanillin, which would exaggerate the effects demonstrated by PG/VG and nicotine here (Hickman et al., 2019). Previously, mitochondrial inhibition has been shown to have no impact on neutrophil effector functions (Borregaard and Herlin, 1982, Reiss and Roos, 1978), demonstrating the high dependence of neutrophil functions on glycolytic ability. Phagocytosis is a glycolysis-dependent process, with glycolytic inhibitors diminishing neutrophil ability to phagocytose (Borregaard and Herlin, 1982, Sbarra and Karnovsky,

1959). Therefore, dysfunctional phagocytosis caused by e-cigarette vapour exposure could be partially explained by diminished ability to amount a glycolytic response in this model. However, there was not an effect on glycolysis caused by 2nd generation e-cigarette vapour but this thesis showed defects in phagocytosis, suggesting there were further drivers of phagocytic dysfunction.

NET generation in response to PMA is dependent on glycolysis (Rodriguez-Espinosa et al., 2015, Awasthi et al., 2019), and therefore the reduced glycolytic capacity of e-cigarette exposed neutrophils in our model could explain the reduction in ability to amount a NET response to PMA described in Chapter 4. Oxidative burst responses are dependent on NADPH oxidases, the substrate of which is generated from the pentose-phosphate pathway which utilises an intermediate substrate from glycolysis (Kumar and Dikshit, 2019, Jeon et al., 2020). Chapter 4 showed a significant inhibition of oxidative burst response caused by 4th generation e-cigarette vapour exposure, but not 2nd generation; which evidence here suggests could have been contributed to by a reduction in glycolytic capacity.

Neutrophil chemotaxis depends heavily on ATP, the majority of which is generated by glycolysis (Jeon et al., 2020, Kumar and Dikshit, 2019), however, there is evidence to show mitochondria and purinergic signalling govern chemotactic responses in neutrophils (Bao et al., 2015). Therefore, it was unlikely that impaired neutrophil chemotaxis could be explained by the reduced glycolytic capacity of neutrophils described here.

This suggests inability of neutrophils to amount a glycolytic response could partially explain some of the glycolysis-dependent functional defects described in Chapter 4, including NET generation and phagocytosis, but that functional defects in 2nd generation e-cigarette vapour exposed neutrophils shows there is more to this potential mechanism of harm. Mechanistic experiments trialling neutrophil function after e-cigarette exposure, with glycolytic inhibitors would help to understand the contribution of reduced glycolytic capacity to neutrophil effector functions.

5.5.3 Nicotine receptors

There is extensive literature debate on the expression of nAChR subunits on the surface of human neutrophils. Some studies have suggested via qPCR and inhibitor work that neutrophils do not possess α4, α7, β2 nAChR subunits (Iho et al., 2003, Ghosh et al., 2019); however, in the work presented here to address the third aim of this chapter, inhibition of these subunits appeared to partially restored phagocytosis in neutrophils exposed to e-cigarette vapour, suggesting they do express these subunits. The nicotine receptor inhibition data presented here was preliminary data collected to inform future work, but was not powered sufficiently to perform statistical analysis or draw firm conclusions from. Therefore, results discussed represent patterns and signals of potential benefit as opposed to firm conclusions, and should be interpreted accordingly. This work supports previous data the presence of α7 nAChR subunits on the surface of human neutrophils via confocal imaging (Lee et al., 2017). Detection of α7 nAChR subunits via RT-PCR revealed heterogeneity in expression across the population (De Rosa et al., 2005) and in non-small-cell lung cancers, different subunits have been shown to be expressed between smokers and non-smokers (Lam et al.,

2007), indicating the impact of environment on nicotine receptor expression heterogeneity. Population heterogeneity may explain why one donor in this study did not respond to Benzethonium chloride pre-treatment prior to e-cigarette vapour exposure here. α7 nAChR subunits are the most extensively investigated in human neutrophils, but the work using Benzethonium chloride presented in this chapter may represent action on α7, α4 or β2 nAChR subunits, which could only be separated out by further work using specific subunit inhibitors. Previous work has shown nicotine interaction with α7 nAChR subunits drives unstimulated and PMA-stimulated NET generation (Lee et al., 2017) however, in Chapter 4 NET responses to PMA appeared to be supressed after e-cigarette vapour exposure, therefore there was likely to be a different mechanism driving this dysfunction.

Nicotine-related effects of e-cigarettes have been previously reported, with changes in degranulation, phagocytosis and chemotaxis caused by nicotine treatment (Seow et al., 1994, Ghosh et al., 2019). The data presented here supported this, demonstrating recovery of phagocytic function was possible by blocking nicotine interaction with α4, α7, β2 nAChR subunits, via treatment with Benzethonium chloride. However, there were nicotine-independent effects on neutrophil functions, described both in Chapter 4 and in existing literature (Clapp et al., 2017, Corriden et al., 2020), meaning there ere further mechanisms to uncover other than nicotine receptor dependent effects.

5.5.3.1 Calcium signalling

Following analysis of nAChR inhibition, an investigation into the effects of e-cigarette vapour on intracellular calcium signalling in neutrophils was pursued to address the

fourth aim. Neutrophils exposed to nicotine-free e-cigarette vapour produced a lower calcium signal compared to their nicotine-containing counterparts due absence of nAChR engagement, which usually causes Ca^{2+} influx. However, neutrophils exposed to nicotine free vapour generated from 2nd generation devices produced a higher calcium signal than those exposed to 4GNF vapour. 4GNF vapour-exposed neutrophils may have reduced intracellular calcium signalling due to an earlier spike and subsequent depletion of calcium stores, but this was not a nAChR response as neutrophils in this treatment group were not exposed to nicotine. Neutrophil degranulation has been shown to be a calcium-dependent function (Perez et al., 1987) and work in the e-cigarette field has shown an increase in protease secretion and activity in neutrophils exposed to 5 mM nicotine following a spike in intracellular calcium signalling after nAChR engagement (Ghosh et al., 2019). However, as reported by the authors, the detection of GAPDH in the cell media and the higher EC_{50} for protease release than Calcium signalling suggests neutrophil lysis caused by this treatment (Ghosh et al., 2019). Therefore, further investigations into the link between nicotine, calcium signalling and neutrophil functions are needed for this to be fully understood.

There is evidence for nicotine, nAChR and calcium dependent effects of e-cigarettes in cell types other than neutrophils. Cystic fibrosis transmembrane conductance regulator (CFTR) function is suppressed in airway epithelial cells by calcium signalling caused by nicotine interacting with α7 nAChRs (Maouche et al., 2013). Flavoured e-liquid containing nicotine also induced persistent elevations in calcium signalling in airway epithelial cells (Rowell et al., 2019). It should be noted that due to

methodological limitations in the calcium signalling assay protocol, there was a delay of 2 hours between e-cigarette vapour exposure and first calcium signalling readout measurement when following these steps. Therefore, a fast calcium spike in response to e-cigarette vapour will have been missed. Further advances allowing real time analysis of calcium levels in during exposure to e-cigarette vapour would enable the full deciphering of the contribution of calcium signalling to neutrophil dysfunction caused by e-cigarettes.

5.5.4 Restoration of function – Pi3K signalling

The fifth aim of this chapter was to investigate whether Pi3K inhibition could improve neutrophil function after e-cigarette vapour exposure. Pi3K signalling has previously been shown to contribute to the control of neutrophil functions including chemotaxis and phagocytosis (Gambardella and Vermeren, 2013, Rossi and Lord, 2013). Pi3K inhibition improves neutrophil function in older adults (Sapey et al., 2014, Wilson et al., 2020) and the critically ill (Scott et al., 2021), where constitutive Pi3K activation drives neutrophil dysfunction. Here, Pi3K inhibitors did not appear to improve phagocytosis of *E. coli* or *S. aureus* or restore neutrophil transwell migration to 100 nM CXCL8 when exposed to 4th generation e-cigarette vapour. However, without western blot confirmation of Pi3K inhibition, this cannot be fully determined. This could be because aberrant Pi3K signalling is not a driver of neutrophil dysfunction after e-cigarette vapour exposure. Alternatively, Pi3K signalling may not be a driver of transmigratory and phagocytic dysfunction, but contributes to other dysfunctions which weren't tested, such as NET generation or oxidative burst responses. Published data revealed Pi3K inhibition improved neutrophil function in older adults (Sapey et al., 2014), yet the

donors used here were significantly younger, and therefore may have regulated Pi3K signalling, even after e-cigarette vapour treatment. Previously, Pi3K inhibitors were shown to attenuate the negative effects of e-cigarettes on alveolar macrophage viability (Scott et al., 2018). α7 nAChR subunit has been shown to be highly expressed on the surface of alveolar macrophages, and engagement of the α7 nAChR subunit transduces a Pi3K signalling cascade (Galvis et al., 2006, Kihara et al., 2001). However, partial Pi3K inhibition did not appear to affect e-cigarette vapour-induced neutrophil dysfunction in this model, suggesting a different mechanism of harm in neutrophils compared to alveolar macrophages.

Evidence from cigarette smoke extract and nicotine treatments on neutrophils shows upregulation of p38 MAPK, ERK and NF-κB pathways (Koethe et al., 2000). In response to high-dose e-cigarette vapour extract treatment, neutrophils exhibit p38 MAPK activation, which drives MMP-9 secretion, but no change in ERK or NF-κB pathway activation were found (Higham et al., 2016). This suggests that there are both differential and overlapping mechanisms of e-cigarette damage compared with cigarette damage, which need further investigating to understand the possible impacts of chronic vaping. In conclusion, Pi3K did not appear to be a driving signalling molecule of dysfunction in e-cigarette exposed neutrophils, but investigations into signalling pathways such as p38 MAPK could uncover further mechanistic insights.

5.5.5 Restoration of function – antioxidants

E-cigarette vapour has been estimated to contain 2.5 x 10^{13}-10.3 x 10^{13} free radicals per puff from a second generation device (Goel et al., 2015). In addition, reactive

carbonyls such as formaldehyde and acetaldehyde present in e-cigarette vapour increase up to 200 times with increasing battery power output, in ranges equivalent to tobacco smoke (Kosmider et al., 2014). Further, e-cigarette vapour has been shown to increase ROS in alveolar macrophages (Scott et al., 2018) and epithelial cells (Anderson et al., 2016). NAC is a well categorised antioxidant and anti-aldehyde (Zhitkovich, 2019), the previous application of which to the e-cigarette setting found an amelioration of toxic effects of e-cigarette vapour condensate on alveolar macrophages and restoration of phagocytic function (Scott et al., 2018). Work detailed in chapter 4 showed a significant impairment of neutrophil functions, even in the absence of nicotine. This suggested there were fundamental drivers of e-cigarette related potential harm to neutrophils caused by exposure to vapourised PG and VG, which could have been driven by the RCS/ROS effects of e-cigarette vapour. Preliminary data presented in this chapter show NAC pre-treatment appeared to improve phagocytosis of *E. coli* and *S. aureus* bioparticles and transmigration to CXCL8 in neutrophils exposed to 4th generation e-cigarette vapour. This data suggested neutrophil phagocytosis and migration was a ROS/RCS driven effect, independent of nicotine and flavourings. This is the first data to have applied the pre-treatment of an antioxidant to e-cigarette treated neutrophils and to have alluded to a potential beneficial effect, albeit in a very small data set.

5.5.6 Limitations

The major limitation of this chapter was low replicate numbers for which the tests were performed. Despite appearing to improve function, these results may have shown statistical significance had they been adequately powered. Further repeats were not

possible due to time pressures exacerbated by the COVID-19 pandemic. This made interpretation and drawing definite conclusions from this work a challenge, but as preliminary data this work was valuable.

The transcriptomic analysis is limited as it is focussed only on one time point. By expanding this to look at transcriptomic changes over time would capture a possible later signal and provide a more insightful look into expressional changes associated with e-cigarette vapour exposed neutrophils. In addition, the p value could have been made less stringent to detect genes of interest, and these could have been followed up by further investigations.

In this investigation of neutrophil metabolism using the seahorse analyser, ECAR was still increasing at the point of oligomycin injection during the glyco stress test, as well as 2DG, meaning this could be an underestimation of glycolysis, capacity, and reserve, though it would be underestimated by the same degree in each group so it would likely not impact the overall trend. Despite showing an e-cigarette device-dependent impact on neutrophil glycolysis, this data was limited by the lack of functional tests examining glycolysis pathway inhibitors to pinpoint the stages of the glycolytic pathway that are affected by e-cigarette vapour.

Previously, dysregulated calcium signalling was suggested as a mechanism by which e-cigarette vapour could induce a negative effect on neutrophils. We were unable to replicate these experiments due to technical limitations. The plate reader used could not meet the exact wavelengths suggested by the assay protocol, which may have

impacted the sensitivity of the readings, however, the wavelengths used were still within range. Also, the calcium signalling was likely to be a very fast response, as shown by adding nicotine to the wells part way through the assay readout. Therefore, the other e-cigarette treatments may have shown a stronger calcium release signal, but we did not have access to methods of measuring real time calcium, so this protocol could be missing the calcium influx signal entirely. Attaching a microscope to a vapour chamber and monitoring cytosolic calcium levels over time, such as that in the Rasmussen study would be a possiblility to recifty this in the future (Rasmussen et al., 2014). A plate reader system with injection ports and a band pass filter would allow this to be assayed in real time. Also, a control for cell numbers or dye loading could add robustness to these results.

Finally, use of wide-spanning pre-treatment agents including NAC (antioxidant and anti-aldehyde) and Benzethonium chloride (α7, α4 or β2 nAChR subunit inhibitor) do not allow for the differentiation of which action is having the main effect. Confirmatory western blots could have been performed to show inhibition of Pi3K and downstream nicotine receptor signalling molecules, but this was not possible due to time limitations. As preliminary data, there appeared to be an improvement of function with these agents, however further work is needed to uncover the specific function of the treatment that is actioning the restorative effects.

5.5.7 Conclusion

This investigation into the mechanism of e-cigarette-related neutrophil dysfunction provided preliminary data to highlight potential avenues for further investigation.

Further data is necessary to build on altered neutrophil function, potential deleterious effects, and ascribe a mechanism through careful enquiry. From this work, treatment with NAC appeared to have the greatest restoration of neutrophil dysfunction, indicating neutrophil dysfunction is a largely RCS/ROS driven mechanism and providing initial data for a potential protective compound against e-cigarette related harm.

Chapter 6 -

GENERAL

DISCUSSION

6.1 Overall findings

This thesis aimed to investigate the impact of e-cigarette vapour on neutrophil function and gather some preliminary data on mechanisms of harm. It was important to first validate the application of previously utilised experimental techniques to the context of e-cigarette vapour exposure, to ensure results were reproducible and addressed the aims of this project. The data presented in Chapter 3 detailed how this validation was performed and how the results support the application of these techniques to the current project. In addition, details of the establishment and validation of a novel, inexpensive, adaptable model of direct e-cigarette vapour exposure provide the ability for laboratories to trial e-cigarette vapour exposure without investing in expensive vaping equipment. The optimised protocols were applied to neutrophils treated with e-cigarette vapour in the newly established model to assess the effects of e-cigarette vapour exposure on important neutrophil functions. Data collection revealed that direct e-cigarette vapour exposure impairs neutrophil effector functions including migration, phagocytosis and oxidative burst. In chapter 5, preliminary data which investigated the contribution of transcriptional changes, Pi3K signalling, nicotine receptor inhibitors, glycolysis and antioxidants to e-cigarette-induced neutrophil dysfunction was collected to uncover information on the driving mechanisms of dysfunction. The data collected did not show transcriptomic changes in neutrophils exposed to e-cigarette vapour but did demonstrate reductions in glycolysis, a key source of ATP in neutrophils. In addition, pre-treatment of neutrophils with nicotine receptor inhibitors and antioxidant and anti-aldehyde NAC appeared to show some restoration of transmigration and phagocytic functions. Overall, the work presented here supports the hypothesis that neutrophil function is impaired by e-cigarette vapour exposure, which is exaggerated

by higher device power, but it is not possible to say whether nicotine exacerbated e-cigarette related neutrophil dysfunction.

6.1.1 Neutrophil migration

Neutrophil transmigration plus speed and velocity of chemotaxis to CXCL8 were significantly impaired by exposure to e-cigarette vapour. This has previously been observed in transwell models (Corriden et al., 2020), but for the first time here has been recapitulated in an Insall chamber, uncovering speed and velocity defects which could be driving migrational dysfunction. In the published study by Corriden et al., the number of neutrophils migrating through a transwell was measured by adding a cell lysis compound to the transwell supernatant and performing an ELISA-like colorimetric assay to measure protein content as a representative measure of neutrophil transmigration. Previous work has shown upregulation of neutrophil granule proteins in the BALF of e-cigarette users, and in neutrophils exposed to e-cigarette vapour extract (Higham et al., 2016, Reidel et al., 2018, Ghosh et al., 2019). Therefore, measuring protein content as a readout of transmigration could be skewed by e-cigarette vapour extract-induced degranulation before neutrophils were even added to the transwell system. In the present study, transwell migration was assessed by counting the number of neutrophils in the supernatant, a more accurate measure of transmigration which is not affected by neutrophil degranulation or other functional defects. Here, transwell migration appeared to be improved by NAC treatment prior to e-cigarette vapour exposure, representing a potential method of protecting against the harmful effects of e-cigarette vapour. The model employed by this study simulates the local effects of e-cigarette vapour exposure on neutrophils in the airspaces. In this

context, neutrophil transmigration may not have been the most critical function to investigate as theoretically neutrophils would have already migrated into the airspaces. Despite this limitation, neutrophils are capable of migrating out of tissues, back into the vasculature, in a process called reverse transmigration (Hirano et al., 2016). Therefore, after exposure to e-cigarette vapour in the airspaces, the inability to accurately migrate out of the lung has the potential to cause excessive tissue damage.

6.1.2 Neutrophil phagocytosis

Similarly, phagocytosis of *E. coli* and *S. aureus* was significantly impaired by exposure to e-cigarette vapour at both time points measured. This work supports previous findings of impaired neutrophil phagocytosis of opsonised pHrodo™ *S. aureus* bioparticles after e-liquid treatment (Clapp et al., 2017) as well as impaired phagocytosis of fluorescently labelled *S. aureus* and *E. coli* bacteria (Corriden et al., 2020) after e-cigarette vapour extract treatment. Despite different models of e-cigarette exposure and different bacterial targets, both studies demonstrated reduced phagocytic ability of neutrophils after e-cigarette exposure.

In addition, previous studies have found impaired phagocytosis by human alveolar macrophages caused by e-cigarette exposure. Studies have reported increases in MRSA population size, reduction in *E. coli* and *S. aureus* phagocytosis by e-cigarette vapour extract and condensate respectively (Hwang et al., 2016, Scott et al., 2018, Clapp et al., 2017). Furthermore, phagocytosis of *M. Tuberculosis* was shown to be reduced by macrophage-like THP-1 cells after e-cigarette vapour extract treatment (Gómez et al., 2020). This indicates an impairment of innate immune cells to clear

bacteria from the lung after being exposed to e-cigarette vapour, potentially leading to increased frequency and severity of respiratory infections. This hypothesis is supported murine model findings that e-cigarette exposed mice exhibit increased bacterial loads and an inability to clear *pseudomonas* and *S. pneumoniae* compared to air-treated mice (Corriden et al., 2020, Sussan et al., 2015). The effect of increased bacterial burdens is exacerbated by evidence of increased virulence of bacterial strains after e-cigarette vapour exposure, including MRSA, similar to that seen in cigarette smoke (Gilpin et al., 2019, Hwang et al., 2016, McEachern et al., 2015).

However, there is a lack of evidence of observed increases in frequency or severity of respiratory infections in e-cigarette users. Recently, e-cigarette users were described to be more likely to experience COVID-19 related symptoms, and five times more likely to be diagnosed with COVID-19 than non-users, however, hospitalisation rates were not elevated in this group (McFadden et al., 2022, Gaiha et al., 2020). Nonetheless, there is no evidence this is due to e-cigarette-driven neutrophil dysfunction, rather e-cigarette vapour has been shown to upregulate angiotensin-converting enzyme 2 (ACE-2) receptor expression, which the SARS-CoV-2 virus exploits to enter cells (Naidu et al., 2021, Ghosh et al., 2021b, Maggi et al., 2021, Masso-Silva et al., 2021, McAlinden et al., 2021).

E-cigarette vapour delivers a high burden of ROS (2.5×10^{13}-10.3×10^{13} per puff compared to 1×10^{15} per puff of cigarette smoke (Pryor and Stone, 1993)), which cells are directly exposed to in a vapour exposure model, such as that employed in the present study. To examine whether the ROS/RCS burden drives neutrophil

dysfunctions, neutrophils were treated with NAC prior to exposure to e-cigarette vapour. NAC appeared to partially restore neutrophil phagocytosis and transmigration, as had previously been shown in alveolar macrophages (Scott et al., 2018). Phagocytic dysfunction induced locally in the airspaces by e-cigarette vapour may prevent clearance of invading pathogens. However, if this dysfunction can be improved by NAC treatment, there is the potential for less persistent inflammation and consequent tissue damage. Nebulised NAC is used in the management of COPD patients, reducing exacerbation rates and minimising the number of hospitalised days (Sadowska et al., 2006b) as well as in idiopathic pulmonary fibrosis (IPF) patients, slowing progression of the disease (Feng et al., 2019). This indicates NAC is a clinically relevant therapeutic which could be repurposed for lung protection in e-cigarette users if e-cigarette associated damage is proven, and NAC is established as a protectant. However, it should be noted that NAC is not thermally stable (> 60ºC) and so would be broken down by the high temperatures reached by e-cigarettes. Alternatively, thermally stable antioxidants such as epigallocatechin gallate, hydroxytyrosol and gallic acid could be added to e-liquid to substantially reduce the concentrations of formaldehyde and other RCS in e-cigarette vapour.

6.1.3 Neutrophil degranulation

Degranulation was largely unchanged when neutrophils were exposed to e-cigarette vapour in our model. Conversely, previous findings have reported significant increases in neutrophil granule proteins in BALF from e-cigarette users (Reidel et al., 2018, Ghosh et al., 2019). In BALF, increased neutrophil degranulation represents the cumulative effect of activation and subsequent inflammation involving epithelial and

endothelial cells, which is a different measure to isolated neutrophils exposed to e-cigarette vapour. Evidence of elevated degranulation (NE, MMP-2 and MMP-9 secretion) has been demonstrated in response to e-cigarette vapour extract treatment and nicotine treatment alone (Higham et al., 2016). It should be noted that neutrophils treated by e-cigarette vapour extract in the aforementioned study were treated for a total of 6 hours and in the high concentrations of e-cigarette vapour extract found reduced NE and MMP-9 secretion and the authors who found elevated proteases after nicotine exposure did not find the same with PG/VG treatment. Potentially, long-term e-cigarette use or long duration of neutrophil exposure to e-cigarette vapour, such as that with chronic e-cigarette use, induces excessive degranulation, but this isn't recapitulated in short exposures *in vitro*. Alternatively, neutrophil granule subsets have been shown to be differentially sensitive to intracellular Ca^{2+} signalling (Perez et al., 1987) and there is evidence linking e-liquids and nicotine exposure with increases in Ca^{2+} levels in epithelial cells, alveolar macrophages and neutrophils (Ghosh et al., 2019, Rowell et al., 2020). This suggests excessive neutrophil degranulation could be driven by e-cigarette induced Ca^{2+} signalling. These findings were not recapitulated in this study, but this was likely due to methodological limitations resulting in a time lag between e-cigarette exposure and calcium measurement. If the link between e-cigarettes, calcium signalling and neutrophil degranulation is true, a greater effect on tertiary and secondary granules than primary granules would be expected due to the dose response effect of calcium (Hann et al., 2020). However, further work is required to determine the full extent of the role of calcium in e-cigarette-induced cellular dysfunction.

6.1.4 Neutrophil oxidative burst

Oxidative burst response was significantly lower in e-cigarette vapour exposed neutrophils in a device-power dependent manner but independent of nicotine content. Bacterial killing and NET generation by neutrophils rely upon oxidative burst responses, due to the involvement of NADPH oxidase in both processes (Babior, 2004, Papayannopoulos et al., 2010). Here, neutrophils exposed to vapour from 2nd generation e-cigarette devices demonstrated reduced phagocytic ability, but not oxidative burst generation. This suggests there are further drivers of this dysfunction to be uncovered. Previously, e-liquid flavours- particularly cinnamaldehyde and ethyl vanillin- have been shown to diminish oxidative burst responses to the same concentration of PMA, using Seahorse analysers (Hickman et al., 2019). ROS production, which is linked to oxidative burst response, has been shown to be significantly reduced at baseline, but upon PMA-stimulation, oxidative burst was not different to controls in neutrophils treated with e-cigarette vapour extract (Corriden et al., 2020). If this were true, it would be suggestive of a normal oxidative burst response being observed in the seahorse analysers, which has not been demonstrated in either study applying Seahorse models. This could be due to lower PMA concentrations (25 nM) used to measure oxidative burst compared to those used to measure oxidative burst (160 nM). Further work is required to fully elucidate the consequences of e-cigarette vapour exposure on neutrophil oxidative burst.

If neutrophils do exhibit supressed oxidative burst after e-cigarette exposure, this would contrast to previous findings in macrophages. E-cigarette vapour condensate has been shown to induce a 50-fold increase in oxidative burst by alveolar

macrophages, potentially compounding local oxidative stress (Scott et al., 2018, Davis et al., 2022). One explanation for this potential differential response is that in contrast to macrophages, neutrophils appear to exhibit an almost functional exhaustion after e-cigarette exposure whereby key effector functions including phagocytosis, migration, NET generation, and degranulation appear blunted. The mechanism for this remains uncertain, but the inability to perform their normal functions may have consequences for neutrophil oxidative burst. Functional exhaustion has previously been described in sepsis to contribute to multi-organ failure, and studies of murine neutrophils have revealed the involvement of TIR domain-containing adapter molecule 2 (TICAM2) and downstream activation of the interferon regulator factor 3 (IRF3) and signal transducer and activator of transcription 1 (STAT1) pathways in the exhausted neutrophil phenotype (Lin et al., 2020). Further investigations into these pathways would be needed to determine if they are contributors to the e-cigarette-induced neutrophil dysfunction described.

6.1.5 NET formation

PMA-stimulated NET generation appeared to be reduced by e-cigarette vapour exposure. This supports previous findings of no change in spontaneous NET generation caused by e-cigarette vapour extract exposure, but a suppression of PMA-induced NET generation (Corriden et al., 2020). Published data has shown that neutrophils from e-cigarette users are significantly more sensitive to PMA than cigarette smokers and non-smokers (Reidel et al., 2018). This could represent a difference between short-term *in vitro* exposure and long-term *in vivo* exposure of e-cigarette-effects on NET generation, with the potential for systemic alterations

associated with e-cigarette use. If long-term e-cigarette use increases NET sensitivity, this effect would be exacerbated by reported reduced efferocytosis by macrophage-like THP-1 cells, which could lead to reduced clearance of apoptotic neutrophils and NETs, causing persistent inflammation (Ween et al., 2020).

As this thesis models the local effects of e-cigarette vapour exposure on neutrophils which are in the airspaces, application of pre-treatments such as NAC, Pi3K and Benzethonium chloride to the restoration of NET function may have been more applicable than transmigration. However, neutrophils are known to be able to transmigrate back out of the lungs during reverse transmigration, so this remains an applicable function to measure restoration of. Furthermore, the lack of a statistically different NET response by neutrophils exposed to e-cigarette vapour compared to UTC means this function was not proved to be affected here, so restoration would not have been logical. Further information on the dynamics of NET generation induced by e-cigarette use, and the consequences of direct vapour exposure to NET generation in the airspaces is an important focus for future work.

6.1.6 Driving mechanisms

This thesis presents preliminary data investigating the mechanistic drivers of e-cigarette-induced neutrophil dysfunction. Neutrophil transcriptome analysis showed no significant DEGs in any treatment, suggesting these rapid changes in function are not caused by transcriptional alterations in this model. However, it might be that transcriptional changes would have been apparent if neutrophils were exposed for a longer duration or if more replicates were included. This is the first study in which

neutrophil transcriptome has been analysed in the context of e-cigarette vapour exposure. RNAseq analysis on lung tissue from e-cigarette exposed mice revealed downregulation of leukocyte extravasation signalling genes, which could amplify the impairment of neutrophil transmigration demonstrated (Corriden et al., 2020). In human epithelial cells from biopsy samples, a study has suggested that 191 proteins are up or down regulated in vapers compared to non-smokers and 78 of which are common with smokers (Ghosh et al., 2018). Similarly, when analysing nasal epithelial gene expression after live-attenuated influenza virus (LAIV) inoculation, 191 genes were found to be differentially expressed in e-cigarette users compared to non-smoker controls, with 52 in common with smokers (Rebuli et al., 2021). Similar analysis of proteomal or transcriptomal changes in neutrophils have not been published, with only western blot analysis showing neutrophil upregulation of p38 MAPK phosphorylation after e-cigarette vapour extract treatment (Higham et al., 2016). Further proteome and transcriptome analysis of neutrophils after e-cigarette exposure would highlight proteins and genes of interest.

Glycolysis was significantly impaired by 4th generation e-cigarette vapour. Neutrophils rely heavily on glycolysis for their effector functions, meaning the inability to amount a glycolytic response could reduce ATP availability and prevent normal functions. However, work presented in chapter 4 reported neutrophils exposed to 2nd generation e-cigarette vapour are functionally impaired, but in chapter 5 did not exhibit reduced glycolytic responses, suggesting there are further contributors to neutrophil dysfunction after e-cigarette vapour exposure than reduced glycolysis alone. Some neutrophils functions rely more heavily on glycolysis than others. For example,

glycolytic inhibitors interfere with neutrophil phagocytosis, NET generation, and oxidative burst, but migration has been shown to rely more heavily on mitochondrial respiration and purinergic signalling (Kumar and Dikshit, 2019). E-liquid flavourings, particularly cinnamaldehyde and ethyl vanillin have been shown to reduce total glycolysis response, which would amplify the effects demonstrated in chapter 5, where PG/VG alone have been used (Hickman et al., 2019). PG/VG (55:45) (vaped and treated directly) has been shown to inhibit glucose uptake and glycolysis in human epithelial airway cell line and HBEC samples from participants (Woodall et al., 2020). In chapter 5, glycolysis was only significantly impaired in neutrophils exposed to high power 4th generation devices. Therefore, the 3% dilution of PG/VG in the study of glycolysis in HBECs may have been a high dosage, representing more powerful devices. There is a lack of data on PG/VG clearance from the lungs. It has been shown that PG can be excreted in the urine (Cotta et al., 2017), but the proportion which reaches the kidneys after inhalation is unknown. In the neutrophil work presented in chapter 5, there was no effect of e-cigarette vapour exposure on glucose uptake, but a reduction in glycolysis was demonstrated. Further investigation into neutrophil metabolism, including mitochondrial respiration, after e-cigarette exposure would help determine whether there is a link between functional defects and metabolic derailment.

As discussed in section 5.1.3, nicotine acts on nAChRs which are expressed on a variety of cell types. The combination of receptor subunits expressed on the neutrophil membrane has been disputed, in part due to heterogeneity in the population (De Rosa et al., 2005). Nicotine has been shown to have consequences for neutrophil functions, so by blocking nicotinic receptors, the contribution of nicotine to neutrophil dysfunction

was assessed. Pre-treatment of neutrophils with Benzethonium chloride (a nicotine receptor subunit inhibitor) appeared to improve post-e-cigarette exposure migration and phagocytosis, but impairments in these functions in neutrophils exposed to nicotine-free e-cigarette vapour demonstrate other factors are involved. Other studies examining pre-treatment of neutrophils with nicotine receptor inhibitors have not been published to date. Nicotine has been shown to increase neutrophil f-actin formation and intracellular Ca^{2+} levels while significantly impairing neutrophil phagocytosis of opsonised microspheres (Ryder, 1994). Finally, nicotine has been shown to be a NET inducer, via nAChRs in an Akt dependent manner (Hosseinzadeh et al., 2016). This indicates nicotine has an impact on human neutrophils, however, there is a lack of understanding of the mechanisms and reversibility of these effects which needs further attention.

Pi3K is a signalling molecule involved in the formation of pseudopods and has been implicated in neutrophil migration and phagocytosis, as discussed in section 5.1.4. Pi3K inhibition did not appear to improve phagocytosis or transmigration of neutrophils exposed to e-cigarettes, suggesting dysfunction may not have been caused by Pi3K signalling defects, unlike has previously been reported in alveolar macrophages (Scott et al., 2018). Pi3K may still be implicated in neutrophil function after e-cigarette vapour exposure, as this work only focused on 2 subunits: δ and γ, the importance of which is discussed in section 5.1.4. Experiments using pan Pi3K inhibitors would help determine if Pi3K is a key contributor to neutrophil dysfunction after e-cigarette vapour exposure. To date, Pi3K has not been investigated Pi3K in the context of neutrophils challenged with e-cigarettes.

NAC is an antioxidant and anti-aldehyde agent which is a precursor to glutathione, promoting scavenging of free radicals and protecting cells against oxidative stress, as detailed in section 5.1.5. To determine whether neutrophil dysfunction was a consequence of ROS burden, neutrophils were pre-treated with NAC prior to e-cigarette vapour exposure. Of the pre-treatments tested in chapter 5, the antioxidant/anti-aldehyde NAC appeared to provide the greatest indication of a protective effect to neutrophils exposed to e-cigarette vapour. Endothelial cells treated with exogenous H_2O_2 have been shown to exhibit decreased actin polymerisation, which, if this effect translated into human neutrophils would drive reduced phagocytosis and migration (Mittal et al., 2014). In addition, murine models have demonstrated a diminished intrinsic antioxidant system (glutathione/glutathione disulfide) after exposure to e-cigarette vapour for 5 hours a day for 3 days (Lerner et al., 2015). Previous work by our group has shown e-cigarettes induce oxidative burst and pro-inflammatory cytokine release from alveolar macrophages (Scott et al., 2018). This has the potential to activate a self-perpetuating cycle of damage, recruiting neutrophils to the alveolar spaces and causing excessive tissue damage. However, having shown a beneficial effect on alveolar macrophages (Scott et al., 2018) and now an indication of benefit to neutrophils, NAC has the potential to break this self-perpetuating cycle of harm. More work is needed to determine the extent of the potential benefit of NAC before its translation into humans.

6.2 *In vivo* evidence of e-cigarette-induced harm

Documented EVALI cases reveal indications that *in vitro* indicators of e-cigarette induced harm are translating into *in vivo* respiratory ill-health. Despite mounting evidence of innate immune dysfunction, dysregulation in pulmonary homeostasis and increased risk of respiratory infections, there is a scarcity of published case reports detailing presentation of these symptoms in human subjects. The scarcity of reported e-cigarette associated illness may be partly due to lack of recording of e-cigarette use and history in clinical settings. Unlike smoking history, which has a measurable unit of use (pack years), e-cigarette history does not have a standardised formal recording method.

Cohort studies have provided some evidence on the biological changes and clinical symptoms of e-cigarette users. Bronchoscopies revealed the airways of e-cigarettes users appear friable and erythematous compared to healthy individuals under inspection (Ghosh et al., 2018). In a study of 60 otherwise healthy males with no previous smoking history, the 30 participants who were e-cigarette users exhibited significant reductions in lung function parameters including FEV_1, FEV_1/FVC ratio, and FEF rates compared to controls (Meo et al., 2019). This was a cross-sectional study of daily e-cigarette users who had used nicotine-containing e-liquid for at least the past 6 months, however, the lack of longitudinal follow up prevents the understanding of the physiological changes associated with e-cigarette use over time. Data published from the Population Assessment of Tobacco Health (PATH) study revealed e-cigarette users were 40% more likely to develop respiratory conditions such as COPD, asthma, chronic bronchitis or emphysema compared to controls (Xie et al., 2020). The PATH

study is an annual survey used to collect data on tobacco product users in the US, meaning this is limited its self-reported nature. The studies mentioned indicate e-cigarette use may not be without its effects on respiratory health, however, there remains a lack of longitudinal data examining effects of e-cigarette use on lung health over time, nor is there evidence of development of symptoms such as recurrent respiratory infections translated from *in vitro* effects on immune cells.

Despite paucity of human data, murine *in vivo* data reveals the potential impact of e-cigarette use on respiratory health by observing development of disease-associated respiratory symptoms. The disease aetiology of EVALI has been recapitulated in murine models of the disease, caused by exposure to vitamin E acetate and PG-VG (Matsumoto et al., 2020, Bhat et al., 2020). Mice exposed to e-cigarette vapour for 60 min/day for 1 month exhibited physiological changes associated with COPD in humans, including airspace enlargement, airway hypersensitivity and elevated pro-inflammatory cytokines (Garcia-Arcos et al., 2016). In a study by Lerner et al., mice were exposed to e-cigarette vapour for 5 hours/day over 3 days and evidence of lung inflammation including elevated immune cells and proinflammatory mediators was documented (Lerner et al., 2015). Mice exposed to e-cigarette vapour for 1.5 hours, twice per day for 2 weeks exhibited significantly increased pulmonary bacterial and viral burdens independent of neutrophil and alveolar macrophage numbers (Sussan et al., 2015). Similarly, mice exposed to e-cigarette vapour for 60 minutes per day, 5 days per week for 4 weeks exhibited higher *pseudomonas* burden than control mice (Corriden et al., 2020). These studies signal a decline in respiratory health in murine

models after a range of exposure durations, supporting the potential for e-cigarette associated disease development in humans.

6.3 What does this study contribute to the field?

The work presented in this thesis details the utilisation of an inexpensive and effective e-cigarette vapour exposure system which can be adapted to any cell type and any device. This is the first study of neutrophil function after e-cigarette exposure to investigate all key neutrophil effector functions and to follow with transcriptomic and metabolic investigations as well as inhibitor and antioxidant treatments to attempt restoration of function. Here, preliminary data showed that the anti-aldehyde NAC appears to provide the greatest restoration of migratory and phagocytic function out of the compounds tested, providing evidence that RCS is driving neutrophil impairment and hope that neutrophil dysfunction can eventually be perturbed. Nicotine receptor subunit inhibition appeared to provide some benefit while Pi3K inhibition did not appear to improve neutrophil migration or phagocytosis. The data presented in this thesis goes beyond previous work, as it directly compares the functional implications of 2nd generation and 4th generation devices as well as nicotine-containing and nicotine-free e-cigarette vapour to delineate the consequences on neutrophil function. 4th generation e-cigarettes were consistently harsher than 2nd generation e-cigarette devices, and inhibited neutrophil functions to a greater extent.

6.4 Clinical implications

Neutrophil dysfunction has been reported in a range of respiratory diseases including COPD, pneumonia, and cystic fibrosis. Table 6.1 details how neutrophils function in

these disease contexts, as well as the effects of e-cigarettes and smoking on the same effector functions. There are common neutrophil dysfunctions across a range of these diseases or behaviours, including increased neutrophilia and degranulation and reduced migration and phagocytosis. E-cigarette induced neutrophil dysfunction has common features with all respiratory-related diseases mentioned in Table 6.1, and are thought to be contributors to these pathophysiologies. For example, impaired neutrophil phagocytosis, seen in Bronchiectasis, asthma, sepsis, and pneumonia as well as e-cigarette and cigarette use, is thought to increase the frequency and severity of respiratory infections and drive increased tissue damage and inflammation in these diseases. Furthermore, reduced neutrophil migration, such as is seen in smoking and vaping as well as COPD, bronchiectasis, asthma, and sepsis is thought to increase obligate tissue damage due to excessive breakdown of the extracellular matrix and a proteinase-antiproteinase imbalance. Neutrophil dysfunction reported to be induced by e-cigarette use has the most common features with those from COPD patients and smokers. Smoking is the leading cause of COPD, and neutrophils are thought to be central contributor to the pathogenesis of COPD, which may explain this link. However, sharing common features of dysfunction with smoking and COPD could be an indicator of the long-term effects of e-cigarette use. In COPD, neutrophil dysfunction is thought to be a key driver of tissue damage, persistent inflammation, and progressive loss of lung function. If e-cigarette vapour does induce neutrophils to behave in the same way as those in COPD, some e-cigarette users may develop COPD-like symptoms. Approximately 30-40% of smokers develop COPD, indicating there are genetic factors which protect some individuals against the development of COPD, but the disease develops 25+ years after initiation of smoking (Lokke et al., 2006). Therefore, if there

is a link between e-cigarettes and COPD, it would be decades before such a link would be established in cohort studies. If e-cigarettes drive COPD development, COPD will remain the leading cause of morbidity and mortality, and its global burden will continue to increase. This highlights the importance of *in vitro* work to model cell behaviours after e-cigarette vapour exposure, detecting early indicators of potential harm and accelerating understanding of the consequences of e-cigarette use.

	Neutrophilia	Migration	Phagocytosis	NETosis	Degranulation / cytokine release	Apoptosis	ROS / oxidative burst
E-cigarettes	↔	↓	↓	↑	↑	↔	↓
COPD	↑	↓	↔	↑	↑	↔	↓
AATD	↑	↔	↔	↔	↑	↑	↑
Bronchiectasis	↑	↓	↓	↑	↑	↑	↓
Asthma	↑	↓	↔	↑	↑	↓	↑
Cystic fibrosis	↔	↔	↓	↑	↓	↓	↓
Sepsis	↑	↓	↓	↓	↑	↓	↑
Pneumonia	↑	↓	↓	↓	↑	↑	↑
Smoking	↑	↓	↓	↓	↑	↓	↓

Table 6.1: Details of current understandings of neutrophil functions in a range of diseases as well as the effect of smoking and e-cigarettes on the same functions.
Key neutrophil effector functions, along with the effect the disease/behaviour has on them is detailed. E-cigarettes have the most dysfunctional features in common with neutrophils from smokers, and from COPD patients. It is also evident that there are shared dysfunctions of neutrophils across a whole range of disease types which may contribute to their pathogenesis. It should be noted that this is a generalisation of existing data, and that there are some contradictory findings in the literature, but an overview or the consensus has been presented here. In addition, reported effects of e-cigarettes on neutrophil functions do not just represent the findings of this thesis but also of the e-cigarette research field. ↑ = there is a reported increase in that function compared to controls, ↔ = there is reportedly no change in the function compared to controls, or it is unknown, ↓ = there is a reduction in that function compared to controls. Information collated from: (Alves-Filho et al., 2010, Kovach and Standiford, 2012, Gotts et al., 2019, Jasper et al., 2019, Domon and Terao, 2021, Jasper et al., 2021) and other primary research papers.

6.5 Study strengths

Working with *ex vivo* human neutrophils requires delicate, efficient, and precise technique to avoid activation. The application of dextran sedimentation followed by percoll separation employed in the current study has been shown to minimise disruption to neutrophils, and allows the isolation of granulocytes without needing red blood cell lysis chemicals (Vuorte et al., 2001). In addition, many previous studies have isolated neutrophils using this technique, allowing the direct comparison of neutrophil functions in this study to cohort studies published using the same protocols. This technique was practiced extensively until high purity, yields and viability were achieved consistently before any functional test protocols were added to the workflow.

This is the first study to employ the use of a modified hypoxia chamber to create a system where cells can be exposed directly to e-cigarette vapour. This is an inexpensive model which can be employed by any researchers who have access to a vacuum pump and can be applied to any cell type or ENDS device. The model used here employed a modified hypoxia chamber which had a volume of 5.5 L, equivalent to the average lung capacity of a healthy adult. In the chamber, e-cigarette vapour is evenly distributed and not compressed compared to that experienced under physiological conditions.

This study directly compares the impact of e-cigarette device power on neutrophil functions. In addition, the application of nicotine-free vapour (50/50 PG/VG only) has unveiled the fundamental impacts of vapourised PG/VG on neutrophil functions before the addition of any flavourings or nicotine.

In addition, existing literature on the functional implications of e-cigarettes on neutrophils have not covered all key neutrophil effector functions and have not unpicked the underlying mechanism(s) of harm caused. This study presented preliminary data on the effects of e-cigarettes on calcium signalling, transcriptome, glycolysis and applied inhibitors and antioxidants to the restoration of function.

6.6 Study limitations

Firstly, *in vivo*, neutrophils which have been recruited into the lung will be primed before being directly exposed to e-cigarette vapour in the alveolar space. In the vapour exposure model employed here, priming agents (e.g. TNF-α, G-CSF or LPS) could have been used to treat peripheral blood neutrophils prior to direct vapour exposure in the chamber to fully mimic the *in vivo* process. However, all e-cigarette vapour exposure systems have limitations on their physiological relevance, and no study on *in vitro/ex vivo* neutrophils can exactly mimic *in vivo* conditions.

With regards to the setup of the vapour chamber, it was not possible to measure and monitor either vacuum air flow or vapour temperature due to limitations in the apparatus. The information gathered from being able to measure vacuum air flow and vapour temperature would have provided valuable data for validation of this model. However, as far as was possible, these factors were controlled for by constant application of minimum suction required for operation and maintaining constant e-cigarette devices temperature settings. Careful maintenance of e-cigarettes was taken including not overusing atomisers and regularly deep cleaning the devices. Mechanical

vaping machines are available which provide lower puff-to-puff variability than this model requiring human operation however, this level of consistency may not be required when trying to replicate a human vaping and the inherent variability in that experience.

Due to the time-sensitive nature of neutrophil studies, a maximum of two e-cigarette vapour exposures could be performed at a time, to avoid excessive lag time which could affect their viability, and consequently functions if more conditions were assayed at once. If multiple exposures could have been done at the same time, this limitation could have been avoided. This did, however mean that some data represents different individuals between treatment groups, however each repeat included a biological UTC control for every functional test. With regards to limitations of functional tests, some do not represent the physiological conditions in which neutrophils would be experiencing *in vivo*. For example, pHrodo™ bioparticles may have more closely represented a physiological environment if opsonised with human serum or neutrophils would physiologically be exposed to e-cigarette vapour after transmigrating into the airway, which may have affected this finding. However, published work has applied the use of unopsonised (Corriden et al., 2020) and opsonised (Clapp et al., 2017) bioparticles to this context, and both show a similar pattern of reduction in phagocytosis.

The biggest limitation of these data is the fully *in vitro* nature of the study. Due to disruption by the COVID-19 pandemic, greater power and depth to this study were not possible. However, this work adds to a growing body of evidence of the effects of e-cigarette vapour on human neutrophils. Despite providing insight into signals of harm,

a large, longitudinal cohort study will be needed to fully define the effects of e-cigarette vapour on human neutrophils.

6.7 Future directions

The work detailed here provided preliminary evidence for mechanisms of e-cigarette induced neutrophil dysfunction, but further work is needed to determine the full extent of the effects of e-cigarettes on human neutrophils, whether there are deleterious physiological effects and ascribe a mechanism of action. This study models the local effect of e-cigarette vapour exposure on neutrophils, translating to the effect of this exposure to neutrophils in the airspaces. The dysfunctions detailed here outline how e-cigarettes could have consequences for respiratory health. However, there is the opportunity for further work to understand whether neutrophil-related changes represent long term, short term, widespread or local effects.

Future work should investigate extensively the expression of nicotine receptors on human neutrophils by performing next generation sequencing, confirming by qPCR and assessing expressed protein by flow cytometry and western blots. This would require a large sample size as published material indicates significant inter-person variation (Benhammou et al., 2000, De Rosa et al., 2005). To confirm transcriptomic changes aren't caused by e-cigarette exposure in neutrophils, more replicate samples should be trialled, to confirm non-significance was caused by under-powering. In addition, longer durations of exposure which would capture the later upregulation of gene expression should be trialled, however, this would not represent the driver of dysfunction in the short period studied here. Extending on this work, analysis of the

neutrophil proteome would help identify key molecular targets and help to understand the response to e-cigarette vapour exposure of neutrophils.

To expand on neutrophil metabolism and oxidative burst tests, the presence of NADPH oxidase and glycolytic enzymes should be assessed by PCR and at the protein level by western blot. Then, applying metabolic inhibitors to functional tests after e-cigarette vapour exposure would help to determine the contribution of metabolic dysfunction to neutrophil behaviours. Further *in vitro* studies are needed to expand on the potential benefits seen in this study using nicotine receptor blockade and NAC. Data presented here suggested constitutive Pi3Kδ and γ activation did not appear to be a driving mechanism of dysfunction in e-cigarette vapour exposed neutrophils, but signalling molecules in different pathways could be driving dysfunction. Other signalling molecules that have been implicated in neutrophil function in response to e-cigarette vapour include p38 MAPK, which should be further investigated. Together, these experiments would help unravel the mechanism of action on the effector functions delineated in this study and other *in vitro* reports.

Previously, cohort studies assessing neutrophils at one time point has compared BALF uncovering elevated NE, MMP-2 and MMP-9 in smokers and vapers BALF and induced sputum compared to non-smoker (Ghosh et al., 2019, Reidel et al., 2018). This work was suggestive of long-term harm from e-cigarettes, however the full impact of e-cigarettes on neutrophils and further on human lung health remains unknown. It is necessary to take this study further, carrying out a large longitudinal cohort study comparing BALF, lung function and immune cell function between never smokers,

vapers who didn't previously smoke, ex-smokers who now vape and current smokers at multiple time points over the duration of the study. By monitoring the same patients over years, the extent at which e-cigarette use affects health status, respiratory symptoms, lung function, immune cell function in both BALF and blood samples over time can be determined and compared to cigarette smoking. Robust execution of a study of this kind, by controlling for inter-person variability in device, e-liquid and pattern of use, would be invaluable to the future of e-cigarette research.

Finally, it is most important that these longitudinal studies are applied to cohorts of at-risk populations (e.g. COPD patients) to determine whether previous development of respiratory diseases leads to an exaggerated or blunted inflammatory response to e-cigarettes compared to healthy individuals. Together, this data will help inform the UK Health Security Agency and MHRA on whether e-cigarettes truly are 95% safer than tobacco cigarettes and how prescribed e-cigarettes can be implemented.

6.8 Conclusions

In conclusion, an inexpensive, adaptable e-cigarette vapour exposure model has been developed, validated, and applied to the exposure of human peripheral blood neutrophils. Considerations for optimisation and validation of existing protocols in the context of a new research question has been detailed and executed for the application to e-cigarette exposure. After exposure to e-cigarette vapour with and without nicotine, key neutrophil effector functions including chemotaxis, transmigration, phagocytosis, oxidative burst and NET generation appear suppressed. No effector functions measured demonstrated an increase from controls after exposure to e-cigarette

vapour. Nicotine was not the key driver of these functional defects, as shown by functional implications caused by nicotine-free vapour. However, nicotine receptor inhibition did provide a protective effect on neutrophil migration and phagocytosis. All effector functions tested were more significantly impaired by exposure to high-power 4th generation e-cigarette vapour, compared to vapour from 2nd generation devices. The ability of neutrophils to upregulate glycolysis was greatly impaired by exposure to e-cigarette vapour, representing a limited ability to respond to environmental stimuli. Preliminary data suggested neutrophil migration and phagocytosis appeared to be partially restored by NAC treatment, indicating neutrophil dysfunction is a largely ROS and RCS-driven effect. Taken together, this data supports the hypothesis that neutrophil function is impaired by e-cigarette vapour and this effect is exaggerated by higher power e-cigarette device power. Work presented in this thesis supports previous findings of neutrophil dysfunction after e-cigarette vapour exposure which could have persistent consequences for lung health, and raises the concern over the long-term safety of e-cigarette use.

Chapter 7 -

REFERENCES

Euromonitor International. Smokeless tobacco and vapour products. [Online]. Available: https://www.euromonitor.com/smokeless-tobacco-and-vapour-products [Accessed].
(ASH), A. o. S. a. H. 2021. Use of e-cigarettes (vapes) among adults in Great Britain.
(NCCDPHP), N. C. f. C. D. P. a. H. P. U. 2014. *The Health Consequences of Smoking—50 Years of Progress: A Report of the Surgeon General.,* Atlanta (GA): Centers for Disease Control and Prevention (US).
Alberts, B. J., A; Lewis, J 2002. *Molecular Biology of the Cell. 4th edition.,* New York, Garland Science.
Allard, B., Panariti, A. & Martin, J. G. 2018. Alveolar Macrophages in the Resolution of Inflammation, Tissue Repair, and Tolerance to Infection. *Front Immunol,* 9**,** 1777.
Alves-Filho, J. C., Spiller, F. & Cunha, F. Q. 2010. NEUTROPHIL PARALYSIS IN SEPSIS. *Shock,* 34.
Amin, K., Ekberg-Jansson, A., Löfdahl, C. G. & Venge, P. 2003. Relationship between inflammatory cells and structural changes in the lungs of asymptomatic and never smokers: a biopsy study. *Thorax,* 58**,** 135-42.
Amulic, B., Cazalet, C., Hayes, G. L., Metzler, K. D. & Zychlinsky, A. 2012. Neutrophil function: from mechanisms to disease. *Annu Rev Immunol,* 30**,** 459-89.
Andelid, K., Bake, B., Rak, S., Lindén, A., Rosengren, A. & Ekberg-Jansson, A. 2007. Myeloperoxidase as a marker of increasing systemic inflammation in smokers without severe airway symptoms. *Respiratory Medicine,* 101**,** 888-895.
Anderson, C., Majeste, A., Hanus, J. & Wang, S. 2016. E-Cigarette Aerosol Exposure Induces Reactive Oxygen Species, DNA Damage, and Cell Death in Vascular Endothelial Cells. *Toxicol Sci,* 154**,** 332-340.
Antigny, F., Jousset, H., König, S. & Frieden, M. 2011. Thapsigargin activates Ca^{2+} entry both by store-dependent, STIM1/Orai1-mediated, and store-independent, TRPC3/PLC/PKC-mediated pathways in human endothelial cells. *Cell Calcium,* 49**,** 115-27.
Armstrong, L. W., Rom, W. N., Martiniuk, F. T., Hart, D., Jagirdar, J. & Galdston, M. 1996. Nicotine enhances expression of the neutrophil elastase gene and protein in a human myeloblast/promyelocyte cell line. *Am J Respir Crit Care Med,* 154**,** 1520-4.
Awasthi, D., Nagarkoti, S., Sadaf, S., Chandra, T., Kumar, S. & Dikshit, M. 2019. Glycolysis dependent lactate formation in neutrophils: A metabolic link between NOX-dependent and independent NETosis. *Biochimica et Biophysica Acta (BBA) - Molecular Basis of Disease,* 1865**,** 165542.
Babior, B. M. 2004. NADPH oxidase. *Current Opinion in Immunology,* 16**,** 42-47.
Bahl, V., Lin, S., Xu, N., Davis, B., Wang, Y. H. & Talbot, P. 2012. Comparison of electronic cigarette refill fluid cytotoxicity using embryonic and adult models. *Reprod Toxicol,* 34**,** 529-37.
Bannenberg, G. & Serhan, C. N. 2010. Specialized pro-resolving lipid mediators in the inflammatory response: An update. *Biochim Biophys Acta,* 1801**,** 1260-73.
Bao, Y., Ledderose, C., Graf, A. F., Brix, B., Birsak, T., Lee, A., Zhang, J. & Junger, W. G. 2015. mTOR and differential activation of mitochondria orchestrate neutrophil chemotaxis. *J Cell Biol,* 210**,** 1153-64.

Bedi, P., Davidson, D. J., McHugh, B. J., Rossi, A. G. & Hill, A. T. 2018. Blood Neutrophils Are Reprogrammed in Bronchiectasis. *Am J Respir Crit Care Med,* 198**,** 880-890.

Behar, R. Z., Davis, B., Wang, Y., Bahl, V., Lin, S. & Talbot, P. 2014. Identification of toxicants in cinnamon-flavored electronic cigarette refill fluids. *Toxicol In Vitro,* 28**,** 198-208.

Behar, R. Z., Hua, M. & Talbot, P. 2015. Puffing topography and nicotine intake of electronic cigarette users. *PLoS One,* 10**,** e0117222.

Belchamber, K. B. R., Singh, R., Batista, C. M., Whyte, M. K., Dockrell, D. H., Kilty, I., Robinson, M. J., Wedzicha, J. A., Barnes, P. J. & Donnelly, L. E. 2019. Defective bacterial phagocytosis is associated with dysfunctional mitochondria in COPD macrophages. *European Respiratory Journal,* 54**,** 1802244.

Belchamber, K. B. R., Walker, E. M., Stockley, R. A. & Sapey, E. 2020. Monocytes and Macrophages in Alpha-1 Antitrypsin Deficiency. *Int J Chron Obstruct Pulmon Dis,* 15**,** 3183-3192.

Benhammou, K., Lee, M., Strook, M., Sullivan, B., Logel, J., Raschen, K., Gotti, C. & Leonard, S. 2000. [3H]Nicotine binding in peripheral blood cells of smokers is correlated with the number of cigarettes smoked per day. *Neuropharmacology,* 39**,** 2818-2829.

Bhat, T. A., Kalathil, S. G., Bogner, P. N., Blount, B. C., Goniewicz, M. L. & Thanavala, Y. M. 2020. An Animal Model of Inhaled Vitamin E Acetate and EVALI-like Lung Injury. *New England Journal of Medicine,* 382**,** 1175-1177.

Bianchi, M., Hakkim, A., Brinkmann, V., Siler, U., Seger, R. A., Zychlinsky, A. & Reichenbach, J. 2009. Restoration of NET formation by gene therapy in CGD controls aspergillosis. *Blood,* 114**,** 2619-22.

Blagev, D. P., Harris, D., Dunn, A. C., Guidry, D. W., Grissom, C. K. & Lanspa, M. J. 2019. Clinical presentation, treatment, and short-term outcomes of lung injury associated with e-cigarettes or vaping: a prospective observational cohort study. *Lancet,* 394**,** 2073-2083.

Blount, B. C., Karwowski, M. P., Shields, P. G., Morel-Espinosa, M., Valentin-Blasini, L., Gardner, M., Braselton, M., Brosius, C. R., Caron, K. T., Chambers, D., Corstvet, J., Cowan, E., De Jesús, V. R., Espinosa, P., Fernandez, C., Holder, C., Kuklenyik, Z., Kusovschi, J. D., Newman, C., Reis, G. B., Rees, J., Reese, C., Silva, L., Seyler, T., Song, M.-A., Sosnoff, C., Spitzer, C. R., Tevis, D., Wang, L., Watson, C., Wewers, M. D., Xia, B., Heitkemper, D. T., Ghinai, I., Layden, J., Briss, P., King, B. A., Delaney, L. J., Jones, C. M., Baldwin, G. T., Patel, A., Meaney-Delman, D., Rose, D., Krishnasamy, V., Barr, J. R., Thomas, J. & Pirkle, J. L. 2019. Vitamin E Acetate in Bronchoalveolar-Lavage Fluid Associated with EVALI. *New England Journal of Medicine,* 382**,** 697-705.

Borregaard, N. 2010. Neutrophils, from marrow to microbes. *Immunity,* 33**,** 657-70.

Borregaard, N. & Herlin, T. 1982. Energy metabolism of human neutrophils during phagocytosis. *The Journal of clinical investigation,* 70**,** 550-557.

Borregaard, N., Kjeldsen, L., Lollike, K. & Sengelov, H. 1993. Granules and vesicles of human neutrophils. The role of endomembranes as source of plasma membrane proteins. *Eur J Haematol,* 51**,** 318-22.

Boxer, L. A., Oliver, J. M., Spielberg, S. P., Allen, J. M. & Schulman, J. D. 1979. Protection of granulocytes by vitamin E in glutathione synthetase deficiency. *N Engl J Med,* 301**,** 901-5.

Branzk, N., Lubojemska, A., Hardison, S. E., Wang, Q., Gutierrez, M. G., Brown, G. D. & Papayannopoulos, V. 2014. Neutrophils sense microbe size and selectively release neutrophil extracellular traps in response to large pathogens. *Nature Immunology,* 15**,** 1017-1025.

Brinkmann, V., Reichard, U., Goosmann, C., Fauler, B., Uhlemann, Y., Weiss, D. S., Weinrauch, Y. & Zychlinsky, A. 2004. Neutrophil extracellular traps kill bacteria. *Science,* 303**,** 1532-5.

Brody, J. S. 2012. Transcriptome alterations induced by cigarette smoke. *Int J Cancer,* 131**,** 2754-62.

Burnett, D., Chamba, A., Hill, S. L. & Stockley, R. A. 1987. Neutrophils from subjects with chronic obstructive lung disease show enhanced chemotaxis and extracellular proteolysis. *Lancet,* 2**,** 1043-6.

Butcher, S., Chahel, H. & Lord, J. M. 2000. Review article: ageing and the neutrophil: no appetite for killing? *Immunology,* 100**,** 411-6.

Carlisle, D. L., Hopkins, T. M., Gaither-Davis, A., Silhanek, M. J., Luketich, J. D., Christie, N. A. & Siegfried, J. M. 2004. Nicotine signals through muscle-type and neuronal nicotinic acetylcholine receptors in both human bronchial epithelial cells and airway fibroblasts. *Respir Res,* 5**,** 27.

Carson, J. L., Zhou, L., Brighton, L., Mills, K. H., Zhou, H., Jaspers, I. & Hazucha, M. 2017. Temporal structure/function variation in cultured differentiated human nasal epithelium associated with acute single exposure to tobacco smoke or E-cigarette vapor. *Inhal Toxicol,* 29**,** 137-144.

Carter, R. I., Mumford, R. A., Treonze, K. M., Finke, P. E., Davies, P., Si, Q., Humes, J. L., Dirksen, A., Piitulainen, E., Ahmad, A. & Stockley, R. A. 2011. The fibrinogen cleavage product Aα-Val360, a specific marker of neutrophil elastase activity in vivo. *Thorax,* 66**,** 686-91.

Carter, T., Tucker, D., Kilic, A., Papadimos, T. J., Barlow, A. & Berry, E. 2017. Life-threatening Vesicular Bronchial Injury Requiring Veno-venous Extracorporeal Membrane Oxygenation Rescue in an Electronic Nicotine Delivery System User. *Clin Pract Cases Emerg Med,* 1**,** 212-217.

CDC. 2020. *Outbreak of Lung Injury Associated with E-cigarette use, or Vaping* [Online]. Centers for Disease Control and Prevention. Available: https://www.cdc.gov/tobacco/basic_information/e-cigarettes/severe-lung-disease.html [Accessed 1st July 2020].

Centers for Disease Control and Prevention 2010. *How Tobacco Smoke Causes Disease: The Biology and Behavioral Basis for Smoking-Attributable Disease: A Report of the Surgeon General,* Atlanta (GA), Centers for Disease Control and Prevention (US); National Center for Chronic Disease Prevention and Health Promotion (US); Office on Smoking and Health (US).

Charest, P. G. & Firtel, R. A. 2007. Big roles for small GTPases in the control of directed cell movement. *Biochem J,* 401**,** 377-90.

Chen, Y. & Junger, W. G. 2012. Measurement of oxidative burst in neutrophils. *Methods in molecular biology (Clifton, N.J.),* 844**,** 115-124.

Christopher, M. J., Liu, F., Hilton, M. J., Long, F. & Link, D. C. 2009. Suppression of CXCL12 production by bone marrow osteoblasts is a common and critical pathway for cytokine-induced mobilization. *Blood,* 114**,** 1331-9.

Churg, A., Cosio, M. & Wright, J. L. 2008. Mechanisms of cigarette smoke-induced COPD: insights from animal models. *American Journal of Physiology-Lung Cellular and Molecular Physiology,* 294**,** L612-L631.

Clapp, P. W., Pawlak, E. A., Lackey, J. T., Keating, J. E., Reeber, S. L., Glish, G. L. & Jaspers, I. 2017. Flavored e-cigarette liquids and cinnamaldehyde impair respiratory innate immune cell function. *Am J Physiol Lung Cell Mol Physiol,* 313**,** L278-L292.

Clunes, L. A., Bridges, A., Alexis, N. & Tarran, R. 2008. In vivo versus in vitro airway surface liquid nicotine levels following cigarette smoke exposure. *Journal of analytical toxicology,* 32**,** 201-207.

Coates, K. M. & Flood, P. 2001. Ketamine and its preservative, benzethonium chloride, both inhibit human recombinant alpha7 and alpha4beta2 neuronal nicotinic acetylcholine receptors in Xenopus oocytes. *Br J Pharmacol,* 134**,** 871-9.

Condliffe, A. M., Kitchen, E. & Chilvers, E. R. 1998. Neutrophil priming: pathophysiological consequences and underlying mechanisms. *Clin Sci (Lond),* 94**,** 461-71.

Corriden, R., Moshensky, A., Bojanowski, C. M., Meier, A., Chien, J., Nelson, R. K. & Crotty Alexander, L. E. 2020. E-cigarette use increases susceptibility to bacterial infection by impairment of human neutrophil chemotaxis, phagocytosis, and NET formation. *Am J Physiol Cell Physiol,* 318**,** C205-c214.

Cotta, K., Stephen, C. & Mohammad, N. 2017. A Review on the Safety of Inhalation of Propylene Glycol in E-cigarettes. *Glob J Pharmaceu Sci 2 (2),* 555584.

Counts, M. E., Morton, M. J., Laffoon, S. W., Cox, R. H. & Lipowicz, P. J. 2005. Smoke composition and predicting relationships for international commercial cigarettes smoked with three machine-smoking conditions. *Regul Toxicol Pharmacol,* 41**,** 185-227.

Crisford, H., Newby, P. R., Sapey, E. & Stockley, R. A. 2018. S15 Proteinase 3 activity in PiSZ alpha-1 antitrypsin deficiency and non-deficient chronic obstructive pulmonary disease. *Thorax,* 73**,** A10.

Crisford, H., Sapey, E., Rogers, G. B., Taylor, S., Nagakumar, P., Lokwani, R. & Simpson, J. L. 2021. Neutrophils in asthma: the good, the bad and the bacteria. *Thorax,* 76**,** 835-44.

Dancey, J. T., Deubelbeiss, K. A., Harker, L. A. & Finch, C. A. 1976. Neutrophil kinetics in man. *J Clin Invest,* 58**,** 705-15.

Dautzenberg, B. & Bricard, D. 2015. Real-Time Characterization of E-Cigarettes Use: The 1 Million Puffs Study. *Journal of Addiction Research and Therapy,* 2015**,** 1-5.

Davis, E. S., Sassano, M. F., Goodell, H. & Tarran, R. 2017. E-Liquid Autofluorescence can be used as a Marker of Vaping Deposition and Third-Hand Vape Exposure. *Sci Rep,* 7**,** 7459.

Davis, L. C., Sapey, E., Thickett, D. R. & Scott, A. 2022. Predicting the pulmonary effects of long-term e-cigarette use: are the clouds clearing? *European Respiratory Review,* 31**,** 210121.

de Falco, B., Petridis, A., Paramasivan, P., Troise, A. D., Scaloni, A., Deeni, Y., Stephens, W. E. & Fiore, A. 2020. Reducing toxic reactive carbonyl species in e-cigarette emissions: testing a harm-reduction strategy based on dicarbonyl trapping. *RSC Advances,* 10**,** 21535-21544.

De Rosa, M. J., Esandi Mdel, C., Garelli, A., Rayes, D. & Bouzat, C. 2005. Relationship between alpha 7 nAChR and apoptosis in human lymphocytes. *J Neuroimmunol,* 160**,** 154-61.

Del Arroyo, A. G., Hadjihambi, A., Sanchez, J., Turovsky, E., Kasymov, V., Cain, D., Nightingale, T. D., Lambden, S., Grant, S. G. N., Gourine, A. V. & Ackland, G. L. 2019. NMDA receptor modulation of glutamate release in activated neutrophils. *EBioMedicine,* 47**,** 457-469.

Delgado BJ, B. T. 2021. *Physiology, Lung Capacity,* Treasure Island (FL).

Delgado-Rizo, V., Martínez-Guzmán, M., Iñiguez-Gutierrez, L., García-Orozco, A., Alvarado-Navarro, A. & Fafutis-Morris, M. 2017. Neutrophil extracellular traps and its implications in inflammation: an overview. *Frontiers in Immunology,* 8.

Dewhurst, J. A., Lea, S., Hardaker, E., Dungwa, J. V., Ravi, A. K. & Singh, D. 2017. Characterisation of lung macrophage subpopulations in COPD patients and controls. *Sci Rep,* 7**,** 7143.

Dinsdale, R. J. 2017. *Production and impaired regulation of neutrophil extracellular traps following severe thermal injury, implications for sepsis and multiple organ failure.* PhD, University of Birmingham

Doll, R. & Hill, A. B. 1950. Smoking and Carcinoma of the Lung. *British Medical Journal,* 2**,** 739-748.

Domon, H. & Terao, Y. 2021. The Role of Neutrophils and Neutrophil Elastase in Pneumococcal Pneumonia. *Frontiers in Cellular and Infection Microbiology,* 11.

Donaldson, G. C., Seemungal, T. A., Patel, I. S., Bhowmik, A., Wilkinson, T. M., Hurst, J. R., Maccallum, P. K. & Wedzicha, J. A. 2005. Airway and systemic inflammation and decline in lung function in patients with COPD. *Chest,* 128**,** 1995-2004.

Donaldson, G. C. & Wedzicha, J. A. 2006. COPD exacerbations .1: Epidemiology. *Thorax,* 61**,** 164-8.

Duell, A. K., Pankow, J. F. & Peyton, D. H. 2018. Free-Base Nicotine Determination in Electronic Cigarette Liquids by 1H NMR Spectroscopy. *Chemical Research in Toxicology,* 31**,** 431-434.

Dupré-Crochet, S., Erard, M. & Nüβe, O. 2013. ROS production in phagocytes: why, when, and where? *J Leukoc Biol,* 94**,** 657-70.

Dutra, L. M. & Glantz, S. A. 2014. High international electronic cigarette use among never smoker adolescents. *J Adolesc Health,* 55**,** 595-7.

Eash, K. J., Greenbaum, A. M., Gopalan, P. K. & Link, D. C. 2010. CXCR2 and CXCR4 antagonistically regulate neutrophil trafficking from murine bone marrow. *J Clin Invest,* 120**,** 2423-31.

Edwards, S. W. 1994. *Biochemistry and physiology of the neutrophil,* Cambridge, UK, Cambridge University Press.

Edwards, S. W., Hallett, M. B. & Campbell, A. K. 1984. Oxygen-radical production during inflammation may be limited by oxygen concentration. *Biochemical Journal,* 217**,** 851-854.

El-Benna, J., Dang, P. M. & Gougerot-Pocidalo, M. A. 2008. Priming of the neutrophil NADPH oxidase activation: role of p47phox phosphorylation and NOX2 mobilization to the plasma membrane. *Semin Immunopathol,* 30**,** 279-89.

Evans, S. E. & Hoffman, A. C. 2014. Electronic cigarettes: abuse liability, topography and subjective effects. *Tob Control,* 23 Suppl 2**,** ii23-9.

Fagon, J.-Y., Chastre, J., Trouillet, J.-L., Domart, Y., Dombret, M.-C., Bornet, M. & Gibert, C. 1990. Characterization of Distal Bronchial Microflora during Acute Exacerbation of Chronic Bronchitis: Use of the Protected Specimen Brush Technique in 54 Mechanically Ventilated Patients. *American Review of Respiratory Disease,* 142**,** 1004-1008.

Farsalinos, K. E., Kistler, K. A., Gillman, G. & Voudris, V. 2015. Evaluation of Electronic Cigarette Liquids and Aerosol for the Presence of Selected Inhalation Toxins. *Nicotine & Tobacco Research,* 17**,** 168-174.

Farsalinos, K. E., Romagna, G., Tsiapras, D., Kyrzopoulos, S. & Voudris, V. 2013. Evaluation of electronic cigarette use (vaping) topography and estimation of liquid consumption: implications for research protocol standards definition and for public health authorities' regulation. *Int J Environ Res Public Health,* 10**,** 2500-14.

Faurschou, M. & Borregaard, N. 2003. Neutrophil granules and secretory vesicles in inflammation. *Microbes Infect,* 5**,** 1317-27.

Feng, F., Zhang, J., Wang, Z., Wu, Q. & Zhou, X. 2019. Efficacy and safety of N-acetylcysteine therapy for idiopathic pulmonary fibrosis: An updated systematic review and meta-analysis. *Exp Ther Med,* 18**,** 802-816.

Fernandez-de-Cossio-Diaz, J. & Vazquez, A. 2018. A physical model of cell metabolism. *Sci Rep,* 8**,** 8349.

Fietta, A., Bersani, C., De Rose, V., Grassi, F. A., Mangiarotti, P., Uccelli, M. & Grassi, C. 1988. Evaluation of systemic host defense mechanisms in chronic bronchitis. *Respiration,* 53**,** 37-43.

Forrest, O. A., Ingersoll, S. A., Preininger, M. K., Laval, J., Limoli, D. H., Brown, M. R., Lee, F. E., Bedi, B., Sadikot, R. T., Goldberg, J. B., Tangpricha, V., Gaggar, A. & Tirouvanziam, R. 2018. Frontline Science: Pathological conditioning of human neutrophils recruited to the airway milieu in cystic fibrosis. *J Leukoc Biol,* 104**,** 665-675.

Fossati, G., Moulding, D. A., Spiller, D. G., Moots, R. J., White, M. R. & Edwards, S. W. 2003. The mitochondrial network of human neutrophils: role in chemotaxis, phagocytosis, respiratory burst activation, and commitment to apoptosis. *J Immunol,* 170**,** 1964-72.

Fuchs, T. A., Abed, U., Goosmann, C., Hurwitz, R., Schulze, I., Wahn, V., Weinrauch, Y., Brinkmann, V. & Zychlinsky, A. 2007. Novel cell death program leads to neutrophil extracellular traps. *The Journal of cell biology,* 176**,** 231-241.

Gaiha, S. M., Cheng, J. & Halpern-Felsher, B. 2020. Association Between Youth Smoking, Electronic Cigarette Use, and COVID-19. *J Adolesc Health,* 67**,** 519-523.

Galvis, G., Lips, K. S. & Kummer, W. 2006. Expression of nicotinic acetylcholine receptors on murine alveolar macrophages. *J Mol Neurosci,* 30**,** 107-8.

Gambardella, L. & Vermeren, S. 2013. Molecular players in neutrophil chemotaxis—focus on PI3K and small GTPases. *Journal of Leukocyte Biology,* 94**,** 603-612.

Garcia-Arcos, I., Geraghty, P., Baumlin, N., Campos, M., Dabo, A. J., Jundi, B., Cummins, N., Eden, E., Grosche, A., Salathe, M. & Foronjy, R. 2016. Chronic electronic cigarette exposure in mice induces features of COPD in a nicotine-dependent manner. *Thorax,* 71**,** 1119-1129.

Ghosh, A., Ahmad, S., Coakley, R. D., Sassano, M. F., Alexis, N. E. & Tarran, R. 2021a. Lipid-laden Macrophages Are Not Unique to Patients with E-Cigarette

or Vaping Product Use-associated Lung Injury. *Am J Respir Crit Care Med,* 203**,** 1030-1033.

Ghosh, A., Coakley, R. C., Mascenik, T., Rowell, T. R., Davis, E. S., Rogers, K., Webster, M. J., Dang, H., Herring, L. E., Sassano, M. F., Livraghi-Butrico, A., Van Buren, S. K., Graves, L. M., Herman, M. A., Randell, S. H., Alexis, N. E. & Tarran, R. 2018. Chronic E-Cigarette Exposure Alters the Human Bronchial Epithelial Proteome. *American journal of respiratory and critical care medicine,* 198**,** 67-76.

Ghosh, A., Coakley, R. D., Ghio, A. J., Muhlebach, M. S., Esther, C. R., Jr., Alexis, N. E. & Tarran, R. 2019. Chronic E-Cigarette Use Increases Neutrophil Elastase and Matrix Metalloprotease Levels in the Lung. *Am J Respir Crit Care Med,* 200**,** 1392-1401.

Ghosh, A., Girish, V., Yuan, M. L., Coakley, R. D., Wrennall, J. A., Alexis, N. E., Sausville, E. L., Vasudevan, A., Chait, A. R., Sheltzer, J. M. & Tarran, R. 2021b. Combustible and Electronic Cigarette Exposures Increase ACE2 Activity and SARS-CoV-2 Spike Binding. *American Journal of Respiratory and Critical Care Medicine,* 205**,** 129-133.

Gilpin, D. F., McGown, K.-A., Gallagher, K., Bengoechea, J., Dumigan, A., Einarsson, G., Elborn, J. S. & Tunney, M. M. 2019. Electronic cigarette vapour increases virulence and inflammatory potential of respiratory pathogens. *Respiratory Research,* 20**,** 267.

Gindele, J. A., Kiechle, T., Benediktus, K., Birk, G., Brendel, M., Heinemann, F., Wohnhaas, C. T., LeBlanc, M., Zhang, H., Strulovici-Barel, Y., Crystal, R. G., Thomas, M. J., Stierstorfer, B., Quast, K. & Schymeinsky, J. 2020. Intermittent exposure to whole cigarette smoke alters the differentiation of primary small airway epithelial cells in the air-liquid interface culture. *Scientific Reports,* 10**,** 6257.

Goel, R., Durand, E., Trushin, N., Prokopczyk, B., Foulds, J., Elias, R. J. & Richie, J. P., Jr. 2015. Highly reactive free radicals in electronic cigarette aerosols. *Chem Res Toxicol,* 28**,** 1675-7.

Goldfinger, L. E., Han, J., Kiosses, W. B., Howe, A. K. & Ginsberg, M. H. 2003. Spatial restriction of alpha4 integrin phosphorylation regulates lamellipodial stability and alpha4beta1-dependent cell migration. *J Cell Biol,* 162**,** 731-41.

Gómez, A.-C., Rodríguez-Fernández, P., Villar-Hernández, R., Gibert, I., Muriel-Moreno, B., Lacoma, A., Prat-Aymerich, C. & Domínguez, J. 2020. E-cigarettes: Effects in phagocytosis and cytokines response against Mycobacterium tuberculosis. *PloS one,* 15**,** e0228919-e0228919.

Goniewicz, M. L., Knysak, J., Gawron, M., Kosmider, L., Sobczak, A., Kurek, J., Prokopowicz, A., Jablonska-Czapla, M., Rosik-Dulewska, C., Havel, C., Jacob, P., 3rd & Benowitz, N. 2014. Levels of selected carcinogens and toxicants in vapour from electronic cigarettes. *Tob Control,* 23**,** 133-9.

Goniewicz, M. L., Kuma, T., Gawron, M., Knysak, J. & Kosmider, L. 2013. Nicotine levels in electronic cigarettes. *Nicotine Tob Res,* 15**,** 158-66.

Gorlin, R. J., Gelb, B., Diaz, G. A., Lofsness, K. G., Pittelkow, M. R. & Fenyk, J. R., Jr. 2000. WHIM syndrome, an autosomal dominant disorder: clinical, hematological, and molecular studies. *Am J Med Genet,* 91**,** 368-76.

Gotts, J. E., Jordt, S.-E., McConnell, R. & Tarran, R. 2019. What are the respiratory effects of e-cigarettes? *BMJ,* 366**,** l5275.

Grabcanovic-Musija, F., Obermayer, A., Stoiber, W., Krautgartner, W. D., Steinbacher, P., Winterberg, N., Bathke, A. C., Klappacher, M. & Studnicka, M. 2015. Neutrophil extracellular trap (NET) formation characterises stable and exacerbated COPD and correlates with airflow limitation. *Respir Res,* 16**,** 59.

Greenwood, H. L. 2014. *Neutrophil migration in the healthy elderly: causes and consequences for the resolution of inflammation.* PhD, University of Birmingham.

Grinnell, F. & Zhu, M. 1994. Identification of neutrophil elastase as the proteinase in burn wound fluid responsible for degradation of fibronectin. *J Invest Dermatol,* 103**,** 155-61.

Grudzinska, F. S., Brodlie, M., Scholefield, B. R., Jackson, T., Scott, A., Thickett, D. R. & Sapey, E. 2020. Neutrophils in community-acquired pneumonia: parallels in dysfunction at the extremes of age. *Thorax,* 75**,** 164-171.

Guzik, K., Skret, J., Smagur, J., Bzowska, M., Gajkowska, B., Scott, D. A. & Potempa, J. S. 2011. Cigarette smoke-exposed neutrophils die unconventionally but are rapidly phagocytosed by macrophages. *Cell Death Dis,* 2**,** e131.

Hager, M., Cowland, J. B. & Borregaard, N. 2010. Neutrophil granules in health and disease. *J Intern Med,* 268**,** 25-34.

Hajek, P., Phillips-Waller, A., Przulj, D., Pesola, F., Myers Smith, K., Bisal, N., Li, J., Parrott, S., Sasieni, P., Dawkins, L., Ross, L., Goniewicz, M., Wu, Q. & McRobbie, H. J. 2019. A Randomized Trial of E-Cigarettes versus Nicotine-Replacement Therapy. *N Engl J Med,* 380**,** 629-637.

Hallmann, R., Horn, N., Selg, M., Wendler, O., Pausch, F. & Sorokin, L. M. 2005. Expression and function of laminins in the embryonic and mature vasculature. *Physiol Rev,* 85**,** 979-1000.

Hampson, P., Dinsdale, R. J., Wearn, C. M., Bamford, A. L., Bishop, J. R. B., Hazeldine, J., Moiemen, N. S., Harrison, P. & Lord, J. M. 2017. Neutrophil Dysfunction, Immature Granulocytes, and Cell-free DNA are Early Biomarkers of Sepsis in Burn-injured Patients: A Prospective Observational Cohort Study. *Annals of Surgery,* 265.

Hann, J., Bueb, J. L., Tolle, F. & Bréchard, S. 2020. Calcium signaling and regulation of neutrophil functions: Still a long way to go. *Journal of Leukocyte Biology,* 107**,** 285-297.

Harris, J. O., Olsen, G. N., Castle, J. R. & Maloney, A. S. 1975. Comparison of proteolytic enzyme activity in pulmonary alveolar macrophages and blood leukocytes in smokers and nonsmokers. *Am Rev Respir Dis,* 111**,** 579-86.

Hazeldine, J., Dinsdale, R. J., Harrison, P. & Lord, J. M. 2019. Traumatic Injury and Exposure to Mitochondrial-Derived Damage Associated Molecular Patterns Suppresses Neutrophil Extracellular Trap Formation. *Frontiers in Immunology,* 10.

Hazeldine, J., Harris, P., Chapple, I. L., Grant, M., Greenwood, H., Livesey, A., Sapey, E. & Lord, J. M. 2014. Impaired neutrophil extracellular trap formation: a novel defect in the innate immune system of aged individuals. *Aging cell,* 13**,** 690-698.

Hazeldine, J., Naumann, D. N., Toman, E., Davies, D., Bishop, J. R. B., Su, Z., Hampson, P., Dinsdale, R. J., Crombie, N., Duggal, N. A., Harrison, P., Belli, A. & Lord, J. M. 2017. Prehospital immune responses and development of multiple organ dysfunction syndrome following traumatic injury: A prospective cohort study. *PLoS Med,* 14**,** e1002338.

Hernandez, P. A., Gorlin, R. J., Lukens, J. N., Taniuchi, S., Bohinjec, J., Francois, F., Klotman, M. E. & Diaz, G. A. 2003. Mutations in the chemokine receptor gene CXCR4 are associated with WHIM syndrome, a combined immunodeficiency disease. *Nat Genet,* 34**,** 70-4.

Herr, C., Tsitouras, K., Niederstrasser, J., Backes, C., Beisswenger, C., Dong, L., Guillot, L., Keller, A. & Bals, R. 2020. Cigarette smoke and electronic cigarettes differentially activate bronchial epithelial cells. *Respir Res,* 21**,** 67.

Hickman, E., Herrera, C. A. & Jaspers, I. 2019. Common E-Cigarette Flavoring Chemicals Impair Neutrophil Phagocytosis and Oxidative Burst. *Chemical research in toxicology,* 32**,** 982-985.

Higham, A., Rattray, N. J., Dewhurst, J. A., Trivedi, D. K., Fowler, S. J., Goodacre, R. & Singh, D. 2016. Electronic cigarette exposure triggers neutrophil inflammatory responses. *Respir Res,* 17**,** 56.

Hirano, Y., Aziz, M. & Wang, P. 2016. Role of reverse transendothelial migration of neutrophils in inflammation. *Biol Chem,* 397**,** 497-506.

Hock, H., Hamblen, M. J., Rooke, H. M., Traver, D., Bronson, R. T., Cameron, S. & Orkin, S. H. 2003. Intrinsic requirement for zinc finger transcription factor Gfi-1 in neutrophil differentiation. *Immunity,* 18**,** 109-20.

Hogg, R. C., Raggenbass, M. & Bertrand, D. 2003. Nicotinic acetylcholine receptors: from structure to brain function. *Rev Physiol Biochem Pharmacol,* 147**,** 1-46.

Hollander, C., Sitkauskiene, B., Sakalauskas, R., Westin, U. & Janciauskiene, S. M. 2007. Serum and bronchial lavage fluid concentrations of IL-8, SLPI, sCD14 and sICAM-1 in patients with COPD and asthma. *Respir Med,* 101**,** 1947-53.

Hoshino, Y., Mio, T., Nagai, S., Miki, H., Ito, I. & Izumi, T. 2001. Cytotoxic effects of cigarette smoke extract on an alveolar type II cell-derived cell line. *American Journal of Physiology-Lung Cellular and Molecular Physiology,* 281**,** L509-L516.

Hosseinzadeh, A., Thompson, P. R., Segal, B. H. & Urban, C. F. 2016. Nicotine induces neutrophil extracellular traps. *J Leukoc Biol,* 100**,** 1105-1112.

Houston, N., Stewart, N., Smith, D. S., Bell, S. C., Champion, A. C. & Reid, D. W. 2013. Sputum neutrophils in cystic fibrosis patients display a reduced respiratory burst. *J Cyst Fibros,* 12**,** 352-62.

Hua, M., Yip, H. & Talbot, P. 2013. Mining data on usage of electronic nicotine delivery systems (ENDS) from YouTube videos. *Tob Control,* 22**,** 103-6.

Hwang, J. H., Lyes, M., Sladewski, K., Enany, S., McEachern, E., Mathew, D. P., Das, S., Moshensky, A., Bapat, S., Pride, D. T., Ongkeko, W. M. & Crotty Alexander, L. E. 2016. Electronic cigarette inhalation alters innate immunity and airway cytokines while increasing the virulence of colonizing bacteria. *J Mol Med (Berl),* 94**,** 667-79.

Iho, S., Tanaka, Y., Takauji, R., Kobayashi, C., Muramatsu, I., Iwasaki, H., Nakamura, K., Sasaki, Y., Nakao, K. & Takahashi, T. 2003. Nicotine induces human neutrophils to produce IL-8 through the generation of peroxynitrite and subsequent activation of NF-kappaB. *J Leukoc Biol,* 74**,** 942-51.

Immler, R., Simon, S. I. & Sperandio, M. 2018. Calcium signalling and related ion channels in neutrophil recruitment and function. *European journal of clinical investigation,* 48 Suppl 2**,** e12964-e12964.

Injarabian, L., Devin, A., Ransac, S. & Marteyn, B. S. 2019. Neutrophil Metabolic Shift during their Lifecycle: Impact on their Survival and Activation. *Int J Mol Sci,* 21.

Invitrogen 2020. pHrodo™ Red, Deep Red, and Green BioParticles™ conjugates for

phagocytosis *Product information sheet.*
Iwasaki, H., Somoza, C., Shigematsu, H., Duprez, E. A., Iwasaki-Arai, J., Mizuno, S., Arinobu, Y., Geary, K., Zhang, P., Dayaram, T., Fenyus, M. L., Elf, S., Chan, S., Kastner, P., Huettner, C. S., Murray, R., Tenen, D. G. & Akashi, K. 2005. Distinctive and indispensable roles of PU.1 in maintenance of hematopoietic stem cells and their differentiation. *Blood,* 106**,** 1590-600.
Jaegers, N. R., Hu, W., Weber, T. J. & Hu, J. Z. 2021. Low-temperature (< 200 °C) degradation of electronic nicotine delivery system liquids generates toxic aldehydes. *Scientific Reports,* 11**,** 7800.
Jankowski, A., Scott, C. C. & Grinstein, S. 2002. Determinants of the Phagosomal pH in Neutrophils*. *Journal of Biological Chemistry,* 277**,** 6059-6066.
Janoff, A. & Scherer, J. 1968. Mediators of inflammation in leukocyte lysosomes. IX. Elastinolytic activity in granules of human polymorphonuclear leukocytes. *J Exp Med,* 128**,** 1137-55.
Jasper, A. E., McIver, W. J., Sapey, E. & Walton, G. M. 2019. Understanding the role of neutrophils in chronic inflammatory airway disease. *F1000Res,* 8.
Jasper, A. E., Sapey, E., Thickett, D. & Scott, A. 2021. Understanding potential mechanisms of harm: the drivers of electronic cigarette-induced changes in alveolar macrophages, neutrophils and lung epithelial cells. *American Journal of Physiology-Lung Cellular and Molecular Physiology*.
Jensen, R. P., Luo, W., Pankow, J. F., Strongin, R. M. & Peyton, D. H. 2015. Hidden formaldehyde in e-cigarette aerosols. *N Engl J Med,* 372**,** 392-4.
Jeon, J.-H., Hong, C.-W., Kim, E. Y. & Lee, J. M. 2020. Current Understanding on the Metabolism of Neutrophils. *Immune Netw,* 20.
Jepsen, L. V. & Skottun, T. 1982. A rapid one-step method for the isolation of human granulocytes from whole blood. *Scand J Clin Lab Invest,* 42**,** 235-8.
Jerzyński, T., Stimson, G. V., Shapiro, H. & Król, G. 2021. Estimation of the global number of e-cigarette users in 2020. *Harm Reduct J,* 18**,** 109.
Jiang, H., Kuang, Y., Wu, Y., Xie, W., Simon, M. I. & Wu, D. 1997. Roles of phospholipase C beta2 in chemoattractant-elicited responses. *Proc Natl Acad Sci U S A,* 94**,** 7971-5.
Jiao, Z. X., Ao, Q. L. & Xiong, M. 2006. Cigarette smoke extract inhibits the proliferation of alveolar epithelial cells and induces apoptosis. *Sheng Li Xue Bao,* 58**,** 244-54.
Kafienah, W., Buttle, D. J., Burnett, D. & Hollander, A. P. 1998. Cleavage of native type I collagen by human neutrophil elastase. *Biochem J,* 330 (Pt 2)**,** 897-902.
Kansas, G. S. 1996. Selectins and their ligands: current concepts and controversies. *Blood,* 88**,** 3259-3287.
Kaplan, M. J. & Radic, M. 2012. Neutrophil extracellular traps: double-edged swords of innate immunity. *Journal of immunology (Baltimore, Md. : 1950),* 189**,** 2689-2695.
Karimi, R., Tornling, G., Grunewald, J., Eklund, A. & Skold, C. M. 2012. Cell recovery in bronchoalveolar lavage fluid in smokers is dependent on cumulative smoking history. *PLoS One,* 7**,** e34232.
Karsunky, H., Zeng, H., Schmidt, T., Zevnik, B., Kluge, R., Schmid, K. W., Duhrsen, U. & Moroy, T. 2002. Inflammatory reactions and severe neutropenia in mice lacking the transcriptional repressor Gfi1. *Nat Genet,* 30**,** 295-300.

Khan, M. A. & Palaniyar, N. 2017. Transcriptional firing helps to drive NETosis. *Scientific Reports,* 7**,** 41749.

Kharazmi, A., Nielsen, H. & Schiøtz, P. O. 1988. N-acetylcysteine inhibits human neutrophil and monocyte chemotaxis and oxidative metabolism. *Int J Immunopharmacol,* 10**,** 39-46.

Kihara, T., Shimohama, S., Sawada, H., Honda, K., Nakamizo, T., Shibasaki, H., Kume, T. & Akaike, A. 2001. α7 Nicotinic Receptor Transduces Signals to Phosphatidylinositol 3-Kinase to Block A ß2;-Amyloid-induced Neurotoxicity *. *Journal of Biological Chemistry,* 276**,** 13541-13546.

Ko, H. K., Lee, H. F., Lin, A. H., Liu, M. H., Liu, C. I., Lee, T. S. & Kou, Y. R. 2015. Regulation of Cigarette Smoke Induction of IL-8 in Macrophages by AMP-activated Protein Kinase Signaling. *J Cell Physiol,* 230**,** 1781-93.

Kobayashi, S. D., Malachowa, N. & DeLeo, F. R. 2018. Neutrophils and Bacterial Immune Evasion. *Journal of Innate Immunity,* 10**,** 432-441.

Kode, A., Yang, S. R. & Rahman, I. 2006. Differential effects of cigarette smoke on oxidative stress and proinflammatory cytokine release in primary human airway epithelial cells and in a variety of transformed alveolar epithelial cells. *Respir Res,* 7**,** 132.

Koethe, S. M., Kuhnmuench, J. R. & Becker, C. G. 2000. Neutrophil priming by cigarette smoke condensate and a tobacco anti-idiotypic antibody. *Am J Pathol,* 157**,** 1735-43.

Kolaczkowska, E. & Kubes, P. 2013. Neutrophil recruitment and function in health and inflammation. *Nature Reviews Immunology,* 13**,** 159-175.

Kosmider, L., Cox, S., Zaciera, M., Kurek, J., Goniewicz, M. L., McRobbie, H., Kimber, C. & Dawkins, L. 2020. Daily exposure to formaldehyde and acetaldehyde and potential health risk associated with use of high and low nicotine e-liquid concentrations. *Scientific Reports,* 10**,** 6546.

Kośmider, L., Kimber, C. F., Kurek, J., Corcoran, O. & Dawkins, L. E. 2018. Compensatory Puffing With Lower Nicotine Concentration E-liquids Increases Carbonyl Exposure in E-cigarette Aerosols. *Nicotine & Tobacco Research,* 20**,** 998-1003.

Kosmider, L., Sobczak, A., Fik, M., Knysak, J., Zaciera, M., Kurek, J. & Goniewicz, M. L. 2014. Carbonyl compounds in electronic cigarette vapors: effects of nicotine solvent and battery output voltage. *Nicotine Tob Res,* 16**,** 1319-26.

Kosmider, L., Sobczak, A., Prokopowicz, A., Kurek, J., Zaciera, M., Knysak, J., Smith, D. & Goniewicz, M. L. 2016. Cherry-flavoured electronic cigarettes expose users to the inhalation irritant, benzaldehyde. *Thorax,* 71**,** 376-7.

Kovach, M. A. & Standiford, T. J. 2012. The function of neutrophils in sepsis. *Current Opinion in Infectious Diseases,* 25.

Kreiss, K., Gomaa, A., Kullman, G., Fedan, K., Simoes, E. J. & Enright, P. L. 2002. Clinical Bronchiolitis Obliterans in Workers at a Microwave-Popcorn Plant. *New England Journal of Medicine,* 347**,** 330-338.

Kuek, L. E. & Lee, R. J. 2020. First contact: the role of respiratory cilia in host-pathogen interactions in the airways. *American Journal of Physiology-Lung Cellular and Molecular Physiology,* 319**,** L603-L619.

Kumar, S. & Dikshit, M. 2019. Metabolic Insight of Neutrophils in Health and Disease. *Front Immunol,* 10**,** 2099.

Lacy, P. 2006. Mechanisms of degranulation in neutrophils. *Allergy Asthma Clin Immunol,* 2**,** 98-108.

Lakschevitz, F. S., Visser, M. B., Sun, C. & Glogauer, M. 2015. Neutrophil transcriptional profile changes during transit from bone marrow to sites of inflammation. *Cell Mol Immunol,* 12**,** 53-65.

Lam, D. C., Girard, L., Ramirez, R., Chau, W. S., Suen, W. S., Sheridan, S., Tin, V. P., Chung, L. P., Wong, M. P., Shay, J. W., Gazdar, A. F., Lam, W. K. & Minna, J. D. 2007. Expression of nicotinic acetylcholine receptor subunit genes in non-small-cell lung cancer reveals differences between smokers and nonsmokers. *Cancer Res,* 67**,** 4638-47.

Larson-Casey, J. L., Gu, L., Jackson, P. L., Briles, D. E., Hale, J. Y., Blalock, J. E., Wells, J. M., Deshane, J. S., Wang, Y., Davis, D., Antony, V. B., Massicano, A. V. F., Lapi, S. E. & Carter, A. B. 2018. Macrophage Rac2 Is Required to Reduce the Severity of Cigarette Smoke-induced Pneumonia. *Am J Respir Crit Care Med,* 198**,** 1288-1301.

Layden, J. E., Ghinai, I., Pray, I., Kimball, A., Layer, M., Tenforde, M. W., Navon, L., Hoots, B., Salvatore, P. P., Elderbrook, M., Haupt, T., Kanne, J., Patel, M. T., Saathoff-Huber, L., King, B. A., Schier, J. G., Mikosz, C. A. & Meiman, J. 2019. Pulmonary Illness Related to E-Cigarette Use in Illinois and Wisconsin — Final Report. *New England Journal of Medicine,* 382**,** 903-916.

Lee, A., Whyte, M. K. & Haslett, C. 1993. Inhibition of apoptosis and prolongation of neutrophil functional longevity by inflammatory mediators. *J Leukoc Biol,* 54**,** 283-8.

Lee, J., Luria, A., Rhodes, C., Raghu, H., Lingampalli, N., Sharpe, O., Rada, B., Sohn, D. H., Robinson, W. H. & Sokolove, J. 2017. Nicotine drives neutrophil extracellular traps formation and accelerates collagen-induced arthritis. *Rheumatology,* 56**,** 644-653.

Lee, J., Taneja, V. & Vassallo, R. 2012. Cigarette smoking and inflammation: cellular and molecular mechanisms. *J Dent Res,* 91**,** 142-9.

Lee, M. S., Allen, J. G. & Christiani, D. C. 2019. Endotoxin and [Formula: see text] Contamination in Electronic Cigarette Products Sold in the United States. *Environ Health Perspect,* 127**,** 47008.

Lee, Y. O., Nonnemaker, J. M., Bradfield, B., Hensel, E. C. & Robinson, R. J. 2018. Examining Daily Electronic Cigarette Puff Topography Among Established and Nonestablished Cigarette Smokers in their Natural Environment. *Nicotine Tob Res,* 20**,** 1283-1288.

Lerner, C. A., Sundar, I. K., Yao, H., Gerloff, J., Ossip, D. J., McIntosh, S., Robinson, R. & Rahman, I. 2015. Vapors Produced by Electronic Cigarettes and E-Juices with Flavorings Induce Toxicity, Oxidative Stress, and Inflammatory Response in Lung Epithelial Cells and in Mouse Lung. *PLOS ONE,* 10**,** e0116732.

Levine, A. P., Duchen, M. R., de Villiers, S., Rich, P. R. & Segal, A. W. 2015. Alkalinity of neutrophil phagocytic vacuoles is modulated by HVCN1 and has consequences for myeloperoxidase activity. *PLoS One,* 10**,** e0125906.

Levy, B. D. & Serhan, C. N. 2014. Resolution of acute inflammation in the lung. *Annual review of physiology,* 76**,** 467-492.

Ley, K., Laudanna, C., Cybulsky, M. I. & Nourshargh, S. 2007. Getting to the site of inflammation: the leukocyte adhesion cascade updated. *Nat Rev Immunol,* 7**,** 678-89.

Ley, K., Smith, E. & Stark, M. A. 2006. IL-17A-producing neutrophil-regulatory Tn lymphocytes. *Immunol Res,* 34**,** 229-42.
Liew, P. X. & Kubes, P. 2019. The Neutrophil's Role During Health and Disease. *Physiol Rev,* 99**,** 1223-1248.
Lin, R., Zhang, Y., Pradhan, K. & Li, L. 2020. TICAM2-related pathway mediates neutrophil exhaustion. *Scientific Reports,* 10**,** 14397.
Lin, V. Y., Fain, M. D., Jackson, P. L., Berryhill, T. F., Wilson, L. S., Mazur, M., Barnes, S. J., Blalock, J. E., Raju, S. V. & Rowe, S. M. 2019. Vaporized E-Cigarette Liquids Induce Ion Transport Dysfunction in Airway Epithelia. *Am J Respir Cell Mol Biol,* 61**,** 162-173.
Liu, C. L., Tangsombatvisit, S., Rosenberg, J. M., Mandelbaum, G., Gillespie, E. C., Gozani, O. P., Alizadeh, A. A. & Utz, P. J. 2012. Specific post-translational histone modifications of neutrophil extracellular traps as immunogens and potential targets of lupus autoantibodies. *Arthritis research & therapy,* 14**,** R25-R25.
Lokke, A., Lange, P., Scharling, H., Fabricius, P. & Vestbo, J. 2006. Developing COPD: a 25 year follow up study of the general population. *Thorax,* 61**,** 935-9.
Love, M. I., Huber, W. & Anders, S. 2014. Moderated estimation of fold change and dispersion for RNA-seq data with DESeq2. *Genome Biology,* 15**,** 550.
Lugg, S. T., Scott, A., Parekh, D., Naidu, B. & Thickett, D. R. 2022. Cigarette smoke exposure and alveolar macrophages: mechanisms for lung disease. *Thorax,* 77**,** 94-101.
Maggi, F., Rosellini, A., Spezia, P. G., Focosi, D., Macera, L., Lai, M., Pistello, M., de Iure, A., Tomino, C., Bonassi, S. & Russo, P. 2021. Nicotine upregulates ACE2 expression and increases competence for SARS-CoV-2 in human pneumocytes. *ERJ Open Research,* 7**,** 00713-2020.
Mahida, R. Y., Scott, A., Parekh, D., Lugg, S. T., Belchamber, K. B. R., Hardy, R. S., Matthay, M. A., Naidu, B. & Thickett, D. R. 2021. Assessment of Alveolar Macrophage Dysfunction Using an in vitro Model of Acute Respiratory Distress Syndrome. *Frontiers in Medicine,* 8.
Maianski, N. A., Geissler, J., Srinivasula, S. M., Alnemri, E. S., Roos, D. & Kuijpers, T. W. 2004. Functional characterization of mitochondria in neutrophils: a role restricted to apoptosis. *Cell Death Differ,* 11**,** 143-53.
Maianski, N. A., Mul, F. P., van Buul, J. D., Roos, D. & Kuijpers, T. W. 2002. Granulocyte colony-stimulating factor inhibits the mitochondria-dependent activation of caspase-3 in neutrophils. *Blood,* 99**,** 672-9.
Malcolm, K. C., Arndt, P. G., Manos, E. J., Jones, D. A. & Worthen, G. S. 2003. Microarray analysis of lipopolysaccharide-treated human neutrophils. *Am J Physiol Lung Cell Mol Physiol,* 284**,** L663-70.
Maouche, K., Medjber, K., Zahm, J. M., Delavoie, F., Terryn, C., Coraux, C., Pons, S., Cloëz-Tayarani, I., Maskos, U., Birembaut, P. & Tournier, J. M. 2013. Contribution of α7 nicotinic receptor to airway epithelium dysfunction under nicotine exposure. *Proc Natl Acad Sci U S A,* 110**,** 4099-104.
Martin, C., Burdon, P. C., Bridger, G., Gutierrez-Ramos, J. C., Williams, T. J. & Rankin, S. M. 2003. Chemokines acting via CXCR2 and CXCR4 control the release of neutrophils from the bone marrow and their return following senescence. *Immunity,* 19**,** 583-93.

Martin, E. M., Clapp, P. W., Rebuli, M. E., Pawlak, E. A., Glista-Baker, E., Benowitz, N. L., Fry, R. C. & Jaspers, I. 2016. E-cigarette use results in suppression of immune and inflammatory-response genes in nasal epithelial cells similar to cigarette smoke. *Am J Physiol Lung Cell Mol Physiol,* 311**,** L135-44.

Martin, K. J., Muessel, M. J., Pullar, C. E., Willars, G. B. & Wardlaw, A. J. 2015. The role of phosphoinositide 3-kinases in neutrophil migration in 3D collagen gels. *PLoS One,* 10**,** e0116250.

Massey, J. B., She, H. S. & Pownall, H. J. 1982. Interaction of vitamin E with saturated phospholipid bilayers. *Biochemical and Biophysical Research Communications,* 106**,** 842-847.

Masso-Silva, J. A., Moshensky, A., Shin, J., Olay, J., Nilaad, S., Advani, I., Bojanowski, C. M., Crotty, S., Li, W. T., Ongkeko, W. M., Singla, S. & Crotty Alexander, L. E. 2021. Chronic E-Cigarette Aerosol Inhalation Alters the Immune State of the Lungs and Increases ACE2 Expression, Raising Concern for Altered Response and Susceptibility to SARS-CoV-2. *Frontiers in Physiology,* 12.

Matsumoto, S., Fang, X., Traber, M. G., Jones, K. D., Langelier, C., Hayakawa Serpa, P., Calfee, C. S., Matthay, M. A. & Gotts, J. E. 2020. Dose-Dependent Pulmonary Toxicity of Aerosolized Vitamin E Acetate. *Am J Respir Cell Mol Biol,* 63**,** 748-757.

Matthews, J. B., Chen, F. M., Milward, M. R., Ling, M. R. & Chapple, I. L. 2012. Neutrophil superoxide production in the presence of cigarette smoke extract, nicotine and cotinine. *J Clin Periodontol,* 39**,** 626-34.

Matthews, J. B., Chen, F. M., Milward, M. R., Wright, H. J., Carter, K., McDonagh, A. & Chapple, I. L. 2011. Effect of nicotine, cotinine and cigarette smoke extract on the neutrophil respiratory burst. *J Clin Periodontol,* 38**,** 208-18.

May, R. C. & Machesky, L. M. 2001. Phagocytosis and the actin cytoskeleton. *J Cell Sci,* 114**,** 1061-77.

Mayadas, T. N., Cullere, X. & Lowell, C. A. 2014. The multifaceted functions of neutrophils. *Annu Rev Pathol,* 9**,** 181-218.

McAlinden, K. D., Lu, W., Ferdowsi, P. V., Myers, S., Markos, J., Larby, J., Chia, C., Weber, H. C., Haug, G., Eapen, M. S. & Sohal, S. S. 2021. Electronic Cigarette Aerosol Is Cytotoxic and Increases ACE2 Expression on Human Airway Epithelial Cells: Implications for SARS-CoV-2 (COVID-19). *Journal of Clinical Medicine,* 10.

McEachern, E. K., Hwang, J. H., Sladewski, K. M., Nicatia, S., Dewitz, C., Mathew, D. P., Nizet, V. & Crotty Alexander, L. E. 2015. Analysis of the effects of cigarette smoke on staphylococcal virulence phenotypes. *Infect Immun,* 83**,** 2443-52.

McFadden, D. D., Bornstein, S. L., Vassallo, R., Salonen, B. R., Bhuiyan, M. N., Schroeder, D. R. & Croghan, I. T. 2022. Symptoms COVID 19 Positive Vapers Compared to COVID 19 Positive Non-vapers. *J Prim Care Community Health,* 13**,** 21501319211062672.

McNeill, A., Brose, L. S., Calder, R., Simonavicius, E. & Robson, D. 2021. Vaping in England: An evidence update including vaping for smoking cessation, February 2021: a report commissioned by PHE. London: PHE.

McNeill, A., Brose, L.S., Calder, R., Simonavicius, E. and Robson, D. 2021. Vaping in England: An evidence update including vaping for smoking cessation, February 2021: a report commissioned by PHE. London: PHE.

McPhail, L. C., Clayton, C. C. & Snyderman, R. 1984. The NADPH oxidase of human polymorphonuclear leukocytes. Evidence for regulation by multiple signals. *J Biol Chem,* 259**,** 5768-75.

Meo, S. A., Ansary, M. A., Barayan, F. R., Almusallam, A. S., Almehaid, A. M., Alarifi, N. S., Alsohaibani, T. A. & Zia, I. 2019. Electronic Cigarettes: Impact on Lung Function and Fractional Exhaled Nitric Oxide Among Healthy Adults. *Am J Mens Health,* 13**,** 1557988318806073.

Metcalfe, H. J., Lea, S., Hughes, D., Khalaf, R., Abbott-Banner, K. & Singh, D. 2014. Effects of cigarette smoke on Toll-like receptor (TLR) activation of chronic obstructive pulmonary disease (COPD) macrophages. *Clin Exp Immunol,* 176**,** 461-72.

Metzler, K. D., Fuchs, T. A., Nauseef, W. M., Reumaux, D., Roesler, J., Schulze, I., Wahn, V., Papayannopoulos, V. & Zychlinsky, A. 2011. Myeloperoxidase is required for neutrophil extracellular trap formation: implications for innate immunity. *Blood,* 117**,** 953-9.

MHRA 2020. Drug Safety Update.

MHRA 2022. E-cigarettes: regulations for consumer products.

Miech, R., Johnston, L., O'Malley, P. M., Bachman, J. G. & Patrick, M. E. 2019. Trends in Adolescent Vaping, 2017–2019. *New England Journal of Medicine,* 381**,** 1490-1491.

Miksa, M., Komura, H., Wu, R., Shah, K. G. & Wang, P. 2009. A novel method to determine the engulfment of apoptotic cells by macrophages using pHrodo succinimidyl ester. *J Immunol Methods,* 342**,** 71-7.

Miller, M. L. & Hurd, Y. L. 2017. Testing the Gateway Hypothesis. *Neuropsychopharmacology,* 42**,** 985-986.

Mio, T., Romberger, D. J., Thompson, A. B., Robbins, R. A., Heires, A. & Rennard, S. I. 1997. Cigarette smoke induces interleukin-8 release from human bronchial epithelial cells. *Am J Respir Crit Care Med,* 155**,** 1770-6.

Miralda, I., Uriarte, S. M. & McLeish, K. R. 2017. Multiple Phenotypic Changes Define Neutrophil Priming. *Frontiers in cellular and infection microbiology,* 7**,** 217-217.

Mishra, S. & Mishra, M. B. 2013. Tobacco: Its historical, cultural, oral, and periodontal health association. *J Int Soc Prev Community Dent,* 3**,** 12-8.

Mittal, M., Siddiqui, M. R., Tran, K., Reddy, S. P. & Malik, A. B. 2014. Reactive oxygen species in inflammation and tissue injury. *Antioxid Redox Signal,* 20**,** 1126-67.

Mocsai, A., Walzog, B. & Lowell, C. A. 2015. Intracellular signalling during neutrophil recruitment. *Cardiovasc Res,* 107**,** 373-85.

Mokhtari, V., Afsharian, P., Shahhoseini, M., Kalantar, S. M. & Moini, A. 2017. A Review on Various Uses of N-Acetyl Cysteine. *Cell J,* 19**,** 11-17.

Morris, A. C., Brittan, M., Wilkinson, T. S., McAuley, D. F., Antonelli, J., McCulloch, C., Barr, L. C., McDonald, N. A., Dhaliwal, K., Jones, R. O., Mackellar, A., Haslett, C., Hay, A. W., Swann, D. G., Anderson, N., Laurenson, I. F., Davidson, D. J., Rossi, A. G., Walsh, T. S. & Simpson, A. J. 2011. C5a-mediated neutrophil dysfunction is RhoA-dependent and predicts infection in critically ill patients. *Blood,* 117**,** 5178-88.

Morris, A. M., Leonard, S. S., Fowles, J. R., Boots, T. E., Mnatsakanova, A. & Attfield, K. R. 2021. Effects of E-Cigarette Flavoring Chemicals on Human Macrophages and Bronchial Epithelial Cells. *Int J Environ Res Public Health,* 18.

Mortaz, E., Henricks, P. A., Kraneveld, A. D., Givi, M. E., Garssen, J. & Folkerts, G. 2011. Cigarette smoke induces the release of CXCL-8 from human bronchial epithelial cells via TLRs and induction of the inflammasome. *Biochim Biophys Acta,* 1812**,** 1104-10.

Muinonen-Martin, A. J., Veltman, D. M., Kalna, G. & Insall, R. H. 2010. An Improved Chamber for Direct Visualisation of Chemotaxis. *PLOS ONE,* 5**,** e15309.

Müns, G., Rubinstein, I. & Bergmann, K. C. 1995. Phagocytosis and oxidative burst of blood phagocytes in chronic obstructive airway disease. *Scand J Infect Dis,* 27**,** 369-73.

Naidu, V., Zeki, A. A. & Sharma, P. 2021. Sex differences in the induction of angiotensin converting enzyme 2 (ACE-2) in mouse lungs after e-cigarette vapor exposure and its relevance to COVID-19. *Journal of Investigative Medicine,* 69**,** 954.

Nerlov, C. & Graf, T. 1998. PU.1 induces myeloid lineage commitment in multipotent hematopoietic progenitors. *Genes Dev,* 12**,** 2403-12.

Nicod, L. P. 2005. Lung defences: an overview. *European Respiratory Review,* 14**,** 45.

Nordenfelt, P. & Tapper, H. 2011. Phagosome dynamics during phagocytosis by neutrophils. *J Leukoc Biol,* 90**,** 271-84.

Norton, K. J., June, K. M. & O'Connor, R. J. 2014. Initial puffing behaviors and subjective responses differ between an electronic nicotine delivery system and traditional cigarettes. *Tob Induc Dis,* 12**,** 17.

Nutt, D. J., Phillips, L. D., Balfour, D., Curran, H. V., Dockrell, M., Foulds, J., Fagerstrom, K., Letlape, K., Milton, A., Polosa, R., Ramsey, J. & Sweanor, D. 2014. Estimating the harms of nicotine-containing products using the MCDA approach. *Eur Addict Res,* 20**,** 218-25.

Ogunwale, M. A., Li, M., Ramakrishnam Raju, M. V., Chen, Y., Nantz, M. H., Conklin, D. J. & Fu, X. A. 2017. Aldehyde Detection in Electronic Cigarette Aerosols. *ACS Omega,* 2**,** 1207-1214.

Owen, J. B. & Butterfield, D. A. 2010. Measurement of oxidized/reduced glutathione ratio. *Methods Mol Biol,* 648**,** 269-77.

Pace, E., Ferraro, M., Siena, L., Melis, M., Montalbano, A. M., Johnson, M., Bonsignore, M. R., Bonsignore, G. & Gjomarkaj, M. 2008. Cigarette smoke increases Toll-like receptor 4 and modifies lipopolysaccharide-mediated responses in airway epithelial cells. *Immunology,* 124**,** 401-11.

Papayannopoulos, V. 2018. Neutrophil extracellular traps in immunity and disease. *Nature Reviews Immunology,* 18**,** 134-147.

Papayannopoulos, V., Metzler, K. D., Hakkim, A. & Zychlinsky, A. 2010. Neutrophil elastase and myeloperoxidase regulate the formation of neutrophil extracellular traps. *J Cell Biol,* 191**,** 677-91.

Park, H. R., O'Sullivan, M., Vallarino, J., Shumyatcher, M., Himes, B. E., Park, J. A., Christiani, D. C., Allen, J. & Lu, Q. 2019. Transcriptomic response of primary human airway epithelial cells to flavoring chemicals in electronic cigarettes. *Sci Rep,* 9**,** 1400.

Parr, D. G., White, A. J., Bayley, D. L., Guest, P. J. & Stockley, R. A. 2006. Inflammation in sputum relates to progression of disease in subjects with COPD: a prospective descriptive study. *Respiratory Research,* 7**,** 136.

Patel, J. M., Sapey, E., Parekh, D., Scott, A., Dosanjh, D., Gao, F. & Thickett, D. R. 2018. Sepsis Induces a Dysregulated Neutrophil Phenotype That Is Associated with Increased Mortality. *Mediators Inflamm,* 2018**,** 4065362.

Pauly, J. L., Allison, E. M., Hurley, E. L., Nwogu, C. E., Wallace, P. K. & Paszkiewicz, G. M. 2005. Fluorescent human lung macrophages analyzed by spectral confocal laser scanning microscopy and multispectral cytometry. *Microscopy Research and Technique,* 67**,** 79-89.

Peachman, K. K., Lyles, D. S. & Bass, D. A. 2001. Mitochondria in eosinophils: functional role in apoptosis but not respiration. *Proc Natl Acad Sci U S A,* 98**,** 1717-22.

Perez, H. D., Marder, S., Elfman, F. & Ives, H. E. 1987. Human neutrophils contain subpopulations of specific granules exhibiting different sensitivities to changes in cytosolic free calcium. *Biochemical and Biophysical Research Communications,* 145**,** 976-981.

Peto, R., Darby, S., Deo, H., Silcocks, P., Whitley, E. & Doll, R. 2000. Smoking, smoking cessation, and lung cancer in the UK since 1950: combination of national statistics with two case-control studies. *Bmj,* 321**,** 323-9.

Phillips, B., Veljkovic, E., Peck, M. J., Buettner, A., Elamin, A., Guedj, E., Vuillaume, G., Ivanov, N. V., Martin, F., Boué, S., Schlage, W. K., Schneider, T., Titz, B., Talikka, M., Vanscheeuwijck, P., Hoeng, J. & Peitsch, M. C. 2015. A 7-month cigarette smoke inhalation study in C57BL/6 mice demonstrates reduced lung inflammation and emphysema following smoking cessation or aerosol exposure from a prototypic modified risk tobacco product. *Food and Chemical Toxicology,* 80**,** 328-345.

Phillipson, M., Heit, B., Colarusso, P., Liu, L., Ballantyne, C. M. & Kubes, P. 2006. Intraluminal crawling of neutrophils to emigration sites: a molecularly distinct process from adhesion in the recruitment cascade. *J Exp Med,* 203**,** 2569-75.

Phillipson, M. & Kubes, P. 2011. The neutrophil in vascular inflammation. *Nat Med,* 17**,** 1381-90.

Pilette, C., Colinet, B., Kiss, R., André, S., Kaltner, H., Gabius, H. J., Delos, M., Vaerman, J. P., Decramer, M. & Sibille, Y. 2007. Increased galectin-3 expression and intra-epithelial neutrophils in small airways in severe COPD. *Eur Respir J,* 29**,** 914-22.

Porter, L., Toepfner, N., Bashant, K. R., Guck, J., Ashcroft, M., Farahi, N. & Chilvers, E. R. 2018. Metabolic Profiling of Human Eosinophils. *Frontiers in immunology,* 9**,** 1404-1404.

Pospieszalska, M. K. & Ley, K. 2009. Dynamics of Microvillus Extension and Tether Formation in Rolling Leukocytes. *Cell Mol Bioeng,* 2**,** 207-217.

Pryor, W. A. & Stone, K. 1993. Oxidants in cigarette smoke. Radicals, hydrogen peroxide, peroxynitrate, and peroxynitrite. *Ann N Y Acad Sci,* 686**,** 12-27; discussion 27-8.

Pullan, J., Greenwood, H., Walton, G. M., Stockley, R. A. & Sapey, E. 2015. Neutrophil extracellular traps (NETs) in COPD: A potential novel mechanism for host damage in acute exacerbations. *European Respiratory Journal,* 46**,** PA5055.

Rasmussen, J. E., Sheridan, J. T., Polk, W., Davies, C. M. & Tarran, R. 2014. Cigarette Smoke-induced Ca^{2+} Release Leads to Cystic Fibrosis Transmembrane Conductance Regulator (CFTR) Dysfunction *. *Journal of Biological Chemistry,* 289**,** 7671-7681.

Reboul, E. 2017. Vitamin E Bioavailability: Mechanisms of Intestinal Absorption in the Spotlight. *Antioxidants (Basel),* 6.

Rebuli, M. E., Glista-Baker, E., Hoffman, J. R., Duffney, P. F., Robinette, C., Speen, A. M., Pawlak, E. A., Dhingra, R., Noah, T. L. & Jaspers, I. 2021. Electronic-Cigarette Use Alters Nasal Mucosal Immune Response to Live-attenuated Influenza Virus. A Clinical Trial. *Am J Respir Cell Mol Biol,* 64**,** 126-137.

Reidel, B., Radicioni, G., Clapp, P. W., Ford, A. A., Abdelwahab, S., Rebuli, M. E., Haridass, P., Alexis, N. E., Jaspers, I. & Kesimer, M. 2018. E-Cigarette Use Causes a Unique Innate Immune Response in the Lung, Involving Increased Neutrophilic Activation and Altered Mucin Secretion. *Am J Respir Crit Care Med,* 197**,** 492-501.

Reiss, M. & Roos, D. 1978. Differences in oxygen metabolism of phagocytosing monocytes and neutrophils. *J Clin Invest,* 61**,** 480-8.

Reyes, A. Z., Hu, K. A., Teperman, J., Wampler Muskardin, T. L., Tardif, J. C., Shah, B. & Pillinger, M. H. 2021. Anti-inflammatory therapy for COVID-19 infection: the case for colchicine. *Ann Rheum Dis,* 80**,** 550-557.

Robinson, R. J., Hensel, E. C., Morabito, P. N. & Roundtree, K. A. 2015. Electronic Cigarette Topography in the Natural Environment. *PLoS One,* 10**,** e0129296.

Rodriguez-Espinosa, O., Rojas-Espinosa, O., Moreno-Altamirano, M. M., Lopez-Villegas, E. O. & Sanchez-Garcia, F. J. 2015. Metabolic requirements for neutrophil extracellular traps formation. *Immunology,* 145**,** 213-24.

Rossi, A. & Lord, J. 2013. Adiponectin inhibits neutrophil phagocytosis of Escherichia coli by inhibition of PKB and ERK 1/2 MAPK signalling and Mac-1 activation. *PloS one,* 8**,** e69108-e69108.

Rowell, T. R., Keating, J. E., Zorn, B. T., Glish, G. L., Shears, S. B. & Tarran, R. 2019. Flavored e-liquids increase cytoplasmic Ca2+ levels in airway epithelia. *American Journal of Physiology-Lung Cellular and Molecular Physiology,* 318**,** L226-L241.

Rowell, T. R., Keating, J. E., Zorn, B. T., Glish, G. L., Shears, S. B. & Tarran, R. 2020. Flavored e-liquids increase cytoplasmic Ca(2+) levels in airway epithelia. *Am J Physiol Lung Cell Mol Physiol,* 318**,** L226-l241.

Ryder, M. I. 1994. Nicotine effects on neutrophil F-actin formation and calcium release: implications for tobacco use and pulmonary diseases. *Exp Lung Res,* 20**,** 283-96.

Sabroe, I., Dower, S. K. & Whyte, M. K. 2005. The role of Toll-like receptors in the regulation of neutrophil migration, activation, and apoptosis. *Clin Infect Dis,* 41 Suppl 7**,** S421-6.

Sadhu, C., Masinovsky, B., Dick, K., Sowell, C. G. & Staunton, D. E. 2003. Essential role of phosphoinositide 3-kinase delta in neutrophil directional movement. *J Immunol,* 170**,** 2647-54.

Sadik, C. D., Kim, N. D. & Luster, A. D. 2011. Neutrophils cascading their way to inflammation. *Trends Immunol,* 32**,** 452-60.

Sadowska, A. M., Manuel-y-Keenoy, B., Vertongen, T., Schippers, G., Radomska-Lesniewska, D., Heytens, E. & De Backer, W. A. 2006a. Effect of N-acetylcysteine on neutrophil activation markers in healthy volunteers: In vivo and in vitro study. *Pharmacological Research,* 53**,** 216-225.

Sadowska, A. M., Verbraecken, J., Darquennes, K. & De Backer, W. A. 2006b. Role of N-acetylcysteine in the management of COPD. *Int J Chron Obstruct Pulmon Dis,* 1**,** 425-34.

Salamanca, J. C., Meehan-Atrash, J., Vreeke, S., Escobedo, J. O., Peyton, D. H. & Strongin, R. M. 2018. E-cigarettes can emit formaldehyde at high levels under conditions that have been reported to be non-averse to users. *Sci Rep,* 8**,** 7559.

Sansone, R. A. & Sansone, L. A. 2011. Getting a Knack for NAC: N-Acetyl-Cysteine. *Innov Clin Neurosci,* 8**,** 10-4.

Sapey, E., Greenwood, H., Walton, G., Mann, E., Love, A., Aaronson, N., Insall, R. H., Stockley, R. A. & Lord, J. M. 2014. Phosphoinositide 3-kinase inhibition restores neutrophil accuracy in the elderly: toward targeted treatments for immunosenescence. *Blood,* 123**,** 239-48.

Sapey, E., Patel, J. M., Greenwood, H., Walton, G. M., Grudzinska, F., Parekh, D., Mahida, R. Y., Dancer, R. C. A., Lugg, S. T., Howells, P. A., Hazeldine, J., Newby, P., Scott, A., Nightingale, P., Hill, A. T. & Thickett, D. R. 2019. Simvastatin Improves Neutrophil Function and Clinical Outcomes in Pneumonia. A Pilot Randomized Controlled Clinical Trial. *Am J Respir Crit Care Med,* 200**,** 1282-1293.

Sapey, E., Patel, J. M., Greenwood, H. L., Walton, G. M., Hazeldine, J., Sadhra, C., Parekh, D., Dancer, R. C. A., Nightingale, P., Lord, J. M. & Thickett, D. R. 2017. Pulmonary Infections in the Elderly Lead to Impaired Neutrophil Targeting, Which Is Improved by Simvastatin. *Am J Respir Crit Care Med,* 196**,** 1325-1336.

Sapey, E., Stockley, J. A., Greenwood, H., Ahmad, A., Bayley, D., Lord, J. M., Insall, R. H. & Stockley, R. A. 2011. Behavioral and structural differences in migrating peripheral neutrophils from patients with chronic obstructive pulmonary disease. *Am J Respir Crit Care Med,* 183**,** 1176-86.

Sapey, E. & Stockley, R. A. 2014. Red, amber and green: the role of the lung in de-priming active systemic neutrophils. *Thorax,* 69**,** 606.

Sapey, E., Wood, A. M., Ahmad, A. & Stockley, R. A. 2010. Tumor necrosis factor-{alpha} rs361525 polymorphism is associated with increased local production and downstream inflammation in chronic obstructive pulmonary disease. *Am J Respir Crit Care Med,* 182**,** 192-9.

Sbarra, A. J. & Karnovsky, M. L. 1959. The biochemical basis of phagocytosis. I. Metabolic changes during the ingestion of particles by polymorphonuclear leukocytes. *J Biol Chem,* 234**,** 1355-62.

Scapini, P., Carletto, A., Nardelli, B., Calzetti, F., Roschke, V., Merigo, F., Tamassia, N., Pieropan, S., Biasi, D., Sbarbati, A., Sozzani, S., Bambara, L. & Cassatella, M. A. 2005. Proinflammatory mediators elicit secretion of the intracellular B-lymphocyte stimulator pool (BLyS) that is stored in activated neutrophils: implications for inflammatory diseases. *Blood,* 105**,** 830-7.

Scapini, P., Lapinet-Vera, J. A., Gasperini, S., Calzetti, F., Bazzoni, F. & Cassatella, M. A. 2000. The neutrophil as a cellular source of chemokines. *Immunol Rev,* 177**,** 195-203.

Schaff, U. Y., Yamayoshi, I., Tse, T., Griffin, D., Kibathi, L. & Simon, S. I. 2008. Calcium flux in neutrophils synchronizes beta2 integrin adhesive and signaling events that guide inflammatory recruitment. *Ann Biomed Eng,* 36**,** 632-46.

Schliwa, M. 1982. Action of cytochalasin D on cytoskeletal networks. *J Cell Biol,* 92**,** 79-91.

Schröder, J. M., Sticherling, M., Henneicke, H. H., Preissner, W. C. & Christophers, E. 1990. IL-1 alpha or tumor necrosis factor-alpha stimulate release of three NAP-1/IL-8-related neutrophil chemotactic proteins in human dermal fibroblasts. *J Immunol,* 144**,** 2223-32.

Schwarzenberger, P., Huang, W., Ye, P., Oliver, P., Manuel, M., Zhang, Z., Bagby, G., Nelson, S. & Kolls, J. K. 2000. Requirement of endogenous stem cell factor and granulocyte-colony-stimulating factor for IL-17-mediated granulopoiesis. *J Immunol,* 164**,** 4783-9.

Scott, A., Lugg, S. T., Aldridge, K., Lewis, K. E., Bowden, A., Mahida, R. Y., Grudzinska, F. S., Dosanjh, D., Parekh, D., Foronjy, R., Sapey, E., Naidu, B. & Thickett, D. R. 2018. Pro-inflammatory effects of e-cigarette vapour condensate on human alveolar macrophages. *Thorax,* 73**,** 1161.

Scott, J., Ruchaud-Sparagano, M.-H., Musgrave, K., Roy, A. I., Wright, S. E., Perry, J. D., Conway Morris, A., Rostron, A. J. & Simpson, A. J. 2021. Phosphoinositide 3-Kinase δ Inhibition Improves Neutrophil Bacterial Killing in Critically Ill Patients at High Risk of Infection. *The Journal of Immunology***,** ji2000603.

Segal, A. W., Geisow, M., Garcia, R., Harper, A. & Miller, R. 1981. The respiratory burst of phagocytic cells is associated with a rise in vacuolar pH. *Nature,* 290**,** 406-409.

Sehgal, P., Szalai, P., Olesen, C., Praetorius, H. A., Nissen, P., Christensen, S. B., Engedal, N. & Møller, J. V. 2017. Inhibition of the sarco/endoplasmic reticulum (ER) Ca(2+)-ATPase by thapsigargin analogs induces cell death via ER Ca(2+) depletion and the unfolded protein response. *The Journal of biological chemistry,* 292**,** 19656-19673.

Sengelov, H., Follin, P., Kjeldsen, L., Lollike, K., Dahlgren, C. & Borregaard, N. 1995. Mobilization of granules and secretory vesicles during in vivo exudation of human neutrophils. *J Immunol,* 154**,** 4157-65.

Seow, W. K., Thong, Y. H., Nelson, R. D., MacFarlane, G. D. & Herzberg, M. C. 1994. Nicotine-induced release of elastase and eicosanoids by human neutrophils. *Inflammation,* 18**,** 119-27.

Shapiro, S. D., Goldstein, N. M., Houghton, A. M., Kobayashi, D. K., Kelley, D. & Belaaouaj, A. 2003. Neutrophil elastase contributes to cigarette smoke-induced emphysema in mice. *Am J Pathol,* 163**,** 2329-35.

Shen, Y., Wolkowicz, M. J., Kotova, T., Fan, L. & Timko, M. P. 2016. Transcriptome sequencing reveals e-cigarette vapor and mainstream-smoke from tobacco cigarettes activate different gene expression profiles in human bronchial epithelial cells. *Scientific reports,* 6**,** 23984-23984.

Sheppard, F. R., Kelher, M. R., Moore, E. E., McLaughlin, N. J., Banerjee, A. & Silliman, C. C. 2005. Structural organization of the neutrophil NADPH oxidase: phosphorylation and translocation during priming and activation. *J Leukoc Biol,* 78**,** 1025-42.

Shields, P. G., Song, M. A., Freudenheim, J. L., Brasky, T. M., McElroy, J. P., Reisinger, S. A., Weng, D. Y., Ren, R., Eissenberg, T., Wewers, M. D. & Shilo, K. 2020. Lipid laden macrophages and electronic cigarettes in healthy adults. *EBioMedicine,* 60**,** 102982.

Shivalingappa, P. C., Hole, R., Westphal, C. V. & Vij, N. 2016. Airway Exposure to E-Cigarette Vapors Impairs Autophagy and Induces Aggresome Formation. *Antioxidants & redox signaling,* 24**,** 186-204.

Silver, I. A. 1977. Local factors in tissue oxygenation. *J Clin Pathol Suppl (R Coll Pathol),* 11**,** 7-13.

Singh, K. P., Lawyer, G., Muthumalage, T., Maremanda, K. P., Khan, N. A., McDonough, S. R., Ye, D., McIntosh, S. & Rahman, I. 2019. Systemic biomarkers in electronic cigarette users: implications for noninvasive assessment of vaping-associated pulmonary injuries. *ERJ Open Res,* 5.

Sivaraman, S. K., Zachariah, G. & Annamala, P. 2014. Effect of Smoking on Metalloproteinases (MMPs) Activity in Patients with Acute Myocardial Infarction (AMI). *J Clin Diagn Res,* 8**,** 27-30.

Sohal, S. S., Eapen, M. S., Naidu, V. G. M. & Sharma, P. 2019. IQOS exposure impairs human airway cell homeostasis: direct comparison with traditional cigarette and e-cigarette. *ERJ Open Res,* 5.

Soneji, S., Barrington-Trimis, J. L., Wills, T. A., Leventhal, A. M., Unger, J. B., Gibson, L. A., Yang, J., Primack, B. A., Andrews, J. A., Miech, R. A., Spindle, T. R., Dick, D. M., Eissenberg, T., Hornik, R. C., Dang, R. & Sargent, J. D. 2017. Association Between Initial Use of e-Cigarettes and Subsequent Cigarette Smoking Among Adolescents and Young Adults: A Systematic Review and Meta-analysis. *JAMA Pediatr,* 171**,** 788-797.

Sørensen, O. E., Follin, P., Johnsen, A. H., Calafat, J., Tjabringa, G. S., Hiemstra, P. S. & Borregaard, N. 2001. Human cathelicidin, hCAP-18, is processed to the antimicrobial peptide LL-37 by extracellular cleavage with proteinase 3. *Blood,* 97**,** 3951-9.

Speert, D. P. 2006. Bacterial infections of the lung in normal and immunodeficient patients. *Novartis Found Symp,* 279**,** 42-51; disussion 51-5, 216-9.

Splettstoesser, W. D. & Schuff-Werner, P. 2002. Oxidative stress in phagocytes--"the enemy within". *Microsc Res Tech,* 57**,** 441-55.

Staudt, M. R., Salit, J., Kaner, R. J., Hollmann, C. & Crystal, R. G. 2018. Altered lung biology of healthy never smokers following acute inhalation of E-cigarettes. *Respir Res,* 19**,** 78.

Stockley, J. A., Walton, G. M., Lord, J. M. & Sapey, E. 2013. Aberrant neutrophil functions in stable chronic obstructive pulmonary disease: the neutrophil as an immunotherapeutic target. *Int Immunopharmacol,* 17**,** 1211-7.

Strieter, R. M., Kunkel, S. L., Showell, H. J., Remick, D. G., Phan, S. H., Ward, P. A. & Marks, R. M. 1989. Endothelial cell gene expression of a neutrophil chemotactic factor by TNF-alpha, LPS, and IL-1 beta. *Science,* 243**,** 1467-9.

Stringer, K. A., Tobias, M., O'Neill, H. C. & Franklin, C. C. 2007. Cigarette smoke extract-induced suppression of caspase-3-like activity impairs human neutrophil phagocytosis. *American Journal of Physiology-Lung Cellular and Molecular Physiology,* 292**,** L1572-L1579.

Subrahmanyam, Y. V., Yamaga, S., Prashar, Y., Lee, H. H., Hoe, N. P., Kluger, Y., Gerstein, M., Goguen, J. D., Newburger, P. E. & Weissman, S. M. 2001. RNA expression patterns change dramatically in human neutrophils exposed to bacteria. *Blood,* 97**,** 2457-68.

Sukumaran, B., Carlyon, J. A., Cai, J.-L., Berliner, N. & Fikrig, E. 2005. Early Transcriptional Response of Human Neutrophils to Anaplasma phagocytophilum Infection. *Infection and Immunity,* 73**,** 8089-8099.

Summers, C., Rankin, S. M., Condliffe, A. M., Singh, N., Peters, A. M. & Chilvers, E. R. 2010. Neutrophil kinetics in health and disease. *Trends Immunol,* 31**,** 318-24.

Summers, C., Singh, N. R., White, J. F., Mackenzie, I. M., Johnston, A., Solanki, C., Balan, K. K., Peters, A. M. & Chilvers, E. R. 2014. Pulmonary retention of primed neutrophils: a novel protective host response, which is impaired in the acute respiratory distress syndrome. *Thorax,* 69**,** 623-9.

Suratt, B. T., Petty, J. M., Young, S. K., Malcolm, K. C., Lieber, J. G., Nick, J. A., Gonzalo, J.-A., Henson, P. M. & Worthen, G. S. 2004. Role of the CXCR4/SDF-1 chemokine axis in circulating neutrophil homeostasis. *Blood,* 104**,** 565-571.

Sussan, T. E., Gajghate, S., Thimmulappa, R. K., Ma, J., Kim, J. H., Sudini, K., Consolini, N., Cormier, S. A., Lomnicki, S., Hasan, F., Pekosz, A. & Biswal, S. 2015. Exposure to electronic cigarettes impairs pulmonary anti-bacterial and anti-viral defenses in a mouse model. *PLoS One,* 10**,** e0116861.

Swain, P. M., Romero, N., Jastromb, N. & Dranka, B. P. 2018. Quantitative Analysis of Neutrophil Activation Using Agilent Seahorse XF Technology. Agilent Technologies, USA.

Taghavi, S., Khashyarmanesh, Z., Moalemzadeh-Haghighi, H., Nassirli, H., Eshraghi, P., Jalali, N. & Hassanzadeh-Khayyat, M. 2012. Nicotine content of domestic cigarettes, imported cigarettes and pipe tobacco in iran. *Addict Health,* 4**,** 28-35.

Taylor, A. E., Finney-Hayward, T. K., Quint, J. K., Thomas, C. M., Tudhope, S. J., Wedzicha, J. A., Barnes, P. J. & Donnelly, L. E. 2010. Defective macrophage phagocytosis of bacteria in COPD. *Eur Respir J,* 35**,** 1039-47.

Theilgaard-Mönch, K., Knudsen, S., Follin, P. & Borregaard, N. 2004. The transcriptional activation program of human neutrophils in skin lesions supports their important role in wound healing. *J Immunol,* 172**,** 7684-93.

Thompson, A. B., Daughton, D., Robbins, R. A., Ghafouri, M. A., Oehlerking, M. & Rennard, S. I. 1989. Intraluminal airway inflammation in chronic bronchitis. Characterization and correlation with clinical parameters. *Am Rev Respir Dis,* 140**,** 1527-37.

Tortorella, C., Ottolenghi, A., Moretti, A. M., Jirillo, E. & Antonaci, S. 1992. Thymostimulin administration modulates polymorph metabolic pathway in patients with chronic obstructive pulmonary disease. *Immunopharmacol Immunotoxicol,* 14**,** 421-37.

Totti, N., 3rd, McCusker, K. T., Campbell, E. J., Griffin, G. L. & Senior, R. M. 1984. Nicotine is chemotactic for neutrophils and enhances neutrophil responsiveness to chemotactic peptides. *Science,* 223**,** 169-71.

Tsukahara, Y., Lian, Z., Zhang, X., Whitney, C., Kluger, Y., Tuck, D., Yamaga, S., Nakayama, Y., Weissman, S. M. & Newburger, P. E. 2003. Gene expression in human neutrophils during activation and priming by bacterial lipopolysaccharide. *J Cell Biochem,* 89**,** 848-61.

U.S. Department of Health, E. a. W. U. 1964. Smoking and Health. Report of the Advisory Committee to the Surgeon General of the Public Health Service *Washington: U.S.,* Publication No. 1103.

Uribe-Querol, E. & Rosales, C. 2020. Phagocytosis: Our Current Understanding of a Universal Biological Process. *Frontiers in Immunology,* 11.

Valavanidis, A., Vlachogianni, T. & Fiotakis, K. 2009. Tobacco smoke: involvement of reactive oxygen species and stable free radicals in mechanisms of oxidative damage, carcinogenesis and synergistic effects with other respirable particles. *International journal of environmental research and public health,* 6**,** 445-462.

Van Keymeulen, A., Wong, K., Knight, Z. A., Govaerts, C., Hahn, K. M., Shokat, K. M. & Bourne, H. R. 2006. To stabilize neutrophil polarity, PIP3 and Cdc42 augment RhoA activity at the back as well as signals at the front. *J Cell Biol,* 174**,** 437-45.

Vlahos, R., Bozinovski, S., Jones, J. E., Powell, J., Gras, J., Lilja, A., Hansen, M. J., Gualano, R. C., Irving, L. & Anderson, G. P. 2006. Differential protease, innate immunity, and NF-kappaB induction profiles during lung inflammation induced by subchronic cigarette smoke exposure in mice. *Am J Physiol Lung Cell Mol Physiol,* 290**,** L931-45.

Vogt, K. L., Summers, C., Chilvers, E. R. & Condliffe, A. M. 2018. Priming and de-priming of neutrophil responses in vitro and in vivo. *European Journal of Clinical Investigation,* 48**,** e12967.

Völs, S., Sionov, R. & Granot, Z. 2017. Always Look On the Bright Side: Anti-Tumor Functions of Neutrophils. *Current pharmaceutical design,* 23.

Vorobjeva, N. V. & Chernyak, B. V. 2020. NADPH Oxidase Modulates Ca2+-Dependent Formation of Neutrophil Extracellular Traps. *Moscow University Biological Sciences Bulletin,* 75**,** 104-109.

Vuorte, J., Jansson, S. E. & Repo, H. 2001. Evaluation of red blood cell lysing solutions in the study of neutrophil oxidative burst by the DCFH assay. *Cytometry,* 43**,** 290-6.

Wang, F. 2009. The signaling mechanisms underlying cell polarity and chemotaxis. *Cold Spring Harb Perspect Biol,* 1**,** a002980.

Ween, M. P., Hamon, R., Macowan, M. G., Thredgold, L., Reynolds, P. N. & Hodge, S. J. 2020. Effects of E-cigarette E-liquid components on bronchial epithelial cells: Demonstration of dysfunctional efferocytosis. *Respirology,* 25**,** 620-628.

Weinreich, U. M. & Korsgaard, J. 2008. Bacterial colonisation of lower airways in health and chronic lung disease. *The Clinical Respiratory Journal,* 2**,** 116-122.

Weitz, J. I., Crowley, K. A., Landman, S. L., Lipman, B. I. & Yu, J. 1987. Increased Neutrophil Elastase Activity in Cigarette Smokers. *Annals of Internal Medicine,* 107**,** 680-682.

White, P. C., Hirschfeld, J., Milward, M. R., Cooper, P. R., Wright, H. J., Matthews, J. B. & Chapple, I. L. C. 2018. Cigarette smoke modifies neutrophil chemotaxis, neutrophil extracellular trap formation and inflammatory response-related gene expression. *Journal of Periodontal Research,* 53**,** 525-535.

WHO 2021. WHO REPORT ON THE GLOBAL TOBACCO EPIDEMIC, 2021: Addressing new and emerging products. Geneva: World Health Organization; 2021.

Wilson, D., Drew, W., Jasper, A., Crisford, H., Nightingale, P., Newby, P., Jackson, T., Lord, J. M. & Sapey, E. 2020. Frailty Is Associated With Neutrophil Dysfunction Which Is Correctable With Phosphoinositol-3-Kinase Inhibitors. *J Gerontol A Biol Sci Med Sci,* 75**,** 2320-2325.

Woodall, M., Jacob, J., Kalsi, K. K., Schroeder, V., Davis, E., Kenyon, B., Khan, I., Garnett, J. P., Tarran, R. & Baines, D. L. 2020. E-cigarette constituents propylene glycol and vegetable glycerin decrease glucose uptake and its

metabolism in airway epithelial cells in vitro. *American Journal of Physiology-Lung Cellular and Molecular Physiology,* 319**,** L957-L967.
Woodfin, A., Voisin, M. B., Imhof, B. A., Dejana, E., Engelhardt, B. & Nourshargh, S. 2009. Endothelial cell activation leads to neutrophil transmigration as supported by the sequential roles of ICAM-2, JAM-A, and PECAM-1. *Blood,* 113**,** 6246-57.
Wrench, C., Belchamber, K. B. R., Bercusson, A., Shah, A., Barnes, P. J., Armstrong-James, D. & Donnelly, L. E. 2018. Reduced Clearance of Fungal Spores by Chronic Obstructive Pulmonary Disease GM-CSF- and M-CSF-derived Macrophages. *Am J Respir Cell Mol Biol,* 58**,** 271-273.
Wu, Q., Jiang, D., Minor, M. & Chu, H. W. 2014. Electronic cigarette liquid increases inflammation and virus infection in primary human airway epithelial cells. *PLoS One,* 9**,** e108342.
Wyatt, T. A., Schmidt, S. C., Rennard, S. I., Tuma, D. J. & Sisson, J. H. 2000. Acetaldehyde-stimulated PKC activity in airway epithelial cells treated with smoke extract from normal and smokeless cigarettes. *Proc Soc Exp Biol Med,* 225**,** 91-7.
Xie, W., Kathuria, H., Galiatsatos, P., Blaha, M. J., Hamburg, N. M., Robertson, R. M., Bhatnagar, A., Benjamin, E. J. & Stokes, A. C. 2020. Association of Electronic Cigarette Use With Incident Respiratory Conditions Among US Adults From 2013 to 2018. *JAMA Network Open,* 3**,** e2020816-e2020816.
Xu, Y., Li, H., Bajrami, B., Kwak, H., Cao, S., Liu, P., Zhou, J., Zhou, Y., Zhu, H., Ye, K. & Luo, H. R. 2013. Cigarette smoke (CS) and nicotine delay neutrophil spontaneous death via suppressing production of diphosphoinositol pentakisphosphate. *Proc Natl Acad Sci U S A,* 110**,** 7726-31.
Yago, T., Shao, B., Miner, J. J., Yao, L., Klopocki, A. G., Maeda, K., Coggeshall, K. M. & McEver, R. P. 2010. E-selectin engages PSGL-1 and CD44 through a common signaling pathway to induce integrin αLβ2-mediated slow leukocyte rolling. *Blood,* 116**,** 485-494.
Yang, S.-R., Chida, A. S., Bauter, M. R., Shafiq, N., Seweryniak, K., Maggirwar, S. B., Kilty, I. & Rahman, I. 2006. Cigarette smoke induces proinflammatory cytokine release by activation of NF-κB and posttranslational modifications of histone deacetylase in macrophages. *American Journal of Physiology-Lung Cellular and Molecular Physiology,* 291**,** L46-L57.
Zelinkova, Z. & Wenzl, T. 2020. Influence of battery power setting on carbonyl emissions from electronic cigarettes. *Tobacco Induced Diseases,* 18**,** 1-5.
Zhao, J., Zhang, Y., Sisler, J. D., Shaffer, J., Leonard, S. S., Morris, A. M., Qian, Y., Bello, D. & Demokritou, P. 2018. Assessment of reactive oxygen species generated by electronic cigarettes using acellular and cellular approaches. *Journal of hazardous materials,* 344**,** 549-557.
Zhitkovich, A. 2019. N-Acetylcysteine: Antioxidant, Aldehyde Scavenger, and More. *Chem Res Toxicol,* 32**,** 1318-1319.
Zhu, S. H., Sun, J. Y., Bonnevie, E., Cummins, S. E., Gamst, A., Yin, L. & Lee, M. 2014. Four hundred and sixty brands of e-cigarettes and counting: implications for product regulation. *Tob Control,* 23 Suppl 3**,** iii3-9.
Zia, S., Ndoye, A., Nguyen, V. T. & Grando, S. A. 1997. Nicotine enhances expression of the alpha 3, alpha 4, alpha 5, and alpha 7 nicotinic receptors modulating calcium metabolism and regulating adhesion and motility of respiratory epithelial cells. *Res Commun Mol Pathol Pharmacol,* 97**,** 243-62.

Zuo, Y. Y., Veldhuizen, R. A., Neumann, A. W., Petersen, N. O. & Possmayer, F. 2008. Current perspectives in pulmonary surfactant--inhibition, enhancement and evaluation. *Biochim Biophys Acta,* 1778**,** 1947-77.